5. Crew Exploration Vehicle

5.1 CEV Overview and Recommendations

One of the keys to enable a successful human space exploration program is the development and implementation of a vehicle capable of transporting and housing crew on Low Earth Orbit (LEO), lunar and Mars missions. A major portion of the Exploration Systems Architecture Study (ESAS) effort focused on the definition and design of the Crew Exploration Vehicle (CEV), the the fundamental element by which NASA plans to accomplish these mission objectives. This section provides a summary of the findings and recommendations specific to the CEV.

While the CEV design was sized for lunar missions carrying a crew of four, the vehicle was also designed to be reconfigurable to accommodate up to six crew for International Space Station (ISS) and future Mars mission scenarios. The CEV can transfer and return crew and cargo to the ISS and stay for 6 months in a quiescent state for emergency crew return. The lunar CEV design has direct applications to International Space Station (ISS) missions without significant changes in the vehicle design. The lunar and ISS configurations share the same Service Module (SM), but the ISS mission has much lower delta-V requirements. Hence, the SM propellant tanks can be loaded with additional propellant for ISS missions to provide benefits in launch aborts, on-orbit phasing, and ISS reboost. Other vehicle block derivatives can deliver pressurized and unpressurized cargo to the ISS.

The ESAS team's first recommendation addresses the vehicle shape. It is recommended that the CEV incorporate a separate Crew Module (CM), SM, and Launch Abort System (LAS) arrangement similar to that of Apollo. Using an improved blunt-body capsule was found to be the least costly, fastest, and safest approach for bringing ISS and lunar missions to reality. The key benefits for a blunt-body configuration were found to be lighter weight, a more familiar aerodynamic design from human and robotic heritage (resulting in less design time and cost), acceptable ascent and entry ballistic abort load levels, crew seating orientation ideal for all loading events, and easier Launch Vehicle (LV) integration and entry controllability during off-nominal conditions. Improvements on the Apollo shape will offer better operational attributes, especially by increasing the Lift-to-Drag (L/D) ratio, improving Center of Gravity (CG) placement, potentially creating a monostable configuration, and employing a lower angle of attack for reduced sidewall heating.

A CM measuring 5.5 m in diameter was chosen to support the layout of six crew without stacking the crew members above or below each other. A crew tasking analysis also confirmed the feasibility of the selected vehicle volume. The pressurized volume afforded by a CM of this size is approximately three times that of the Apollo Command Module. The available internal volume provides flexibility for future missions without the need for developing an expendable mission module. The vehicle scaling also considered the performance of the proposed Crew Launch Vehicle (CLV), which is a four-segment Solid Rocket Booster (SRB) with a single Space Shuttle Main Engine (SSME) upper stage. The CEV was scaled to maximize vehicle size while maintaining adequate performance margins on the CLV.

The CEV will utilize an androgynous Low-Impact Docking System (LIDS) to mate with other exploration elements and to the ISS. This requires the CEV-to-ISS docking adapters to be LIDS-compatible. It is proposed that two new docking adapters replace the Pressurized Mating Adapter (PMA) and Androgynous Peripheral Attachment System (APAS) adapters on the ISS after Shuttle retirement.

An integrated pressure-fed Liquid Oxygen (LOX) and methane service propulsion system/ Reaction Control System (RCS) propulsion system is recommended for the SM. Selection of this propellant combination was based on performance and commonality with the ascent propulsion system on the Lunar Surface Access Module (LSAM). The risk associated with this type of propulsion for a lunar mission can be substantially reduced by developing the system early and flying it to the ISS. There is schedule risk in developing a LOX/methane propulsion system by 2011, but development schedules for this type of propulsion system have been studied and are in the range of hypergolic systems.

Studies were performed on the levels of radiation protection required for the CEV CM. Based on an aluminum cabin surrounded by bulk insulation and composite skin panels with a Thermal Protection System (TPS), no supplemental radiation protection is required.

Solar arrays combined with rechargeable batteries were selected for the SM due to the long mission durations dictated by some of the Design Reference Missions (DRMs). The ISS crew transfer mission and long-stay lunar outpost mission require the CEV to be on orbit for 6–9 months, which is problematic for fuel cell reactants.

The choice of a primary land-landing mode was primarily driven by a desire for land landing in the Continental United States (CONUS) for ease and minimal cost of recovery, post-landing safety, and reusability of the spacecraft. However, the design of the CEV CM should incorporate both a water- and land-landing capability. Ascent aborts will require the ability to land in water, while other off-nominal conditions could lead the spacecraft to a land landing, even if not the primary intended mode. However, a vehicle designed for a primary land-landing mode can more easily be made into a primary water lander than the reverse situation. For these reasons, the study attempted to create a CONUS land-landing design from the outset, with the intention that a primary water lander would be a design off-ramp if the risk or development cost became too high.

In order for CEV entry trajectories from LEO and lunar return to use the same landing sites, it is proposed that NASA utilize skip-entry guidance on the lunar return trajectories. The skip-entry lunar return technique provides an approach for returning crew to a single CONUS landing site anytime during a lunar month. The Apollo-style direct-entry technique requires water or land recovery over a wide range of latitudes. The skip-entry includes an exo-atmospheric correction maneuver at the apogee of the skip maneuver to remove dispersions accumulated during the skip maneuver. The flight profile is also standardized for all lunar return entry flights. Standardizing the entry flights permits targeting the same range-to-landing site trajectory for all return scenarios so that the crew and vehicle experience the same heating and loads during each flight. This does not include SM disposal considerations, which must be assessed on a case-by-case basis.

For emergencies, the CEV also includes an LAS that will pull the CM away from the LV on the pad or during ascent. The LAS concept utilizes a 10-g tractor rocket attached to the front of the CM. The LAS is jettisoned from the launch stack shortly after second stage ignition. Launch aborts after LAS jettison are performed by using the SM service propulsion system. Launch abort study results indicate a fairly robust abort capability for the CEV/CLV and a 51.6-deg-inclination ISS mission, given 1,200 m/s of delta-V and a Thrust-to-Weight (T/W) ratio of at least 0.25. Abort landings in the mid-North Atlantic can be avoided by either an Abort-To-Orbit (ATO) or posigrade Trans-Atlantic Abort Landing (TAL) south of Ireland. Landings in the Middle East, the Alps, or elsewhere in Europe can be avoided by either an ATO or a retrograde TAL south of Ireland. For 28.5-deg-inclination lunar missions, abort landings in Africa can be avoided by either an ATO or a retrograde TAL to the area between the Cape Verde islands and Africa. However, it appears that even with 1,724 m/s of delta-V, some abort landings could occur fairly distant from land. However, once the ballistic impact point crosses roughly 50°W longitude, posigrade burns can move the abort landing area downrange near the Cape Verde islands.

5.2 CEV Description

5.2.1 CEV Ground Rules and Assumptions

The following Ground Rules and Assumptions (GR&As) were drafted at the beginning of the ESAS for consistency among the team in studying the ESAS Initial Reference Architecture (EIRA). As the study progressed, some of the assumptions were modified or deleted.

In response to the ESAS charter, the first crewed flight of the CEV system to the ISS was assumed to occur in 2011. The CEV design requirements were, however, to be focused on exploration needs beyond LEO. Therefore, the team started with the existing ESMD Revision E Crew Transportation System (CTS) requirements and assessed these against ISS needs for areas of concern where CEV may fall short of ISS expectations. Any such shortcomings were then examined on a case-by-case basis to determine whether they were critical to performing the ISS support function. If they were found not to be critical, such shortcomings were considered as guidelines and not requirements on the CEV.

The CEV reference design includes a pressurized CM to support the Earth launch and return of a crew of up to six, a LAS, and an unpressurized SM to provide propulsion, power, and other supporting capabilities to meet the CEV's in-space mission needs. Operations at ISS will require the CEV pressurized module to be capable of 14.7 psi. The CEV may launch at a lower pressure but must support equalization with the ISS. The CEV docking system was selected to meet exploration needs and, therefore, was assumed to not be APAS-compatible. This approach will require a docking adaptor to (or in place of) the United States On-orbit Segment (USOS) PMA that remains on ISS.

ISS interfaces to CEV (either direct or through intermediate adaptor) will include:

- Hard-line and Radio Frequency (RF) voice channels (two);
- Basic ECLS System (ECLSS) for habitability air exchange via flexhose—the ISS provides temperature and humidity control and air revitalization capabilities;
- Minimal keep-alive/habitability power provided by the ISS;
- Status telemetry and hard-line command via ISS bent pipe;
- Automated Rendezvous and Docking (AR&D) RF interfaces; and
- Transfer of high-pressure oxygen and nitrogen to ISS airlock.

ISS support assumptions include:

- Two crewed flights per year for crew rotation;
- One uncrewed, unpressurized cargo flight per year; and
- Three uncrewed, pressurized cargo flights per year.

ISS pressurized cargo CEV variant (Block 1B) assumptions include:

- The pressurized cargo module is the crewed CEV CM with seats removed and outfitted with stowage accommodations;
  - Stowage unit size is limited to Shuttle Mid-deck Locker Equivalent (MLE) dimensions compatible with APAS-size hatch.
- The pressurized cargo module supports both up- and down-mass capability (i.e., the module lands and is recovered);

- The AR&D system meets ISS requirements for approach and docking of automated vehicles;
- In addition to dry cargo, the CEV also supports delivery of water, gaseous oxygen, and the transfer of high-pressure oxygen and nitrogen to airlock tanks; and
- The SM provides delta-V for transfer from LV insertion orbit to ISS rendezvous and deorbit from ISS.

ISS crewed CEV variant (Block 1A) assumptions include:

- Same as Block 1B variant, with the following exceptions:
- CEV CM nominally outfitted for three crew plus logistics;
  - Assume the Russians continue to support the ISS with Soyuz—it is considered unrealistic to expect the Russians to stop producing Soyuz.
- The CEV will support a docking as early as Rev3 on flight day 1;
- Assume no less than 6 days of stand-alone free-flight capability;
  - Three days for a flight day 3 rendezvous and docking profile;
  - One contingency rendezvous delay day; and
  - Two contingency post-undock days dwell time for resolving systems problems.
- Option of piloted approach/manual docking based on direct targeting (versus offset targeting used for AR&D case); and
- CEV will support a crew of three docked to the station with hatches closed for up to 48 hours.

ISS unpressurized Cargo Delivery Vehicle (CDV) assumptions include.

- Utilizes the same SM as other blocks;
- Delivers unpressurized cargo to ISS;
- Common Berthing Mechanism (CBM) and grapple fixture for capture and berthing with Space Station Remote Manipulator System (SSRMS); and
- Vehicle expended at the end of the mission.

Lunar CEV variant (Block 2) assumptions include:

- Same as Block 1A variant, with the following exceptions:
- The CEV CM outfitted for four people plus To Be Determined (TBD) cargo;
- Assume no less than 16 days of stand-alone free-flight capability;
- TBD supplemental radiation protection;
- The SM provides delta-V for Low Lunar Orbit (LLO) rendezvous, ascent plane change, and Trans-Earth Injection (TEI); and
- Supports first lunar landing in 2018.

Mars CEV variant (Block 3) assumptions include:

- Same as Lunar Block 2 variant, with the following exceptions:
- The CEV CM outfitted for six people plus TBD cargo; and
- Assume no less than 2 days of stand-alone free-flight capability.

5.2.2 Design Approach

The CEV design was approached with the focus on a lunar polar mission. In addition to optimizing the design for exploration missions, the team also assessed the possible means by which the CEV could access the ISS. The lunar design starting point was very important, as a vehicle optimized for the ISS and then adapted for lunar missions may have a very different outcome. Past studies, such as the Orbital Space Plane (OSP) and the Crew Return Vehicle (CRV), designed vehicles to solely go to the ISS and, therefore, did not address transit out of LEO. The biggest difference with this study is that the CEV does not have a 24-hour medical return mission from the ISS coupled with an emergency evacuation mission that required system power-up in 3 minutes. These requirements would drive vehicle system design and landing site selection. Neither the Space Shuttle nor Soyuz were designed to go to the ISS and meet these requirements, and the CEV is modeled after the capabilities that these two vehicles provide to the ISS. The CEV will be the United States' next human spacecraft for the next 20 to 30 years and should have the flexibility to meet the needs for missions to the Moon, Mars, and beyond.

Vehicle size, layout, and mass were of central importance in this study, because each factors into vital aspects of mission planning considerations. Detailed subsystem definitions were developed and vehicle layouts were completed for a four-crew lunar DRM and a six-crew Mars DRM. The lunar mission was a design driver since it had the most active days with the crew inside. The Mars DRM, which was a short-duration mission of only 1 to 2 days to and from an orbiting Mars Transfer Vehicle (MTV), drove the design to accommodate a crew of six. Ultimately, the CEV CM was sized to be configurable for accommodating six crew members even for an early mission to the ISS.

The different CEV configurations were each assigned a block number to distinguish their unique functionality. The Block 1 vehicles support the ISS with transfer of crew and cargo. The Block 1A vehicle transfers crew to and from the ISS. This vehicle can stay at the ISS for 6 months. Varying complements of crew and pressurized cargo can be transported in the Block 1A CM. The Block 1B CM transports pressurized cargo to and from the ISS. The crew accommodations are removed and replaced with secondary structure to support the cargo complement. The relationship between the Block 1A and Block 1B CMs is similar to that of the Russian Soyuz and Progress vehicles. Unpressurized cargo can be transported to the ISS via the CDV. The CDV replaces the CM with a structural "strong back" that supports the cargo being transferred. The CDV uses the same SM as the other blocks and also requires a suite of avionics to perform this mission. The CDV is expended after its delivery mission. The Block 2 CEV is the reference platform sized to transfer crew to the lunar vicinity and back. Detailed sizing was performed for this configuration and the other blocks were derived from its design. The Block 3 configuration is envisioned as a crewed transfer vehicle to and from an MTV in Earth orbit. The crew complement for this configuration is six. No detailed design requirements were established for this block and detailed mass estimates were never derived.

Design details for each block configuration are discussed in later sections. A mass summary for each block is shown in **Figure 5-1**. Detailed mass statements were derived for each block and are provided in **Appendix 5A**, **CEV Detailed Mass Breakdowns**.

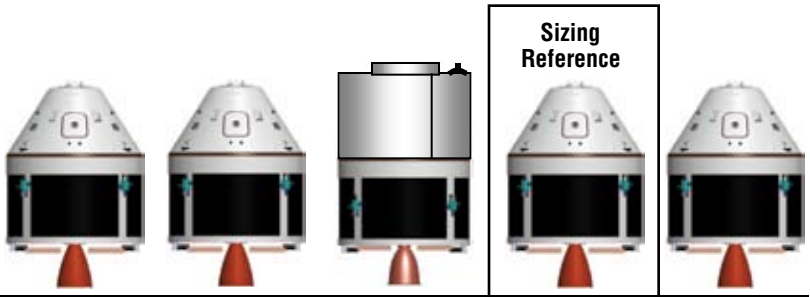

	Block 1A ISS Crew	Block 1B ISS Press Cargo	CDV ISS Unpress Cargo	Block 2 Lunar Crew	Block 3 Mars Crew
Crew Size	3	0	0	4	6
LAS Required	4,218	None	None	4,218	4,218
Cargo Capability (kg)[1]	400	3,500	6,000	Minimal	Minimal
CM (kg)	9,342	11,381	12,200	9,506	TBD
SM (kg)	13,558	11,519	6,912	13,647	TBD
Service Propulsion System delta-V (m/s)	1,544[2]	1,098[2]	330	1,724	TBD
EOR–LOR 5.5-m Total Mass (kg)	22,900	22,900	19,112	23,153	TBD

Note 1: Cargo capability is the total cargo capability of the vehicle including Flight Support Equipment (FSE) and support structure.
Note 2: A packaging factor of 1.29 was assumed for the pressurized cargo and 2.0 for unpressurized cargo.
Extra Block 1A and 1B service propulsion system delta-V used for late ascent abort coverage.

Figure 5-1. Block Mass Summaries

The design and shape of the CEV CM evolved in four design cycles throughout the study, beginning with an Apollo derivative configuration 5 m in diameter and a sidewall angle of 30-deg. This configuration provided an Outer Mold Line (OML) volume of 36.5 m^3 and a pressurized volume of 22.3 m^3. The CM also included 5 g/cm^2 of supplemental radiation protection on the cabin walls for the crew's protection. Layouts for a crew of six and the associated equipment and stowage were very constrained and left very little habitable volume for the crew.

A larger CEV was considered in Cycle 2, which grew the outer diameter to 5.5 m and reduced the sidewall angles to 25 deg. Both of these changes substantially increased the internal volume. The pressurized volume increased by 75 percent to 39.0 m^3 and the net habitable volume increased by over 50 percent to 19.4 m^3. The desire in this design cycle was to provide enough interior volume for the crew to be able to stand up in and don/doff lunar EVA suits for the surface direct mission. Most of the system design parameters stayed the same for this cycle including the 5 g/cm^2 of supplemental radiation protection.

Cycle 3 reduced the sidewall angles even further to 20 deg in an effort to achieve monostability on Earth entry. The sidewall angle increased the volume further. Because the increases in volume were also increasing the vehicle mass, the height of the vehicle was reduced by 0.4 m, reducing the height-to-width aspect ratio. This configuration showed the most promise in the quest for monostability, but the proper CG was still not achieved. Analysis in this design cycle showed that the supplemental radiation protection could be reduced to 2 g/cm^2. **Figure 5-2** illustrates the progression of the configurations through Cycle 3 of the study as compared to Apollo and the attached table details the changes in diameter, sidewall angle, and volume. Data for Cycle 4 is also shown and is described in the following paragraphs.

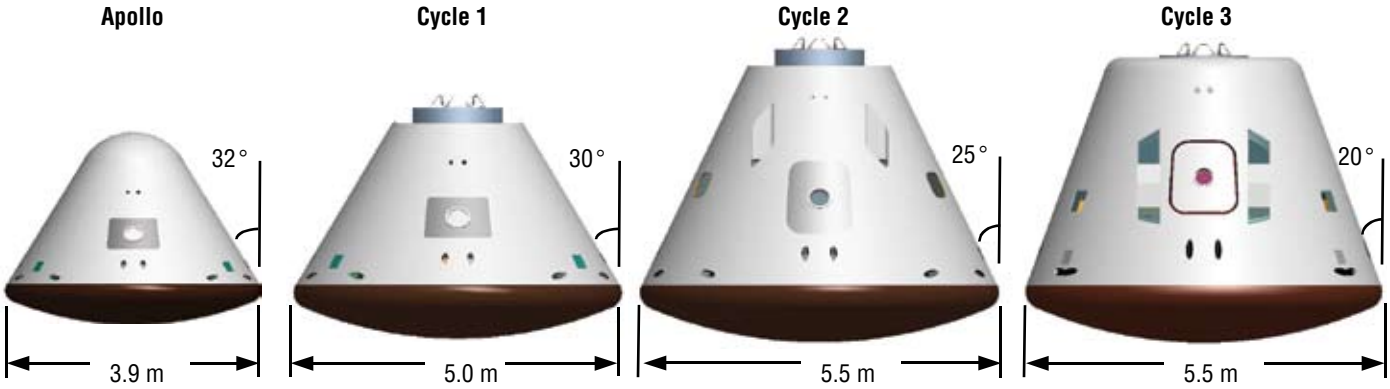

Configuration	Diameter (m)	Sidewall Angle (deg)	OML Volume (m^3)	Pressurized Volume(m^3)
Apollo	3.9	32.5	15.8	10.4
Cycle 1 (EIRA)	5.0	30.0	36.5	22.3
Cycle 2	5.5	25.0	56.7	39.0
Cycle 3	5.5	20.0	63.6	39.5
Cycle 4	5.5	32.5	45.9	30.6

Figure 5-2. CEV Crew Module Sizing Progression

Cycle 4 was the final CEV design cycle and began after the decision was made to no longer consider the lunar surface direct mission. The design implications to the CEV (i.e., difficulty including an airlock and complex operatives) and the low mass margins surrounding the lunar surface direct mission mode were the primary reasons for taking the mode out of consideration. The Cycle 4 CEV was sized for a dual-launch Earth Orbit Rendezvous-Lunar Orbit Rendezvous (EOR–LOR) mission mode where the CEV performs a rendezvous with the Earth Departure Stage (EDS) and LSAM in LEO, stays in lunar orbit while the LSAM descends to the lunar surface, and performs another rendezvous with the LSAM in lunar orbit. No supplemental radiation protection was included in the mass estimates for this design analysis due to results from a radiation study reported in **Section 4**, **Lunar Architecture**.

The resulting Cycle 4 CM shape is a geometric scaling of the Apollo Command Module (**Figure 5-3**). The vehicle is 5.5 m in diameter and the CM has a sidewall angle of 32.5 deg. The resulting CM pressurized volume is approximately 25 percent less than the Cycle 3 volume, but has almost three times the internal volume as compared to the Apollo Command Module. The CEV was ultimately designed for the EOR–LOR 1.5-launch solution, and volume reduction helps to reduce mass to that required for the mission. **Figure 5-4** depicts how vehicle sidewall angle and diameter affect pressurized volume and the resulting design point for each cycle.

The following sections detail the design of the lunar CEV CM, SM, and LAS, as well as the other block variants.

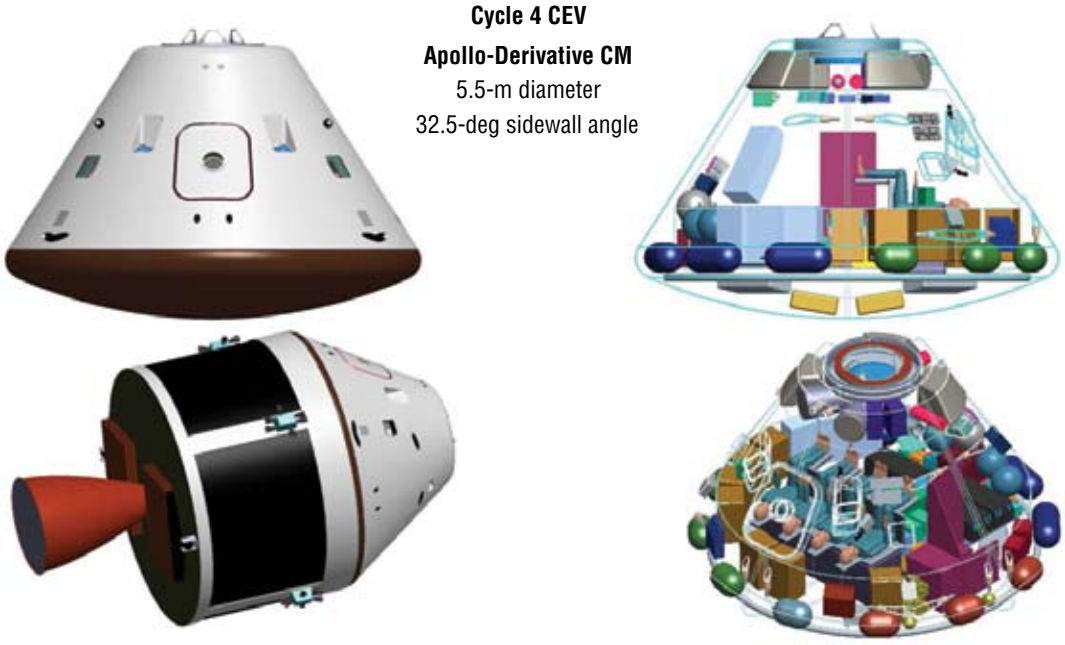

Figure 5-3. Cycle 4 CEV CM

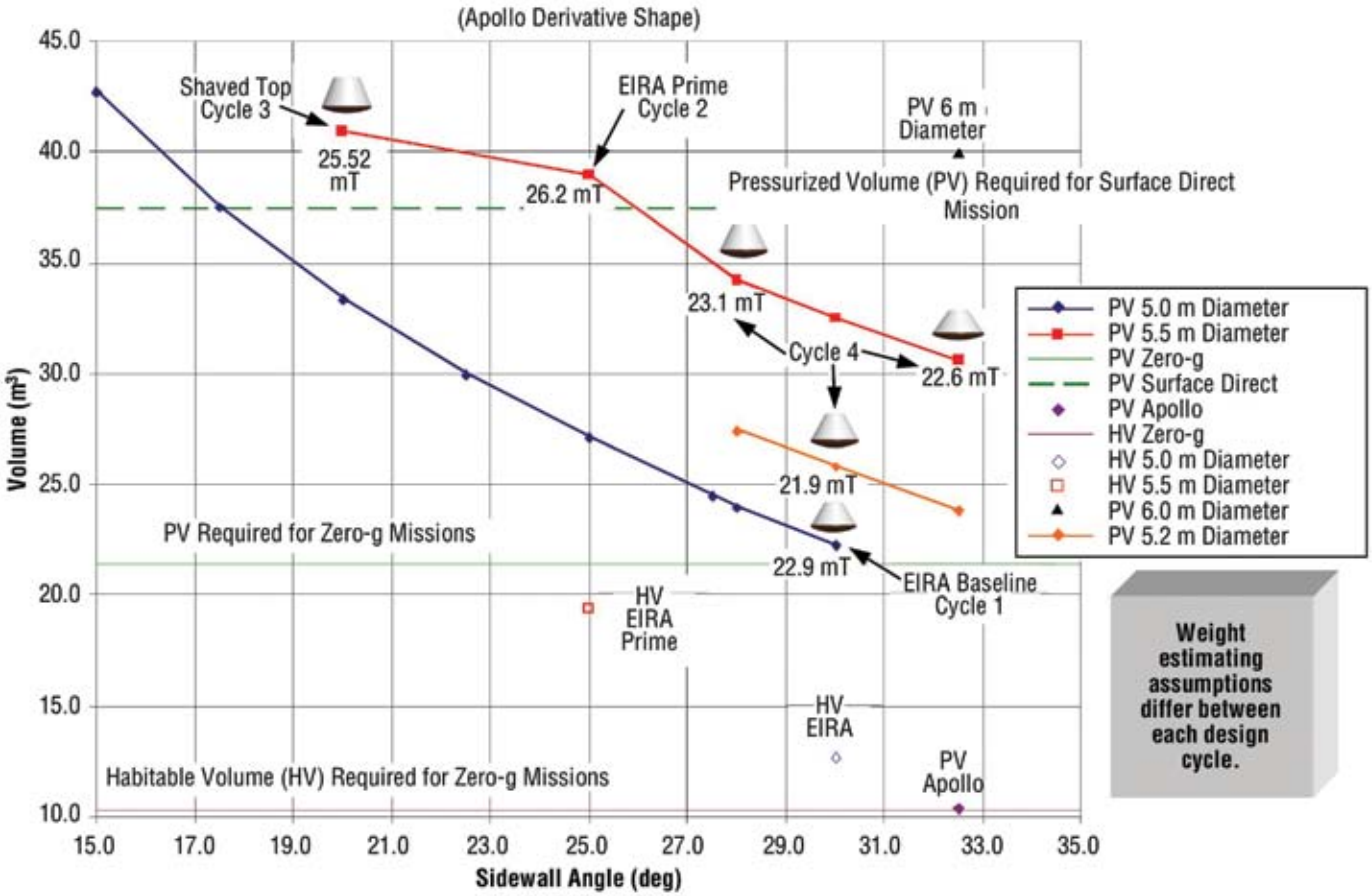

Figure 5-4. CEV Volume Relationships

5.2.3 Block 2 - Lunar CEV

5.2.3.1 Lunar CEV CM

5.2.3.1.1 Vehicle Description

The lunar CEV CM, in conjunction with the SM and LV/EDS, is used to transport four crew members from Earth to lunar orbit and return the crew members to Earth. The CM provides habitable volume for the crew, life support, docking and pressurized crew transfer to the LSAM, and atmospheric entry and landing capabilities. Upon return, a combination of parachutes and airbags provide for a nominal land touchdown with water flotation systems included for water landings following an aborted mission. Three main parachutes slow the CEV CM to a steady-state sink rate of 7.3 m/s (24 ft/s), and, prior to touchdown, the ablative aft heat shield is jettisoned and four Kevlar airbags are deployed for soft landing. After recovery, the CEV is refurbished and reflown with a lifetime up to 10 missions.

A scaled Apollo Command Module shape with a base diameter of 5.5 m and sidewall angle of 32.5 deg was selected for the OML of the CEV CM. This configuration provides 29.4 m^3 of pressurized volume and 12–15 m^3 of habitable volume for the crew during transits between Earth and the Moon. The CEV CM operates at a nominal internal pressure of 65.5 kPa (9.5 psia) with 30 percent oxygen composition for lunar missions, although the pressure vessel structure is designed for a maximum pressure of 101.3 kPa (14.7 psia). Operating at this higher pressure allows the CEV to transport crew to the ISS without the use of an intermediate airlock. For the lunar missions, the CM launches with a sea-level atmospheric pressure (101.3 kPa), and the cabin is depressurized to 65.5 kPa prior to docking with the LSAM.

The lunar CEV CM propulsion system provides vehicle attitude control for atmospheric entry following separation from the SM and range error corrections during the exoatmospheric portion of a lunar skip-entry return trajectory. A gaseous oxygen/ethanol bipropellant system is assumed with a total delta-V of 50 m/s.

Illustrations of the reference lunar CEV CM are shown in **Figure 5-5**.

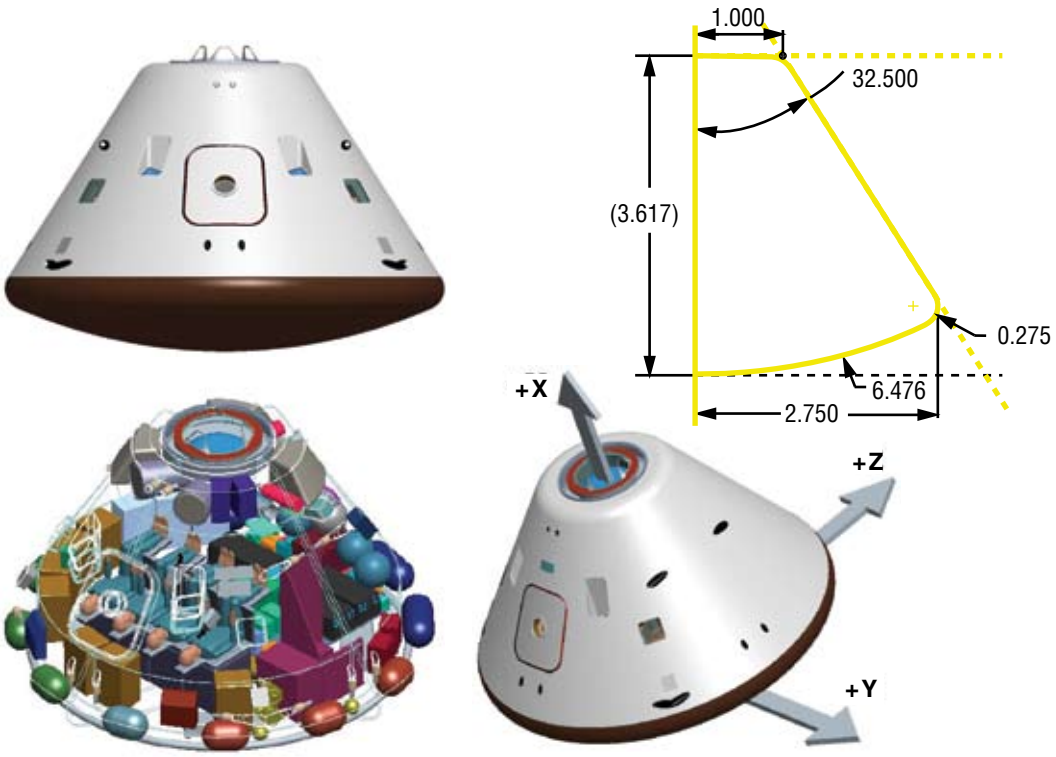

Figure 5-5. Reference Lunar CEV CM

5.2.3.1.2 Overall Mass Properties

Table 5-1 provides overall vehicle mass properties for the lunar CEV CM. The mass properties reporting standard is outlined in JSC-23303, Design Mass Properties. A detailed mass statement is provided in **Appendix 5A**, **CEV Detailed Mass Breakdowns**.

Table 5-1. Vehicle Mass Properties for the Lunar CEV CM

Lunar CEV CM	% of Vehicle Dry Mass	Mass (kg)	Volume (m^3)
1.0 Structure	23%	1,883	0
2.0 Protection	11%	894	1
3.0 Propulsion	5%	413	1
4.0 Power	10%	819	1
5.0 Control	0%	0	0
6.0 Avionics	5%	435	1
7.0 Environment	14%	1,091	4
8.0 Other	14%	1,159	2
9.0 Growth	17%	1,339	2
10.0 Non-Cargo		821	3
11.0 Cargo		100	1
12.0 Non-Propellant		367	0
13.0 Propellant		184	0
Dry Mass	**100%**	**8,034 kg**	
Inert Mass		**8,955 kg**	
Total Vehicle		**9,506 kg**	

5.2.3.1.3 Subsystem Description

Structure

The CEV CM structure includes vehicle primary structures and consists of the following components:

- Pressure vessel structure,
- Windows, and
- OML unpressurized structure.

The selected shape for the CEV CM is the Apollo Command Module shape scaled in dimension by approximately 141 percent to a base diameter of 5.5 m (18 ft), while the original Apollo Command Module sidewall angle of 32.5 deg has been maintained for this analysis. Selecting this shape provides a total CEV pressurized volume of 29.4 m^3 (1,038 ft^3).

The CEV pressure vessel structure provides habitable volume for the crew and enclosure for necessary systems of the CEV through ascent until rendezvous with the LSAM in LEO, through transit to the Moon and transfer to the LSAM in lunar orbit, and through undocking from the LSAM until reentry and crew recovery on Earth. The CEV CM pressure vessel structure construction is an Aluminum (Al) honeycomb sandwich using materials such as Al 2024 or the equivalent for the face sheets and Al 5052 for the honeycomb core. The mass-estimating method used for estimating pressure vessel structure (including secondary structure) in this assessment was to assume a uniform structure mass per unit area and scale by the external surface area of the pressure vessel. The assumed scaling factor for aluminum honeycomb is 20.3 kg/m^2 (4.15 lb/ft^2) and the surface area of the pressure vessel less windows and hatches is 52.7 m^2. The pressure vessel structure mass for the CEV was designed to withstand a higher 14.7 psia nominal internal cabin pressure required for ISS crew rotation missions instead of the lower 9.5 psia nominal internal pressure for lunar missions.

Five windows are included on the CEV for rendezvous and docking operations, observation, and photography. Two forward-facing windows on the vehicle sidewalls provide a view toward the apex of the CM for docking with the ISS and the LSAM, while two side windows and a fifth circular window located within the side ingress/egress hatch provide additional external views. The windows are double-paned fused silica panels similar to the optical windows on the Shuttle Orbiter.

The OML for the CEV CM is composed of graphite epoxy/Bismaleimide (BMI) composite skin panels similar to those developed for the X–37 Approach and Landing Test Vehicle (ALTV). This structure provides the vehicle's aerodynamic shape and serves as the attachment structure for windward and leeward TPS. The mass-estimating method used for estimating OML structure mass in this assessment was to assume a uniform structure mass per unit area and scale by the external surface area of the outer structure. The assumed scaling factor for composite skin panels, including attachment structure, is 11.6 kg/m^2 (2.38 lb/ft^2), and the surface area of the OML, less windows and hatches, is 66.9 m^2. Graphite epoxy/BMI has a maximum service temperature of 450°K (350°F) for aerothermal analysis.

Protection

The CEV CM spacecraft protection consists of the materials dedicated to providing passive spacecraft thermal control during all mission phases including ascent, ascent aborts, in-space operations, and atmospheric entry, and includes the following components: External TPS and internal insulation.

For the CEV CM, spacecraft protection is the TPS that includes ablative TPS on the windward (aft) side of the vehicle, reusable surface insulation for the external leeward (central and forward) TPS, and internal insulation between the pressurized structure and OML. There are a number of potential materials available for use in the CEV CM protection system and the eventual TPS materials selected will be the result of a rigorous trade study based on performance and cost. Some of these materials may include carbon-carbon, carbon-phenolic, AVCO, Phenolic Impregnated Carbonaceous Ablator (PICA), PhenCarb-28, Alumina Enhanced Thermal Barrier-8 (AETB–8))/TUFI, Advanced Flexible Reusable Surface Insulation (AFRSI, LI-900 or LI-2200, CRI, SLA-561S, cork, and many others.

TPS mass for the present CEV CM concept is scaled from an analysis conducted for a vehicle of the same base diameter but lower sidewall angle and higher mass at Entry Interface (EI). A 5.5-m, 28-deg sidewall concept with a total mass of approximately 11,400 kg requires an aft TPS mass of 630 kg and forward TPS mass of 180 kg. The assumed TPS materials for this analysis were PICA for the aft side and a combination of LI-2200, LI-900, AFRSI, and Flexible Reusable Surface Insulation (FRSI) at equal thicknesses for the central and forward side. The maximum heating rate for the TPS is driven by ballistic entry trajectories at lunar return speeds (11 km/s), and TPS thickness is sized by the total integrated heat load of a skip-entry trajectory. For the lighter 5.5-m, 32.5-deg CM, the 630-kg aft TPS mass from the larger, heavier concept has been retained to provide additional margin, while the central and forward TPS mass has been scaled based on the lower surface area. The current CEV CM mass, including external TPS, is 9,301 kg at atmospheric EI for the nominal lunar mission.

Finally, the mass-estimating method used for internal insulation was to assume Saffil high-temperature fibrous alumina insulation wrapped around the exterior of the CM pressure vessel at a mass penalty of 2 kg/m^2 of surface area. The pressure vessel external surface area is 52.7 m^2.

Propulsion

The CEV CM propulsion consists of an RCS and includes the following components:

- Primary RCS thrusters,
- Primary RCS tanks,
- Primary RCS pressurization,
- Backup RCS thrusters, and
- Backup RCS tanks.

The CEV CM propulsion RCS provides vehicle attitude control following SM separation through atmospheric entry. Following SM separation, the vehicle is reoriented using the primary RCS to a proper attitude for entry; and, during atmospheric flight, the RCS provides roll torque to control the direction of the CM lift vector and to counteract induced spin torques, provides dampening of induced pitch and yaw instabilities, and corrects range dispersions during skip-out portions of a lunar skip return trajectory. A backup, fully independent RCS is also included on the CEV to provide emergency attitude control and a ballistic entry mode in the event of complete loss of primary power and attitude control during entry. A ballistic entry is a non-lifting flight mode where a controlled roll rate is introduced to the vehicle to effectively null the net lift vector, thereby avoiding "lift vector down" flight modes that may exceed maximum crew g-loads and TPS temperature limits during lunar return.

The assumed primary RCS propulsion system for the CEV CM is a Gaseous Oxygen (GOX) and liquid ethanol bipropellant system selected for its nontoxicity and commonality with the life support system's high-pressure oxygen supply system. A similar system has been developed and ground-tested for potential use as a Shuttle Orbiter RCS replacement and for attitude control use on the Kistler K–1 LV. The system consists of twelve 445 N (100 lbf) thrusters arranged to thrust in the pitch, roll, and yaw directions, with two thrusters pointed in each of the six directions (+pitch, –pitch, +roll, –roll, +yaw, –yaw). The assumed Specific Impulse (Isp) for the RCS system is 274 sec at a chamber pressure of 300 psia, oxidizer to fuel mixture ratio of 1.4:1 by mass, and nozzle area ratio of 40:1. The Oxygen (O2) gas for the CM primary RCS and life support system is stored in four cylindrical 5,000 psia graphite composite overwrapped-Inconel 718-lined tanks mounted at the CM base, exterior to the crew pressure vessel. Each tank has an outer diameter of 0.39 m and total length of 0.96 m, and holds 0.092 m^3 (5,553 in^3), or 43 kg, of oxygen. The liquid ethanol for the primary RCS is stored in two cylindrical graphite composite overwrapped-Inconel 718-lined bellows tanks of the same size as the tanks used to store the Nitrogen (N2) gas required for the CEV life support system. Each tank has an outer diameter of 0.39 m and total length of 0.66 m, and holds 0.053 m^3 (3,230 in^3), or 39 kg, of ethanol.

Ethanol tank pressure for the primary RCS is regulated using a high-pressure Gaseous Helium (GHe) pressurization system. Two spherical 6,000 psia tanks hold the required helium gas, 0.4 kg per tank, and have outer diameters of 0.19 m each. The tanks are the same construction as the RCS propellant tanks—graphite composite overwrapped with Inconel 718 liners.

The backup RCS is a fully independent CEV attitude control system and is used to provide emergency vehicle attitude control following complete loss of the primary system. The backup system may be used to reorient the vehicle from an “apex forward” to a “heat shield forward” configuration for entry, or to induce a slow roll rate for an emergency zero-lift ballistic entry flight mode. In the former scenario, the CEV CM, much like the Apollo Command Module, may be bi-stable and have a secondary trim point where the vehicle apex points during entry in the direction of the velocity vector. Such an orientation is clearly undesirable, as the CEV would be unable to withstand the intense heat of atmospheric entry. If the vehicle’s CG can be lowered close enough to the aft heat shield, this trim point can be eliminated and the vehicle will have a single trim point (monostable) where the heat shield points toward the velocity vector. Therefore, for a given range of initial vehicle state conditions at entry (e.g., static with apex forward, 3-axis tumbling, etc.), a monostable CEV would eventually trim in the proper orientation due to the pitching moment characteristics of the vehicle. Depending on the initial vehicle state, however, a monostable vehicle may take longer to trim at the proper angle of attack than would be allowed before the onset of induced aerothermal heating exceeded vehicle temperature limits. Thus, while a monostable CEV CM is highly desired, a backup attitude control capability is required. In addition, a monostable vehicle could still trim at an angle of attack that pointed the lift vector down, and, for that possibility, the backup attitude control system can induce a slow, lift-nulling roll rate for a zero-lift ballistic mode.

GOX and liquid ethanol are also used as propellants for the backup RCS. The system, which for simplicity operates in blowdown mode instead of being helium-pressure-regulated, consists of four 445 N (100 lbf) thrusters arranged near the CM apex to thrust in the pitch and roll directions, with two thrusters each pointing in the +pitch and –pitch directions. To induce a roll moment, the +pitch/–Z thruster fires in tandem with the –pitch/+Z thruster, or vice versa. Pitching moments are generated by firing both +pitch or –pitch thrusters in tandem. The backup RCS thrusters are identical to the primary system. Oxygen gas for the CM backup RCS is stored in a single cylindrical 5,000 psia graphite composite overwrapped Inconel 718-lined tank identical to the oxygen tanks for the primary system. The tank has an outer diameter of 0.39 m and total length of 0.96 m. The liquid ethanol for the backup RCS is stored in a single cylindrical graphite composite overwrapped Inconel 718-lined diaphragm tank, again identical to the primary ethanol tanks. The tank has an outer diameter of 0.39 m and total length of 0.66 m.

There are several propellant alternatives to GOX/ethanol also worthy of consideration for the CEV CM propulsion system. These include, but are not limited to, Tridyne, GOX/Gaseous Methane (GCH4), monopropellant hydrazine, monopropellant Hydrogen Peroxide (H2O2), Nitrous Oxide (N2O), Nitrogen Tetroxide (NTO)/Monomethyl Hydrazine (MMH), cold gas nitrogen, and monopropellant Hydroxyl Ammonium Nitrate- (HAN-) based propellants. A warm gas Tridyne system is particularly attractive for the CM but was considered infeasible due to the high delta-V currently associated with the lunar skip-entry.

Power

The power subsystem for the CEV CM encompasses the primary electrical power and distribution and energy storage functions for the CEV and includes the following components:

- Rechargeable Lithium-ion (Li-ion) batteries for primary power,
- 28 Volts Direct Current (VDC) electrical power buses,
- Power control units,
- Remote PCUs, and
- Backup battery.

Four rechargeable Li-ion batteries provide CEV power during LEO and lunar orbit eclipse periods and power following CM–SM separation through landing. These batteries were selected for their high specific energy and volume, low drain rate, long wet life, and good charge retention. The total CM energy storage requirement is 6.0 kW (the CEV's maximum average power for the mission) for 2.25 hours (the time from SM separation to landing). Three batteries are sized to meet this 13.5 kW-hr requirement with a fourth battery included for redundancy. Including power management and distribution losses (10 percent) and a battery depth-of-discharge of 80 percent, each of the four batteries is sized to store a maximum of 223.2 Amp-hr at 28 VDC. Battery mass and volume were estimated using linear scaling factors for rechargeable Li-ion batteries, 100 W-hr/kg and 200 W-hr/L, respectively. The total battery mass was further increased by 10 percent for battery installation.

The four Li-ion batteries, in conjunction with two solar arrays mounted on the SM, provide electrical power to the CEV power distribution system. The primary power distribution system then distributes 28 VDC power to the vehicle across three main distribution buses, with each main bus sized to handle the peak electrical load for two-fault tolerance. CEV average power for the entire mission with crew on board is 4.5 kW, with a peak power of 8 kW. The wiring harness for the electrical power distribution system consists of primary and secondary distribution cables, jumper cables, data cabling, RF coaxial cable, and miscellaneous brackets, trays, and cable ties. Mass for the entire CM wiring harness, including electrical power and avionics wiring and associated items, is estimated at 317 kg.

Power Control Units (PCUs) on the CEV CM monitor and control current from the solar arrays and batteries and distribute power among the vehicle loads. A PCU includes the relays, switches, current sensors, and bus interfaces necessary to control and distribute power, as well as solar array switch modules and battery charge modules for monitoring and regulating output current. There are three PCUs included in the CEV CM (one per bus), with each unit capable of switching 160 amps at 28 VDC continuously (4,500 W) or 285 Amps at 28 VDC over a short duration (8,000 W). PCUs have an estimated mass of 41.1 kg each.

Remote Power Control Units (RPCUs) monitor and control power from the PCUs and distribute 28 VDC power to vehicle loads. Each unit has an estimated mass of 32.6 kg each and three units are included on the CEV CM (one per bus).

The CEV also includes a single rechargeable Li-ion backup battery for emergency power during ballistic entry modes. In the event of complete loss of primary power during entry, the backup battery supplies 500 W of 28 VDC power for 45 minutes.

Control
Items typically included in the spacecraft control category are aerodynamic control surfaces, Thrust Vector Control (TVC), actuators, cockpit controls such as rudder pedals, and others. There are no control components on the CEV CM.

Avionics
The CEV CM avionics subsystem provides Command and Control (C&C) over all CEV operations and consists of the following components:

- Command, Control, and Data Handling (CCDH);
- Guidance and navigation;
- Communications; and
- Cabling and instrumentation.

CCDH includes the components necessary to process and display flight-critical spacecraft data and collect crew input. These components on the CEV CM include: four flight critical computers for implementing dual fault-op tolerant processing, eight data interface units to collect and transmit data, two multifunction liquid crystal displays and two control panel sets to provide a crew interface for system status and command input, and two sets of translational/rotational/throttle hand controllers to provide manual vehicle flight control. Masses for CCDH components are derived from estimates for X–38 or commercially available hardware.

Guidance and navigation comprises the equipment needed to provide on-orbit vehicle attitude information for the CEV, perform vehicle guidance and navigation processing, and execute AR&D. This includes an integrated Global Positioning System (GPS)/Inertial Navigation System (INS), including four space-integrated GPS/INS units, one GPS combiner unit and four GPS antennas; two star trackers; and two video guidance sensors and two Three-Dimensional (3–D) scanning Laser Detection and Ranging (LADAR) units to provide AR&D capability.

The communications and tracking subsystem consists of the equipment for the CEV CM to provide communications and tracking between other architecture elements and to the ground. Information on the communication links will include command, telemetry, voice, video, and payload data. Assumed communications components are: S-band/Search and Rescue Satellite-aided Tracking (SARSAT)/Ultrahigh Frequency Television (UHF) communications systems, network signal processors, information storage units, a Television (TV)/video system, an operations recorder, and a digital audio system. A high data rate Ka-band communications system is included on the SM.

Avionics instrumentation for the CEV CM consists of instrumentation to collect spacecraft health data and includes 120 sensor clusters at 0.29 kg per cluster.

Environment
The CEV environment components consist of the equipment needed to maintain vehicle health and a habitable volume for the crew and include the following:

- Environmental Control and Life Support (ECLS);
- Active Thermal Control System (ATCS); and
- Crew accommodations.

Environmental Control and Life Support (ECLS)
Items included in ECLS are nitrogen storage, oxygen storage, atmosphere supply and control, atmosphere contaminant control, fire detection and suppression, venting and thermal conditioning, water management, and Extra-Vehicular Activity (EVA) umbilicals and support. The assumed cabin pressure for the lunar CEV CM is 65.5 kPa (9.5 psia) with nitrogen and oxygen partial pressures of 43.90 kPa (67 percent) and 19.65 kPa (30 percent), respectively.

The CM includes the atmosphere gases needed for a nominal 13.3 days of crew time in the CEV. Thirty-two (32) kg of Gaseous Nitrogen (GN2) for cabin atmosphere makeup is stored in two cylindrical 5,000 psia graphite composite overwrapped Inconel 718-lined tanks with outer diameters of 0.39 m and lengths of 0.66 m. GOX for one full contingency cabin atmosphere repressurization and nominal crew metabolic consumption (0.8 kg per crew member per day) is stored in the four primary RCS oxygen tanks.

Environment atmosphere supply and control includes the components needed to regulate and distribute oxygen and nitrogen, monitor and control atmospheric pressure, and provide atmosphere relief and venting. Masses and volumes for these items are taken directly from the Space Shuttle Operations Data Book.

The chosen systems to provide atmosphere contaminant control on the CEV CM are a combined regenerative Carbon Dioxide (CO2) and Moisture Removal System (CMRS) for CO2 control, ambient temperature catalytic oxidation (ATCO) for trace contaminant control, and O2/CO2 sensors for atmosphere contaminant monitoring. The mass for the CMRS is scaled from improved Shuttle Regenerative CO2 Removal System (RCRS) heritage data based on the required CO2 removal rate for six crew members, while masses for other atmosphere contaminant control are taken directly from Shuttle heritage components. The CMRS is internally redundant.

Fire detection and suppression on the CEV consists of smoke detectors, a fixed halon fire suppression system, and halon fire extinguishers. Masses and volumes for these components are taken directly from ISS heritage.

Atmosphere venting and thermal conditioning includes cabin fans, air ducting, and humidity condensate separators. Cabin fans and air ducting mass, power, and volumes are scaled from Shuttle data based on the CEV pressurized volume, while the humidity condensate separator is identical to that of the Shuttle.

For the CEV CM, water management includes the tanks and distribution lines necessary to hold potable water for crew consumption, water for the fluid evaporator system, and waste water. Four spherical metal bellows water tanks, pressurized with GN2, are sized to store the mission's potable water supply with a diameter of 0.47 m per tank. The tanks are similar to the Shuttle's potable water tanks and each hold 0.053 m^3 (3,217 in^3) or 53 kg of water. A single waste water tank stores up to 25 kg of waste water and is periodically vented to space. The waste water tank is identical in size and construction to the potable water tanks.

The final components in ECLS are the umbilicals and support equipment needed to support contingency EVAs and suited crew members inside the CEV CM. The assumed EVA method is for the four CEV crew members to don their launch and entry suits, fully depressurize the CEV cabin, and egress from the side or docking hatch in the same manner as was done in the Gemini or Apollo programs. Umbilicals connect the in-space suits to the CM life support

system. In the event of an unplanned cabin depressurization, the life support system must support the crew via EVA umbilicals until the internal atmosphere has been restored or the vehicle has returned to Earth. For this, a suit oxygen supply assembly and suit ventilation manifold system has been included.

Active Thermal Control System (ATCS)
Active thermal control for the CEV is provided by a single-loop propylene glycol fluid loop with a radiator and a fluid evaporator system. The fluid loop heat rejection system includes cold plates for collecting CM equipment waste heat, a cabin heat exchanger for atmosphere temperature control (sized for six crew members), a Ground Support Equipment (GSE) heat exchanger for vehicle thermal control while the CEV is on the launch pad, a Liquid-Cooled Ventilation Garment (LCVG) heat exchanger for suit cooling, fluid pumps, fluid lines, and radiator panels. A total heat load of 6.25 kW is assumed for the ATCS, with 5.0 kW collected by the internal cold plates, 0.75 kW collected by the cabin air heat exchanger, and 0.5 kW collected by external cold plates (if necessary). The GSE heat exchanger transfers 6.25 kW of vehicle heat to the ground.

The assumed working fluid for the fluid loop system is a 60 percent propylene glycol/40 percent water blend, selected for its low toxicity and freeze tolerance. Two continuous single-phase fluid loops pump the propylene glycol/water blend through the cabin cold plates and heat exchangers, exit the pressure vessel to external cold plates (if necessary), and finally pump the fluid to the SM radiators where the heat is radiated away. The loop temperature is 308 K prior to entering the radiator and 275 K after exiting. Each loop contains two pumps, with one primary and one backup pump package, and each loop is capable of transporting the entire 6.25 kW heat load. The CEV CM portion of the TCS includes the mass and volume for the pumps, cold plates, lines, and heat exchangers, while the radiators are mounted on the structure of the SM.

The ATCS for the CEV CM also includes a dual-fluid evaporator system to handle peak heating loads in excess of the 6.25 kW maximum capacity of the fluid loop and to reject up to 6 kW of CM waste heat for the 2.25 hours from SM separation to landing. The fluid evaporator system operates by boiling expendable water or Freon R–134A in an evaporator to cool the heat rejection loop fluid, which is circulated through the walls of the evaporator. Generated vapor is then vented overboard. A dual-fluid system for the CEV is required because water does not boil at ATCS fluid loop temperatures and atmospheric pressures found at 100,000 ft or less; therefore, the nontoxic fluid Freon R–134A is used for vehicle cooling from that altitude to the ground. The Apollo Command Module did not provide cooling after water boiling became ineffective; however, that may not be appropriate for the CEV since the vehicle lands on land (i.e., the Command Module relied in part on the water landing for post-landing cooling), the CEV is nominally reusable (i.e., the Command Module was expendable), and the assumed heat load is higher. The mass estimate for the fluid evaporator system is based on the Shuttle Fluid Evaporator System (FES), scaled linearly using the heat capacity of that system. FES water is stored with the ECLSS potable water supply, while Freon R–134A is stored in a single 0.47–m diameter metal bellows tank.

Crew Accommodations

The crew accommodations portion of the CEV CM includes a galley, a Waste Collection System (WCS), Cargo Transfer Bags (CTBs) for soft stowage, and seats. For the galley, a water spigot and Shuttle-style food warmer are included to prepare shelf-stable and freeze-dried packaged foods. The mass for these items is taken from Shuttle heritage equipment. The CEV galley also includes accommodations for cooking/eating supplies and cleaning supplies, which are estimated at 0.5 kg per crew member and 0.25 kg per day, respectively.

The assumed WCS for the CM is a passive Mir Space Station-style toilet/commode with appropriate supplies, a privacy curtain, and contingency waste collection bags. In the Mir-style commode, wastes are deposited in a bag-lined can with a suitable user interface. The bags can then be individually isolated and stored in an odor control container. Alternate methods for waste collection could include urine collection devices (Shuttle), bags (Apollo), an active WCS (Shuttle), or personal urine receptacles.

CTBs are used on the CEV to provide soft stowage capability for crew accommodations equipment. Each CTB holds 0.056 m^3 (2 ft^3) of cargo and 26 bags are required for the vehicle.

For seats, four removable/stowable crew couches are included on the CEV CM for launch and landing with 10 inches of seat stroking under the seats for impact attenuation. Specifically, the seats stroke 10 inches at the crew member's feet, 5 inches at the head, 5 inches above the crew member, and 5.5 inches to the sides. The mass for the crew couches, taken from the Apollo Command Module, is scaled by 133 percent to accommodate a fourth crew member.

Other

CEV CM components included in the "Other" category are:

- Parachutes,
- Parachute structure and release mechanisms,
- Shell heaters,
- Landing airbags,
- Water flotation system,
- Doors and hatches, and
- Docking mechanism.

The CEV CM parachute system is comprised of three round main parachutes, two drogue parachutes, three pilot parachutes, and parachute structure and release mechanisms. Parachutes are packed between the CM pressure vessel and OML near the CEV docking mechanism. The three main parachutes, 34 m (111 ft) in diameter each, are sized to provide a nominal landing speed of 24 ft/s with all three parachutes deployed and a landing speed of 29.5 ft/s with one failed parachute. Main parachutes deploy at a dynamic pressure of 30 psf (10,000 ft altitude and 126 mph sink rate) and have a CM suspended mass of 8,654 kg. The two drogue parachutes, 11 m (37 ft) in diameter, stabilize and decelerate the CEV CM from a deployment dynamic pressure of 78 psf (23,000 ft altitude and 252 mph) to the main parachute deployment at 30 psf. Each drogue parachute is individually capable of slowing the CEV to the desired main parachute deployment sink rate. Once that dynamic pressure is reached, the drogue parachutes are pyrotechnically severed and the main parachutes are simultaneously deployed by the three pilot parachutes. Finally, mass is included in the CEV CM for parachute structure and release mechanisms. This mass is estimated as a fixed percentage (22.5 percent) of the main, drogue, and pilot parachute total mass.

The chosen landing mode for the CEV CM is a land landing with four inflatable Kevlar airbags for impact attenuation. Prior to touchdown, the CM aft heat shield is jettisoned and the airbags are inflated with compressed nitrogen gas. The airbags, which are mounted between the pressure vessel and aft heat shield, include both inner and outer bags, with the outer bags deflating after impact while the inner airbags remain inflated for landing stability. Airbags are sized for a worst-case impact speed of 29.5 ft/s with one failed main parachute. The total impact attenuation system includes the airbags, the airbag inflation system, and airbag controls. One cylindrical high-pressure GN2 tank identical to the ECLSS nitrogen tanks holds the gas used for inflating the airbags, with the tank having an outer diameter of 0.39 m and total length of 0.66 m. The four airbags have a stowed volume of 0.095 m^3 at a packing density of 498 kg/m^3.

A water flotation system is also included in the CEV CM to assure proper vehicle orientation in the event of a water landing. The flotation system allows the CM to self-right for safe vehicle and crew extraction by recovery forces.

The CEV CM also includes miscellaneous doors and hatches for crew access and vehicle servicing. An ingress/egress hatch provides a means for vehicle entry and exit while the vehicle is on the launch pad and is identical in size and mass to the Apollo Command Module hatch (29 inches x 34 inches). As part of the LIDS mechanism, a 32-inch docking adapter hatch provides a secondary egress path from the vehicle and is the means for pressurized crew transfer between two spacecraft. The CEV also includes two passive vent assemblies for purge, vent, and thermal conditioning of enclosed unpressurized vehicle compartments. Finally, umbilical and servicing panels allow for fluid loading on the launch pad.

The other CEV CM component assumed in this category is the androgynous LIDS mechanism for mating with the ISS and other exploration architecture elements. The LIDS on the CEV includes the docking mechanism and LIDS avionics. A flight-qualified LIDS has an estimated mass of 304 kg.

Growth
A 20 percent factor for potential vehicle mass growth is included here, applied to all dry mass components.

Non-Cargo
Non-cargo for the CEV CM consists of the following components:

- Personnel,
- Personnel provisions, and
- Residual propellant.

The CEV CM is capable of carrying four persons to the Moon for lunar exploration missions. A mass estimate for a crew of four is included in the vehicle, assuming the mass (100 kg) of a 95th percentile male crew member.

CEV personnel provisions for the DRM include the following:

- Recreational equipment consists of crew preference items and is estimated at 5 kg per crew member;
- Crew health care includes basic medical, dental, and surgical supplies, and four emergency breathing apparatuses;

- Personal hygiene includes basic hygiene kits and consumables for the mission;
- Clothing includes multiple clothing sets for the four crew members at 0.46 kg per crew member per day;
- Housekeeping supplies include a vacuum, disposable wipes for spills, and trash bags;
- Operational supplies include basic operational supplies estimated at 5 kg per crew member; CEV CM lighting (10 kg); zero-g restraints (12 kg); emergency egress kits for pad aborts at 2.3 kg per crew member; a sighting aid kit for dockings including a Crew Optical Alignment Sight (COAS), binoculars, spotlights, etc. (13 kg); and a crew survival kit including beacons, transponders, a life raft, etc. (44 kg);
- Maintenance equipment includes a basic Shuttle-style in-flight maintenance toolkit;
- Sleep accommodations are zero-g sleep aids estimated at 2.3 kg per crew member;
- EVA suits and spares include Gemini-style launch and entry suits capable of performing emergency EVAs. The assumed EVA mode for the CEV CM is to fully depressurize the CEV pressure vessel with all four crew members donning their EVA suits. Each suit is estimated at 20 kg per crew member; and
- Food for the crew is estimated at 1.8 kg per crew member per day.

Residual propellant on the CEV CM is the trapped ethanol and GOX propellant remaining in the propulsion tanks after completion of the nominal delta-V maneuvers. Residuals for RCS propellants are 2 percent of the nominally consumed propellant. Pressurant is the GHe needed to pressurize the ethanol primary RCS tanks.

Cargo
Cargo for the CEV CM consists of the following components: Ballast.

Ballast mass is included in the CEV CM to ensure a proper vehicle CG location prior to atmospheric entry. The ultimate ballast mass requirement will be the product of a detailed aerodynamic and vehicle mass properties study, but a placeholder mass of 100 kg is included in the CEV CM mass estimate until such analyses can be completed.

Non-Propellant
Non-propellant for the CEV CM consists of the following components:

- Oxygen,
- Nitrogen,
- Potable water, and
- FES water and freon.

Oxygen gas is included in the CEV for breathing gas makeup, contingency EVA consumption, atmosphere leakage and venting, and one contingency full-cabin repressurization. The total oxygen mass requirement is estimated at 64 kg for the lunar mission. An alternative to storing oxygen in the CM would be to use the service propulsion system/RCS oxygen tanks in the SM for shared storage; however, that option was not pursued since the CM primary RCS oxygen tanks provide a convenient source of high-pressure GOX.

The amount of nitrogen gas required for the CEV CM atmosphere is estimated using assumptions for cabin leak rate (0.15 kg/day), waste management and regenerative CO2 system venting, and the number of full-cabin repressurizations (one). A nitrogen partial pressure of 43.9 kPa is assumed, with a total cabin pressurized volume of 29.4 m^3 and cabin temperature of 21°C, for a total nitrogen mass requirement of 32 kg.

CM potable water requirements are estimated to supply (1) water for Intra-Vehicular Activity (IVA) crew water usage, (2) EVA water for contingency EVAs, and (3) water for the CEV CM's water evaporator system. IVA crew water usage for drinking water, food preparation water, and hygiene water is included at a consumption rate of 3.5 kg per crew member per day, with 53 crew-days required for the mission. Consumable water is also included for the ATCS's FES, which is sized to reject 37,800 kJ of heat (35,827 Btu) from the time of SM separation to 100,000 ft. FES water requirements are estimated assuming a heat of vaporization of 2,260 kJ/kg and 20 percent margin for consumables.

Once the CEV reaches an altitude where water boiling is no longer effective, the FES switches to using freon R–134A for cooling. The Freon consumable mass is sized to reject 10,800 kJ of heat (10,236 BTU) from 100,000 ft to post-landing vehicle shutdown. FES freon requirements are estimated assuming a heat of vaporization of 216 kJ/kg and 20 percent margin for consumables.

Propellant
Propellant for the CEV CM consists of the following components: Used RCS propellant.

Primary RCS propellant on the CEV CM is used to reorient the vehicle to a proper attitude for entry and, during atmospheric flight, the RCS provides roll torque to control the direction of the CM lift vector and counteract induced spin torques, provides dampening of induced pitch and yaw instabilities, and corrects range dispersions during skip-out portions of a lunar skip return trajectory. The assumed delta-V for these maneuvers is 10 m/s for entry maneuvering and 40 m/s for skip-out error corrections, with a thruster Isp of 274 sec and initial vehicle mass prior to entry of 9,599 kg. The CEV CM mass includes 100 kg of samples returned from the lunar surface.

The backup RCS propellant is used to reorient the vehicle to a proper trim attitude and induce a roll moment for the emergency ballistic down mode.

5.2.3.2 Lunar CEV SM

5.2.3.2.1 Vehicle Description

The Lunar CEV SM is included in the ESAS exploration architecture to provide major translational maneuvering capability, power generation, and heat rejection for the CEV CM. The SM assumes an integrated pressure-fed oxygen/methane service propulsion system and RCS to perform rendezvous and docking with the LSAM in Earth orbit, any contingency plane changes needed prior to lunar ascent, TEI, and self-disposal following separation from the CM. One 66.7 kN (15,000 lbf) service propulsion system and twenty-four 445 N (100 lbf) RCS thrusters, systems common to both the SM and the LSAM ascent stage, are used for on-orbit maneuvering. The SM propellant tanks are sized to perform up to 1,724 m/s for the service propulsion system and 50 m/s of RCS delta-V with the CEV CM attached and 15 m/s of RCS delta-V after separation. In the event of a late ascent abort off the CLV, the SM service propulsion system may also be used for separating from the LV and either aborting to near-coastline water landings or aborting to orbit.

Two deployable, single-axis gimbaling solar arrays are also included to generate the necessary CEV power from Earth-Orbit Insertion (EOI) to CM–SM separation prior to entry. For long-duration outpost missions to the lunar surface, lasting up to 180 days, the CEV remains unoccupied in lunar orbit. Solar arrays were selected instead of fuel cells or other similar power generation options because the reactant mass requirements associated with providing keep-alive power during the long dormant period for fuel cells became significantly higher than the mass of a nonconsumable system such as solar arrays. The solar arrays use state-of-the-art three-junction Photovoltaic (PV) cells. Finally, the SM composite primary structure also provides a mounting location for four radiator panels. These panels provide heat rejection capability for the CEV fluid loop heat acquisition system.

Illustrations of the reference lunar CEV SM are shown in **Figure 5-6**.

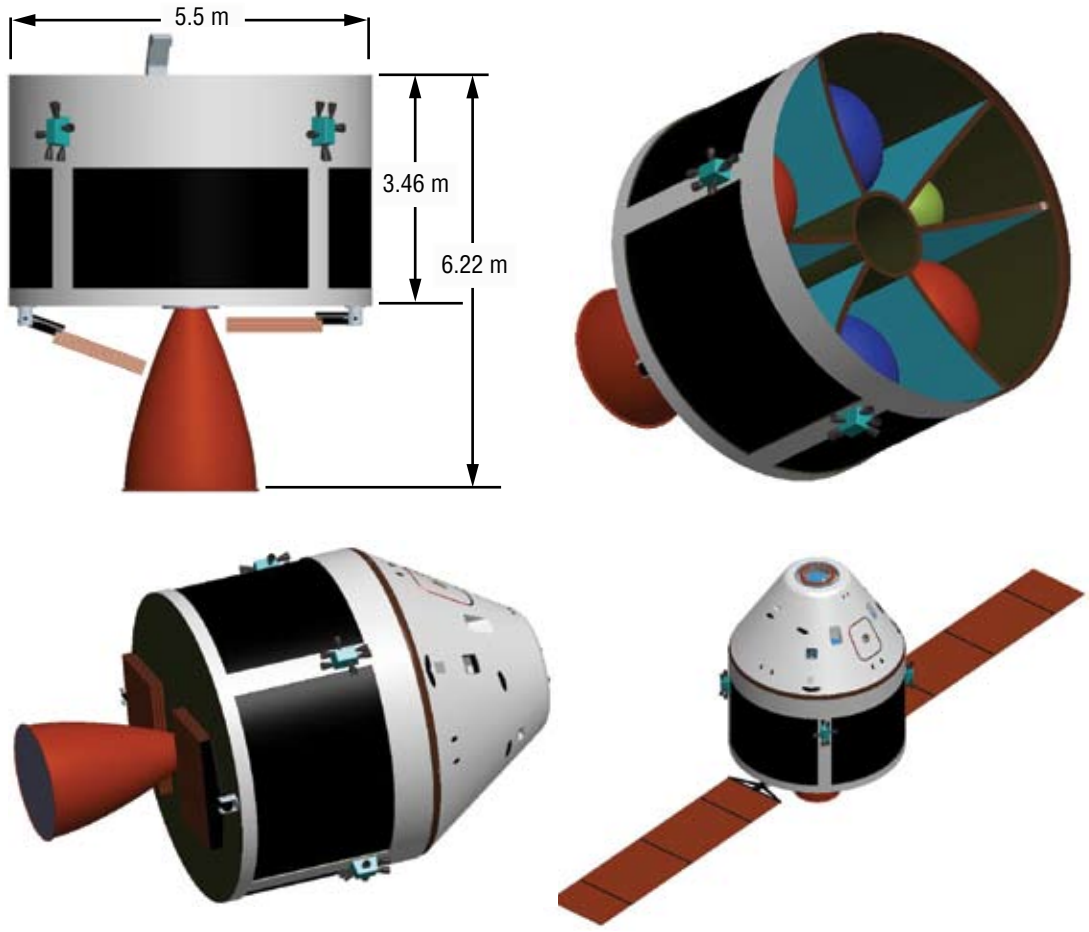

Figure 5-6. Reference Lunar CEV SM

5.2.3.2.2 Overall Mass Properties

Table 5-2 provides overall vehicle mass properties for the SM used for the lunar exploration mission. The mass properties reporting standard is outlined in JSC-23303, Design Mass Properties. A detailed mass statement is provided in **Appendix 5A**, **CEV Detailed Mass Breakdowns**.

Lunar SM	% of Vehicle Dry Mass	Mass (kg)	Volume (m^3)
1.0 Structure	20%	819	0
2.0 Protection	4%	167	1
3.0 Propulsion	36%	1,423	1
4.0 Power	10%	417	1
5.0 Control	0%	0	0
6.0 Avionics	3%	117	1
7.0 Environment	2%	98	4
8.0 Other	7%	290	2
9.0 Growth	17%	666	2
10.0 Non-Cargo		579	3
11.0 Cargo		0	1
12.0 Non-Propellant		0	0
13.0 Propellant		9,071	0
Dry Mass	**100%**	**3,997 kg**	
Inert Mass		**4,576 kg**	
Total Vehicle		**13,647 kg**	

Table 5-2. Overall Vehicle Mass Properties for the SM for the Lunar Exploration Mission

5.2.3.2.3 Subsystem Description

Structure

The CEV SM structure includes vehicle primary structure and consists of the following component: Unpressurized structure.

The CEV SM unpressurized structure provides structural attachment for the CEV power, avionics, and propulsion system components, a mounting location for body-mounted thermal control radiator panels, and an interface for mating to the CEV LV. An SM external diameter of 5.5 m was selected, equal to the diameter of the CEV CM, and the vehicle has a length for the primary structure of 3.46 m. SM structure length was driven by the length of the internal propellant tanks and required acreage for mounting four radiator panels.

The CEV SM is a semimonocoque structure, similar in design and construction to the Apollo SM. Graphite epoxy/BMI composites were selected as the structural material for mass savings, though several aluminum alloys, such as Al 2024 or Al-Li 8090, may also be considered. The mass-estimating method used for composite unpressurized structure mass in this assessment was to assume a power law relationship based on the external surface area of the SM, which is 59.8 m^2. The assumed equation for composites was: Mass = 6.6515 * (surface area)1.1506, where surface area is given in square meters and mass is calculated in kilograms. Mass was further added to the primary structure estimate to account for dedicated tank support structure. This was estimated using a linear relationship of 0.008 kg of tank support structure per kilogram of wet tank mass.

Protection

The CEV SM protection consists of the materials dedicated to providing passive spacecraft thermal control during all mission phases, including ascent and in-space operations, and includes the following component: Internal insulation

The CEV SM contains insulation blankets for passive thermal control. The mass-estimating method used for internal insulation was to assume insulation wrapped around the SM external surface area at a mass penalty of 2 kg/m^2. The unpressurized structure external surface area, including the sidewalls and base heat shield, is 83.6 m^2.

Propulsion

The CEV SM propulsion consists of an integrated service propulsion system/RCS and includes the following components:

- Service propulsion system,
- RCS thrusters,
- Service propulsion system and RCS fuel/oxidizer tanks, and
- Service propulsion system and RCS pressurization system.

The SM propulsion for performing major CEV translational and attitude control maneuvers is a pressure-fed integrated service propulsion system/RCS using LOX and Liquid Methane (LCH4) propellants. This propellant combination was selected for its relatively high Isp, good overall bulk density, space storability, nontoxicity, commonality with the LSAM, and extensibility to In-Situ Resource Utilization (ISRU) and Mars, among other positive attributes. A pressure-fed integrated service propulsion system/RCS was selected for its simplicity, reliability, and lower development cost over other comparable systems. Other tradable propellants for the CEV SM might include bipropellants such as NTO/MMH, LOX/Liquid Hydrogen (LH2), and several other LOX/hydrocarbon propellants such as ethanol or propane. Alternative system configurations might be nonintegrated versus integrated service propulsion system/RCS, pump-fed versus pressure-fed service propulsion system, and common service propulsion system/RCS propellants versus dissimilar service propulsion system/RCS propellants.

The EIRA uses CEV propulsion to rendezvous with the LSAM in LEO, perform any plane changes associated with an emergency anytime return on ascent, and return to Earth from lunar orbit regardless of orbital plane alignment. The assumed delta-Vs for these maneuvers are described below in the CEV SM propellant section.

A single fixed (non-gimbaling) oxygen/methane pressure-fed service propulsion system is included on the SM to perform major translational maneuvers while on-orbit or late-ascent orbits from the LV are necessary. The engine has a maximum vacuum thrust and Isp of 15,000 lbf (66.7 kN) and 363.6 sec, respectively. The regeneratively cooled engine operates at a chamber pressure of 225 psia and an oxygen/methane mixture ratio of 3.6:1 by mass, and has a nozzle expansion ratio of 150:1. The calculated total engine length is 3.41 m, the nozzle length is 2.76 m, and the nozzle exit diameter is 2.01 m. All engine parameters are subject to future optimization trades.

Twenty-four oxygen/methane pressure-fed RCS thrusters are also included for vehicle attitude control and minor translational maneuvers such as terminal approach during rendezvous and docking. Each engine has a maximum vacuum thrust and Isp of 100 lbf (445 N) and 317.0 sec, respectively. The RCS thrusters are film-cooled, operate at chamber pressures and mixture ratios of 125 psia and 3.6:1, and have nozzle expansion ratios of 40:1. As the RCS thrusters operate on liquid propellants, they are able to perform long steady-state burns as a service propulsion system backup, albeit at lower Isp.

Service propulsion system and RCS oxygen/methane propellants are stored in four tanks constructed with Al-Li 2090 liners and graphite epoxy composite overwrappings, with two tanks dedicated per fluid. Each oxygen tank holds 3.49 m^3 or 3,706 kg of subcooled oxygen at a nominal tank pressure of 325 psia and Maximum Expected Operating Pressure (MEOP) of 406 psia. The tanks are cylindrical with external dimensions of 1.80 m for diameter, 2.21 m for overall length, and 0.76 m for dome height. Each methane tank holds 2.63 m^3, or 1,033 kg, of subcooled fluid, has a nominal pressure and MEOP of 325 and 406 psia, respectively, and is cylindrical with external dimensions of 1.80 m for diameter, 1.81 m for overall length, and 0.76 m for dome height.

Oxygen and methane are stored entirely passively on the CEV SM. Each tank includes 60 layers of variable density Multilayer Insulation (MLI) with a total thickness of 0.041 m and a 0.025-m layer of Spray-on Foam Insulation (SOFI), which reduces the average heat leak rate per tank for oxygen and methane to 0.15 and 0.14 W/m^2, respectively. A passive thermodynamic vent system is provided on the tank to periodically vent vaporized propellants. Cryocoolers could be included in the propulsion system to remove the tank heat leak and eliminate propellant boil-off, though such a system would require power and thermal control and would increase tank cost and complexity.

The assumed pressurization system for the SM propellant tanks is GHe stored in two Inconel 718-lined, graphite epoxy composite-overwrapped 6,000 psia tanks. As propellant is consumed, the GHe is distributed to the oxygen/methane tanks to maintain a propellant tank pressure of 325 psia. To minimize helium tank size, the tanks are thermodynamically coupled to the LCH4 tank, thus reducing the helium temperature while stored to 112 K. Each helium tank is spherical with an outer diameter of 1.03 m and holds 86.2 kg of helium.

Power

The power subsystem for the CEV SM encompasses the power generation function for the CEV and includes the following components:

- Triple-junction Gallium Arsenide (GaAs) solar arrays,
- Electrical power distribution, and
- PCUs.

Two 17.9 m^2 (193 ft^2) triple-junction GaAs solar arrays provide CEV power during LEO and lunar orbit operations and during transfer between Earth and the Moon. Each solar array wing is sized to generate the full CEV average power requirement of 4.5 kW with various losses at array end-of-life. Those losses, which include a 90 percent Power Management and Distribution (PMAD) efficiency, 180-day on-orbit lifetime with 2.5 percent degradation per year, 15-deg Sun pointing loss, and 15 percent inherent array degradation, result in arrays theoretically capable of generating 6,167 W in laboratory conditions, assuming a 26 percent maximum conversion efficiency. The beginning-of-life power generation per panel once the CEV is on orbit is 5,242 W. The solar array system includes two array panels, deployment mechanisms, single axis drive actuators, and Sun sensors. Charge control and power conditioning units for the arrays are integrated into the PCUs on the CEV CM. Array system mass for the CEV was estimated for each individual component. Array panel mass was estimated using the array area (17.9 m^2) and a mass scaling factor for state-of-the-art triple-junction GaAs arrays, while other solar array system components were assumed to have masses independent of array power level.

The SM electrical power distribution and control system collects power generated by the solar arrays and distributes it as 28 VDC power to SM loads and the CM power distribution system. CEV average power for the entire mission is 4.5 kW, with the SM distribution system capable of handling a peak power of 8 kW. The wiring harness for the electrical power distribution system consists of primary distribution cables, secondary distribution cables, jumper cables, data cabling, RF coaxial cable, and miscellaneous brackets, trays, and cable ties. Mass for the entire SM wiring harness is estimated at 164 kg.

PCUs on the CEV SM monitor and control power from the solar arrays and distribute power among the vehicle loads. A PCU includes relays, switches, current sensors, and bus interfaces necessary to control and distribute power. There are two units (one primary and one backup) included in the CEV SM, with each unit capable of switching 160 amps at 28 VDC continuously (4,500 W) or 285 amps at 28 VDC over a short duration (8,000 W). PCUs have an estimated mass of 41.1 kg each.

Control

Items typically included in the spacecraft control category are aerodynamic control surfaces, actuators, cockpit controls such as rudder pedals, and others. There are no control components on the CEV SM.

Avionics

The CEV SM avionics subsystem transmits health data and commands between SM components and the CM CCDH system. SM avionics consist of the following components:

- CCDH,
- Communications, and
- Instrumentation.

CCDH on the SM includes four data interface units to collect and transmit health and status data from other SM components. Masses for data interface units are derived from estimates for other commercially available components. A 30 percent installation factor is also included.

The SM also includes a high-gain Ka-band phased array antenna system for sending and receiving high data rate information between Earth and the CEV, though the decision to locate the antenna on the CM or SM is an ongoing trade. The Ka-band antenna is currently mounted near the base (engine) of the SM structure.

Avionics instrumentation for the CEV SM includes 40 sensor clusters at 0.29 kg per cluster.

Environment

The CEV environment components consist of the equipment needed to maintain vehicle health and a habitable volume for the crew and include the following on the SM: ATCS.

Active Thermal Control System (ATCS)

Active thermal control for the CEV is provided by a single-loop propylene glycol fluid loop with radiator and an FES. All ATCS components are mounted in the CM, with the exception of the radiator panels that are mounted on the SM body structure. There are four radiator panels on the SM, each centered 90 deg apart with an area of 7.0 m^2 per panel. The radiator was sized assuming a fluid loop temperature of 275 K exiting the radiator and 308 K entering the radiator. In a worst-case vehicle attitude, two panels are viewing the Sun and two panels are out-of-Sun with a radiation sink temperature of 100 K. The maximum radiator heat load is 8.0 kW.

The assumed coating for the radiator is 10 mil silver-Teflon with a maximum absorptivity of 0.094 and emissivity of 0.888. Radiator panel mass is estimated using total panel area and a radiator mass penalty per unit area of 3.5 kg per m^2.

Other
CEV SM components included in the "Other" category are:

- CEV CM/SM attachment,
- Pyrotechnic separation mechanisms, and
- Doors and hatches.

The CEV CM/SM attachment includes structural mass for physically mating the two vehicles and umbilical lines for sharing power, fluid, and data across the vehicle interface. Mass for this component is estimated by scaling the mass for the Apollo Command Module/SM attachment system. Also included in this category are pyrotechnic separation mechanisms for initiating a mechanical separation of the two vehicles or other SM components. A mass placeholder of 100 kg is included pending further refined analysis.

The SM also includes two passive vent assemblies for purge, vent, and thermal conditioning of enclosed unpressurized vehicle compartments. Umbilical and servicing panels on the SM allow for fluid loading on the launch pad.

Growth
A 20 percent factor for potential vehicle mass growth is included here, applied to all dry mass components.

Non-Cargo
Non-cargo for the CEV SM consists of the following components:

- Residual propellant,
- Propellant boil-off, and
- Pressurant.

Residual propellant on the CEV SM is the trapped oxygen and methane propellant left in the propulsion tanks after completion of the nominal delta-V maneuvers. Residuals for liquid propellants are 2 percent of the nominally consumed propellant.

The LOX and LCH4 used for the SM service propulsion system and RCS are stored entirely passively (i.e., with foam and MLI only); therefore, as heat leaks into the propellant tanks, the cryogenic fluids will slowly vaporize. Vaporized propellant, or boil-off, is vented as it is produced to maintain a nominal tank pressure. Boil-off mass is calculated assuming 60 layers of variable-density MLI per tank and SOFI, a 210 K external environment temperature, and the appropriate heats of vaporization for oxygen and methane.

The assumed pressurization system for the SM propellant tanks is GHe stored in two 6,000 psia tanks. As propellant is consumed, the GHe is distributed to the tanks to maintain a propellant tank pressure of 325 psia. To minimize helium tank size, the tanks are thermodynamically coupled to the LCH4 tank, thus reducing the helium temperature while stored to 112 K.

Cargo
There are no cargo components included on the CEV SM.

Non-Propellant
There are no non-propellant components included on the CEV SM. All non-propellant fluids are stored on the CM.

Propellant
Propellant for the CEV SM consists of the following components:

- Used service propulsion system fuel propellant,
- Used service propulsion system oxidizer propellant,
- Used RCS fuel propellant, and
- Used RCS oxidizer propellant.

CEV total SM service propulsion system/RCS propellant is calculated for four major delta-V maneuvers in the mission. For each maneuver, the assumed service propulsion system Isp is 363.6 sec and the RCS Isp is 317.0 sec.

- The first major maneuver is rendezvous and docking with the LSAM in LEO. The CEV is inserted by the LV upper stage into a 55- x 185-km (30- x 100-nmi) elliptical orbit, while the LSAM and EDS are loitering in a 296-km (160-nmi) circular orbit. The CEV will then rendezvous with the LSAM and dock. The required delta-V for rendezvous and docking is estimated at 119.4 m/s for the service propulsion system and 25.1 m/s for the RCS, while the initial CEV mass prior to the maneuver is 23,149 kg.
- The second major maneuvers are station-keeping in LLO while the crew is on the surface and a contingency 5-deg plane change in the event of a worst-case anytime ascent from a 85-deg latitude landing site. The required delta-V for station-keeping is estimated at 15 m/s for RCS and 156 m/s of service propulsion system delta-V is included for the plane change. The initial CEV mass prior to these maneuvers is 21,587 kg.
- The third major CEV maneuver is TEI from LLO. For a worst-case anytime return from a polar orbit, a 90-deg plane change may first be needed to align the spacecraft's velocity vector with the V-infinity departure vector. The method chosen to accomplish this maneuver is to use a sequence of three impulsive burns, where the first burn raises the CEV orbit apolune from a 100-km orbit to an orbit with a period of 24 hours. The CEV coasts to the correct position to perform the 90-deg plane change and then coasts to perilune to complete TEI. The required delta-V for TEI is estimated at 1,449 m/s for the service propulsion system. This maneuver also includes +/– 90-deg control of the arrival coazimuth at Earth and +/–12-hr control of the nominal 96-hr return time from the third TEI burn. The initial CEV mass prior to the maneuver is 21,057 kg.
- The fourth maneuver is a 10-m/s mid-course correction using an RCS. This is used to correct any errors resulting from an imprecise TEI burn. The initial CEV mass prior to the maneuver is 14,023 kg.
- The fifth and final SM maneuver is to safely dispose of the SM after CM separation. The required RCS delta-V for disposal is 15 m/s, and the initial SM mass prior to the burn is 4,372 kg.

5.2.3.3 Launch Abort System (LAS)

The LAS was sized to pull the CEV CM away from a thrusting LV at 10 g's acceleration. The LAS sizing concept is similar to the Apollo Launch Escape System (LES) in that it is a tractor system that is mounted ahead of the CM. The main difference is that the exhaust nozzles are located near the top of the motor, which will reduce the impingement loads on the CM.

The LAS features an active trajectory control system based on solid propellant, a solid rocket escape motor, forward recessed exhaust nozzles, and a CM adaptor. The motor measures 76 cm in diameter and 5.5 m in length, while eight canted thrusters aid in eliminating plume impingement on the CM. A star fuel grain minimizes motor size and redundant igniters are intended to guarantee the system's start.

The LAS provides abort from the launch pad and throughout powered flight of the booster first stage. The LAS is jettisoned approximately 20–30 seconds after second stage ignition. Further analyses are required to determine the optimum point in the trajectory for LAS jettison. After the LAS is jettisoned, launch aborts for the crew are provided by the SM propulsion system.

The mass for a 10-g LAS for a 21.4 mT CM is 4.2 mT. **Figure 5-7** depicts the LAS on top of the CM.

Figure 5-7. CEV with Launch Abort System

5.2.4 ISS CEV CM (3 Crew with 400 kg Cargo)

5.2.4.1 Vehicle Description

The ISS CEV CM in the ESAS architecture is the Block 1 variant of the lunar CM designed to rotate three to six crew members and cargo to the ISS. The ISS CM is designed largely to support lunar exploration requirements, with a minimal set of modifications made to support ISS crew rotation. Initial mass for the three-crew ISS CM variant is 162 kg less than the lunar CM mass, with the assumed system modifications listed below:

- Removed EVA support equipment for one crew member (–3 kg);
- Sized galley, waste collection consumables, and soft stowage for 18 crew-days instead of 53 crew-days (–19 kg);
- Removed one crew member and sized personnel provisions for 18 crew-days (–238 kg);
- Added ISS cargo (+400 kg);
- Sized oxygen, nitrogen, and potable water for 18 crew-days (–156 kg);
- Sized RCS propellant for smaller vehicle mass and lower delta-V (–145 kg); and
- Less growth allocation for lower vehicle dry mass (–4 kg).

5.2.4.2 Overall Mass Properties

Table 5-3 provides overall vehicle mass properties for the ISS crewed variant of the CEV CM. The mass properties reporting standard is outlined in JSC-23303, Design Mass Properties. A detailed mass statement is provided in **Appendix 5A**, **CEV Detailed Mass Breakdowns**.

Table 5-3. Vehicle Mass Properties for the ISS Crewed Variant of the CEV CM

ISS CEV CM (3 Crew + Cargo)	% of Vehicle Dry Mass	Mass (kg)	Volume (m^3)
1.0 Structure	24%	1,883	0
2.0 Protection	11%	894	1
3.0 Propulsion	5%	413	0
4.0 Power	10%	819	1
5.0 Control	0%	0	0
6.0 Avionics	5%	435	1
7.0 Environment	13%	1,069	3
8.0 Other	14%	1,159	2
9.0 Growth	17%	1,335	1
10.0 Non-Cargo		581	2
11.0 Cargo		500	1
12.0 Non-Propellant		211	0
13.0 Propellant		42	0
Dry Mass	**100%**	**8,008 kg**	
Inert Mass		**9,089 kg**	
Total Vehicle		**9,342 kg**	

5.2.4.3 Subsystem Description

5.2.4.3.1 Structure

The CEV CM structure is identical for the lunar and ISS variants because the lunar CM variant is already designed to withstand an internal cabin pressure of 14.7 psia.

5.2.4.3.2 Protection

The CEV CM spacecraft protection is identical for the lunar and ISS variants because the ISS CM variant uses the ablative aft heat shield designed for the lunar mission.

5.2.4.3.3 Propulsion

The CEV CM propulsion is identical for the ISS and lunar CM variants.

5.2.4.3.4 Power

The power subsystem for the CEV CM is identical for the ISS and lunar variants.

5.2.4.3.5 Control

Items typically included in the spacecraft control category are aerodynamic control surfaces, actuators, cockpit controls such as rudder pedals, and others. There are no control components on the CEV CM.

5.2.4.3.6 Avionics

The CEV CM avionics subsystem is identical for the ISS and lunar variants.

5.2.4.3.7 Environment

The CEV environment components consist of the equipment needed to maintain vehicle health and a habitable volume for the crew and include the following:

- ECLS,
- ATCS, and
- Crew accommodations.

Environmental Control and Life Support (ECLS)

The ISS CEV CM differs from the lunar variant only in that EVA umbilicals and support equipment are included for three crew members rather than four.

Active Thermal Control System (ATCS)

Active thermal control for the CEV is identical for the ISS and lunar variants.

Crew Accommodations

The crew accommodations portion of the CEV CM differs from the lunar variant in that galley equipment, waste collection, and stowage is provided for three crew members (18 crew-days) in the ISS variant versus four crew members (53.3 crew-days) in the lunar mission.

5.2.4.3.8 Other

CEV CM components included in the "Other" category, such as the parachute system, landing system, flotation system, and docking system, are identical for the ISS and lunar CM variants. The ISS CM uses a LIDS docking mechanism for docking to ISS rather than the Shuttle's Androgynous Peripheral Attachment System (APAS) mechanism.

5.2.4.3.9 Growth

Mass growth included on the CEV CM is sized for 20 percent of dry mass.

5.2.4.3.10 Non-Cargo

Mass for personnel and personnel provisions has been reduced on the ISS CM variant to reflect the smaller crew size (three versus four) and shorter mission duration (6 versus 13.3 days).

Residual propellant is estimated at 2 percent of the nominally consumed propellant for the ISS mission.

5.2.4.3.11 Cargo

Cargo for the ISS CEV CM differs from the lunar CM in that 400 kg of pressurized cargo has been added in place of the fourth crew member. The pressurized cargo in Mid-deck Locker Equivalents (MLEs) has a density of 272.7 kg/m^3. Ballast mass for the CM is unchanged at 100 kg.

5.2.4.3.12 Non-Propellant

Mass for oxygen, nitrogen, and potable water has been changed on the ISS CM variant to reflect the smaller crew size (three versus four), shorter mission duration (6 versus 13.3 days), and higher cabin pressure (14.7 versus 9.5 psia).

5.2.4.3.13 Propellant

Propellant for the ISS CEV CM is estimated using a lower delta-V (10 m/s versus 50 m/s), as the lunar skip-entry trajectory is not applicable to the ISS mission. The propellant loading has also changed due to the lower CM mass at entry with the ISS mission. The initial CM mass prior to the maneuver is estimated at 9,335 kg.

5.2.5 ISS CEV CM (Six Crew)

5.2.5.1 Vehicle Description

The ISS CEV CM in the ESAS architecture is the Block 1 variant of the lunar CM designed to rotate three to six crew members and cargo to ISS. The ISS CM is designed largely to support lunar exploration requirements, with a minimal set of modifications made to support ISS crew rotation. Initial mass for the six-crew ISS CM variant is 45 kg more than the lunar CM mass with the assumed system modifications listed below:

- Added EVA support equipment for two crew members (+6 kg);
- Sized galley, waste collection consumables, soft stowage, and seats for six crew and 36 crew-days instead of four crew and 53 crew-days (+31 kg);
- Added two crew members and sized personnel provisions for 36 crew-days (+219 kg);
- Sized oxygen, nitrogen, and potable water for 36 crew-days (–76 kg);
- Sized RCS propellant for larger vehicle mass and lower delta-V (–144 kg); and
- More growth allocation for higher vehicle dry mass (+8 kg).

5.2.5.2 Overall Mass Properties

Table 5-4 provides overall vehicle mass properties for the ISS crewed variant of the CEV CM. The mass properties reporting standard is outlined in JSC-23303, Design Mass Properties. A detailed mass statement is provided in **Appendix 5A**, **CEV Detailed Mass Breakdowns**.

Table 5-4. Vehicle Mass Properties for the ISS Crewed Variant of the CEV CM

ISS CEV CM (6 Crew)	% of Vehicle Dry Mass	Mass (kg)	Volume (m^3)
1.0 Structure	23%	1,883	0
2.0 Protection	11%	894	1
3.0 Propulsion	5%	413	0
4.0 Power	10%	819	1
5.0 Control	0%	0	0
6.0 Avionics	5%	435	1
7.0 Environment	14%	1,129	4
8.0 Other	14%	1,159	2
9.0 Growth	17%	1,346	2
10.0 Non-Cargo		1,038	4
11.0 Cargo		500	1
12.0 Non-Propellant		100	0
13.0 Propellant		43	0
Dry Mass	**100%**	**8,079 kg**	
Inert Mass		**9,217 kg**	
Total Vehicle		**9,551 kg**	

5.2.5.3 Subsystem Description

5.2.5.3.1 Structure

The CEV CM structure is identical for the lunar and ISS variants because the lunar CM variant is already designed to withstand an internal cabin pressure of 14.7 psia.

5.2.5.3.2 Protection

The CEV CM spacecraft protection is identical for the lunar and ISS variants because the ISS CM variant uses the ablative aft heat shield designed for the lunar mission.

5.2.5.3.3 Propulsion

The CEV CM propulsion is identical for the ISS and lunar CM variants.

5.2.5.3.4 Power

The power subsystem for the CEV CM is identical for the ISS and lunar variants.

5.2.5.3.5 Control

Items typically included in the spacecraft control category are aerodynamic control surfaces, actuators, cockpit controls such as rudder pedals, and others. There are no control components on the CEV CM.

5.2.5.3.6 Avionics

The CEV CM avionics subsystem is identical for the ISS and lunar variants.

5.2.5.3.7 Environment

The CEV environment components consist of the equipment needed to maintain vehicle health and a habitable volume for the crew and include the following:

- ECLS,
- ATCS, and
- Crew accommodations.

Environmental Control and Life Support (ECLS)

The ISS CEV CM differs from the lunar variant only in that EVA umbilicals and support equipment are included for six crew members rather than four.

Active Thermal Control System (ATCS)

Active thermal control for the CEV is identical for the ISS and lunar variants.

Crew Accommodations

The crew accommodations portion of the CEV CM differs in that galley equipment, waste collection, seating, and stowage is provided for six crew members (36 crew-days) in the ISS variant versus four crew members (53.3 crew-days) in the lunar mission.

5.2.5.3.8 Other

CEV CM components included in the “Other” category, such as the parachute system, landing system, flotation system, and docking system, are identical for the ISS and lunar CM variants. The ISS CM uses a LIDS docking mechanism for docking to the ISS rather than the Shuttle’s APAS mechanism.

5.2.5.3.9 Growth

Mass growth included on the CEV CM is sized for 20 percent of dry mass.

5.2.5.3.10 Non-Cargo

Mass for personnel and personnel provisions has been reduced on the ISS CM variant to reflect the larger crew size (six versus four) and shorter mission duration (6 versus 13.3 days).

Residual propellant is estimated at 2 percent of the nominally consumed propellant for the ISS mission.

5.2.5.3.11 Cargo

The six crew-to-ISS variant of the lunar CEV CM does not carry any cargo to ISS. Ballast mass for the CM is unchanged at 100 kg.

5.2.5.3.12 Non-Propellant

Mass for oxygen, nitrogen, and potable water has been changed on the ISS CM variant to reflect the greater crew size (six versus four), shorter mission duration (6 versus 13.3 days), and higher cabin pressure (14.7 versus 9.5 psia).

5.2.5.3.13 Propellant

Propellant for the ISS CEV CM is estimated using a lower delta-V than the lunar variant (10 m/s versus 50 m/s), as the lunar skip-entry trajectory is not applicable to the ISS mission. The propellant loading is also affected by the higher CM mass at entry with the ISS mission. The initial CM mass prior to the maneuver is estimated at 9,544 kg.

5.2.6 ISS Pressurized Cargo CEV CM Variant

5.2.6.1 Vehicle Description

The ESAS architecture also includes a variant of the ISS CEV CM that may be used to deliver several tons of pressurized cargo to the ISS without crew on board and return an equivalent mass of cargo to a safe Earth landing. This spacecraft is nearly identical to the ISS crew rotation variant, with the exception that the personnel and most components associated with providing crew accommodations are removed and replaced with cargo. Initial mass for the uncrewed ISS CM variant is 2,039 kg greater than the three-crew ISS crew rotation CM, with the assumed system modifications listed below:

- Removed atmosphere contaminant (CO2, etc.) control equipment (–165 kg);
- Removed EVA support equipment (–21 kg);
- Removed galley, WCS, and CTBs (–84 kg);
- Removed mass for personnel and personnel provisions (–580 kg);
- Removed 500 kg of ISS cargo and ballast, and added 3,500 kg of ISS cargo (+3,000 kg);
- Loaded oxygen, nitrogen, and water as needed for the pressurized cargo mission (–64 kg);
- Increased RCS propellant for higher vehicle mass (+8 kg); and
- Less growth allocation for lower vehicle dry mass (–54 kg).

5.2.6.2 Overall Mass Properties

Table 5-5 provides mass properties for the ISS pressurized cargo delivery variant of the CEV. The mass properties reporting standard is outlined in JSC-23303, Design Mass Properties. A detailed mass statement is provided in **Appendix 5A**, **CEV Detailed Mass Breakdowns**.

Table 5-5. Mass Properties for the ISS Pressurized Cargo Delivery Variant of the CEV

ISS CEV Capsule (Pressurized Cargo)	% of Vehicle Dry Mass	Mass (kg)	Volume (m^3)
1.0 Structure	25%	1,883	0
2.0 Protection	12%	894	1
3.0 Propulsion	5%	413	0
4.0 Power	10%	819	1
5.0 Control	0%	0	0
6.0 Avionics	6%	435	1
7.0 Environment	10%	799	3
8.0 Other	15%	1,159	2
9.0 Growth	17%	1,281	1
10.0 Non-Cargo		1	2
11.0 Cargo		3,500	1
12.0 Non-Propellant		147	0
13.0 Propellant		49	0
Dry Mass	**100%**	**7,683 kg**	
Inert Mass		**11,184 kg**	
Total Vehicle		**11,381 kg**	

5.2.6.3 Subsystem Description

5.2.6.3.1 Structure

The CEV CM structure is identical for the crewed and uncrewed ISS variants.

5.2.6.3.2 Protection

The CEV CM spacecraft protection is identical for the crewed and uncrewed ISS variants. The uncrewed CM is designed to return as much cargo to Earth as it delivers to the ISS; however, lunar entry requirements remain the dominant heat load/heat rate case for TPS sizing.

5.2.6.3.3 Propulsion

The CEV CM propulsion is identical for the crewed and uncrewed ISS variants.

5.2.6.3.4 Power

The power subsystem for the CEV CM is identical for the crewed and uncrewed ISS variants.

5.2.6.3.5 Control

Items typically included in the spacecraft control category are aerodynamic control surfaces, actuators, cockpit controls such as rudder pedals, and others. There are no control components on the CEV CM.

5.2.6.3.6 Avionics

The CEV CM avionics subsystem is identical for the crewed and uncrewed ISS variants.

5.2.6.3.7 Environment

Select CEV environment components required for the crew rotation mission are removed from the uncrewed pressurized cargo delivery variant. Changes between the variants are noted below.

Environmental Control and Life Support (ECLS)
The ISS uncrewed pressurized cargo delivery CM differs from the crew rotation variant in that atmosphere contaminant control equipment and EVA umbilicals and support equipment have been removed from the uncrewed CM. Without crew on board, there is no need for the vehicle to remove CO2 from the atmosphere or support EVAs.

Active Thermal Control System (ATCS)
Active thermal control for the CEV is identical for the ISS and lunar variants.

Crew Accommodations
The crew accommodations portion of the CEV uncrewed CM differs in that the galley equipment, waste collection, and crew seating needed for the crewed CM has been removed.

5.2.6.3.8 Other
CEV CM components included in the "Other" category, such as the parachute system, landing system, flotation system, and docking system, are identical for the crewed and uncrewed ISS variants. Using parachutes designed to support the lunar exploration mission, the pressurized cargo CEV lands with three fully inflated main parachutes at 8.2 m/s (26.9 ft/s) and a landed mass of 10,604 kg. For the lunar CEV with one failed chute, the crewed vehicle lands at 8.9 m/s (29.5 ft/s) and landed mass of 8,475 kg.

5.2.6.3.9 Growth
Mass growth included on the CEV CM is sized for 20 percent of dry mass.

5.2.6.3.10 Non-Cargo
Since the pressurized cargo variant of the CEV CM is uncrewed, all mass dedicated to personnel and personnel provisions have been eliminated from the vehicle. The only remaining non-cargo component is residual propellant, which is estimated at 2 percent of the nominally consumed propellant for the ISS mission.

5.2.6.3.11 Cargo
The uncrewed, pressurized cargo delivery CM has been sized to deliver 3,500 kg of pressurized cargo to the ISS in MLEs. The pressurized cargo has a density of 272.7 kg/m^3. Ballast mass for the CM has been removed.

5.2.6.3.12 Non-Propellant
Mass for oxygen and nitrogen is included on the uncrewed pressurized cargo delivery CM to maintain an appropriate pressurized environment for the cargo. Potable water has been removed because of the lack of need without crew on board.

5.2.6.3.13 Propellant
Propellant for the ISS pressurized cargo CEV CM is estimated using the same 10 m/s delta-V as the crew rotation variant; however, the propellant loading has changed due to the different CM mass at entry. The initial CM mass prior to the maneuver is estimated at 11,374 kg.

5.2.7 ISS SM (Off-loaded Lunar SM)

5.2.7.1 Vehicle Description

The ISS SM is identical to the SM designed for lunar exploration, except that propellant is off-loaded to reflect the lower delta-V requirements of ISS crew rotation compared to LOR. Propellant requirements for the ISS SM are estimated based on using the largest vehicle the SM may deliver to the ISS and subsequently deorbit, which is currently the unpressurized CDV. Other potential ISS payloads for the SM are the crewed CEV CM and pressurized cargo CEV; however, these have total masses less than the unpressurized CDV. The CDV has a total mass of 12,200 kg, compared to 9,342 kg for the three-crew CEV, 9,551 kg for the six-crew CEV, and 11,381 kg for the pressurized cargo delivery CEV.

5.2.7.2 Overall Mass Properties

Table 5-6 provides overall vehicle mass properties for the ISS SM, assuming a common lunar SM with off-loaded consumables. The mass properties reporting standard used in the table is outlined in JSC-23303, Design Mass Properties. A detailed mass statement is provided in **Appendix 5A**, **CEV Detailed Mass Breakdowns**.

Table 5-6. Vehicle Mass Properties for the ISS SM

ISS SM for Unpressurized Cargo Carrier (Off-loaded Lunar SM)	% of Vehicle Dry Mass	Mass (kg)	Volume (m^3)
1.0 Structure	20%	819	0
2.0 Protection	4%	167	1
3.0 Propulsion	36%	1,423	15
4.0 Power	10%	417	0
5.0 Control	0%	0	0
6.0 Avionics	3%	117	0
7.0 Environment	2%	98	1
8.0 Other	7%	290	0
9.0 Growth	17%	666	3
10.0 Non-Cargo		882	0
11.0 Cargo		0	0
12.0 Non-Propellant		0	0
13.0 Propellant		2,033	0
Dry Mass	**100%**	**3,997 kg**	
Inert Mass		**4,879 kg**	
Total Vehicle		**6,912 kg**	

5.2.7.3 Subsystem Description

5.2.7.3.1 Structure

The CEV SM structure is identical for the ISS and lunar variants.

5.2.7.3.2 Protection

The CEV SM protection is identical for the ISS and lunar variants.

5.2.7.3.3 Propulsion

The CEV SM propulsion is identical for the ISS and lunar variants because the ISS variant uses the propulsion system designed for the lunar mission and loads propellant as needed to transfer to the ISS.

5.2.7.3.4 Power
The power subsystem for the CEV SM is identical for the ISS and lunar variants.

5.2.7.3.5 Control
Items typically included in the spacecraft control category are aerodynamic control surfaces, actuators, cockpit controls such as rudder pedals, and others. There are no control components on the CEV SM.

5.2.7.3.6 Avionics
The CEV SM avionics subsystem is identical for the lunar and ISS variants.

5.2.7.3.7 Environment
The CEV environment components are identical for the ISS and lunar variants, as the radiator panels are sized for the worst environment conditions of the two missions and are used for either variant.

5.2.7.3.8 Other
CEV SM components are identical for the ISS and lunar variants.

5.2.7.3.9 Growth
Mass growth is the same for either the lunar or ISS SM.

5.2.7.3.10 Non-Cargo
The amount of residual propellant, propellant boil-off, and pressurant included on the SM varies depending on the needs for the ISS or lunar missions. Residual propellant on the CEV SM is 2 percent of the nominally consumed propellant, which is substantially less for the ISS mission owing to the lower total delta-V.

LOX and LCH4 boil-off for the ISS SM has been calculated assuming an average environment temperature of 250 K while docked to the ISS, while lunar mission boil-off was estimated with an average environment temperature of 210 K. The higher temperature is due to the CEV being placed in a non-optimal fixed attitude at the ISS and greater incoming infrared radiation from Earth and the ISS. While loitering in lunar orbit, the CEV can be placed in a more thermally benign attitude configuration, thus reducing propellant boil-off.

The mass of helium pressurant required is identical for the lunar and ISS variants.

5.2.7.3.11 Cargo
There are no cargo components included on the CEV SM.

5.2.7.3.12 Non-Propellant
There are no non-propellant components included on the CEV SM. All non-propellant fluids are stored on the CM.

5.2.7.3.13 Propellant
Propellant for the CEV SM in the ISS unpressurized cargo carrier delivery mission is loaded as needed for that mission's delta-V requirements. CEV total SM service propulsion system/RCS propellant is calculated for three major delta-V maneuvers in the mission. For each maneuver, the assumed service propulsion system Isp is 353.6 sec and the RCS Isp is 307.0 sec. The engine Isp for the ISS SM has been decremented by 10 sec below the level of the lunar variant to allow for suboptimal performance in the early years of the engine life. All ISS mission delta-Vs include 10 percent reserve.

The major SM maneuvers are described below.

- The first major maneuvers are circularization of the CEV insertion orbit and rendezvous and docking with the ISS. The CEV is first inserted by the CEV LV into a 55- x 296-km (30- x 160-nmi) LEO, and, when the CEV coasts to apogee, the SM uses its service propulsion system to circularize its orbit and then rendezvous and dock with the ISS. Maximum ISS altitude is 460 km (250 nmi) for this analysis. The required delta-V for circularization, rendezvous, and docking is estimated at 191.8 m/s for the service propulsion system and 33.5 m/s for the RCS, while the initial CEV mass prior to the maneuver is 19,104 kg.
- The second major maneuvers are undocking from the ISS and deorbit. Deorbit from the ISS is estimated assuming a maximum ISS altitude of 460 km and deorbit perigee of 46 km. The required service propulsion system delta-V for undocking and deorbit is estimated at 137.7 m/s for the service propulsion system and 19.4 m/s for the RCS. The initial CEV mass prior to these maneuvers is 17,204 kg.
- The third and final SM maneuver is to safely dispose of the SM after CM separation. The required RCS delta-V for disposal is 15 m/s and the initial SM mass prior to the burn is 4,224 kg.

5.2.8 ISS Unpressurized CDV

5.2.8.1 Vehicle Description

The ISS CDV was sized to deliver unpressurized cargo to the ISS. The CDV is mainly a structural "strong back" with a CBM for attachment to the ISS. The CDV utilizes the same SM as the other block configurations for transfer from the LV injection orbit to the ISS. Because the avionics for the other CEV variants are located within the CM, an avionics pallet is required for the CDV. This pallet would support the avionics and provide the connection to the ATCS on the SM.

The CDV was sized to transport two 1,500-kg unpressurized Orbital Replacement Units (ORUs) for the ISS. Examples of ORUs include Control Moment Gyroscopes (CMGs) and pump packages. The packaging factor for these ORUs was assumed to be 100 percent; therefore, the trays and secondary support structure for the cargo is estimated to be 3,000 kg, for a total cargo complement of 6,000 kg. The total estimate for the CDV without the SM is 12,200 kg.

Operationally, the CDV would perform automated rendezvous and proximity operations with the ISS and would then be grappled by the SSRMS and berthed to an available port. Two releasable cargo pallets are used to provide structural attachment for the ORUs. The cargo pallets can be grappled by the SSRMS and relocated to the ISS truss as required. Once the cargo has been relocated on the ISS, the CDV would depart from the ISS and perform an automated deorbit burn for burnup and disposal in the ocean.

Illustrations of the reference CDV are shown in **Figures 5-8** and **5-9**.

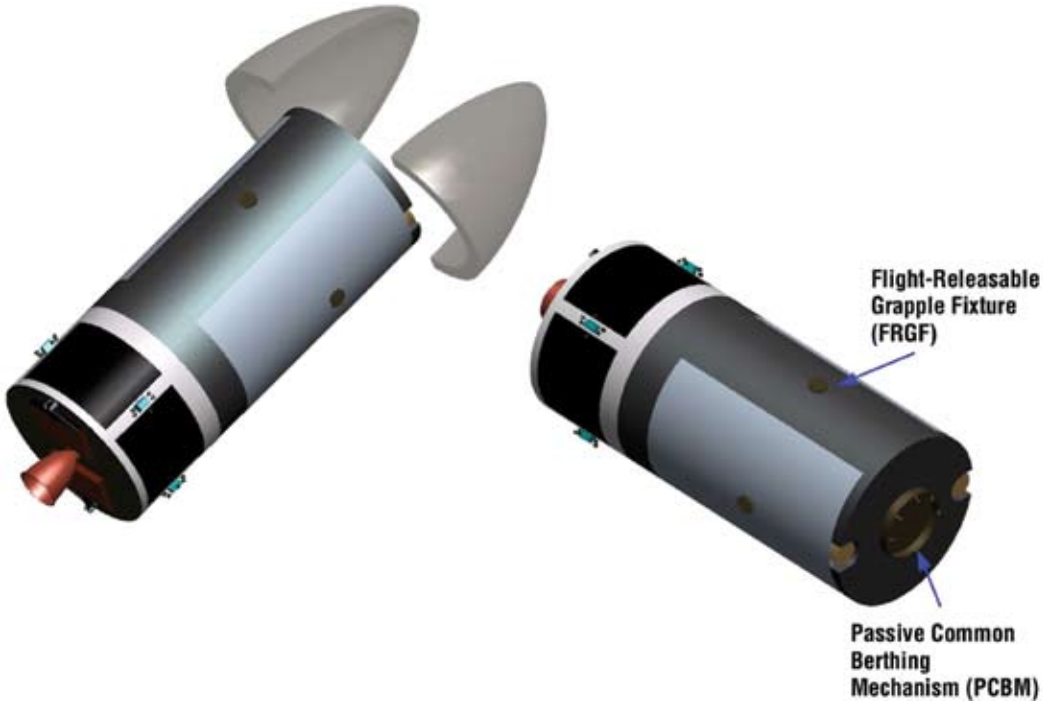

Figure 5-8. CDV

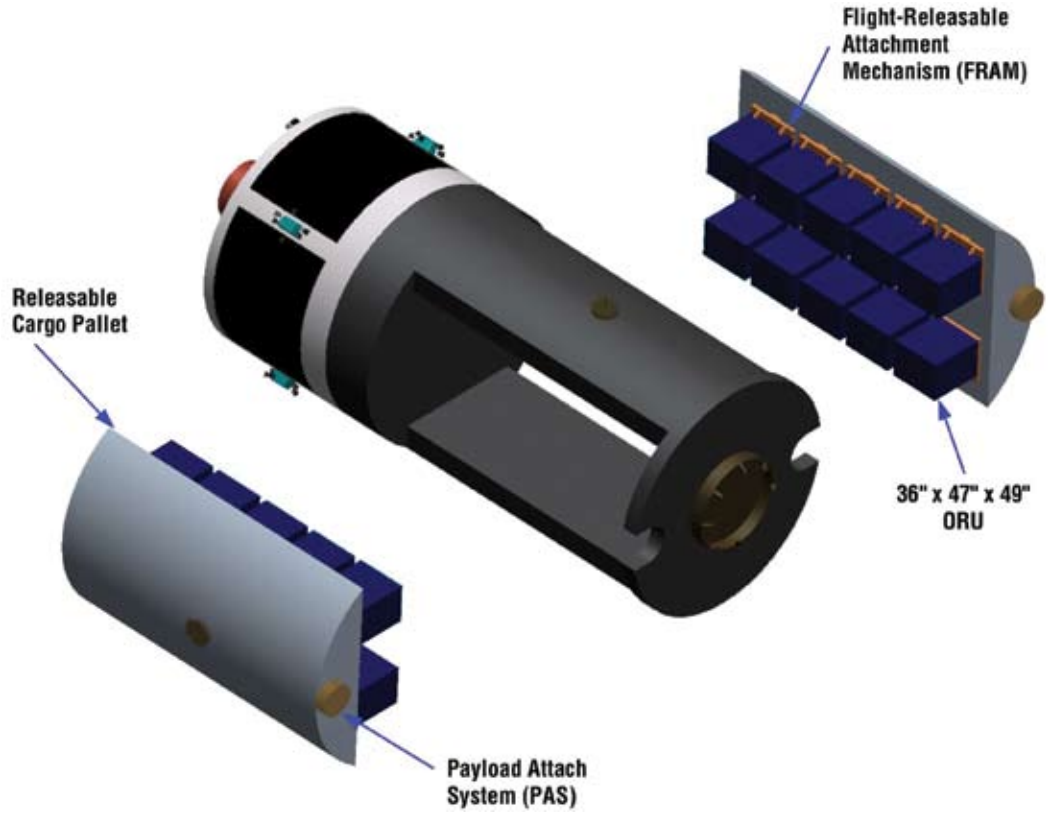

Figure 5-9. CDV Cargo Pallets

5.2.9 Mars Block 3 CEV

5.2.9.1 Vehicle Description

The ESAS reference Mars mission utilizes a Block 3 CEV to transfer a crew of six between Earth and an MTV at the beginning and end of the Mars exploration mission. A Block 3 CEV CM and SM are launched by the CLV into an orbit matching the inclination of the awaiting MTV. The CEV is first injected into a 55- x 296-km altitude orbit while the MTV loiters in a circular orbit of 800–1,200 km altitude. It then takes the CEV up to 2 days to perform orbit-raising maneuvers to close on the MTV, conducting a standard ISS-type rendezvous and docking approach to the MTV. After docking, the CEV crew performs a leak check, equalizes pressure with the MTV, and opens hatches. Once crew and cargo transfer activities are complete, the CEV is configured to a quiescent state and remains docked to the MTV for the trip to and from Mars. Periodic systems health checks and monitoring are performed by the ground and flight crew throughout the mission.

As the MTV approaches Earth upon completion of the 1.5–2.5 year round-trip mission, the crew performs a pre-undock health check of all entry critical systems, transfers to the CEV, closes hatches, performs leak checks, and undocks from the MTV. The CEV departs 24–48 hours prior to Earth entry, and the MTV then either performs a diversion maneuver to fly by Earth or recaptures into Earth orbit. After undocking, the CEV conducts an onboard-targeted, ground-validated burn to target for the proper entry corridor, and, as entry approaches, the CEV CM maneuvers to the proper EI attitude for a direct-guided entry to the landing site. Earth entry speeds from a nominal Mars return trajectory may be as high as 14 km/s, compared to 11 km/s for the Block 2 CEV. The CEV performs a nominal landing at the primary land-based landing site and the crew and vehicle are recovered.

Figure 5-10 shows the Block 3 CEV CM configured to carry six crew members to the MTV.

Figure 5-10. Block 3 CEV CM

5.3 Crew Exploration Vehicle (CEV) Trades

Many trade studies were performed in the development of the CEV design and requirements. Some of these were specific to the CEV and others were more global to the architecture. For example, determining the CM OML shape and internal volume was specific to the CEV, but other trades that addressed propulsion, airlocks, and radiation protection were cross-cutting across the architecture. The following sections describe some of the trades that were performed on the CEV shape, size, systems, and performance.

5.3.1 CM Vehicle Shape

5.3.1.1 Introduction and Requirements

The ESAS team addressed the task of designing the CM vehicle shape. A number of desirable characteristics was identified through requirements allocation and trade studies. The initial goal was to achieve as many of these characteristics as possible with the proper design of an OML shape. These characteristics included:

- Low technical risk for near-term development feasibility;
- Adequate volume to meet the ISS, lunar, and Mars DRMs;
- Satisfaction of acceleration loads across the spectrum of flight conditions within crew limits;
- Efficient dissipation of entry aeroheating loads within existing material temperature limits;
- Adequate crew visibility for rendezvous and docking maneuvers;
- A simple yet robust approach to abort survival in case of primary power or Guidance Navigation and Control (GN&C) failures;
- Land-landing capability for reusability; and
- Highly accurate CONUS landing for ease and minimal cost of recovery and retrieval.

5.3.1.1.1 Monostability

The desire for a simple abort technique led to a goal of producing a vehicle that was monostable. This term implies that the vehicle has only one stable trim angle-of-attack in atmospheric flight. Given enough time, this would guarantee that the vehicle reaches its desired heat shield-forward attitude passively, without assistance from the RCS. The Apollo capsule was not able to achieve monostability due to the inability to place the CG close enough to the heat shield. Conversely, the Soyuz vehicle is monostable, with claims that it is able to achieve its desired trim attitude and a successful reentry with initial tumble rates of up to 2 deg/sec. **Figure 5-11** shows the history of abort ascent and entries that either relied on the monostable characteristic of the vehicle (Soyuz) for survival or would have benefited had the vehicle been monostable.

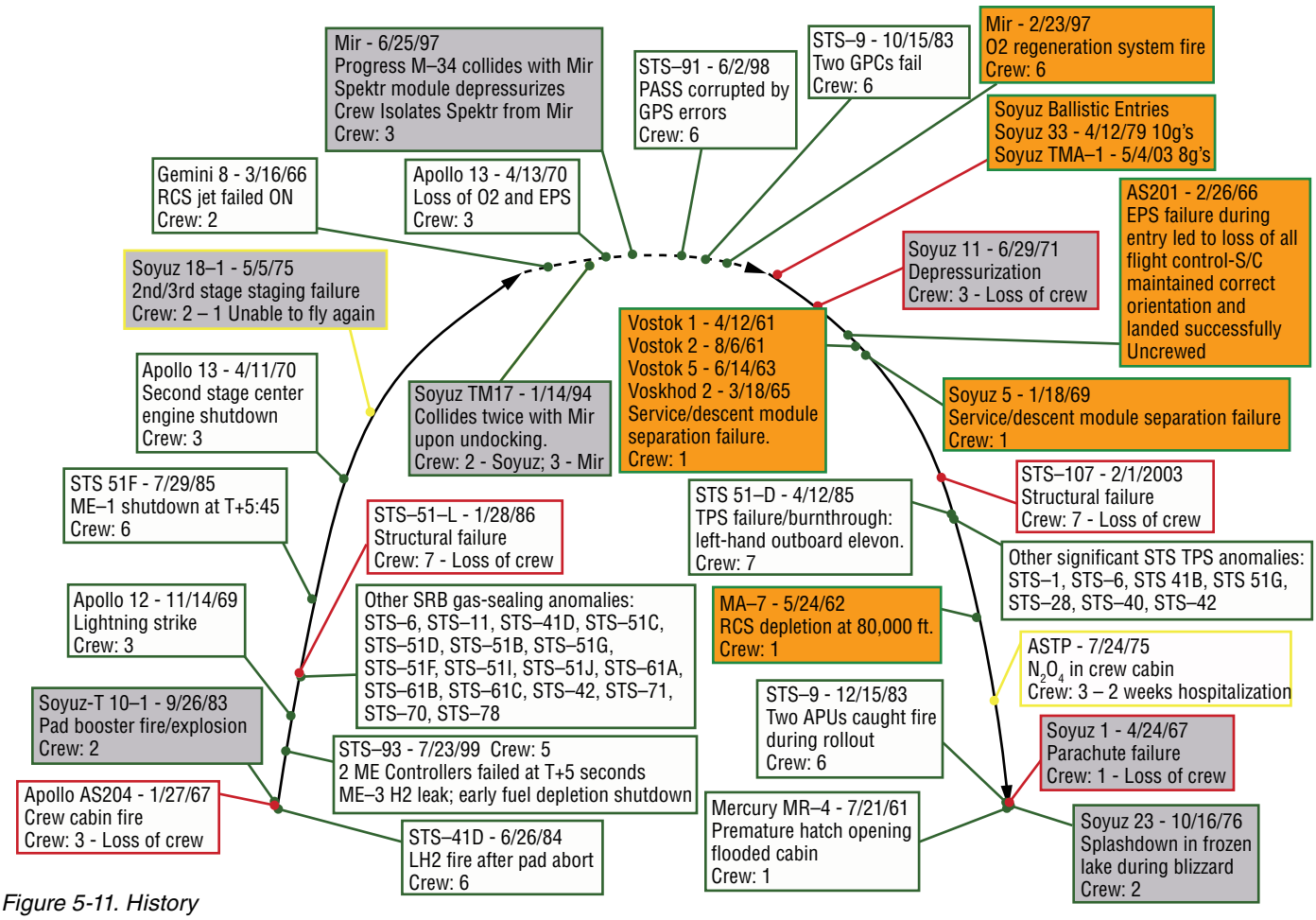

Figure 5-11. History of Manned Capsule Failures

5.3.1.1.2 Ballistic Entry Capability

A second way of achieving a simple abort approach was also examined in detail—to spin-up the vehicle after the proper orientation had been achieved. This spin-up would be a rolling motion about the velocity vector axis so that the lift of the vehicle would gyrate. This would produce a nearly ballistic trajectory through an effective cancellation of the lift vector so that it would have no effect on the entry trajectory. This would allow a vehicle that has lost primary power or control to successfully enter the atmosphere without being stuck in a lift-down roll angle that would exceed crew load limits.

5.3.1.1.3 Lift-to-Drag (L/D) Requirements

The desire for CONUS land landings led to the requirement for at least a 0.4 L/D ratio. This level of L/D is needed to reach attractive landing sites when returning from the ISS while safely disposing of the SM in the Pacific Ocean. In addition, the 0.4 L/D would aid in the performance of the lunar return skip-entry that was necessary to achieve the CONUS landing sites with a single entry technique. Although not enough time was permitted to perform an accurate quantitative trade study to indicate the minimum necessary L/D, it is known that the more L/D provided will produce a more accurate landing and help minimize the correction burn performed in the middle of the skip-entry maneuver. Further work is required to assess the risk and total viability of the CONUS land-landing approach for both lunar and LEO returns.

5.3.1.2 Blunt Bodies Versus Slender Bodies Trade

The shape study trade was initiated between major vehicle classes. The primary classes considered were capsules (blunt bodies), slender bodies, lifting bodies, and winged vehicles. Winged bodies and lifting bodies (such as X–38, X–24, HL–10, etc.) were eliminated at the outset due to several factors, including: (1) the extreme heating (especially on empennages) these would encounter on lunar return entries, (2) the additional development time required due to multiple control surfaces, and (3) the increased mass associated with wings, fins, and control surfaces which are huge liabilities in that they must be carried to the Moon and back simply for use on entry. Thus, the trade space involved capsules versus slender bodies. It was planned that, after a desirable class of vehicle was selected, the shape would be optimized within that class.

An extensive spreadsheet was designed to compare two applicable, fundamental classes of vehicles—blunt bodies and slender bodies. This spreadsheet attempted to delineate all the important performance, design, and operational differences that could be used as discriminators for selecting one class of vehicles over the other. Categories of evaluation included on the spreadsheet were: crew load directions and magnitudes, LV integration, entry heating, landing sites and opportunities, SM disposal, ballistic entry landing, weather avoidance, aerostability, terminal deceleration systems, landing issues, and additional mission and system requirements. Some of these analyses are presented in more detail below. All flight phases from launch to landing were evaluated for the two classes of vehicles, including three lunar return options: direct-entry, skip-entry, and aerocapture. The spreadsheet is provided in **Appendix 5B**, **CEV Crew Module Shape Trade Data**.

A representative vehicle was chosen in each class for analysis purposes. An Apollo-shape CEV configuration was selected as representative of the blunt-body class as seen in **Figure 5-12**. Both a straight biconic and an ellipsled design from earlier NASA studies were chosen as representative of the slender bodies (**Figure 5-13**). The configuration details of these vehicles can be seen in the first page of the spreadsheet in **Appendix 5B**, **CEV Crew Module Shape Trade Data**. For each of the slender bodies, two variations were analyzed—one without an attached SM and one with an attached SM.

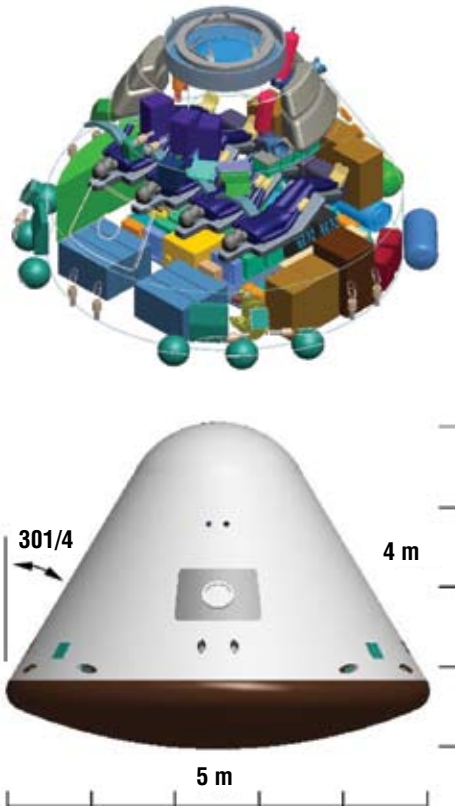

Total Mass:	8,000 kg (17,637 lbs)
Crew Size:	4
Active Duration:	16 days
Passive Duration:	90 days
Pressurized Volume:	22 m^3 (777 ft^3)
Habitable Volume:	12 m^3 (424 ft^3)
Base Diameter:	5 m (16.4 ft)
Max Hypersonic L/D (est.):	0.3
Nominal Return Mode:	Direct Entry
Landing Mode:	Water w/ Contingency Land
Payload:	Crew + 100 kg (220.5 lbs)
Delta-V (Service Propulsion System/RCS):	0/10 m/s (33 ft/sec)
Major Maneuvers:	Aeroentry
Propellant:	Tridyne ($N_2/H_2/O_2$)
Isp:	140 s
Dry Mass Growth:	20%

Vehicle Dry Mass Distribution

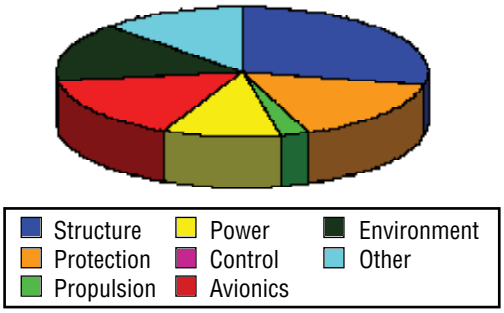

Figure 5-12. Representative Blunt-Body

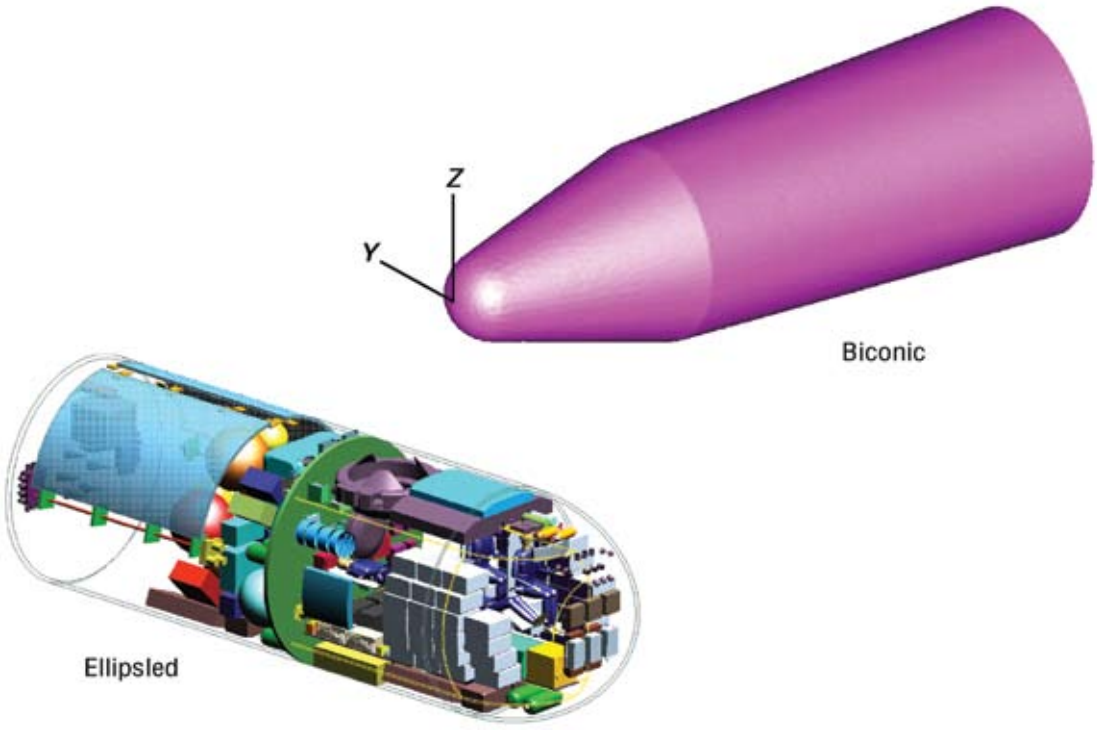

Figure 5-13. Representative Slender Bodies

5.3.1.2.1 Load Directions Analysis

One of the key areas of performance investigation was the area of load directions encountered by the crew in flight. It is important to note that the entry load directions are significantly different between a capsule and a slender body. During entry, the aerodynamic forces on a trimmed blunt-body primarily generate axial loads, as can be seen in **Figure 5-14**. As shown, the majority of the deceleration occurs along the axis of the capsule. This is also the same direction that primary loads are generated during ascent when attached to an LV, during ascent abort, and during landing. Conversely, slender bodies generate primarily normal aerodynamic loads, so that, on entry, the majority of the acceleration occurs normal to the axis of the slender body (**Figure 5-14**). These loads would be 90 deg off from the load direction encountered during ascent or ascent abort. These load directions have implications on the seating orientation of the crew. For a capsule, the logical crew orientation is with their backs parallel to the heat shield. All primary loads would then be carried through the crews' chest towards their backs ("eyeballs in"), which is the most tolerable load direction for a human. For a slender body, the primary load direction changes approximately 90 deg between launch and entry. Thus, either the crew would have to rotate their orientation in flight or a very benign ascent would have to be designed to allow the crew to take the ascent loads sitting up.

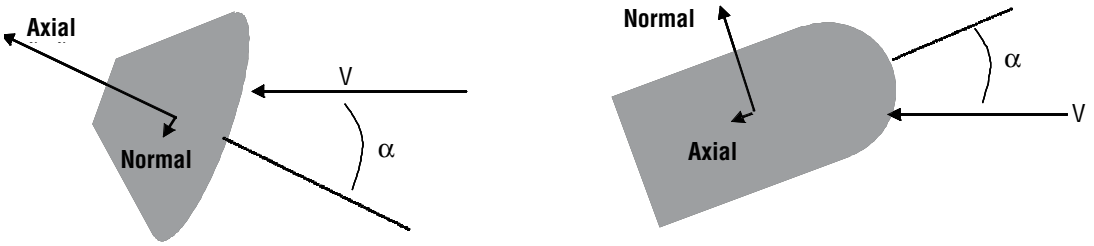

Figure 5-14. Atmospheric Flight (Entry) Aerodynamic Loads Direction

5.3.1.2.2 Load Magnitudes Analysis

During all phases of flight, it is mandatory that accelerations be kept within the crew load limits set forth by the NASA-STD-3000, Volume VIII, Human-Systems Integration Standards document. An example of these limit curves, which are a function of the duration of the load as well as the direction taken in the human body, is shown in **Figure 5-15**. Three limit-curves exist for each of the three human body axis directions. The highest limit-curve is intended for use in abort situations. It represents the maximum loads to ever be applied on the crew with the expectation of survival. The lowest limit-curve applies to crew who have been subjected to zero-gravity or very low gravity for an extended amount of time. The middle curve applies to normal, g-tolerant crew. Each of the vehicle shapes was evaluated in simulations to assess their capacities to meet these limits using the applicable limit-curves. Results can be seen in the spreadsheet in **Appendix 5B**, **CEV Crew Module Shape Trade Data**.

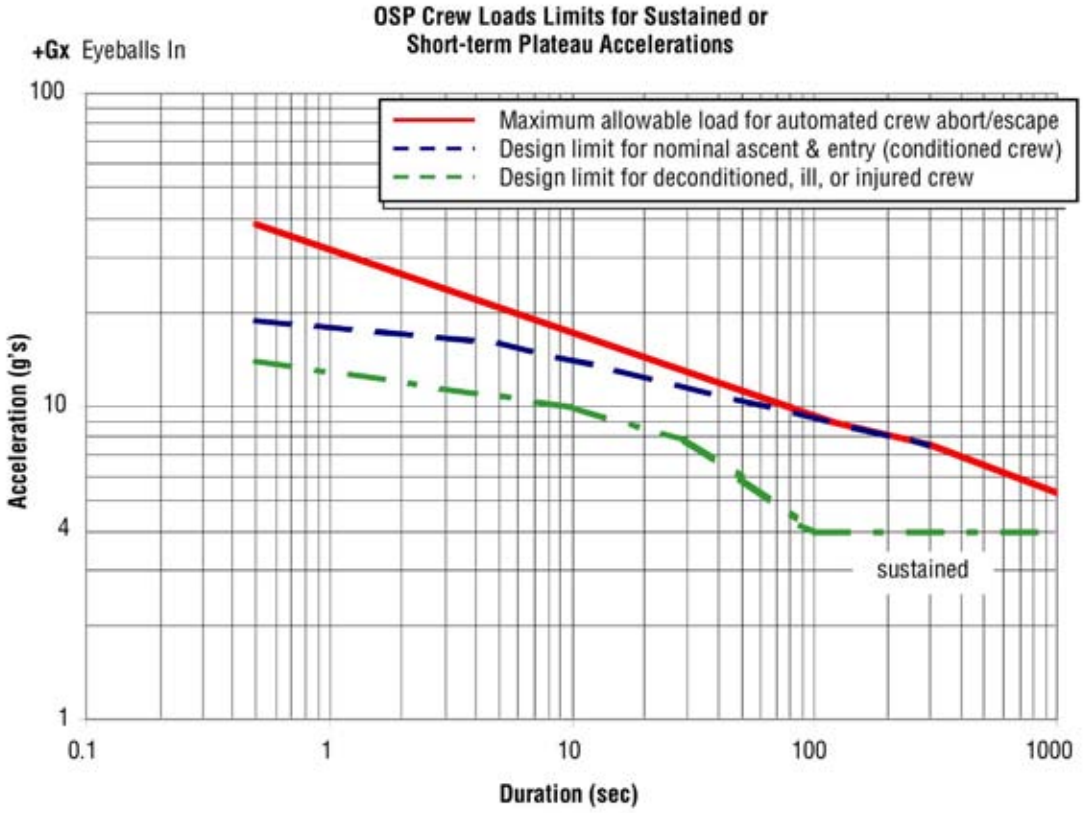

Figure 5-15. Example of NASA Standard 3000 Crew Load Limits

5.3.1.2.3 Aerodynamic Stability Analysis

Another key analysis in the shape trade study involved assessing the inherent aerodynamic stability in the design of the CEV CM as it relates to vehicle shape and CG location. In the presence of an active control system, the natural behavior of a vehicle can be augmented. Still, it is important to design a vehicle that can operate in a passively stable configuration for worst-case situations. An understanding of the stability characteristics of a vehicle cannot be obtained from a single parameter. A number of factors influenced the stability evaluation of the vehicle classes. In this study, monostability (including degree of monostability), pitching moment curve slope ($C_{m\alpha}$), $trim_{\alpha}$, and sensitivity of L/D to CG location were all included. All of these parameters were analyzed, reported, and evaluated for each of the shapes considered.

There are many other important limiting factors that are not related to stability, but are still related to the vehicle aerodynamics. These include CG location placement for desired L/D (which affects systems packaging and landing stability), trajectory range and cross-range capability, loads on vehicle and crew, and heat rates and heat loads (which affect TPS selection and mass). Thus, vehicle trim line information delineating desired CG locations for the proposed L/D was utilized for this analysis, while additional aerodynamic data was supplied to other analysts to perform trades in the other areas.

As discussed earlier, the representative vehicles for the slender bodies included a biconic and an ellipsled configuration. The Apollo capsule was used as the representative for the blunt bodies. The slender body vehicles exhibit a range of L/D ratios much higher than blunt capsules. Thus, the proposed L/D values differed. **Table 5-7** shows the different trim angles and L/D values studied.

	Biconic	Ellipsled	Apollo
L/D	.817	.655	.3
Trim α	40°	40°	19.8°

Table 5-7. L/D Ratios and Trim Angles

The main appeal of the slender bodies is their higher lift capability. **Figure 5-16** shows the CG trim line for the 40-deg angle-of-attack trim for the biconic shape.

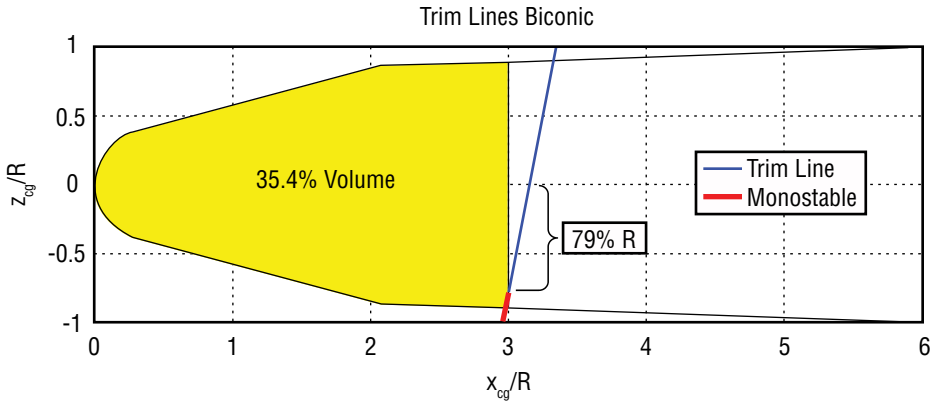

Figure 5-16. Biconic Shape with Trim Line

Figure 5-17 shows that the vehicle, which has an aspect ratio of three, trims with a CG near the center of the vehicle. However, if monostability (one stable trim angle-of-attack) is desired, the required CG location (i.e., the heavy segment of the trim line near the sidewall) is not possible to achieve.

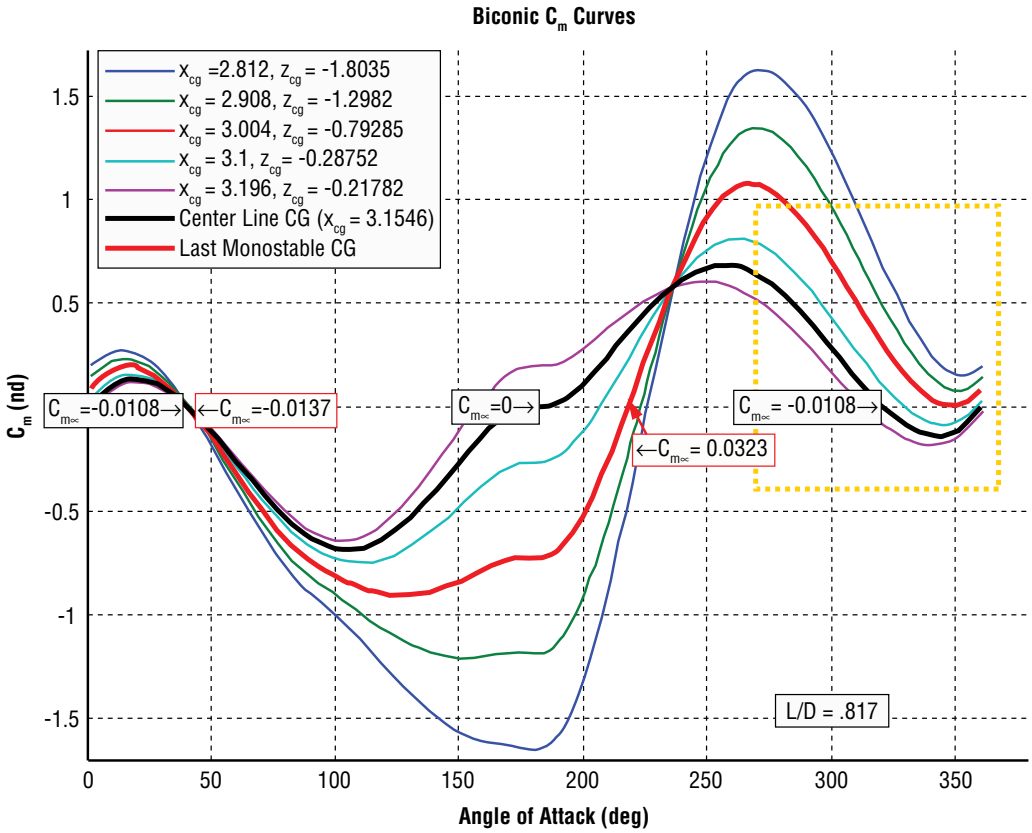

Figure 5-17. C_m Curves for Biconic Vehicle

The plot in **Figure 5-17** shows the pitching moment coefficient (C_m) curves for different points along the blue trim line. The portion of the graph in the gold box highlights the second stable trim point, where the curve crosses zero with a negative slope. The red curve is for a CG at the first monostable point; it is the last curve that does not intersect zero in the gold box. This first monostable CG is the point where the fine blue line ends and the heavy red line begins in the figure.

The data used in this study was generated by a simple, modified Newtonian aerodynamics code. The gold box in **Figure 5-17** is highlighted to indicate the belief that, based on wind tunnel analyses of a related configuration, the second trim point does not really exist in actual flight and would disappear with more robust Computational Fluid Dynamics (CFD) analysis. If the second trim point does exist as these curves suggest and monostability is required, this design is not feasible. However, this does not eliminate slender bodies altogether. Other studies have demonstrated that a bent biconic shape could remove this second trim. The negative aspects to a bent biconic are a loss of symmetry, an increase in configuration complexity, and more volume existing in the opposite direction of the desired CG placement.

The ellipsled vehicle exhibits very similar characteristics to the biconic. The main differences are that the monostable limit is closer to the centerline of the vehicle (37 percent of the vehicle radius as opposed to 79 percent of the radius), and the trim line is less vertical. However, this is still not a realistically achievable CG location to achieve monostability.

The blunt bodies are appealing because they are simpler and have historical precedent. The Apollo capsule vehicle is shown in **Figure 5-18** with two trim lines (0.3 and 0.4 L/D). **Figure 5-19** displays C_m curves for an L/D of 0.3 (CG locations along the solid trim line).

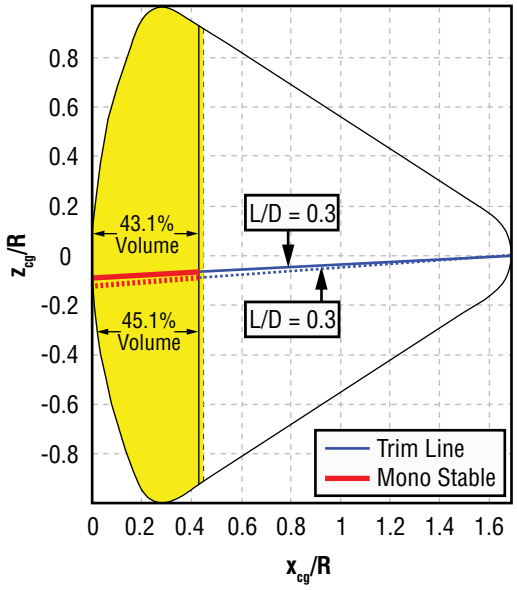

Figure 5-18. Blunt-Body (Apollo) Vehicle: Trim Lines with OML

The Apollo vehicle shows that the trim line is closer to the centerline and gives a larger percent volume that is monostable than the slender vehicles. The location of this trim line is desirable, as it stays close to the centerline throughout the vehicle's length.

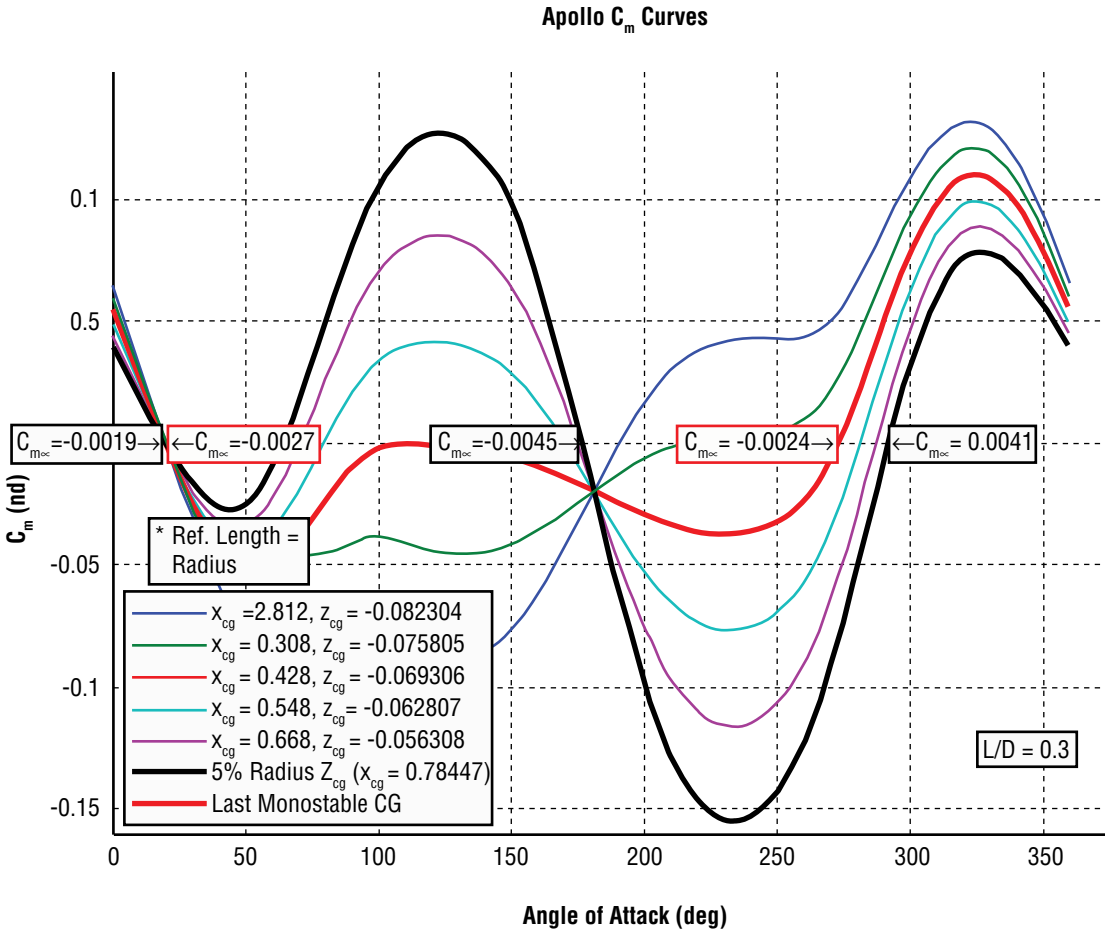

Figure 5-19. Blunt-Body (Apollo) Vehicle: C_m Curves

For comparison purposes, **Table 5-8** shows the stability metrics.

Table 5-8. Stability Comparison Between Slender and Blunt Bodies

		Ellipsled	Biconic	Apollo
Monostability	% Vol	42%	35%	43-45%
	Z_{cg} Offset	37% R	79% R	7% R
L/D Sensitivity	To Z_{cg}	0.001/cm	0.002/cm	0.016/cm
	To X_{cg}	0.002/cm	0.008/cm	0.001/cm

To summarize the aerodynamic stability trade, the Apollo capsule (blunt-body) has more favorable monostability characteristics and the lowest sensitivity to X_{cg} variations, but the least favorable L/D sensitivity to Z-axis CG (Z_{cg}). This is because the trim lines for the capsule are more parallel to the X-axis. For slender bodies, monostability appeared infeasible based on simple Newtonian aerodynamic data, though some existing wind tunnel data suggested it may be better than Newtonian aerodynamic data suggested. In any case, the wind tunnel data would require much more analyses. For blunt bodies, monostability appeared feasible, but the actual Apollo Program could not achieve a CG close enough to the heat shield to produce it. However, it appeared that the capsule shape could be refined to produce an OML that provided monostability, with a CG relatively higher in the capsule than Apollo (i.e., with greater percentage of the OML volume between the needed monostable CG and the heat shield). Obviously, the Soyuz OML has been able to achieve this.

5.3.1.2.4 "Passive," Ballistic Entry Analysis

Another key area of performance investigation was the ability to perform a ballistic entry without an active primary GN&C or power system. In this section, "passive stability" is understood as the capacity of the spacecraft to orient itself to the nominal attitude from an initial off-nominal attitude and/or angular rate without the assistance of an RCS or a stabilizer. Note this requires the vehicle to be monostable, but a backup RCS could also be used to damp rates and/or spin the vehicle for ballistic entry.

This analysis was carried out as a cooperative effort between NASA Centers using both the Six-Degrees of Freedom (6–DOF) simulation tool Decelerator System Simulation (DSS) and the Program to Optimize Simulated Trajectories (POST II) tool. In order to validate both DSS and POST II simulations, a simulation-to-simulation comparison was performed using a scaled Apollo module with excellent comparable results.

Passive stability was investigated for:

- Three shapes:
  - Blunt-body capsule (Apollo),
  - Slender body, biconic, and
  - Slender body, ellipsled.
- Three scenarios:
  - Ascent abort (using CLV - LV 13.1) for worst-case heat rate and heat load cases,
  - Entry from LEO, and
  - Lunar return.

The following specifications for the vehicles were used:

- Blunt-body (Apollo):
  - Actual aerodynamics database,
  - CG on 20-deg alpha trim line (L/D is approximately 0.3),
  - Maximum reasonable monostable position, and
  - $X_{cg}/D = 0.745$; $Z_{cg}/D = 0.04$ (where D is the vehicle diameter).
- Biconic/ellipsled:
  - Modified Newtonian aerodynamics,
  - Secondary trim existed for reasonable CG location listed below,
  - CG on 40-deg alpha trim line,
  - Biconic – $X_{cg}/D = 1.56$; $Z_{cg}/D = –0.0918$; L/D is approximately 0.82, and
  - Ellipsled – $X_{cg}/D = 1.41$; $Z_{cg}/D = –0.0877$; L/D is approximately 0.65.

The assessment of performance includes a heat rate limit criteria and NASA-sanctioned crew load limits criteria. For the heat rate limit criteria, success (or no violation) is declared if, in the time interval when the heat rate is above 20, the attitude oscillations are confined to a safe region. If a small percentage (less than 20 percent) of the oscillations fell outside this heat safe region, no violation would be declared. The heat rate model used in the study was the Detra Kemp Riddell convective model. The radius considered in the model (the corner radius in the blunt-body and the nose radius in the slender bodies) was the smallest one exposed to the flow for each shape.

For the load limit criteria, success is declared if medical maximum allowable load crew limits are not violated in any axis. The medical limits from NASA Standard 3000 are established in charts that show the load in g's as a function of maximum time duration at that load, with each axis having an associated load limit chart. A sample chart depicting the acceleration limit along the X-axis versus the total duration in seconds is shown in **Figure 5-20**.

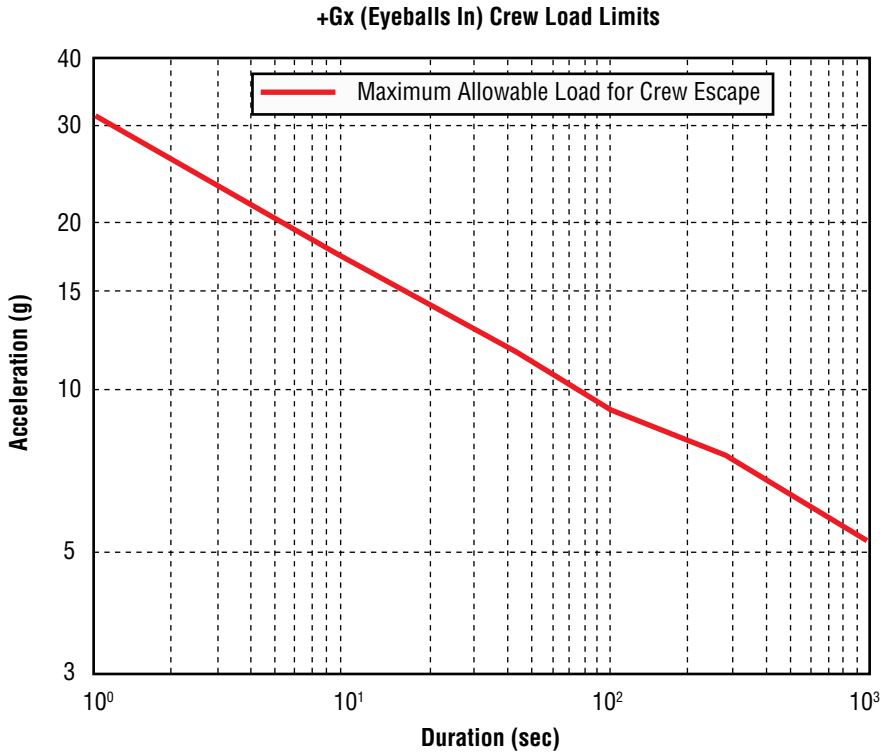

Figure 5-20. Maximum Allowable Load for Crew Escape in the +X Direction (Eyeballs In)

For each scenario and vehicle type, two kinds of 6–DOF tests were run, including:

- With zero initial angular rates and a zero initial sideslip angle, the initial attitude is varied on angle-of-attack (alpha) only.
- With initial attitudes being apex forward in the blunt-body and nose forward in the slender bodies, the initial pitch rate is varied from -10 to +10 deg/s. Yaw and roll rates are initialized to zero.

(Hereafter, these will be referred to as "Test type 1" or "Tt 1" and "Test type 2" or "Tt 2," respectively.)

Conclusions of the trade between slender and blunt bodies' passive stability is summarized in **Table 5-9**. The blunt bodies have slightly more tendency to be able to recover from off-nominal initial attitudes than the slender bodies, but both appear to be able to handle any off-nominal attitude, assuming they are monostable. The axisymmetric slender bodies, however, were shown to require very unreasonable CG locations for monostability.

Table 5-9. Conclusions of the Trade Between Slender and Blunt Bodies' Passive Stability

(Tt = Test type)	Blunt Body (Apollo)	Biconic	Ellipsled
Ascent abort	Tt 1. Acceptable aborts from any initial attitude Tt 2. Acceptable aborts from -2 to +2 deg	*Tt 1. Acceptable aborts from any initial attitude Tt 2. Acceptable aborts from -2 to +1 deg	*Tt 1. Acceptable aborts from any initial attitude Tt 2. Acceptable aborts from 0 to +2 deg
Entry from LEO	Tt 1. Acceptable aborts from any initial attitude Tt 2. Acceptable aborts from -2 to +2 deg	Not performed due to time but assumed similar to the ascent abort case	Not performed due to time but assumed similar to the ascent abort case
Lunar return	High onset of loads and heating associated with lunar return precludes passive stability from working for any appreciable initial attitude rates or off-nominal attitudes		

**These results account for the assumption that the secondary trim point was removed.*

The conclusion for the lunar return cases was later discovered to be an artifact of the analysis technique—multiple cases were skipping or pulling lift-down because the vehicle was not spun-up after the trim attitude was achieved. When proper spin-up of the vehicle is achieved to null the lift vector, results are more favorable.

Introducing a bank rate to null the lift vector effect on the trajectory (ballistic abort) was then investigated. A bank maneuver consists of the rotation of the spacecraft about the velocity vector. This rotation results in gyration of the lift vector, thus producing a ballistic trajectory. An initial bank rate was set via a combination of body axis roll and yaw rates. No damping aerodynamic terms were used, although, at the velocities and altitudes of concern, very little damping would occur in any case. Due to the presence of cross products of inertia and the fact that the principal axis of inertia is not aligned with the trim angle, the initial bank rate oscillates and changes with time—particularly for the slender bodies.

Figures 5-21 and **5-22** show the angle of attack (alpha), sideslip angle (beta), and bank angle time histories with an initial bank rate. The scenario is an ascent abort with worst heat rates at reentry, with the trim attitude being the initial attitude. Initial bank rates are 20 deg in the Apollo and biconic cases and 25 deg for the ellipsled. This is shown as:

Time Histories with Initial Bank Rate = 25 deg/s ellipsled, 20 deg/s biconic.

A comparison between **Figures 5-21** and **5-22** clearly indicates a better performance of the blunt-body with respect to that of the slender bodies. Whereas the Apollo shape is maintaining a reasonable attitude, the biconic and ellipsled shapes are both tumbling at the onset of the simulation. This tumbling is attributed to the principal moments of inertia being nearly aligned with the body axis rather than the trim angle of attack (40 deg away from the principal axis), about which the banking maneuver is being performed.

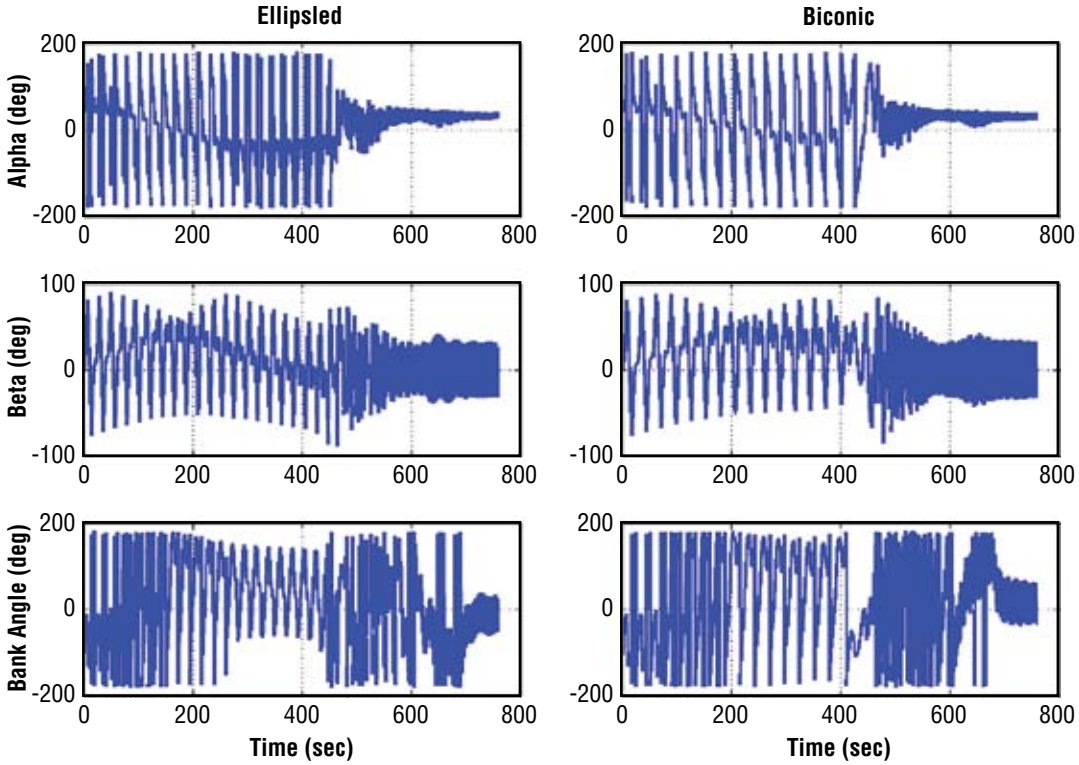

Figure 5-21. Slender Bodies: Angles of Attack (alpha), Sideslip (beta), and Bank

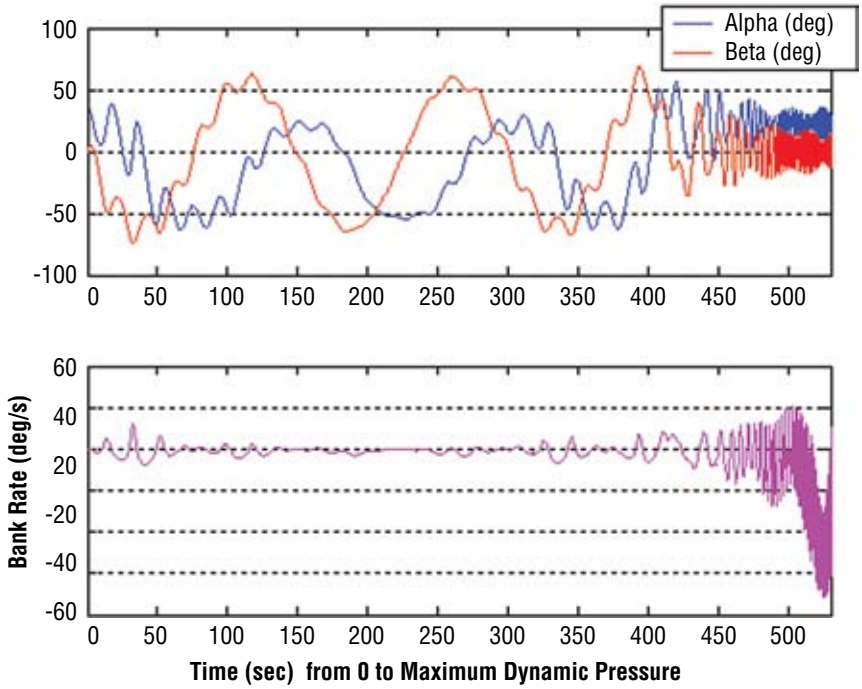

Figure 5-22. Blunt-Body (Apollo): Angles of Attack (alpha), Sideslip (beta), Bank Rate Time Histories with Initial Bank Rate = 20 deg/s (Ascent abort with worst heat rate at reentry. Initial attitude is the trim attitude.)

A lunar return case with initial bank rate was further investigated. As shown in **Figures 5-23** and **5-24**, the presence of cross products of inertia results in larger amplitude of oscillations in alpha, beta, and bank rate for a capsule, although both are acceptable.

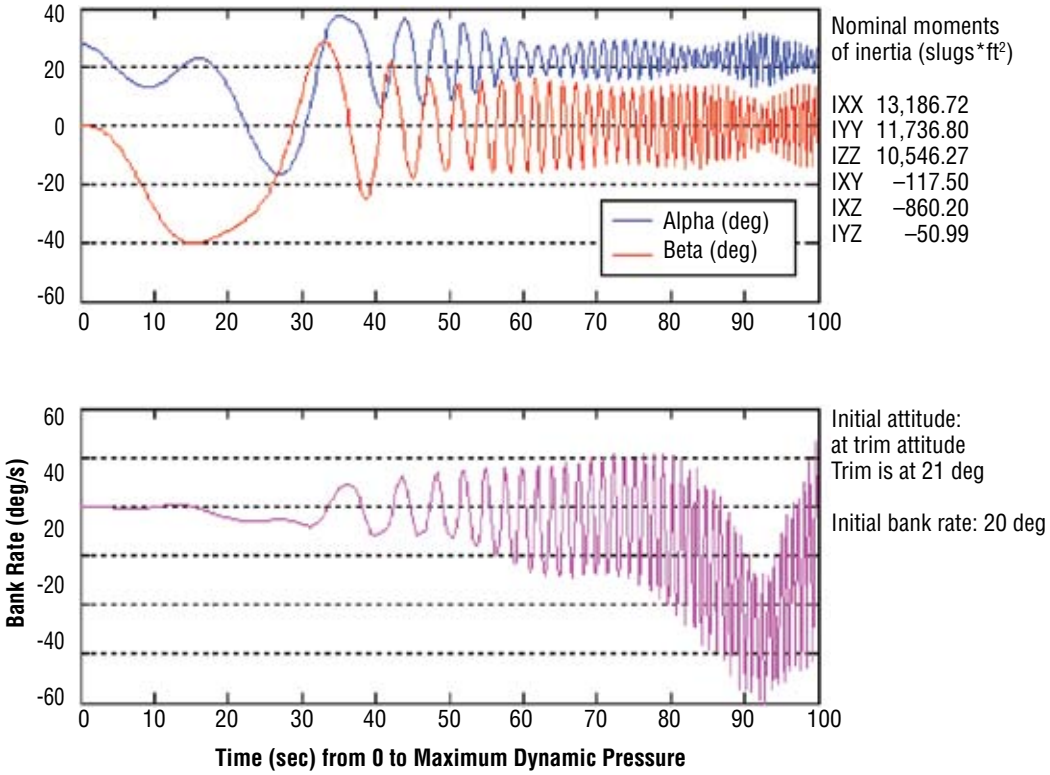

Figure 5-23. Blunt-Body (Apollo) Ballistic Entry with Initial Bank Rate = 20 deg

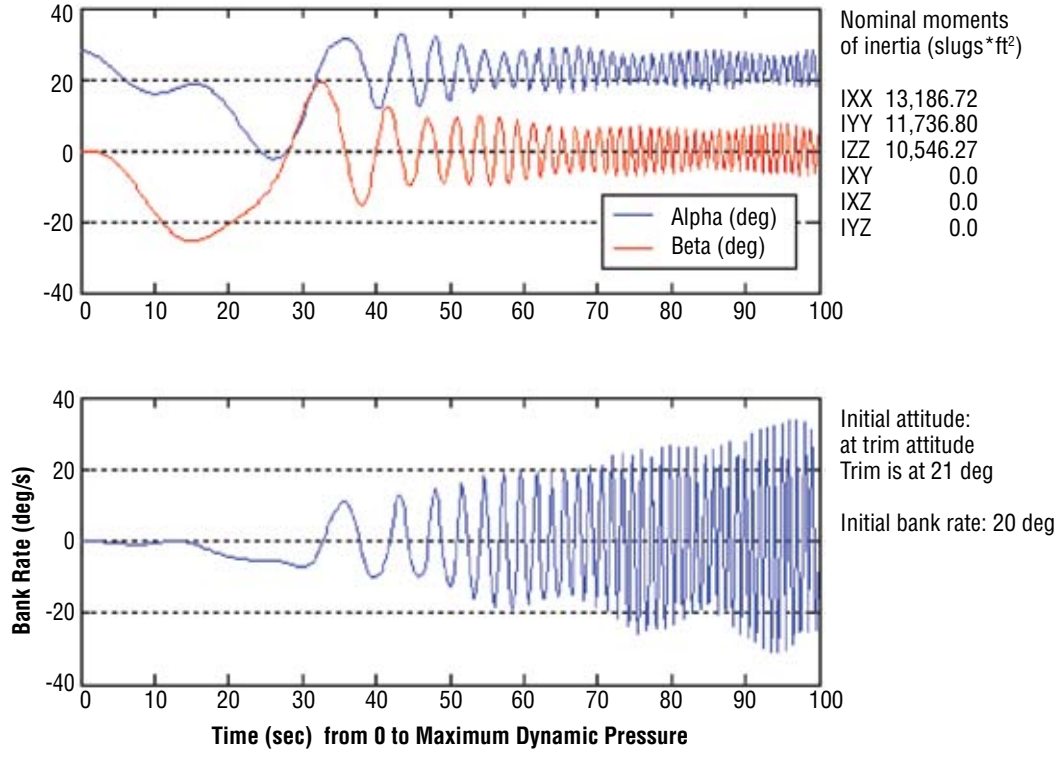

Figure 5-24. Blunt-Body (Apollo) Ballistic Entry with Initial Bank Rate = 20 deg

The tumbling motion of the biconic and ellipsled bodies can be avoided by waiting until there is enough dynamic pressure to fight the effect of the moments of inertia. The effect of a bank rate induced late in the flight in the case of a biconic body is presented in **Figure 5-25**. It is uncertain whether it would be allowable to initiate the bank rate this late in the trajectory under all abort cases. There may be abort situations when it is desirable to have the SM create the bank rate before it separates from the CM. In this case, it appears the slender bodies would have difficulties with dynamics during entry.

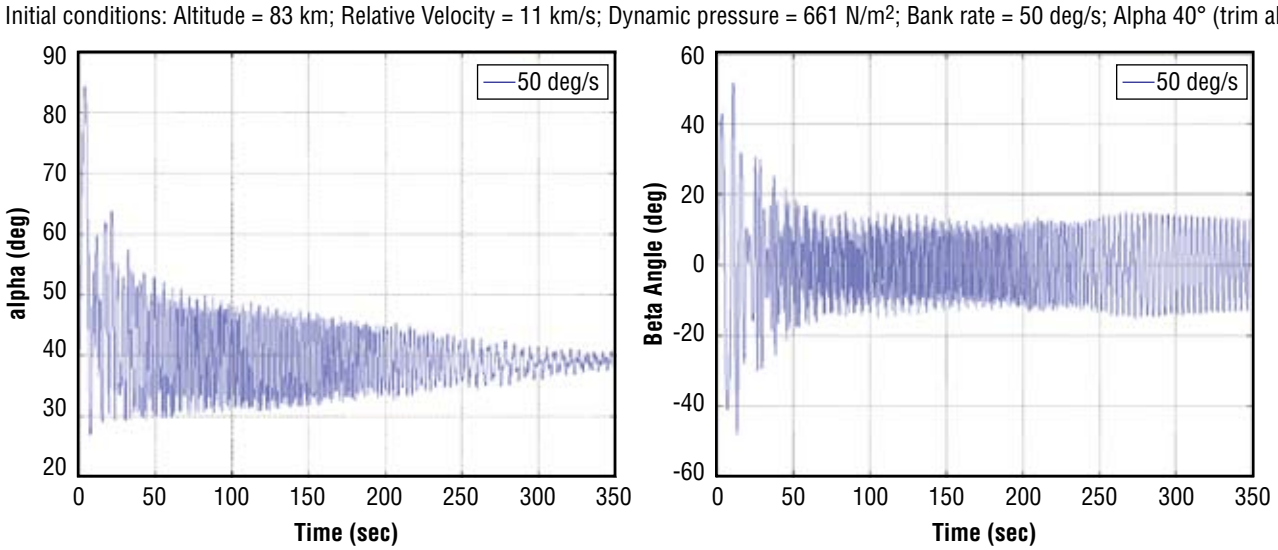

Figure 5-25. Slender Body (Biconic): Angles of Attack (alpha) and Sideslip (beta) Time Histories with Bank Rate Induced Late in the Flight

The conclusions from the trade between slender bodies and blunt bodies using a bank rate to null the lift vector are as follows: Slender bodies are difficult to enter ballistically (without RCS maintenance) unless spin-up occurs very late in the trajectory, after sufficient aerodynamic forces are generated to help stabilize the vehicle. This is due to large inertial cross-coupling. This behavior hinders the ability to spin them up using the SM before entry in case of Command Module RCS total failure. Blunt bodies can be spun up from entry or later.

5.3.1.2.5 Blunt Bodies versus Slender Bodies Comparison Summary

After all performance analyses, simulations, and evaluations were made on the representative vehicles, the spreadsheet in **Appendix 5B**, **CEV Crew Module Shape Trade Data**, was filled out. Key items of discrimination were then flagged as follows:

- Green: a particularly advantageous feature;
- Yellow: a design challenge, operational limitation, or requiring small technology development; and
- Red: a major design challenge, operational impact, or significant technology advancement required.

For the blunt-body, the key benefits were found to be:

- A more familiar aerodynamic design from human and robotic heritage—less design time and cost;
- Acceptable ascent and entry ballistic abort load levels;
- A proven passive, ballistic abort method (as performed on Soyuz);

- Crew seating orientation ideal for all loading events;
- Easier LV integration and controllability;
- TPS not exposed during mission;
- Possible early use of reusable TPS rather than ablator (ISS and LEO missions); and
- If land-landing approach fails, water-landing capability is a known fallback solution.

Major challenges appeared to be:

- Long-range skip-entry or aerocapture techniques must be used to achieve a CONUS land landing from the Moon for anytime return; and
- Land-landing stability (preventing tumbling) and load attenuation may be a significant challenge. (Note that Soyuz tumbles on 80 percent of landings.)

Minor challenges discovered were:

- Requires capsule reshaping or better packaging for CG (compared to Apollo) to achieve a monostable vehicle;
- Requires adequate free-fall time during high-altitude ascent aborts to separate the SM and rotate the capsule to a heat shield-forward attitude;
- Land-landing sites in CONUS must be very near the West Coast for proper SM disposal and potential ballistic abort entry; and
- Land landing generates limitations for ISS return opportunities, which can be solved by proper mission planning and multiple CONUS sites.

For the slender body, the most important benefits were:

- The SM can be integrated and potentially reused, which:
  - Allows use of further inland land-landing sites—at least 550 nmi. (However, this may be extremely limited due to protection for population overflight.)
  - Easily provides necessary delta-V and ECLSS for an aerocapture or skip-entry return.
- The vehicle attitude is pre-set for launch abort, i.e., the vehicle does not need to "flip around" to get the heat shield forward on ascent abort;
- Better separation of alternate landing sites for weather avoidance;
- At least daily land-landing opportunities for routine ISS return or medical mission, although this was not a requirement; and
- Lunar return can land on land in south CONUS using Apollo up-control guidance.

Significant challenges for the slender body were found to be:

- Crew seats (and displays/controls) must rotate 90 deg in flight to achieve proper load direction for ascent versus entry/landing;
- Ballistic ascent abort g-loads are unacceptable to crew survival unless ascent trajectory is significantly depressed like Shuttle; and
- Requires coordinated RCS firings to spin up vehicle properly and may require RCS to maintain banking motion during a ballistic abort due to inertial cross-coupling; hence, no passive re-entry mode would be available during off-nominal entry as Soyuz; and
- Development would take significantly longer and cost more due to added weight and shape complexity.

In addition, minor challenges encountered were:

- TPS exposed on ascent and rest of mission;
- Requires landing orientation control—likely for water or land—and attenuation technology development;
- May require drogue parachute repositioning event (similar problem addressed in X–38);
- Ejection seat design may be challenging to avoid ejection into parachutes;
- Monostable configuration is problematic for axisymmetric shapes—needs detailed aero analysis; and
- Lunar return heating is extremely high (heavy heat shield).

5.3.1.2.6 Blunt Bodies versus Slender Bodies Conclusions

To summarize the results, it appeared that the capsule configurations have more desirable features and fewer technical difficulties or uncertainties than the slender body class of vehicles. Because one of the primary drivers for the selection was the minimal time frame desired to produce and fly a vehicle, the blunt bodies had a definite advantage. All the human and robotic experience NASA has had with blunt bodies has led to a wealth of knowledge about how to design, build, and fly these shapes. A slender, lifting entry body (without wings, fins, or control surfaces) has never been produced or flown by NASA.

The blunt-body has been shown in previous programs to be able to meet the requirements of the LEO and lunar return missions. However, the new desires expressed for a CEV produce some uncertainties and challenges. Perhaps the major concern is the land-landing design challenge, including the skip-entry, sites selection, and impact dynamics. However, the capsule approach has a proven water-landing capability that can be used as a fall-back approach if further studies show the land landing to be too costly, risky, or technically difficult. Another challenge would be to develop a shape to more easily achieve monostability (as compared to Apollo) and achieve more than 0.3 L/D (at least 0.4 L/D). An L/D of 0.4, which appears achievable, is necessary to provide reasonable CONUS land-landing sites in terms of number, size, in-land distance, and weather alternates, and to increase the return opportunities. In addition, it provides lower nominal g-load and better skip-entry accuracy, which reduces skip delta-V requirements. This may result in higher heating on the shoulder and aft side of the vehicle, but this does not appear to be a great TPS concern.

The slender body class of vehicles has several characteristics that create concern about the time required for development. The trade study analysis and spreadsheet results do not indicate that a slender body would be infeasible, simply that there are several concerns and design problems that would require further significant analyses, design iterations, trades, testing, and development. First, they would require substantially more aerodynamic, aerothermodynamic, and TPS design and development work than a blunt-body. Second, the loads directions issue would need to be solved, including potential crew seat rotation, landing orientation control, and landing attenuation. Water-landing impacts and dynamics would need extensive design and test work done. The ascent trajectory would need to be tailored (depressed) to reduce ballistic ascent abort loads due to the fact that slender bodies have high ballistic numbers.

Additionally, the ballistic abort mode problem would need to be solved. At first glance, the slender bodies do not behave dynamically stable when spun up to null the lift vector. They appear to require RCS control or very judicious mass placements for inertias alignment. As an alternative, a configuration with an independent, separable abort capsule could be designed to eliminate the passive, ballistic abort concerns, but this is difficult to design for crew load orientations and difficult to design without adding substantial weight for additional TPS, recovery systems, etc. The ability to integrate an SM into a slender body design is advantageous, but creates an extremely massive entry vehicle and limits descent options to three very large, round chutes due to mass.

The conclusions from the capsules versus slender bodies trade were:

- Using an improved blunt-body capsule is the fastest, least costly, and currently safest approach for bringing lunar missions to reality; and
- Improvements on the Apollo shape will offer better operational attributes, especially with increasing the L/D, improving CG placement feasibility, and potentially creating a monostable configuration.

Based on this preliminary trade study, the class of blunt bodies was selected for further investigation to ultimately define a CEV CM shape.

5.3.1.3 Capsule Shape Trade

5.3.1.3.1 Driving Factors

In the trades between blunt body and slender body classes of vehicles, representative vehicles were adequate for downselect. Within a class, however, optimization requires parameterization. Multiple basic capsule shapes were available to investigate as potential CEV CM OML candidates. The driving factors, particularly for a capsule OML, that resulted from the initial trade study were as follows:

- L/D of 0.4 is required to achieve the necessary range capability between the landing site and SM disposal for the ISS missions, as well as to increase the performance and accuracy of the skip-entry for lunar returns and to reduce delta-V requirements. In addition, increased cross-range capability resulting from increased L/D helps to reduce the number of landing sites and time between opportunities for ISS return;
- Ballistic abort capability, including monostability;
- Satisfaction of acceleration loads across the spectrum of flight conditions within crew limits;
- Feasible, attainable CG requirements;
- Adequate static stability and low sensitivity of L/D to Z_{cg} dispersions (approximately the same or better than Apollo);
- Adequate volume and shape for crewed operations;
- Reusable TPS on the aft-body;
- Low technology requirements; and
- Short development time.

5.3.1.3.2 Axisymmetric Capsule Shape Variations and Effects

The basic capsule shapes shown in **Figure 5-26** were analyzed using a modified Newtonian aerodynamics code. Various shape parameters, such as after-body cone angles, base radii, corner radii, heights, and others, were parametrically changed and evaluated in the aerodynamics generator to assess the effects of these parameters on the desirable criteria. Of primary interest were the sidewall angle (theta), the corner radius (Rc), and the base radius (Rb).

The data quickly indicated the desired path to pursue. The shapes similar to Soyuz could not attain the 0.4 L/D without high angles-of-attack and excessive acreage of after-body sidewall heating. Although after-body TPS could be made to handle the environments (Soyuz and Apollo employed ablative TPS across the entire vehicle), better shapes were available for possibly achieving the desired reusable after-body TPS. The Gemini/Mercury class of shapes showed no significant advantage over plain cones and required more Z_{cg} offset and higher angle-of-attack than plain cones for 0.4 L/D. Although the extended frustum apexes could help increase monostability, a plain cone of the same height was shown to produce more. The Moses-type shapes, while extremely stable with the proper CG, could not attain 0.4 L/D easily. In addition, the crew seating orientation would have to vary to always produce loads perpendicular to crew spines, much as required for the slender bodies. As on the Aero-assist Flight Experiment (AFE) shape, the non-axisymmetric heat shield would produce CG and angle-of-attack benefits but has no flight heritage. The ESAS team decided to leave this AFE shape for further analysis as a potential improvement over a plain conical, axisymmetric shape. The conical, axisymmetric shapes such as Apollo were determined to be preferable since they had the best experience base and aerodynamic familiarity while being capable of producing the desired L/D, monostability, low technology needs, and ease of fabrication due to axisymmetry. Hence, they were found to merit further trade analyses and investigation.

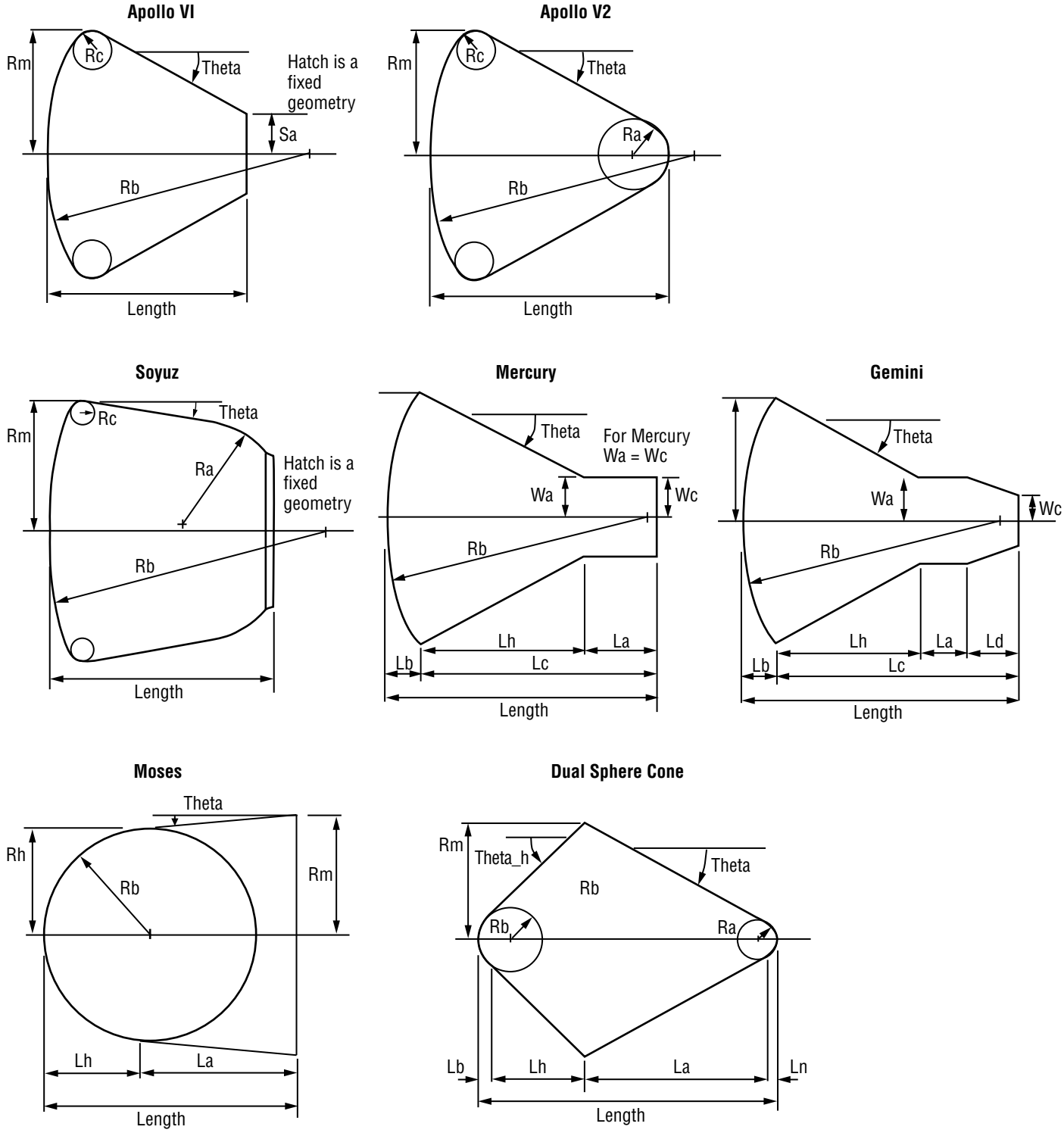

Figure 5-26. Initial Set of Capsule Shapes and Parametric Variables Considered

Figure 5-27 shows an example of how the effect of parameter variations was measured. The figure is a 3–D contour plot. Each intersection point on the colored contour curves represents a different analyzed case. The corresponding value for each case is measured by the values on the Z-axis. In this figure, the quantity of interest is the percent volume below the last monostable CG location (moving away from the heat shield) for 0.4 L/D. This value represents an important quantity for packaging if a monostable vehicle is desired. In this particular figure, a 40 percent contour is also shown—an arbitrary metric for desired volume. An ideal packaging percent volume would be 50 percent if the objects in the vehicle were of uniform density. From this plot, the best vehicle for monostability would have a small sidewall angle (theta), a small base radius, and a large corner radius. Of these three parameters, a corner radius was the largest discriminator, followed by the sidewall angle (theta).

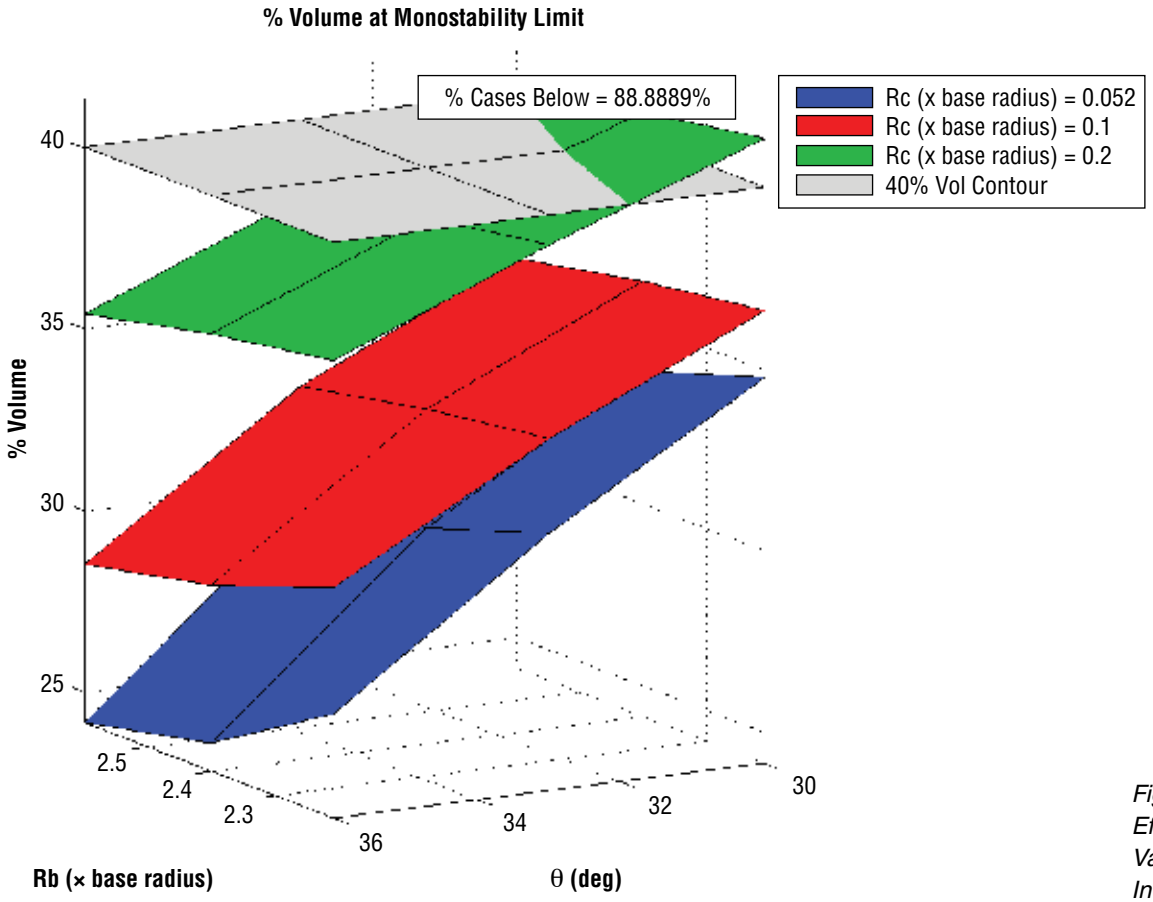

Figure 5-27. Example of Effect of Parameterized Variables on Quantity of Interest (Monostability)

Each of the parameters influenced the important factors in different ways, but all of the blunt-bodied vehicles exhibited similar trends, regardless of their original shape. **Table 5-10** shows the overall affect of this parameterization. The arrows indicate if the parameter (first row) should increase or decrease for a desired quality (left column) to improve.

Table 5-10. Trends Associated with Parameterized Values for Conical Shapes (Based on Constant Height)

	Corner Radius	Base Radius	Cone Angle
To decrease Z_{cg} offset required for 0.4 L/D	↓	↑	↓
To increase % volume below first monostable CG	↑		↓
To increase C_m-alpha magnitude (static stability) at 40% volume CG	↓	↓	
To decrease heat rate	↑	↑	
To decrease sensitivity of L/D to Z_{cg} at 40% volume CG	↑	↓	
To decrease X_{cg}/D at 40% volume CG (effects landing stability)	↓	↑	↑

As illustrated in each column, many of the desired characteristics conflicted with each other. There was no clear variation in a single parameter that would help in all areas. It would require a weighting and compromise of the various desired characteristics to produce a "best" set of vehicle shape parameters. Generally speaking, the desire for monostability corresponded with improved L/D sensitivity to Z_{cg} and heat rate (perhaps two of the least demanding desires), but conflicted with all other (more important) characteristics. Thus, it became difficult to establish an optimal vehicle shape, especially since the requirements for these vehicles were not well defined.

In order to arrive at a desirable sidewall angle, a simultaneous comparison of all parameters was needed. Thus, the vehicles were compared side-by-side with a table of relevant aerodynamic characteristics. The following figures show some of the noted trends.

Figure 5-28 shows how changing only the length affects the vehicle performance characteristics. **Figure 5-29** shows the effect of a changing sidewall angle. A careful study of these vehicles reveals that the length of the aft cone generally has little effect except for one main difference: a longer cone is more monostable. This means there is a greater percentage of the total OML volume below the minimum monostable CG for a longer cone height. Therefore, in theory, the longer cone height OML should be easier to package and attain a monostable condition. If the length is held constant, and the aft cone sidewall angle is changed, the figures show that a smaller (shallower) angle is more monostable. (The CG position for monostability allows a greater percentage volume between the CG position and the heat shield.) However, CG height for constant volume is relatively higher in the vehicle with the smaller sidewall angle. The other parameters vary very little. Other variations were examined, including beveling and rounding of the top of the cone. Besides bringing the trim line only slightly closer to the centerline, the biggest effect of an increase in bevel angle or rounding radius was a decrease in monostability (an undesirable result).

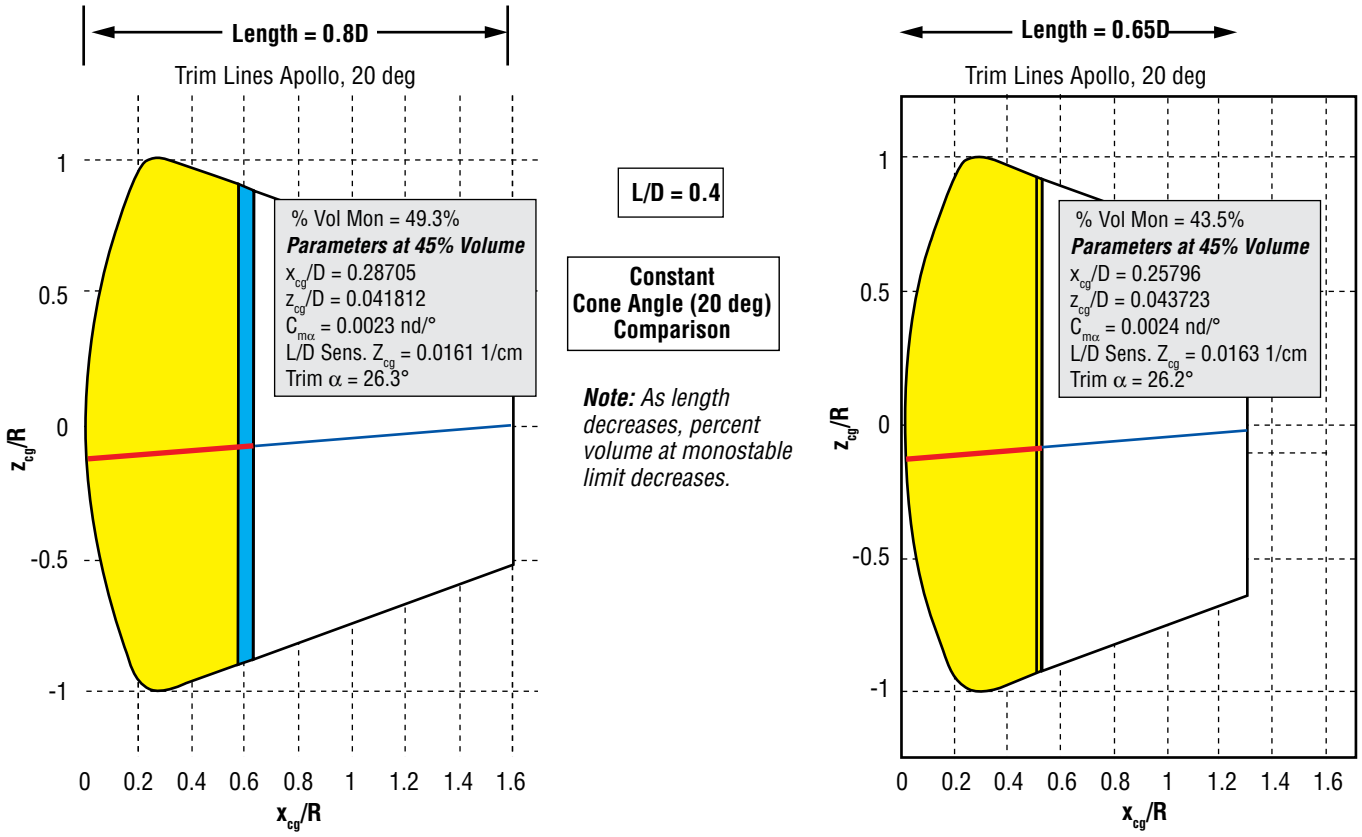

Figure 5-28. Affect of Length on Aerodynamic Characteristics

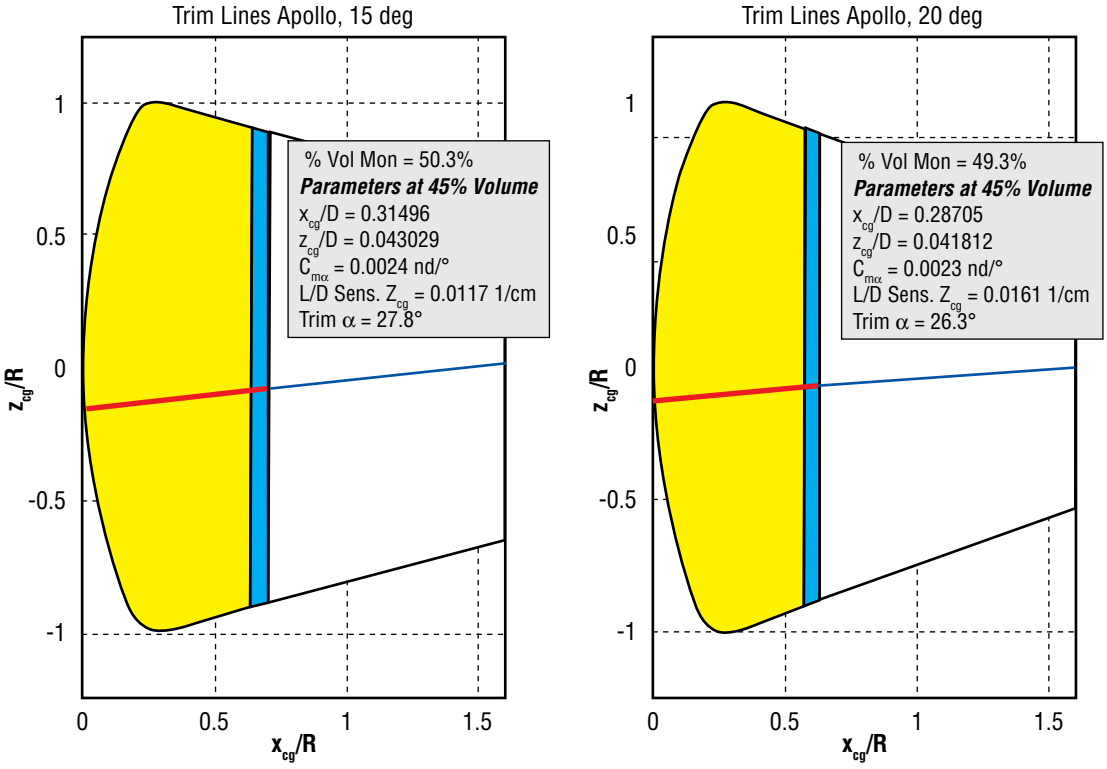

Figure 5-29. Affect of Sidewall Angle on Vehicle Aerodynamics at Constant Length

5.3.1.3.3 Initial Axisymmetric Capsule Shape Downselect

In order to balance the effects of the changing parameters, a baseline vehicle was selected with a shallower cone angle of 20 deg (since this had the least effect on other parameters), with the same base and corner radius as Apollo. This new vehicle trended toward the family of vehicles represented by the Soyuz capsule, which has an even shallower sidewall angle. This vehicle is shown in **Figure 5-30** below. It was estimated that an achievable X-axis center of gravity (X_{cg}) position would lie at or around the 45 percent volume level. In that case, the Z_{cg} offset required for 0.4 L/D would be roughly 0.053 times the diameter. For this shape, the monostable CG position could be as high as the 48.6 percent volume level, which would therefore leave some margin for assured monostability.

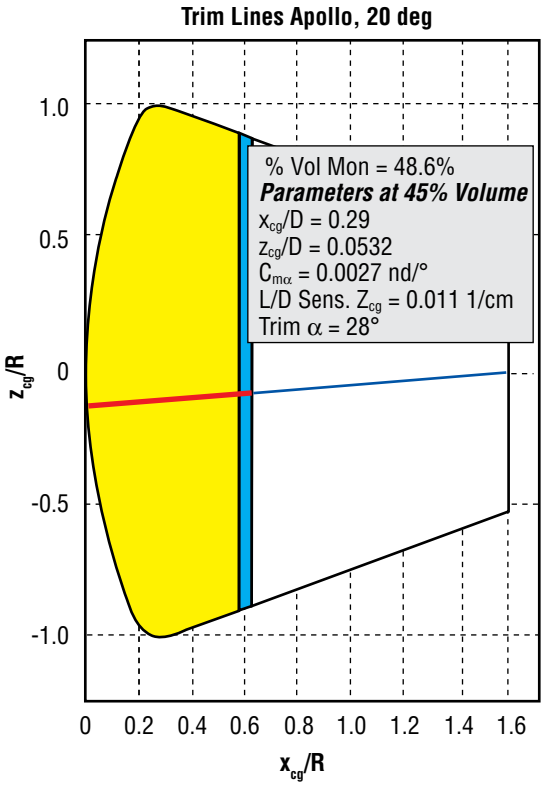

Figure 5-30. Initial Baseline Capsule Data

Figure 5-31 shows the pitching moment coefficient (C_m) curves versus angle-of-attack for this vehicle. The black line shows the C_m curve for the desired CG position at the 45 percent volume level. The red line corresponds to the first monostable CG position at the 48.6 percent volume level. The blue line designates a bi-stable CG position closer to the apex that was arbitrarily chosen for visualization.

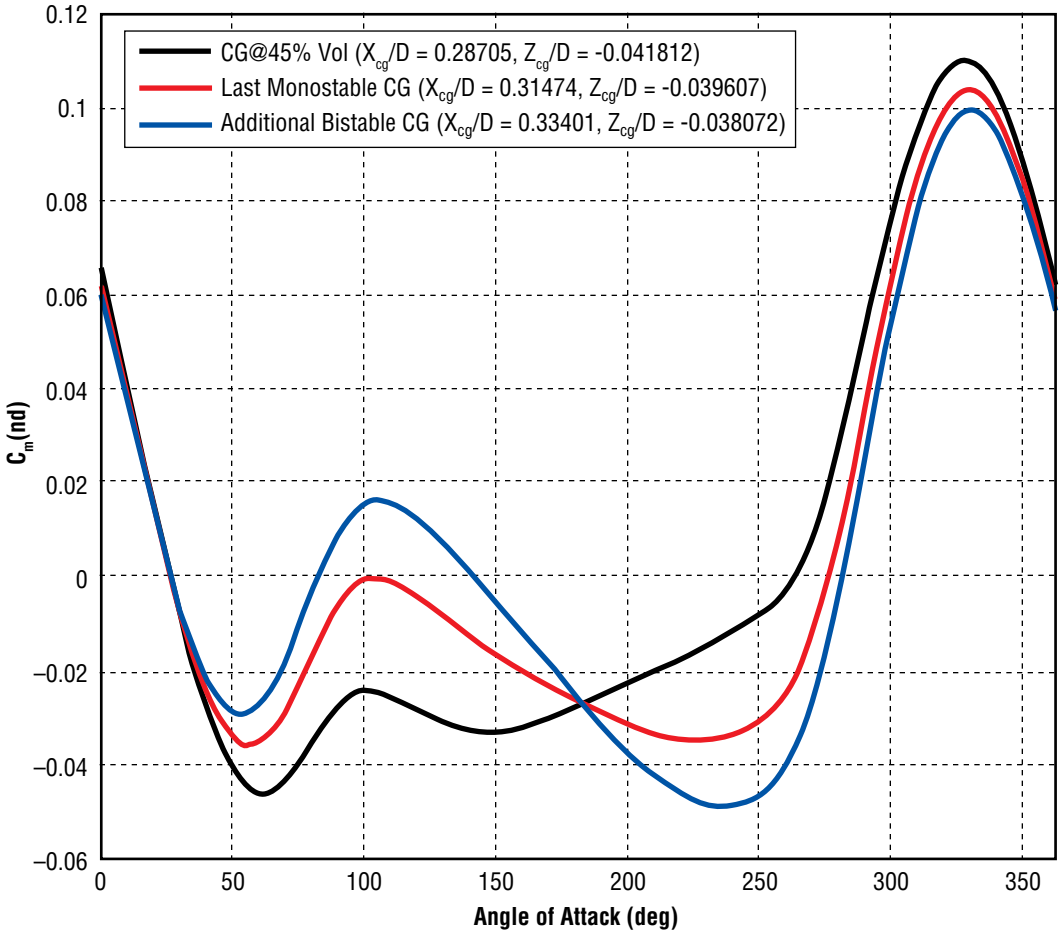

Figure 5-31. Pitching Moment Coefficient Curves for the Baseline Capsule

5.3.1.3.4 Axisymmetric Capsule Shape Variations

One way to achieve the required L/D is to use a nonaxisymmetric shape similar to the AFE shape mentioned previously. A computer-generated shape optimization approach was pursued to attempt to optimize an OML that exhibited some of the desirable characteristics without necessarily being axissymmetric.

The investigation of various "optimized" shapes used the optimization capabilities of the CBAERO computer code. These optimized shapes held the aft-body shape fixed, while the heat shield shape was optimized to meet the trim and L/D constraints. CBAERO permits the very general optimization of the configuration shape, where the actual nodes of the unstructured mesh are used as the design variables. For instance, a typical capsule mesh contained approximately 20,000 triangles and 10,000 nodes. Full shape optimizations were performed where the Cartesian coordinates (x,y,z) of each node were used as design variables. In the example discussed below, there would be 3 x 10,000 = 30,000 design variables.

Often, only the heat shield was optimized, thus reducing the total number of design variables. **Figure 5-32** shows the axisymmetric baseline CBAERO grid. The orange region contains those triangles that lie within the optimization region (2,774 nodes, or 8,322 design variables). **Figure 5-33** shows one optimization result in which L/D was optimized with the moment constrained to zero and the volume held constant. The resultant geometry exhibits a "trim tab" on the upper windward surface, which the optimizer has produced in an attempt to trim the

vehicle while maintaining both the required L/D of 0.4 and the vehicle volume. The surface also exhibits some concavities, which may lead to increased heating or other complex effects. More recent optimization studies have imposed constraints on concavities, and it may be desirable to revisit these optimized shapes or start with the AFE baseline.

Figure 5-32. Baseline Axisymmetric Shape CBAERO Grid

Figure 5-33. An Optimization Result from CBAERO Where the Moment was Constrained to Zero and the Volume Held Constant

The engineering level analysis of CBAERO, as well as efficient coding of the gradient process, enables these optimized solutions to be performed with tens of thousands of design variables and multiple constraints in a matter of minutes-to-hours on a typical desktop Personal Computer (PC). The results shown here typically took 100 to 200 design iterations and less than 60 minutes on a PC laptop.

Various candidate designs were shown to meet both the trim and L/D requirements; however, the complexity of the shapes led to the desire to investigate simpler (but nonaxisymmetric) shapes that might obtain similar results.

Various rotated heat shield concepts were also investigated to examine their ability to reduce the required "z" offset in the CG to trim the vehicle at the desired L/D of 0.4. The various configurations analyzed were capable of reducing the "z" offset; however, the shapes all failed to meet the required L/D of 0.4.

5.3.1.3.5 Initial Capsule Shape Trade Conclusions

For the initial capsule shape trade study, detailed and extensive analysis of parametric effects and trends of various capsule shapes and features indicated that achieving the desired characteristics was indeed a formidable task. A compromise was made to achieve all of the desired characteristics as closely as possible while minimizing the detrimental effects. The resultant axisymmetric shape (shown in **Figures 5-30** and **5-32**) was a 5.5-m diameter capsule with Apollo heat shield and 20-deg aft-body sidewall angle. The capsule offered large volume (i.e., large enough for surface-direct missions), easily developed axisymmetric shape, the best chance for monostability, L/D = 0.4 with attainable CG, adequate static stability, and low L/D sensitivity to CG dispersions. Nonaxisymmetric shape optimization had shown that this technique could indeed reduce CG offset requirements if needed in the future. Further detailed analysis was then required to further define the performance characteristics of the axisymmetric shape.

5.3.1.3.6 Detailed Aerodynamic Analyses of Initial Baseline Capsule Shape

Once the baseline shape for the CEV was defined as a 5.5-m diameter capsule with Apollo heat shield and 20 deg aft-body sidewall angle (shown in **Figure 5-30**), a number of analyses was conducted to further define the performance and suitability of the selected design. Some specifications are shown in **Figure 5-34**. Data shown in the figure for angle-of-attack and CG location were based on modified Newtonian aerodynamics and were later modified by CFD calculations of the aerodynamics. The CFD aerodynamics give a high-fidelity estimate of the required trim angle and radial CG offset needed for L/D = 0.4. The Newtonian results generally give good estimates of the required trim angle for a given L/D, but underestimate the radial CG offset required to achieve the trim angle. In addition, CFD aerothermodynamics results were used to estimate geometry effects on heating, anchor other predictive tools, and provide input to TPS sizing analyses. Details of aerodynamic CFD analysis, the tools used for CFD aerodynamics, CFD aerothermodynamics, and TPS analysis, as well as the process used for the results presented in this report are included in **Appendix 5C**, **CFD Tools and Processes**.

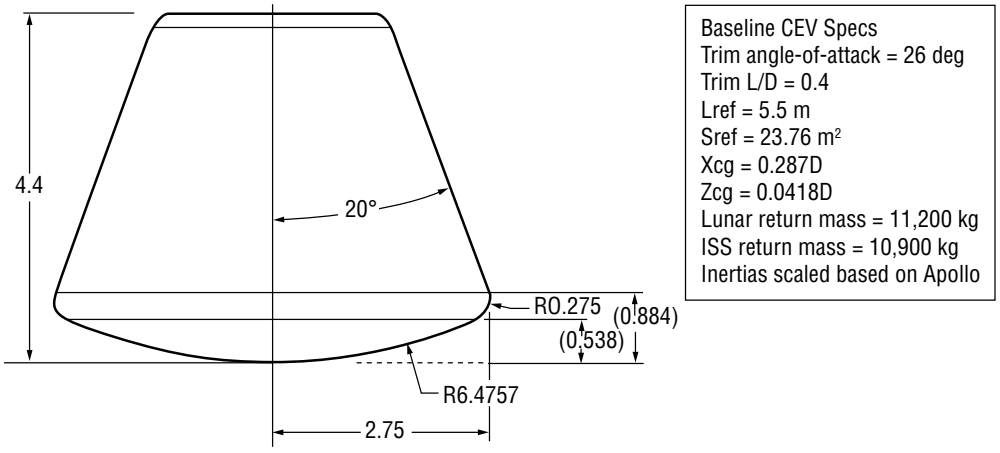

Figure 5-34. Initial CEV Baseline Specifications

5.3.1.3.7 Detailed TPS Analyses of Initial Baseline Capsule Shape

The general GR&As for the CEV TPS design analysis, modeling assumptions, and data sources are presented below.

Geometry

The OML definition for both the baseline axisymmetric capsule and the AFE-based non-axisymmetric capsule were obtained from the same triangulated surface grid used in the engineering-based aerothermal analysis.

Aerothermodynamics

The aerothermal environments were provided by the CFD-anchored engineering-based CBAERO code (Version 2.0.1). The aeroheating environments consisted of the time history throughout the trajectory of the convective heating (recovery enthalpy and film coefficient), the shock layer radiation heating, and the surface pressure for each surface triangle. No margins on the aeroheating environments were used in the TPS analysis and sizing because conservative margins were used in the TPS analysis.

Trajectory

Both guided entry (nominal) and passive ballistic (abort) trajectories were examined for 8 km/sec (LEO) entry and 11 km/sec and 14 km/sec (Lunar return) entries. In addition, for the 11 km/sec entry, a skipping guided and skipping ballistic trajectory were also provided and analyzed. These trajectories were generated for a nominal L/D ratio of 0.4. Among other flight parameters, these trajectories consisted of the time history of the Mach number, angle-of-attack, and free-stream dynamic pressure. This data was interpolated along each trajectory within the aerothermodynamic database to generate the aeroheating environments.

TPS and Aero-Shell Material and Properties

A summary of the structural and carrier panel aero-shell materials is presented in **Table 5-11**, which includes material selection and representative thicknesses. A similar summary of the TPS materials is presented in **Table 5-12**. For the reusable TPS concepts, the thermal, optical and mechanical properties were taken from the Thermal Protection Systems eXpert (TPSX) online database. A detailed listing of the benefits and concerns associated with each TPS material is given in **Table 5-13**.

Table 5-11. Structural Materials and Thicknesses Analyzed in Studies

Structure Choices	Material	Thickness (cm)
8 km/s aft body	Aluminum 2024	0.2540
	RTV	0.0508
All heat shields, 11 km/s aft body	Graphite Polycyanate	0.0381
	Aluminum Honeycomb	1.2700
	Graphite Polycyanate	0.0381
	RTV	0.0508

The carrier panel aero-shell design consisted of a composite honeycomb panel, with 0.015 inch graphite polycynate face sheets bonded to an 0.5 inches aluminum honeycomb core with a mean density of 8.0 lb/ft^3. The ablator TPS materials were direct-bonded onto the carrier panel using a high-temperature adhesive. The reusable TPS concepts were direct-bonded onto the primary structure (modeled as 0.10 inches Aluminum 2024) using Room Temperature Vulcanized (RTV) adhesive for the blanket concepts, while the ceramic tiles used a Nomex Strain Isolation Pad (SIP) with a nominal thickness of 0.090 inches and two RTV transfer coats.

The TPS split-line definition was generated using the non-conducting wall temperatures, multi-use allowable temperature for the nominal trajectory, and single-use for the abort trajectories. For the LEO return CEV design, the heat shield material selected was the Shuttle-derived high-density ceramic tile (LI–2200), while the aft-body TPS material consisted of existing Shuttle ceramic tile (Reaction-Cured Glass (RCG-) coated LI–900) and flexible blanket systems (AFRSI and FRSI). Temperature limits for these materials are presented in **Table 5-14**.

Table 5-12. TPS Materials

TPS Choices	Material	Thickness (cm)
FRSI	FRSI	Varying
	DC92	0.0127
AFRSI	EGLASS	0.0279
	QFELT_mquartz	Varying
	ASTRO_quartz	0.0686
	GrayC9	0.0419
LI–900	Nomex SIP	0.2286
	RTV	0.0305
	LI900	Varying
	RCG	0.0305
LI–2200	Nomex SIP	0.2286
	RTV	0.0305
	LI2200	Varying
	TUFT12	0.2540
Silicon Infused Reusable Ceramic Ablator (SIRCA)	Nomex SIP	0.2286
	RTV	0.0305
	SIRCA-15F_V	Varying
	SIRCA-15F_C	0.2540
SIRCA calculated in Fiat	SIRCA-15	Varying
SLA	SLA-561V	Varying
Avcoat	Avcoat	Varying
PICA	PICA-15	Varying
Carbon Phenolic	Carbon Phenolic	Varying
Mid-Density Carbon Phenolic	Carbon Phenolic Mid-Density	Varying
Carbon Facesheet 0.6-cm	Carbon Fiber	Varying
	Carbon Facesheet	0.6000
Carbon Facesheet 1-cm	Carbon Fiber	Varying
	Carbon Facesheet	1.0000
Carbon Phenolic	Carbon Phenolic	Varying

Table 5-13. Summary of TPS Material Options and Their Characteristics

	Carbon Phenolic	AVCOAT	PICA	C–C facesheet/Carbon fiberform	Mid-density C–P
Characteristics	Heritage tape-wrapped composite developed by USAF used on BRVs, and as heat shields on Pioneer Venus and Galileo probes (many fabricators)	Filled epoxy novolac in fiberglas-phenolic honey comb used as Apollo TPS (developed by Avco; now Textron)	Phenolic impregnated carbon fiberform used as heat shield on Stardust (developed by Ames, fabricated by FMI)	Carbon-carbon facesheet co-bonded to carbon fiberform insulator used as heat shield on Genesis (developed by LMA, fabricated by CCAT)	Notional developmental material to span the density range 480–960 kg/m^3 by densifying PICA or making low-density carbon phenolic (ongoing development at Ames)
Density, kg/m^3 (lbm/ft^3)	1,441.66 (90)	529 (32)	236 (15)	1,890/180 (118/11)	480.55 (30)
Aerothermal performance limit and failure mode	20,000 W/cm^2 and 7 atm; char spall	700 W/cm^2 and 1 atm; char spall	2,000 W/cm^2 and 0.75 atm; char spall	5,000 W/cm^2 and 5 atm (postulated); strain failure at C–C/insulator interface	5,000 W/cm^2 and 1 atm (postulated); char spall
Attachment to substructure	Fabricated and cured on mandrel; secondary bonding	Honeycomb bonded to structure; cells individually filled with caulking gun	Tile bonded to structure (fabricated as one-piece for Stardust)	Tile bonded to structure (fabricated as one-piece for Genesis)	Multiple options dependent on material architecture. Most likely tiles bonded to structure
Manufacturability and scalability (to 5.5 m)	Not possible to tape-wrap a quality composite with suitable shingle angle at that scale	Pot life of composite may preclude filling all cells and curing on aeroshell of this size	Can be fabricated as tiles, but not demonstrated	Can be fabricated as tiles, but not demonstrated	Most likely to be fabricated as tiles, but not demonstrated
Current availability	Heritage material no longer available; USAF developing new generation using foreign precursor	Not made in 20 years. Textron claims they can resurrect	FMI protoype production	Currently available (CCAT for LMA)	Scalability not an issue if fabricated as tiles
Human-rating status	Space-qualified for uncrewed misssions	Human-rated in 1960s	Space-qualified for uncrewed missions (not tiles)	Space-qualified for uncrewed missions (not tiles)	Developmental
Test facility requirements (include radiation and convective heating)	High-density all-carbon system will be opaque to radiant heating over broad spectrum (Galileo experience)	Opacity over radiative spectrum needs to be evaluated but no facility available	Opacity over radiative spectrum needs to be evaluated but no facility available. Opacity at UV wavelengths demonstrated (lamp tests)	High-density all-carbon system will be opaque to radiant heating over broad spectrum	Mid-density all-carbon system will be opaque to radiant heating over broad spectrum
Test set requirements (experience with range of test conditions/sample sizes)	Strong experience so number of required tests would be relatively low	Extensive ground tests in 1960s, augmented by flight tests and lunar return missions. Radiative heating rates for CEV will be higher	Qualified to 1,600 W/cm^2 and 0.65 atm for Stardust. Issues with tile fabrication/gap fillers has not been evaluated	Qualified to 700 W/cm^2 and 0.75 atm for Genesis. Issues with tile fabrication/gap fillers has not been evaluated	Very limited test data on developmental materials. Issues with tile fabrication/gap fillers has not been evaluated
Radiation (CGR) Protection characteristics	Limited data. Some promise	Unknown	Unknown	Unknown but not expected to be of value	Unknown, but could provide some protection
Material response model status	High fidelity model for heritage material (which is no longer available)	High fidelity model developed under Apollo. Currently, only Ames can utilize	High fidelity model developed for Stardust	Material modeling is straightforward; uniformity of 2-layer contact unknown	Developmental materials; no model currently available but could be scaled from existing models
Micrometeroid/Orbital Debris (MMOD) impact tolerance	Denser materials more robust, glass more forgiving than carbon				
Landing shock tolerance	Heat shield is ejected, so landing shock not important for forebody				
Salt water tolerance (water landing)	Any of these materials would need to be dried out after water landing (or replaced). Denser will absorb less moisture.				

Table 5-13. (Continued)
Summary of TPS Material Options and Their Characteristics

	SLA–561	SRAM20	PhenCarb-20	PhenCarb-32	LI–2200
Characteristics	Filled silicone in fiberglass-phenolic honeycomb used as heat shield on Mars Viking, Pathfinder and MER landers. Developed and fabricated by LMA	Filled silicone fabricated by Strip Collar Bonding Approach (SCBA) or large cell honeycomb. Developed and fabricated by ARA	Filled phenolic fabricated by SCBA or large cell honeycomb. Developed and fabricated by ARA	Filled phenolic fabricated by SCBA or large cell honeycomb. Developed and fabricated by ARA	Glass-based tile developed by LMA and used as windside TPS on Shuttle. Several fabricators
Density, kg/m³ (lbm/ft³)	256 (16)	320 (20)	320 (20)	512 (32)	352 (22)
Aerothermal performance limit and failure mode	300 W/cm² and 1 atm (postulated); char spall	400 W/cm² and 0.5 atm (postulated); char spall	800 W/cm² and 0.75 atm (postulated); char spall	2,000 W/cm² and 1 atm (postulated); char spall	Shuttle-certified to 60 W/cm² and 1 atm; glass melt, flow and vaporization at higher heat fluxes
Attachment to substructure	Honeycomb bonded to structure; cells filled by pushing compound into honeycomb	SCBA uses secondary bonding. Compound pushed into cells in honeycomb approach	SCBA uses secondary bonding. Compound pushed into cells in honeycomb approach	SCBA uses secondary bonding. Compound pushed into cells in honeycomb approach	Tile bonded to SIP which is bonded to structure (Shuttle Technology)
Manufacturability and scalability (to 5.5 m)	Pot life of composite may preclude filling all cells and curing on aeroshell of this size	SCBA approach with secondary bonding should scale, but not demonstrated	SCBA approach with secondary bonding should scale, but not demonstrated	SCBA approach with secondary bonding should scale, but not demonstrated	Should scale easily
Current availability	In production (LMA)	Prototype production in small sizes	Prototype production in small sizes	Prototype production in small sizes	Stockpiles of billets at KSC. Manufacturing can be restarted if necessary
Human-rating status	Space-qualified for uncrewed missions (not tiles)	Developmental	Developmental	Developmental	Human-rated for Shuttle
Test facility requirements include radiation and convective heating)	Opacity over radiative spectrum needs to be evaluated but no facility available. Opacity at UV wavelengths demonstrated (lamp tests)	Opacity over radiative spectrum needs to be evaluated but no facility available. Opacity at UV wavelengths demonstrated (lamp tests)	Opacity over radiative spectrum needs to be evaluated but no facility available. Opacity at UV wavelengths demonstrated (lamp tests)	Opacity over radiative spectrum needs to be evaluated but no facility available. Opacity at UV wavelengths demonstrated (lamp tests)	Radiative heating not an issue for Block 1 applications
Test set requirements (experience with range of test conditions/sample sizes)	Qualified to 105 W/cm² and 0.25 atm for Pathfinder. Currently being tested to 300 W/cm for MSL	Developmental material currently being tested to 300 W/cm² for MSL	Developmental material has been tested to 700 W/cm under ISP	Developmental material has been tested to 800 W/cm under ISP	Gaps and gap fillers need to be tested at higher heat fluxes for CEV Block 1 application
Radiation (CGR) Protection characteristics	Unknown	Unknown, but could provide some protection	Unknown, but could provide some protection	Unknown, but could provide some protection	Unknown
Material response model status	Existing model very limited and not high fidelity. High fidelity model will be developed under ISP	Existing ARA model empirical and limited. High fidelity model will be developed under ISP	Existing ARA model empirical and limited.	Existing ARA model empirical and limited.	High fidelity model for Shuttle regime. Needs to be extended to higher heat fluxes where material may become ablator
MMOD impact tolerance	Denser materials more robust, glass more forgiving than carbon				
Landing shock tolerance	Heat shield is ejected, so landing shock not important for forebody				
Salt water tolerance (water landing)	Any of these materials would need to be dried out after water landing (or replaced). Denser will absorb less moisture.				

Table 5-14. Shuttle TPS Allowable Temperature Limits

TPS Material	Multi-Use Temperature (Kelvin, ºF)	Single-Use Temperature (Kelvin, ºF)
LI-2200 Ceramic tile	2,000, 3,140	2,000, 3,140
LI-900 Ceramic Tile	1,495, 2,230	1,756, 2,700
AFRSI	922, 1,200	1,256, 1,800
FRSI	672, 750	728, 850

Several candidate ablative materials were investigated for the lunar-return design heat shield, as presented in **Table 5-12**. On the aft-body, Shuttle-derived reusable TPS materials (LI–2200, LI–900, AFRSI and FRSI) were used for regions where the surface temperatures were within the allowable temperature range for a given material.

Initial Conditions
Initial in-depth temperature distribution was assumed to be 70°F (294.26 Kelvin) for both Earth orbit reentry and lunar return entry.

Internal Boundary Conditions
An adiabatic backwall condition was assumed for both the composite aero-shell and primary structure.

Heat Transfer Analysis and TPS Sizing
The TPS sizing analysis was conducted using a transient 1–D "Plug" model. The required TPS insulation thicknesses were computed by a TPS Sizer using the Systems Improved Numerical Differencing Analyzer (SINDA)/Fluid Integrator (FLUINT) software solver for the reusable concepts and the FIAT software code for the ablative TPS materials. For the aft portion of the capsule, a full soak-out condition was imposed for TPS insulation sizing. Because the heat shield for all capsule configurations was assumed to be ejected before landing, a non-soak-out condition (i.e., the heat transfer analysis was stopped at the end of the flight trajectory) was used for the heat shield TPS sizing. For all TPS materials, the required thickness was computed to limit the composite carrier panel and the primary aluminum structure to 350ºF (450 Kelvin).

TPS Analysis
An extensive set of analyses were performed to analyze and size the TPS for ISS, lunar, and Mars mission entry trajectories. A number of trade studies were also conducted. These results are summarized in **Appendix 5C**, **CFD Tools and Processes**.

5.3.1.3.8 Baseline Capsule "Passive" Stability Analysis

A number of analyses was carried out on the initial baseline capsule shape to assess the benefits of monostability versus bistability and the effects of the degree of monostability on a "passive," ballistic entry. The baseline shape on which these analyses were performed is depicted in **Figures 5-29** and **5-33**.

Several arbitrary CG locations were selected (**Table 5-15**), resulting in different pitching moment curves (**Figure 5-35**). Of the six CG locations, five showed different degrees of monostability and one resulted in a bistable vehicle. CG1 is the most monostable and CG5 the least monostable. CG6 represents a bistable configuration. In order to quantify the degree of monostability, each of the CG locations was associated with a parameter—hereafter referred to as "monostability percentage"—that represented the area under the absolute value of its corresponding pitching moment curve as a percentage of that of the Soyuz. Using this method, the range of initial conditions (away from nominal) that each configuration could be able to withstand without any load or heat rate violations could be represented in terms of this monostability percentage.

Two kinds of tests were run for each CG location and the three scenarios described previously (entry from LEO, ascent abort, and lunar return). These tests are described below.

- With zero initial angular rates and zero initial beta, the initial attitude is varied on alpha only from –180 to +180 deg.
- With initial attitude being the trim attitude, the initial pitch rate is varied from –5 to +5 deg/s. Yaw and roll rates are initialized to zero.

The heat rate and crew limits criteria remained the same as those described in the previous trade analysis.

Table 5-15. Selected CEV CG Locations for Passive Stability Evaluation

	Soyuz Monostable	CEV CG1 Monostable	CEV CG2 Monostable	CEV CG3 Monostable	CEV CG4 Monostable	CEV CG5 Monostable	CEV CG6 Monostable
X_{cg}/D	0.375	0.216	0.241	0.268	0.290	0.315	0.340
Z_{cg}/D	–0.0305	–0.0475	–0.0455	–0.0433	–0.0416	–0.0396	–0.0376
Percent Monostability	100	150	125	100	87	77	11

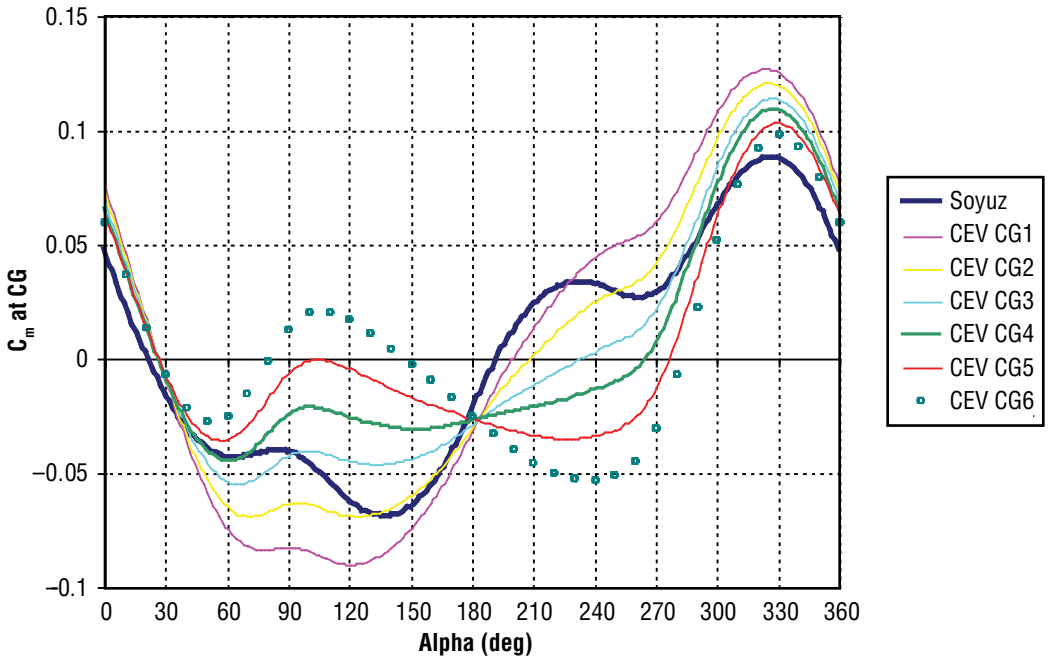

Figure 5-35. Pitching Moment Curves Associated With Each CEV CG Location Used in the Passive Stability Evaluation

The valid ranges for both types of tests for a LEO return are presented in **Figure 5-36**.

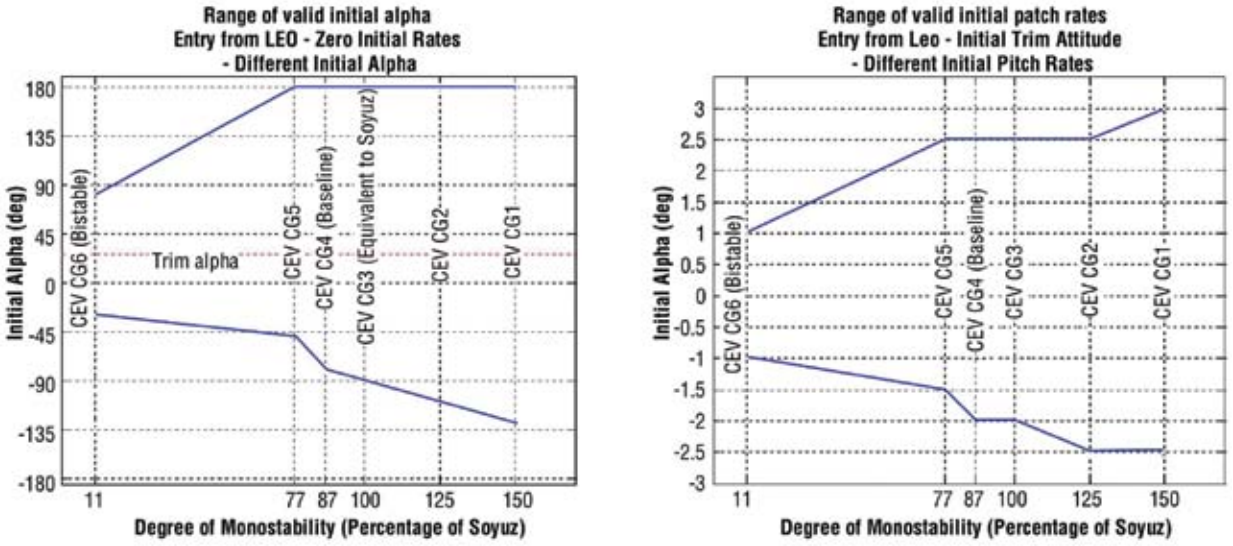

Figure 5-36. Valid Initial Attitudes and Pitch Rates in Entry from LEO versus Different Degrees of Monostability

The valid ranges for Test type 1, for an ascent abort at a trajectory point that produces the worst case heat rates, are presented in **Figure 5-37**. The results for Test type 2 are not easily quantifiable and, therefore, are inconclusive at this point.

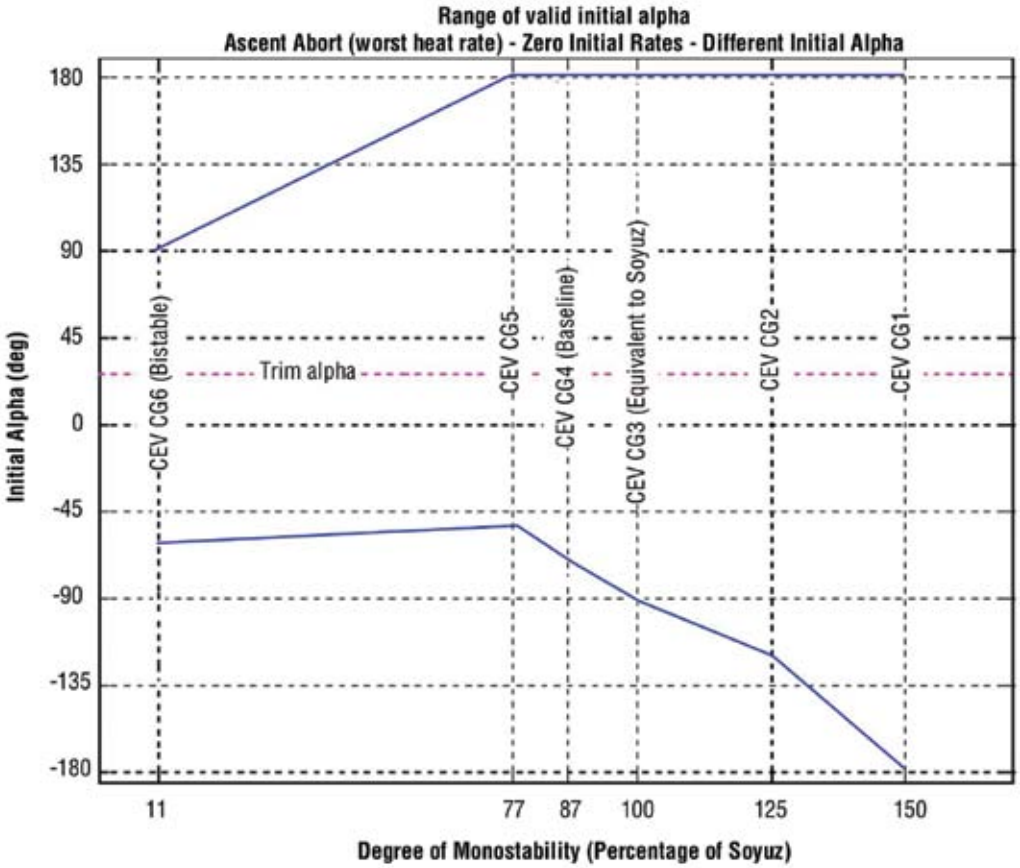

Figure 5-37. Valid Initial Attitudes in Entry from Ascent Abort (Worst Heat Rate) versus Different Degrees of Monostability

In the lunar return case, the L/D characteristics are enough to result in a high number of skip cases for all CGs tested. Therefore, in order to be able to quantify the impact of the degree of monostability in the range of initial conditions that the vehicle could passively recover from, two options were studied. These options were:

- The Z component of the CG location was set to zero. By doing this, the spacecraft was transformed into a ballistic vehicle, permitting the suppression of all the skip cases. The resulting CG locations and monostability percentages are presented in **Table 5-16**. The associated pitching moment curves are depicted in **Figure 5-38**. It can be seen in **Figure 5-38** that the CEV with CG5 becomes a bistable vehicle; therefore, CEV CG6 has been removed from the analysis. The valid ranges of off-nominal initial conditions when Z_{cg} is set to zero are presented in **Figure 5-39**.
- The induction of a spin rate to null the effect of lift, allowed the spacecraft to become close to a ballistic vehicle. A tentative spin rate of 35 deg was imparted before heat rate buildup. In this case, the CG locations are still those of **Table 5-16**. This technique is more realistic in terms of the manner in which a ballistic entry trajectory would actually be achieved. The valid ranges of off-nominal initial conditions when the vehicle is spun up are presented in **Figure 5-40**.

	Soyuz Monostable	CEV CG1 Monostable	CEV CG2 Monostable	CEV CG3 Monostable	CEV CG4 Monostable	CEV CG5 Monostable
X_{cg}/D	0.375	0.216	0.241	0.268	0.290	0.315
Z_{cg}/D	0.0	0.0	0.0	0.0	0.0	0.0
Percent Monostability	100	146	118	87	62	35

Table 5-16. Resulting CEV CG Locations for Ballistic Lunar Return Passive Stability Evaluation

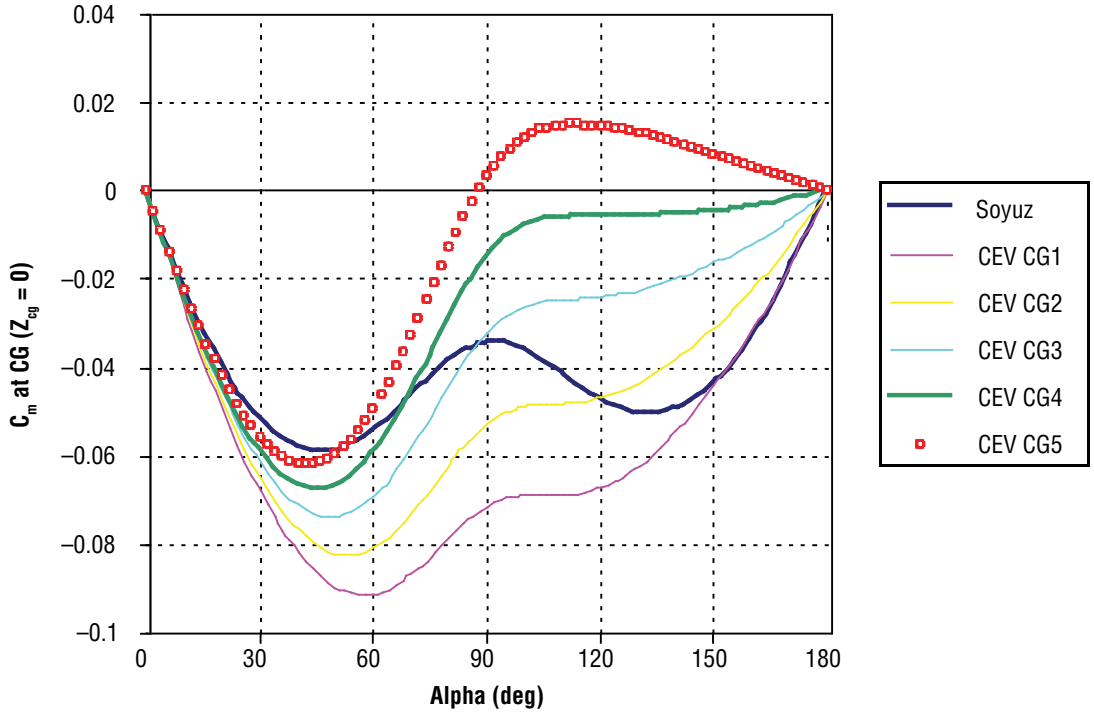

Figure 5-38. Pitching Moment Curves Associated With Each CEV CG Location Used in the Ballistic Lunar Return Passive Stability Evaluation

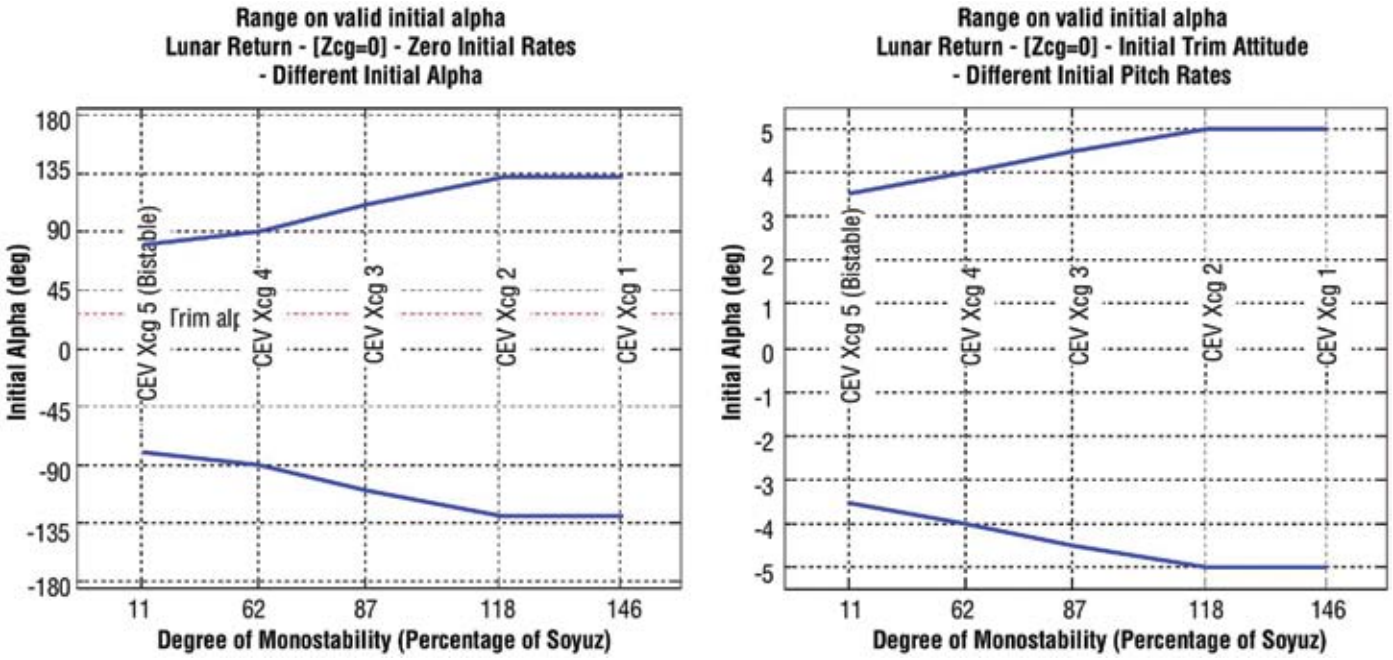

Figure 5-39. Valid Initial Attitudes and Pitch Rates in Ballistic (Z_{cg} = 0) Entry from Lunar Return versus Different Degrees of Monostability

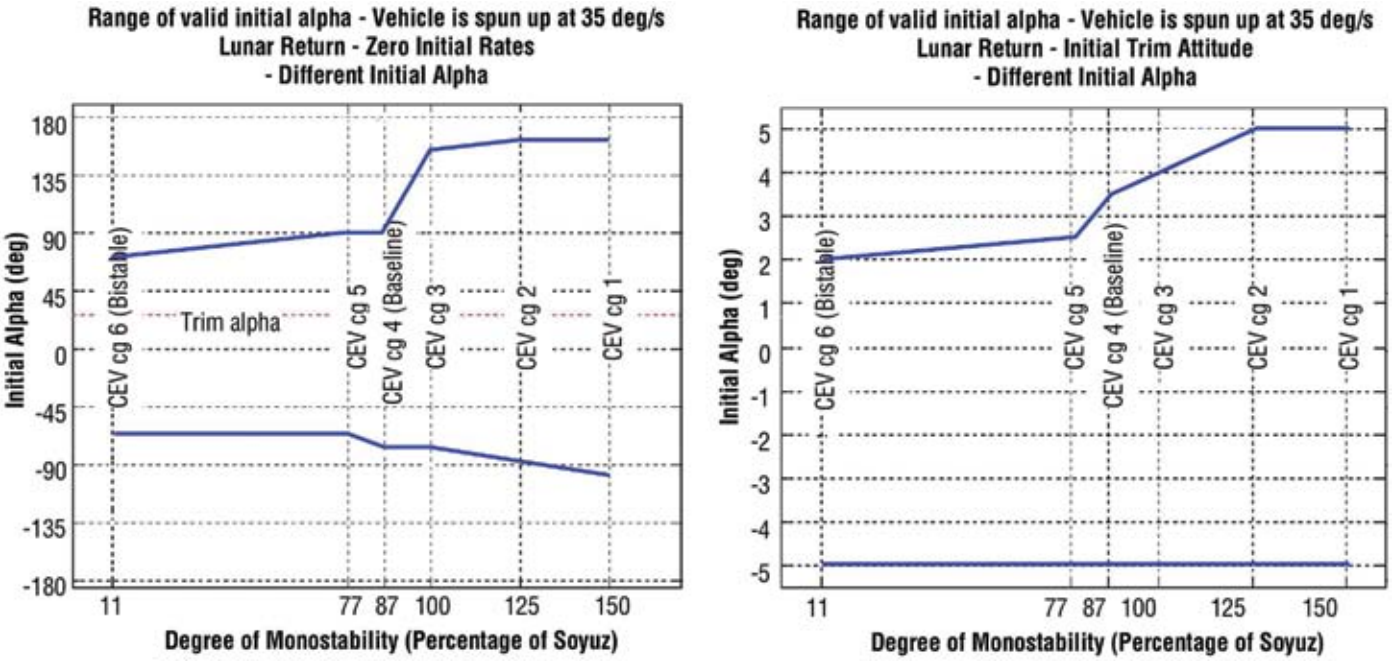

Figure 5-40. Valid Initial Attitudes and Pitch Rates Entry from Lunar Return with Spin Up (35 deg/s) versus Different Degrees of Monostability

5.3.1.3.9 Initial Baseline Capsule Analysis Summary

Detailed CFD investigations of the aerodynamics and aerothermodynamics of the initial baseline capsule validated the initial design results. The trim angle-of-attack for 0.4 L/D was determined to be 28 deg. The vehicle was monostable with up to 49 percent of the volume below the CG. For margin, a desired CG level was established at 45 percent volume, or an X/D location of 0.29. At this location, a Zcg offset of 0.53D would be required, which was approximately the same as required by an Apollo for 0.4 L/D. The vehicle had greater static stability at the desired trim angle than Apollo, and less sensitivity of L/D to a Zcg dispersion than Apollo. Sidewall heating was somewhat influenced by the direct impingement of flow, but only a very small portion of the windward aft-body (near the leading edge corner) would require ablative TPS for the 11 km/sec lunar return velocity. However, a fair amount of LI–2200 was required on the aft-body.

The 6–DOF analysis of the passive, ballistic entry capabilities of the vehicle showed it could handle approximately –90 deg to +180 deg in initial pitch attitude or up to +/–2 deg/sec of initial pitch rate for a LEO entry or ascent abort. For a lunar return, analysis showed that approximately +/– 90 deg initial attitude or +/– 4 deg/sec initial pitch rate could be handled. Even more capability existed if the X_{cg} could be placed lower than the 45 percent volume level.

Some of the attributes of the initial baseline capsule are shown in **Table 5-17**, compared to the actual Apollo with 0.3 L/D, an Apollo with 0.4 L/D, and an AFE shape—all scaled up to the 5.5-m diameter CEV size.

Table 5-17. Comparison of Actual Apollo, Initial Baseline CEV Capsule, and Preliminary AFE-type CEV Parameters

	Apollo (based on flt aero) Actual – 0.3 L/D	**Apollo** (based on flt aero) 0.4 L/D	**Axisym. CEV** (based on CFD) 0.4 L/D	**AFE CEV** (based on CFD) 0.4 L/D
Base radius/D	1.18	1.18	1.18	Original AFE
Corner Radius/D	0.05	0.05	0.05	Original AFE
Cone angle	32.5 deg	32.5 deg	20 deg	20 deg
Height/D (to docking adapter)	0.75 (4.1 m)	0.75 (4.1 m)	0.8 (4.4 m)	0.8 (4.4 m)
α	20 deg	27 deg	28 deg	25 deg
OML Volume	44.3 m_3	44.3 m_3	63.7 m_3	~64 m_3
Xcg/D	0.265 (< 0.22 for monostab.)	0.265 (< 0.23 for monostab.)	0.29 (<0.31 for monostab.)	0.29
Zcg/D	0.038 (> 0.04 for monostab.)	0.05 (> 0.052 for monostab.)	0.053 (> 0.051 for monostab.)	0.032
% Vol below Xcg	55% (< 39% for monostab.)	55% (< 42% for monostab.)	45% (< 49% for monostab.)	~45%
Monostable?	No	No	Yes	Yes
C_m-alpha @ cg	-0.0023	-0.0025	-0.0028	
ΔL/D per ΔZcg	0.022/cm	0.018/cm	0.016/cm	

Note: All are scaled to a 5.5-m diameter.

5.3.1.3.10 Alternative AFE-Type Capsule Shape

The proposed baseline design was disseminated to the systems engineering and aerothermal groups for packaging and TPS estimation, respectively. It became readily apparent that this design could be difficult to package and acquire the desired CG. The primary difficulty rested in attempting to reach the Z_{cg} location. The CG was pushed far off the centerline in order to acquire the desired 0.4 L/D ratio. Thus, in order to keep the general aerodynamics and shape of the baseline vehicle, a slightly modified heat shield, known as the AFE-type, was proposed. The AFE-type shape is intended to bring about two big changes in the aerodynamics. First, it brings the CG closer to the centerline of the vehicle, and secondly, it makes the trim angle-of-attack lower.

The AFE-type shape originated with the AFE of the late 1980s and early 1990s. Although never flown, it offered some advantages over a symmetric blunt-body, particularly in required Z_{cg} offset. The shape was defined by the seven parameters listed below, with the original values shown in parentheses (**Figure 5-41**):

- Cone angle (60 deg),
- Rake angle (73 deg),
- Shoulder turning angle (60 deg),
- Shoulder radius (0.3861 m),
- Nose radius (3.861 m),
- Nose eccentricity, and
- Diameter (3.861 m).

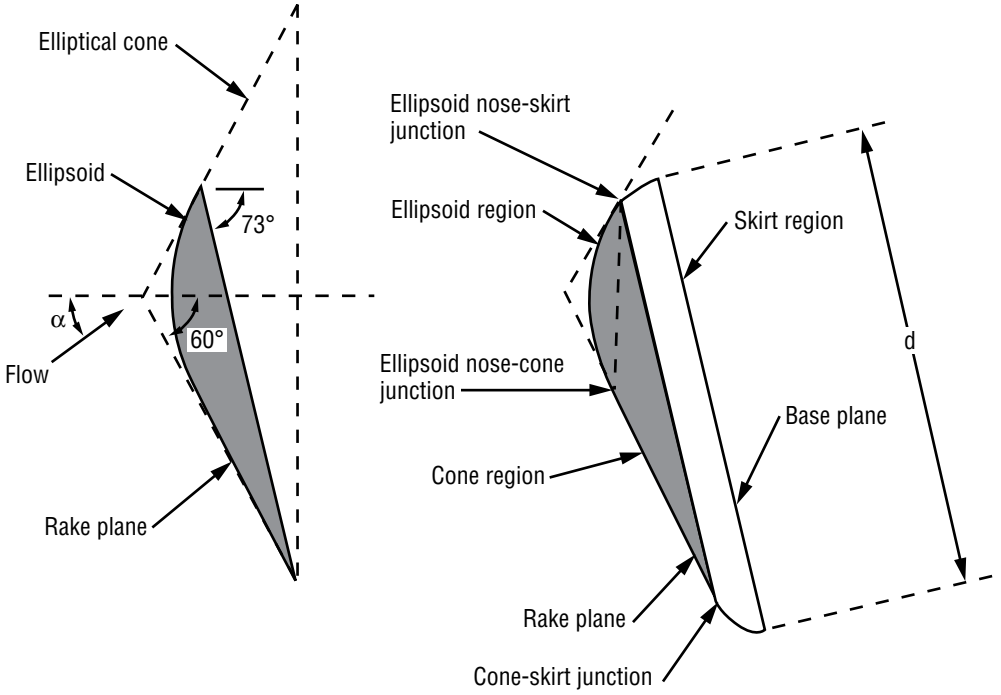

Figure 5-41. AFE-type Shape Parameters

Thus, the AFE-type shape is a well-defined geometry. The design is basically a raked (i.e., cut off at an angle) elliptical cone with a blunted nose (i.e., can be either spherical or elliptic). The rake angle stipulates the position of the blunted nose. If the angle-of-attack is equal to the complement of the rake angle, the velocity vector is aligned with the nose of the heat shield. If the angle-of-attack is smaller than the sidewall angle, the flow will not impinge on the aft cone. The pitch plane elliptical cone angle (for the AFE heat shield) basically determines the thickness of the heat shield. As the difference between the rake and the cone angle increases, the thickness will also increase. Both of these parameters together affect the vehicle aerodynamics. A preliminary analysis of the strengths and weaknesses of employing this shape for the CEV is provided in **Appendix 5C**, **CFD Tools and Processes**, and the geometry tool created by the NASA Ames Research Center (ARC) for AFE-type vehicle model generation is described in **Appendix 5D**, **ARC Geometry Tool for Raked Cone Model**.

5.3.1.3.11 Alternate Proposed CM Shapes

Near the end of the ESAS, it was decided that the direct-to-surface lunar mission architecture would not be prudent. This eliminated the need for a high-volume CEV CM such as the baseline axisymmetric CM shape. In addition, a 1.5-launch solution was selected in which the CEV CM would always be launched on a Shuttle-derived CLV configuration for both LEO and lunar missions. This LV was limited in performance, particularly for the lunar mission and lunar CEV, which created a need to decrease the baseline CEV mass. Because significant mass was created by the extremely large aft-body due to TPS, radiation shielding, and structure, it was desirable to increase the aft-body sidewall angle. In addition, the aft-body flow impingement of the baseline axisymmetric CM shape was not desirable. Finally, the systems packaging at this point had still not achieved the desired CG location for the baseline shape. Although the CG location was low enough to provide monostability, it was not offset far enough to produce the desired 0.4 L/D ratio. All of these factors weighed in against the remaining benefit of the shallow-walled, large aft-body baseline design—the potential monostability. Eventually, the desire for aerodynamic monostability was outweighed by other factors; however, other propulsive or mechanical methods are available to ensure stable ballistic entry, such as employing a flap or RCS jets.

The baseline axisymmetric shape was modified to have a 30-deg back-shell sidewall angle and reduced diameter to 5.2 m. This provided a 2- to 3-deg buffer from the flow direction at a 26–27 trim degree angle-of-attack. The alternative AFE-type vehicle with its 28-deg sidewall angle was already suitable, except for the fact that it was scaled down to a 5.2-m diameter. In addition, its length was decreased to allow for the docking ring diameter and a tighter corner radius was employed to help decrease the Z_{cg} offset requirement. Both changes to the AFE-type shape significantly decreased monostability. These vehicles are shown in **Figure 5-42**.

The C_m curves for these vehicles are shown in **Figure 5-43** at the representative CG locations and monostable limits. The C_m curves are similar, although there is a slight reduction in static stability at the desired trim angle-of-attack of the AFE-type shape compared to Apollo. **Figure 5-44** provides the 0.4 L/D CG trim lines for these configurations. (Note: the significantly reduced Z_{cg} offset requirements of the AFE-type shape.) Both trim lines have roughly equal distance from a representative CG to the monostable CG limit. **Table 5-18** presents some performance specifications for the two vehicles. The overwhelming benefit of the AFE-type configuration is the reduced Z_{cg} offset required for 0.4 L/D, though there is a slight TPS mass cost.

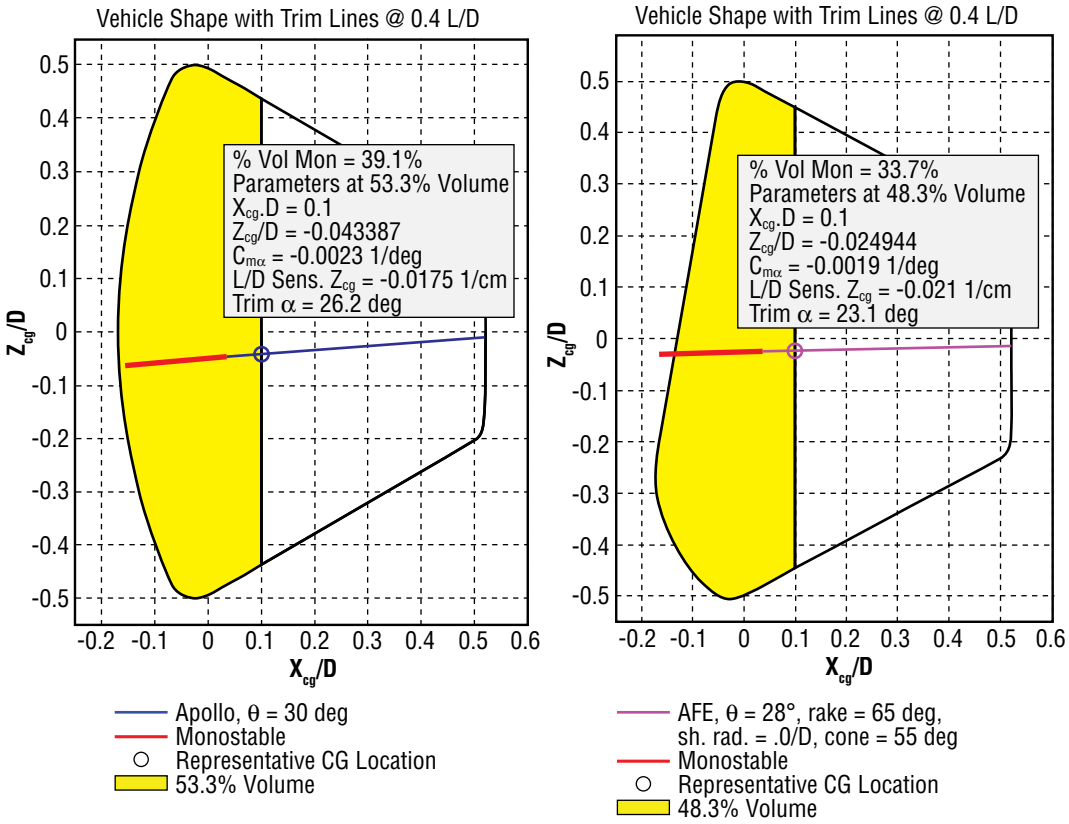

Figure 5-42. Alternate Symmetric and AFE Heat Shield Vehicles

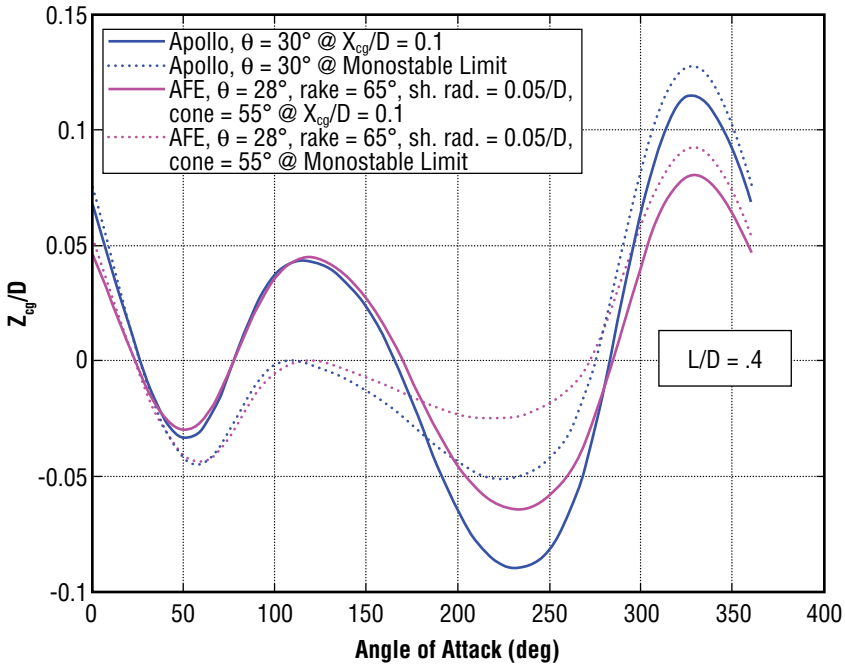

Figure 5-43. C_m Curves for Alternate Vehicles

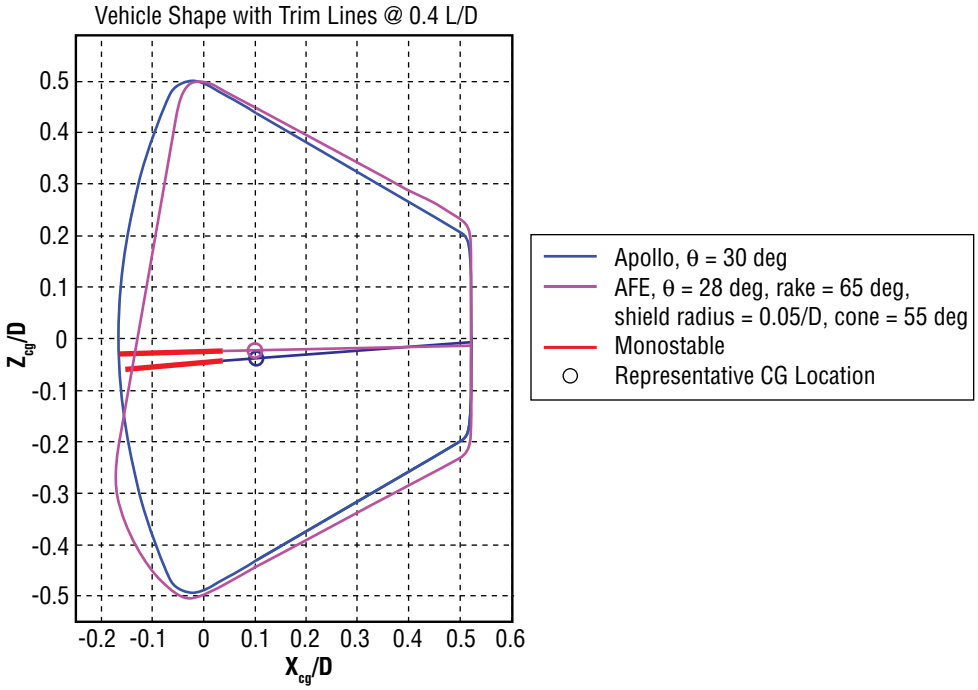

Figure 5-44. Trim CG Lines for Alternate Vehicles

Table 5-18. Comparison of the Alternate Vehicles

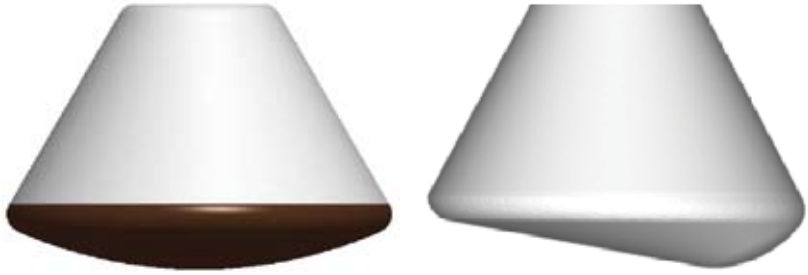

Shape Specifics	5.2-m diameter/30-deg sidewall angle/ Apollo heat shield	5.2-m diameter/28-deg sidewall angle/ AFE heat shield
Angle of Attack for 0.4 L/D	27-deg (CFD)	23-deg (CFD) (more margin from afterbody flow Impingment even with larger aftervody)
Zcg offset for 0.4 L/D with Xcg/D=0.1 (0.52 m)*	23 cm (Newtonian**)	13 cm (Newtonian**) (43% decrease)
Heat shield TPS mass * (non-conservative estimate)**	630 kg (5.5 m dia)	690 kg (5.5 m dia) (9% more TPS mass for heat shield)
Monostability Trending	Xcg limit for monostability @ 0.19 m*	Xcg limit for monostability @ 0.19 m* (same distance to a monostable condition)
Sensitivity to Zcg (ΔL/D per ΔZcg)	0.018/cm	0.021/cm (slightly more sensitive to Zcg)
Development complexity	Lower	Higher (20–25% more aero/aerothermo effot)

** Measured from intersection of heat of heat shield and aftbody cone*

***CFD typically increases the Z_{cg} offset requirement by about 0.01D*

****Designed to handle both ballistic direct entry and skip entry*

5.3.1.3.12 Final ESAS CM Shape

Based primarily on packaging and mass issues, the final proposed baseline CEV CM shape was a 5.5-m diameter Apollo (with the original Apollo 32.5-deg sidewall). Thus, the aerodynamics and aerothermodynamics are well known. TPS estimates were made based on the results presented previously using the heat shield data for the axisymmetric baseline shape and the back-shell data for the AFE-type shape. The trimline for this shape was found to be nearly identical to that shown previously for the 30-deg sidewall Apollo. Also, the ballistic entry analyses provided above is still applicable for the most part.

Concern is warranted, however, over the ability to achieve the Z_{cg} offset that will be required to achieve a 0.4 L/D using this shape. However, the alternative AFE-type shape as shown previously would alleviate this concern. The shape working group is continuing to evolve an AFE-type shape that is directly comparable to the proposed 5.5-m diameter Apollo with a 32.5-deg back-shell, with the only difference being in the heat shield shape. Further risk and performance analyses in the areas of landing (land versus water) may ultimately determine which CEV CM shape is selected.

5.3.2 CM Net Habitable Volume Trades

In the history of human spacecraft design, the volume allocated for crew operations and habitability has typically been the remaining excess after all of the LV constraints and vehicle design, weight, CG, and systems requirements were met. As a result, crew operability has often been compromised as crew sizes are increased, mission needs changed, and new program requirements implemented. CM habitability considerations have often been relegated to a second level behind engineering convenience (e.g., putting the galley next to or collocated with the hygiene facility to simplify plumbing). Whereas flight crews have demonstrated a consistent and, at times, heroic resilience and adaptability on orbit, designs of future crew habitable modules should not sacrifice crew operability. NASA should design new vehicles that allow the crew to safely and efficiently execute the mission, not build vehicles that execute a mission which happens to carry crew.

Net habitable volume is defined for this study as the pressurized volume left available to the crew after accounting for the Loss of Volume (LOV) due to deployed equipment, stowage, trash, and any other structural inefficiency that decreases functional volume. The gravity environment corresponding to the habitable volume must also be taken into consideration. Net habitable volume is the volume the crew has at their disposal to perform all of their operations. In order to estimate the net habitable volume requirement for the CEV for each phase of flight, this study first looked at the crewed operations required in the spacecraft, what operations must be done simultaneously, how many crew members might be expected to perform each operation, how long each operation might last, how often each operation might be required during the mission, the complexity of the task, and the potential impact to the task by vehicle structure, shape, and gravity environment. The analysis took into account the entire spacecraft pressurized volume and the estimated volume and layout of internal systems equipment and stowage volumes by mission type and phase. Pressurized and net habitable volumes of previous and current spacecraft were used for comparison. Full-scale rough mockups were made for the internal volumes of both the CEV CM and LSAM to assist in the visualization and evaluation process.

The initial goal of the study was to determine the minimum net habitable volume required for the CEV for each DRM. However, without more definition of systems and structural

requirements (e.g., how much volume seat stroke, plumbing, cables, and wiring will require), a specific volume number was difficult to derive. Using the mockups, the ESAS team determined a rough estimate of minimum net habitable volume. More detailed analysis may find ways to be more efficient in the design of internal systems and structure; however, requirements for systems and volumes not currently anticipated may also be added in the future, which will compromise the net habitable volume for the crew.

Full-scale high-level mockups of the CEV interior configurations being traded allowed the ESAS team to visualize the impacts of using the CEV as a single vehicle to take crew all the way to the lunar surface and as part of a set of vehicles for the lunar exploration mission where the CEV remains in LLO. The ESAS team provided the designs it felt best supported the requirements of launch, on orbit, and entry. The team also provided best available estimates of both equipment volumes and required task volume.

The number of crew, mission duration, task/operations assumptions, and volume discussions for each of the CEV DRMs are described in the following sections.

5.3.2.1 ISS Crew/Cargo Mission

The CEV will carry three to six crew members to the ISS with nominally a day of launch rendezvous, but, in the worst case, taking 3 days to get to the ISS. Returning from the ISS to Earth will nominally take 6 hours; however, in a contingency this could take a day or more. The crew will not need to exercise, will not require a functional galley, will not conduct planned EVA, will not perform science activities, but will still require privacy for hygiene functions. Consumables required for this mission will be minimal. The CEV and launch and entry suits will be capable of contingency EVA, but, for the ISS mission, it is anticipated that the vehicle would return to Earth or stay at the ISS if a contingency EVA was required. The vehicle and the launch and entry suits will support contingency cabin depressurization to vacuum. The CEV will remain docked to the ISS for a nominal period of 6 months. The CEV will support safe haven operations while docked to the ISS and provide nominal and emergency return of the crew that arrived at the ISS in the vehicle.

Since ascent and descent are the main activities in the CEV for this DRM, seats may not require stowing, and the CM interior will probably not require significant reconfiguration for on-orbit operations. The lunar DRMs will drive minimum net habitable volume for the CEV; therefore, the volume required for the ISS DRM was not examined in detail since the lunar DRM net habitable volume requirement is larger than that required for the ISS DRM.

5.3.2.2 Lunar Mission – CEV Direct to the Lunar Surface

The CEV will carry a crew of four on a 4- to 6-day Earth-to-Moon trip, with up to 7 days on the surface and 4–6 days return. All systems and equipment must function in a variety of environments and orientations (e.g., 1-g ground/pad prelaunch operations, up to 4-g ascent operations, zero-g on-orbit operations, one-sixth-g lunar surface operations, and up to 15-g worst-case Earth reentry/abort environments). The crew will need to exercise, both enroute and on the lunar surface, will require private hygiene capability and a galley, and will need to reconfigure the volume for on-orbit operations, including rendezvous and docking with other exploration elements. All crew members must be able to stand up simultaneously in the vehicle on the lunar surface. The CEV and the launch and entry suits will support contingency EVA operations. Lunar surface suits and support equipment will be carried in the CEV and must be accessible by the crew after landing on the lunar surface. An airlock is required on the lunar surface.

The critical task driving the required volume in this DRM was the volume needed for four crew to don, doff, and maintain the lunar surface EVA suits in partial gravity. The volume sensitivity to both simultaneous and serial suit donning and doffing was evaluated. Utilizing graphics analysis, direct measurement, and indirect measurement of suited operations, a rough estimate of a critical "open area" of net habitable volume of approximately 19 m^3 was derived.

5.3.2.3 Lunar Mission, CEV Left in Lunar Orbit

The CEV will carry a crew of four on a 4- to 6-day Earth-to-Moon trip and remain in orbit uncrewed while the entire crew spends time on the lunar surface in an ascent/descent module (LSAM). The CEV will rendezvous with the LSAM in LEO, and the LSAM volume will be available as living space for the crew on the way to the Moon. The on-orbit assumptions for this DRM are the same as the previous DRM. After the lunar stay, the ascent module will rendezvous with the CEV in lunar orbit and be discarded once the crew has transferred to the CEV. Only the volume in the CEV will be available to the crew for the 4- to 6-day return trip to Earth. Lunar surface suits and support equipment will be carried in the LSAM. An airlock will be required in the LSAM for lunar surface operations.

For this scenario, the donning and doffing of launch and entry suits was the major volume driver, with a minimum required critical "open area" of net habitable volume of 8 (TBR) m^3.

5.3.2.4 Mars Missions

The CEV will carry a crew of six to an MTV in Earth orbit. The time the crew spends in the CEV is expected to be less than 24 hours. The CEV will remain attached to the Mars vehicle for the transit to Mars (6 months), then remain in Mars orbit with the transit vehicle while the crew is on the Martian surface (18 months), and remain with the transit vehicle for the Earth return (6 months). The crew will reenter the CEV for the last 24 hours of the return trip to Earth. The requirements for habitability and operations for this DRM are the same as the ISS DRM.

5.3.2.5 CEV Split Versus Single Volume

A considerable amount of time was spent analyzing the advantages and disadvantages of a CEV split versus single volume. Separating the CEV volume into a CM used primarily for ascent and entry and a mission module that could be sized and outfitted for each particular mission has operational advantages depending on the mission to be supported. Also, separation of the mission module with the SM after the Earth deorbit burn provides the lightest and smallest reentry shape.

The difficulty in minimizing the ascent/entry volume of the vehicle became a driving factor because this volume must accommodate a maximum crew of six for the Mars return mission. Once the ascent/entry volume for six was determined, all other DRM crew sizes by definition will fit in this volume. A CEV sized for the six-crew DRM is the minimum size for the ascent/entry module.

The study found a single volume, which is less complex from a build-and-integrate standpoint, to be more mass-efficient and volume-efficient for a given mass. A larger single-volume vehicle also has lower entry heating and g's as a result of a larger surface area, and thereby lower ballistic coefficient, than a smaller ascent/entry split volume. A mission module was determined to not be required for the ISS and the Mars return DRMs and was of limited value to the lunar DRM, if the single volume is large enough, and the CEV is not taken all the way to the lunar surface.

Finally, the cost and LV analyses determined that the split volume case would be higher cost (building two versus one module) and require a larger throw capability on the booster for the same net habitable volume. Based on these factors, the ESAS team decided that a single volume CEV sized for the six-crew ISS and Mars DRM would provide sufficient volume for both the four-crew lunar DRM and the three-crew ISS DRM.

5.3.3 Airlock Trades

5.3.3.1 Airlock Design Considerations

Early in the ESAS, a proposal was made by the operational community to incorporate an airlock into the CEV design. Depending on the configuration, this requirement could have significant design implications. Because the mass and volume implications of an airlock affect the size and layout of the CEV, justification of the need was addressed.

Integration of an airlock into the CEV design is complex. Non-inflatable airlocks are massive and require significant volume. Inflatable airlocks are not as heavy, but the support system requirements are the same or larger. Inflatable airlocks also bring the risk of not being able to be retracted, thus requiring jettison capability before reentry.

5.3.3.2 Zero-g Missions

The first question to be answered is whether or not the DRMs require an airlock. For missions to the ISS, the CEV docks with the station and returns to Earth. The CEV is only active for 2 to 3 days at a time during transit. Contingency EVAs are not even required for this mission. For lunar EOR/LOR missions, the CEV docks with the LSAM which then goes to the lunar surface. This mission does require contingency EVA capability that can be accomplished with a cabin depressurization. For the Mars DRM, the CEV docks with an MTV in LEO. As in the ISS missions, the CEV in this scenario is only active for 1 or 2 days. This mission does have a possible contingency EVA requirement, which could be accomplished with a cabin depressurization.

5.3.3.3 Lunar Surface Direct Mission

The only mission scenario for the CEV that could significantly benefit from an airlock is the lunar surface-direct mission, in which the CEV is taken all the way to the lunar surface. This mission would require an airlock. Without an airlock, the entire CEV would have to be depressurized, and all four crew would require Extra-vehicular Maneuvering/Mobility Units (EMUs), even if only two crew members performed an EVA. A separate airlock could be left on the lunar surface with all or portions of the EVA equipment, which would reduce the dust issue in zero-g flight. Several concepts were studied for this mission scenario, but further study would be required. The concepts studied show different arrangements for the crew during ascent/entry and for surface operations that have difficult issues to be resolved (e.g., what functionality is within the CM versus the airlock). Since the lunar surface-direct mission is no longer being considered, the requirement for a CEV airlock on the lunar surface shifts to the LSAM.

5.3.3.4 Recommendation

An airlock is not required for any of the current zero-g CEV DRMs. The ascent/entry volume is adequate for an entire mission profile, and a disposable airlock module would increase development and recurring costs.

5.3.4 Docking Mechanism/ISS Docking Module Trades

As indicated in the President's Vision for Space Exploration, the completion of the ISS is a high priority for the Agency and the U.S. aerospace community. As such, CEV access to the ISS is of primary importance, and the mechanism and operations required for mating to the ISS must be factored into the CEV design and operations concept. Also, as stated in the Vision for Space Exploration, there is a need to develop systems and infrastructure that are enabling and allow for an affordable and sustainable exploration campaign. As such, it has been determined that systems developed in support of the CEV ISS missions should be compatible with other exploration missions (e.g., docking of CEV and LSAM).

The three mating systems currently available for the U.S. Space Program are: the U.S. CBM, the Russian APAS docking mechanism, and the Russian Drogue-Probe docking mechanism. The study researched these options as they presently exist and also explored possibilities for optimizing each through adaptation and modification. The study also assessed a next-generation docking/berthing mechanism being developed at the NASA Johnson Space Center (JSC) called LIDS. The four mating concepts are depicted in **Figure 5-45**.

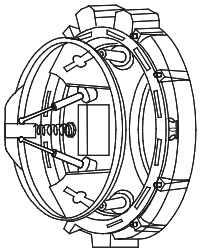

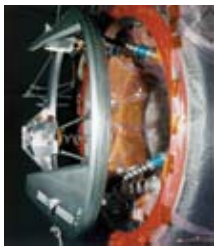

Androgynous Peripheral Docking System (APAS)
Weight: 1,250 lbs (mech/avionics/lights/hatch/ Comm/ranging sys)
Max OD: 69˝ dia
Hatch Pass Through: 31.38˝ dia
Source: JSC-26938, "Procurement Specification for the Androgynous Peripheral Docking System for the ISS Missions";
OSP ISS Port Utilization Study; Final Version, Nov. 8, 2002

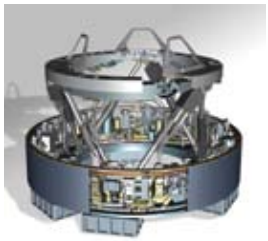

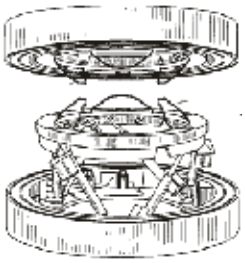

New Mating System based on LIDS/ADBS [1]
Weight: est. 870 lbs (mech/avionics/hatch)
Max OD: 54˝ dia (X-38 CRV scale)
Hatch Pass Through: 32˝ dia
Source: ADBS Project
[1] LIDS/ADBS in development

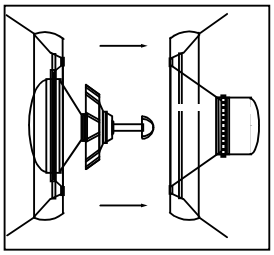

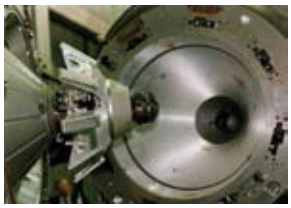

Russian Probe/Cone (P/C)
Weight: 1,150 lbs (mech/avionics/lights/hatch/ Comm/ranging sys)
Max OD: 61˝ dia
Hatch Pass Through: 31.5˝ dia (approximate)
Source: Energia; OSP ISS Port Utilization Study; Final Version, Nov. 8, 2002

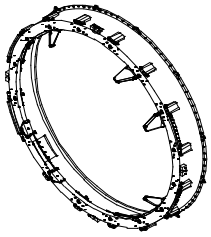

Passive Common Berthing Mechanism (PCBM)
Weight: 900 lbs
(mech/avionics/lights/hatch/ Comm/ranging sys/grapple fixture)
Hatch Pass Through: 54˝ square
Max OD: 86.3˝ dia
Source: SSP 41004, Part 1, "Common Berthing Mechanism to Pressurized Elements ICD" & SSP 41015, Part 1, Common Hatch & Mechanisms To Pressurized Elements ICD; OSP ISS Port Utilization Study; Final Version, Nov. 8, 2002

Figure 5-45. Docking/ Berthing Mechanisms

The two Russian docking mechanisms are complex, do not support berthing operations, and have performance limitations that create dynamically critical operations, increasing risk for missions, vehicles, and crews. With respect to their current usage on the ISS (i.e., in LEO), these limitations are manageable, and consideration of wholesale upgrade and replacement for existing vehicles and programs is not practical. However, after factoring in technical limitations, level of fault tolerance, reliance on foreign suppliers, and the requirement for application beyond the ISS and LEO, it became clear to the ESAS team that existing docking solutions were inadequate.

The ISS berthing mechanism does not support docking dynamics because it requires a robotic arm to deliver and align mating interfaces; therefore, all berthing operations would require involvement of the crew, which is incompatible with lunar applications and autonomous mating operations. Additionally, preliminary CEV architectural sizing has determined that the diameter of the CBM is too great to fit the current CEV configuration, further eliminating it for potential consideration for the CEV.

During the study, it was confirmed that all three existing systems failed to meet dual-fault tolerance requirements for critical operations and those for time-critical release, which are very important for an emergency or expedited separation. While both docking mechanisms provide nominal hook release and a pyrotechnic backup, the Space Shuttle Program accepts the use of a 96-bolt APAS release via a 4-hour EVA to satisfy dual-fault tolerance requirements. CBM-powered bolts do not operate fast enough to support expedited release because of the threaded bolt and nut design, and they are operated in groups of four to prevent binding and galling during unthreading. The CBM uses a pyrotechnic to provide one-fault tolerance for release.

Additionally, all three systems contain uniquely passive and active (male and female) interfaces that are not fully androgynous, offer limited mission mating flexibility, and each has a specific, narrow, operational range of performance for use. **Figure 5-46** depicts the dispositions of the various presented solutions and their associated issues.

	CBM	APAS	P/C	LIDS
Mass				
Diameter				
Docking or Berthing				
Impact/Capture Force				
Fault Tolerance				
Availability				
Time-Critical Separation				
Fully Androgynous				
Supports AR&D				

Figure 5-46. Various Solutions and Associated Issues

These facts indicate that the development of a modular, generic mating infrastructure is a key element needed for the success of CEV and other future NASA exploration missions and programs.

Many of the issues associated with existing systems have been well understood for more than a decade. Since the early 1990s, in response to mitigating these issues, the NASA Advanced Docking Berthing System (ADBS) project has been developing the LIDS as a smaller, lighter, low-impact mating system to reduce the dynamics required for and the risks associated with mating space vehicles. The ADBS project has focused on the development and testing of a low-impact mating system that incorporates lessons learned from previous and current mating systems to better meet future program requirements. As a result, it has been established that an advanced mating system built around low-impact characteristics is feasible and will help ensure meeting anticipated future mating system requirements. **Figure 5-47** depicts the LIDS mechanism in detail.

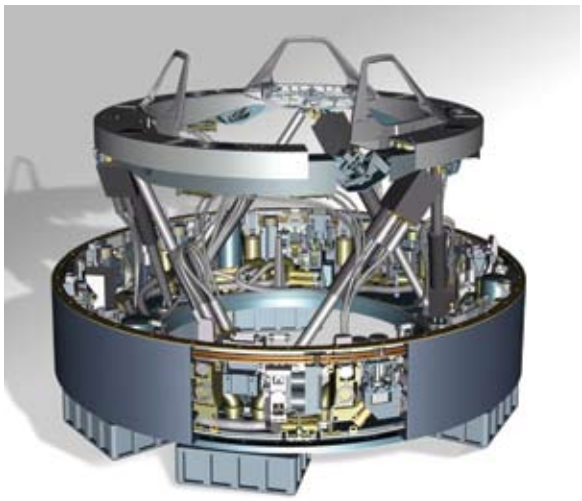

Figure 5-47. LIDS Docking/Berthing Mechanism

Through the course of this study it was also established that over the last decade, except for the LIDS development, no other U.S. activity has been occurring to develop a human-rated, crew transfer mating system. Currently, the project is funded under ESMD's Technology Maturation Program. Of primary concern was the ability of the technology to meet the accelerated CEV schedule and, in response, the ADBS/LIDS project has performed credible planning that demonstrates it can bring the TRL to the level required to support the accelerated CEV schedule. As such, it is recommended that NASA continue the LIDS development for the CEV, but use both the CEV and planned future exploration requirements to develop a mating mechanism and operations approach to form the basis of a standardized mating element that can be used as a key component in new exploration program architectures.

When developing a new mating system, an understanding of the ISS mating ports and locations becomes critical. During the assessment of existing mating options, it was established that the two existing ISS Primary Mating Adapters (PMAs) ports used as the primary and secondary docking ports for the Shuttle would be available (following Shuttle retirement) for modification or replacement and could then be used for CEV docking. However, after assessing the inability of the APAS to meet CEV and exploration requirements, it is recommended that the LIDS mechanism be incorporated onto an adapter, enabling near-term CEV/ISS use as

well as supporting near-term commercial ISS cargo needs. By adapting LIDS to the ISS, this will also allow the LIDS development to proceed focused on requirements from the broader exploration activities and not just those associated with using existing ISS mating hardware.

Study trades indicate that developing a small LIDS-to-ISS adapter to configure the ISS for LIDS mating operations will allow continued accessibility through a direct-docking of the visiting vehicles and Remote Manipulator System (RMS) berthing and unberthing to easily relocate attached vehicles.

The trades have also shown that the adapter could be delivered as a new "PMA" requiring more payload bay space in a Shuttle launch or be designed as a small adapter taking up less space in a future Shuttle flight. A small adapter would also lend itself to be able to "piggy-back" on the first CEV flight should Shuttle launches or payload bay space be unavailable. RMS grappling and berthing would be required to install the adapter in this scenario. An additional scenario was evaluated using a small LIDS-to-APAS adapter to be attached to a PMA, but this requires the adapter and its delivery vehicle to deal with the force-intensive active APAS and its air-cooled avionics pallet, all of which makes this scenario less attractive than other options.

Based on the trade study, the ESAS team's recommendation for the docking mechanism is to develop the LIDS into a common interface for all applicable future exploration elements. Currently already in development at NASA/JSC, the LIDS could be completed and inserted onto the vehicle as Government-Furnished Equipment (GFE) for the early CEV-to-ISS missions. The docking adapter would subsequently be developed to convert the ISS docking points into LIDS interfaces following additional ISS port utilization trades, Shuttle launch and payload bay availability assessments, detailed design studies, and requirements definition.

5.3.5 Landing Mode/Entry Design

5.3.5.1 Summary and Introduction

The choice of a primary landing mode—water or land—was driven primarily by a desire for land landing in the CONUS for ease and minimal cost of recovery, post-landing safety, and reusability of the spacecraft. The design of the CEV CM will need to incorporate both a water- and land-landing capability to accommodate abort contingencies. Ascent aborts can undoubtedly land in water and other off-nominal conditions could lead the spacecraft to a land landing, even if not the primary intended mode. In addition, the study found that, if a vehicle is designed for a primary land-landing mode, it can more easily be altered to perform primarily water landings than the inverse situation. For these reasons, the study attempted to create a CONUS land landing design from the outset, with the intention that, if the risk or development cost became too high, a primary water lander would be a backup design approach.

5.3.5.2 Return for ISS Missions

5.3.5.2.1 Landing Site Location Analysis

A landing site location analysis was performed for the CEV conceptual design that compares the 0.35 L/D (100 nmi cross-range) and the 0.40 L/D (110 nmi cross-range) vehicles. The focus of this study was to show where acceptable landing sites can be located with respect to the SM disposal area. The SM is assumed to be unguided, and its entry state vector unaltered from that of the CEV, except for the small separation maneuver. The SM debris ellipse, which encompasses a track approximately 900 nmi long from toe-to-heel, must not infringe on land areas. This SM footprint was derived from multiple previous studies at NASA JSC, including

the Assured Crew Return Vehicle (ACRV), Soyuz Crew Return Vehicle, X–38, and Orbital Space Plane (OSP) projects. It is based on detailed analyses of, and actual data from, SM-type breakups.

Three landing sites that meet the SM disposal guidelines were analyzed: Edwards Air Force Base (AFB) in California, Carson Flats in Nevada, and Moses Lake in Washington. Vandenberg AFB in California was originally considered as a prime site, but the landing area does not meet minimum size requirements (5–6 nmi diameter). Moses Lake and Carson Flats have not been surveyed as actual NASA landing areas, but have been considered in previous studies. Present satellite photos show that they meet the minimum size requirement with a high probability that they have acceptable terrain for landing. Moses Lake resides near Larson AFB (closed in 1966) and Carson Flats is located near a Naval Target Area. It is highly recommended that these sites be investigated in more detail to assess their viability.

Figure 5-48 represents the 0.35 L/D case, which shows that the SM debris limits the landing site locations to no further than 350 nmi east of the Pacific Ocean (including a 25-nmi safety margin for all U.S. coast lines). This boundary line was computed by using the entry aerodynamic flight characteristics for this vehicle design. The results show that Edwards AFB is accessible only on the ascending passes and that Carson Flats and Moses Lake were very near the safety limits, thus making them marginal for off-nominal approaches.

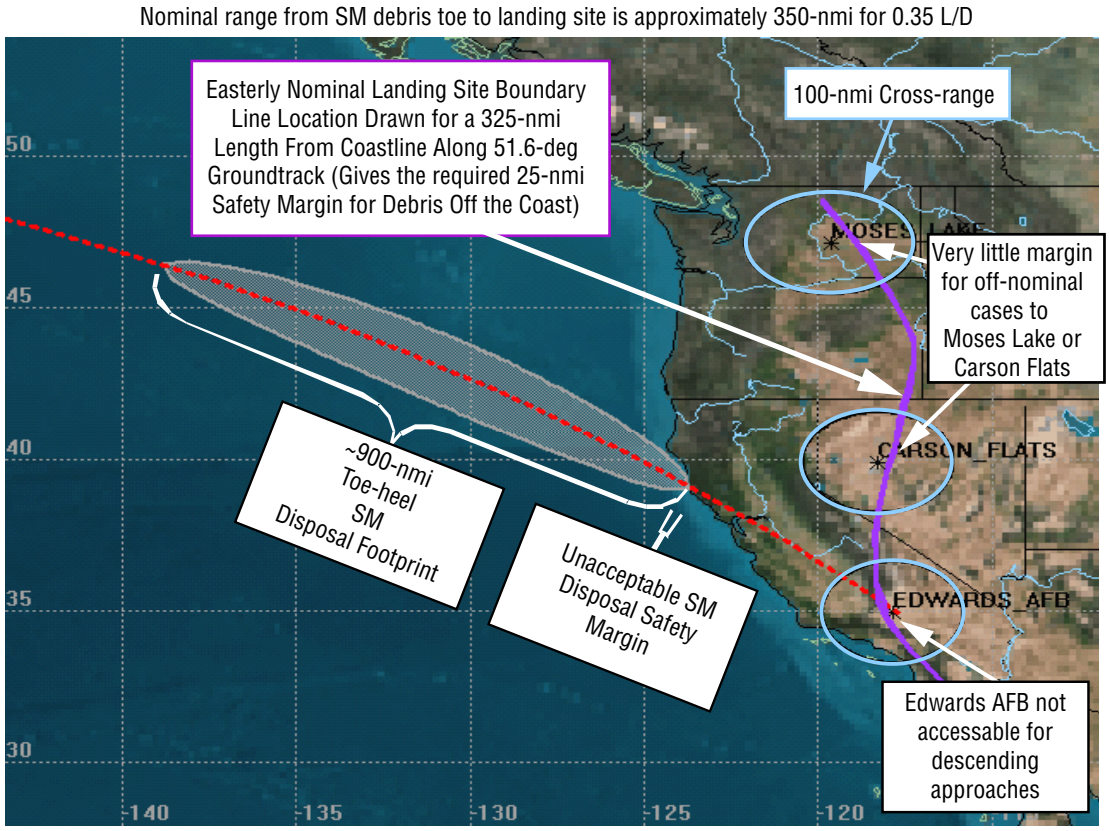

Figure 5-48. Maximum Landing Site Boundary for a 0.35 L/D CM Returning from a 51.6-deg Space Station Orbit

Figure 5-49 shows the 0.40 L/D case, which has an SM debris limit boundary line of 500 nmi (including the 25-nmi safety zone). All three landing sites are shown to have adequate accessibility on both ascending and descending passes without concern for SM debris. There is a safety margin available from the SM debris area to the coast of at least 100 nmi for all three sites. Based on this analysis, an L/D of 0.4 was determined to be desirable for the CEV CM design.

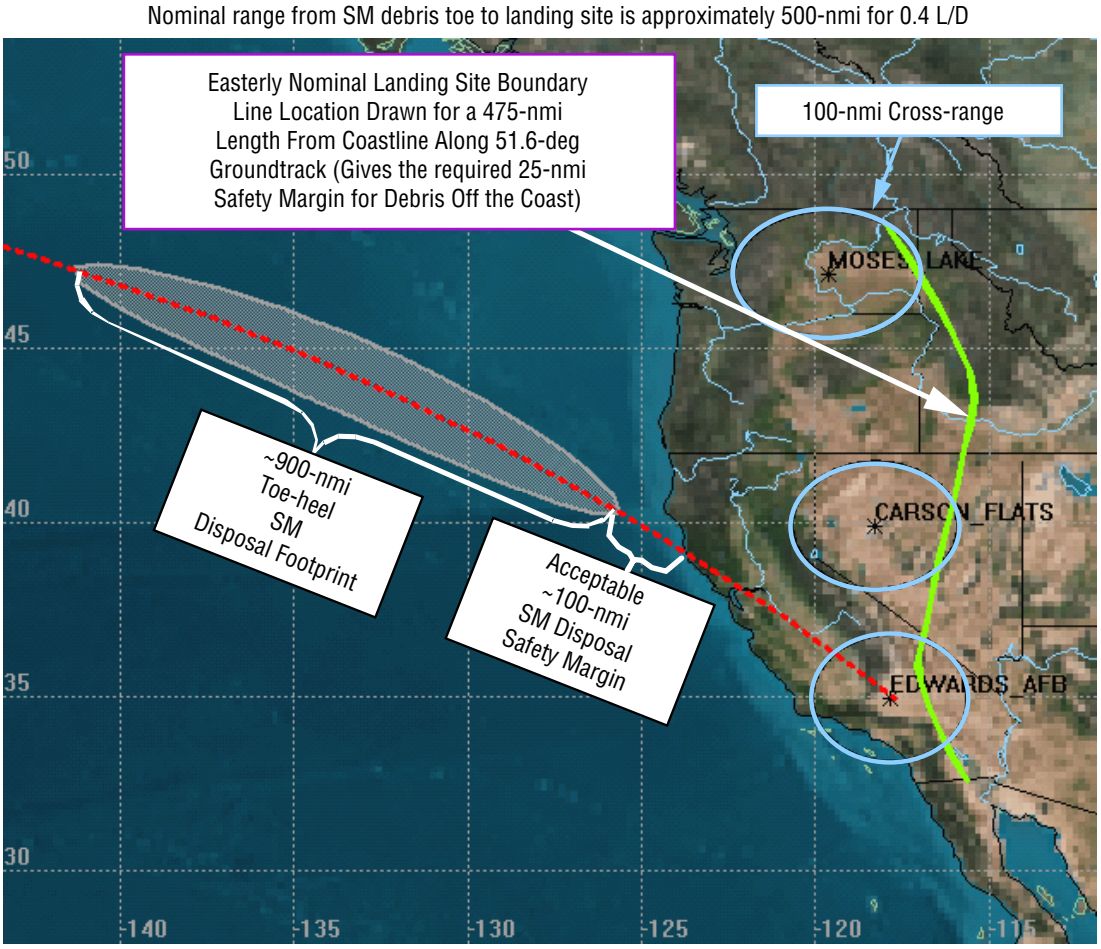

Figure 5-49. Maximum Landing Site Boundary for a 0.4 L/D CM Returning from a 51.6-deg Space Station Orbit

5.3.5.2.2 Landing Site Availability Analysis for 0.4 L/D CEV CM

The objective of this study was to find average and maximum orbital wait times for landing opportunities considering the three different CONUS landing sites located in the western U.S. for a 0.4 L/D CM. The three sites chosen were Edwards AFB, Carson Flats, and Moses Lake.

The trajectory profile used in the analysis is derived from an ISS real-time state vector with an altitude of approximately 207 nmi. This orbit is at the lower end of what is considered nominal, but is well within the operational range of many of the ISS activities.

The nominal orbital wait times, as well as ones that are phased (a procedure that lessens the wait time by shifting the node favorably—with a possible delta-V penalty), were included in this study. Results are shown in **Table 5-19** with supporting plots in **Figures 5-50** through **5-53**. Phasing implies inserting the CEV into a higher or lower orbit, then waiting to achieve a landing opportunity sooner than if one had remained in the circular ISS orbit. Phasing maneuvers can be used when considering the overall propellant budget. For this study, an additional delta-V of 250 ft/sec was assumed available over the normal propellant budget required for the deorbit from ISS altitude.

Table 5-19. Average and Maximum Wait Times for Deorbit Opportunities from 207-nmi Orbit

	Nominal Opportunities		Phasing Maneuver Opportunities	
Landing Site	Average Orbital Wait Time (hrs)	Maximum Orbital Wait Time (hrs)	Average Orbital Wait Time (hrs)	Maximum Orbital Wait Time (hrs)
Edwards AFB (CA)	39	71	18	28
Carson Flats (NV)	35	71	17	31
Moses Lake (WA)	21	28	15	23
All Sites Considered	10	28	8	21

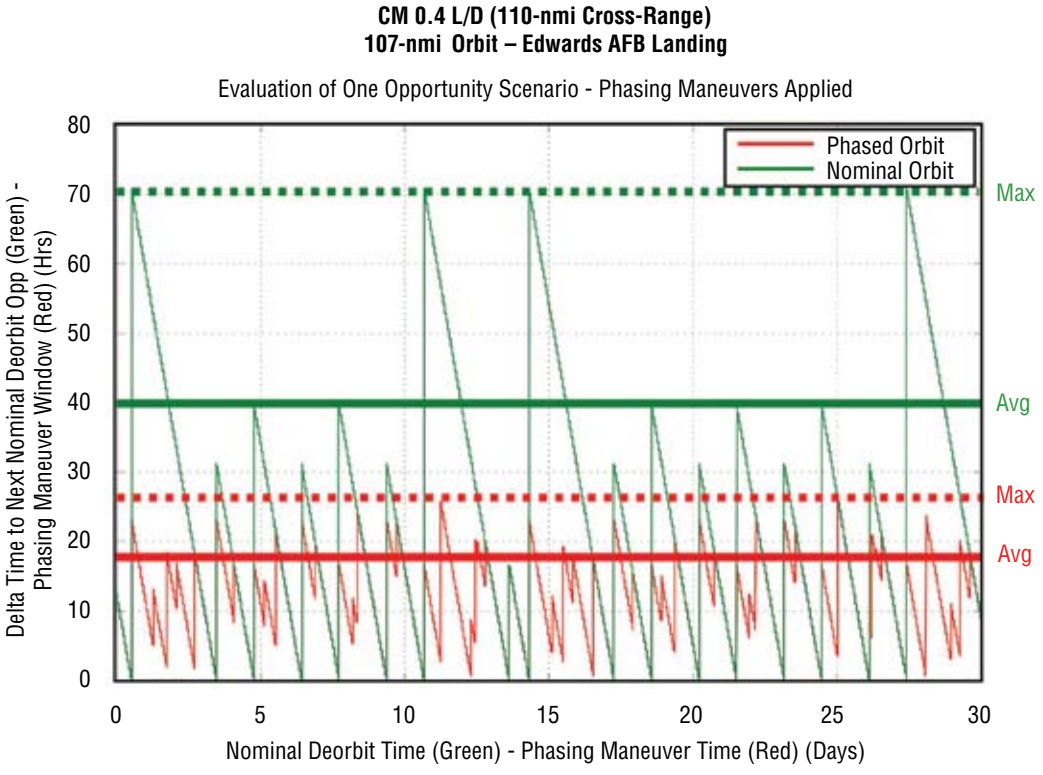

Figure 5-50. Edwards AFB Deorbit Opportunities

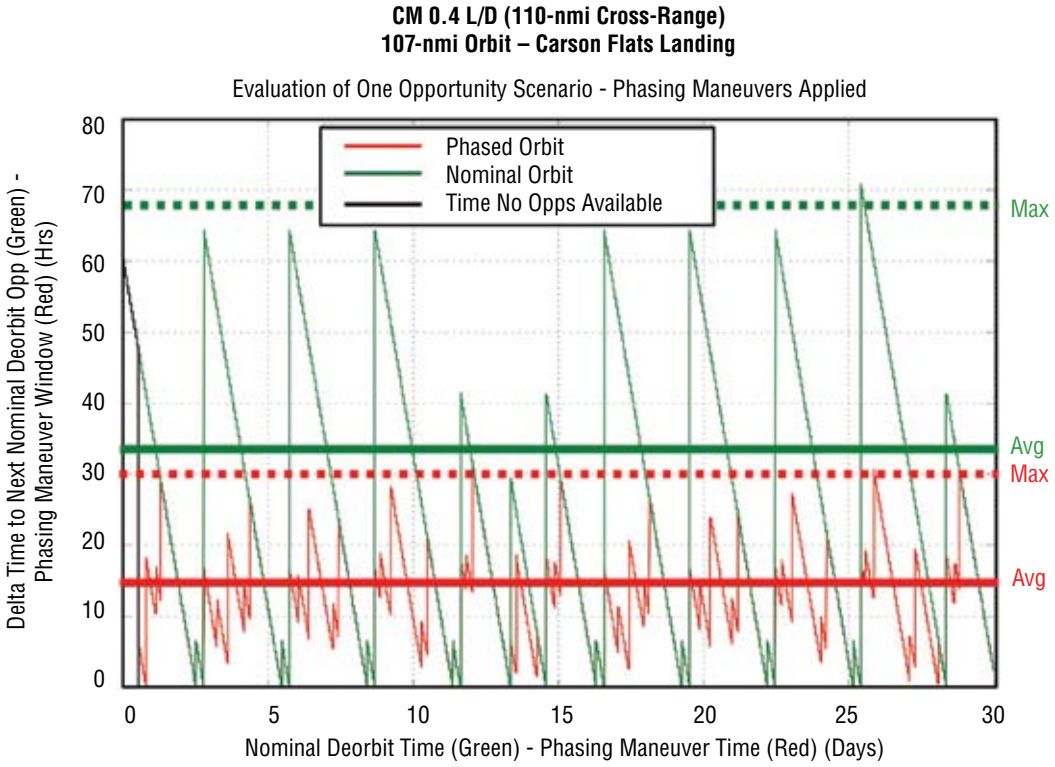

Figure 5-51. Carson Flats Deorbit Opportunities

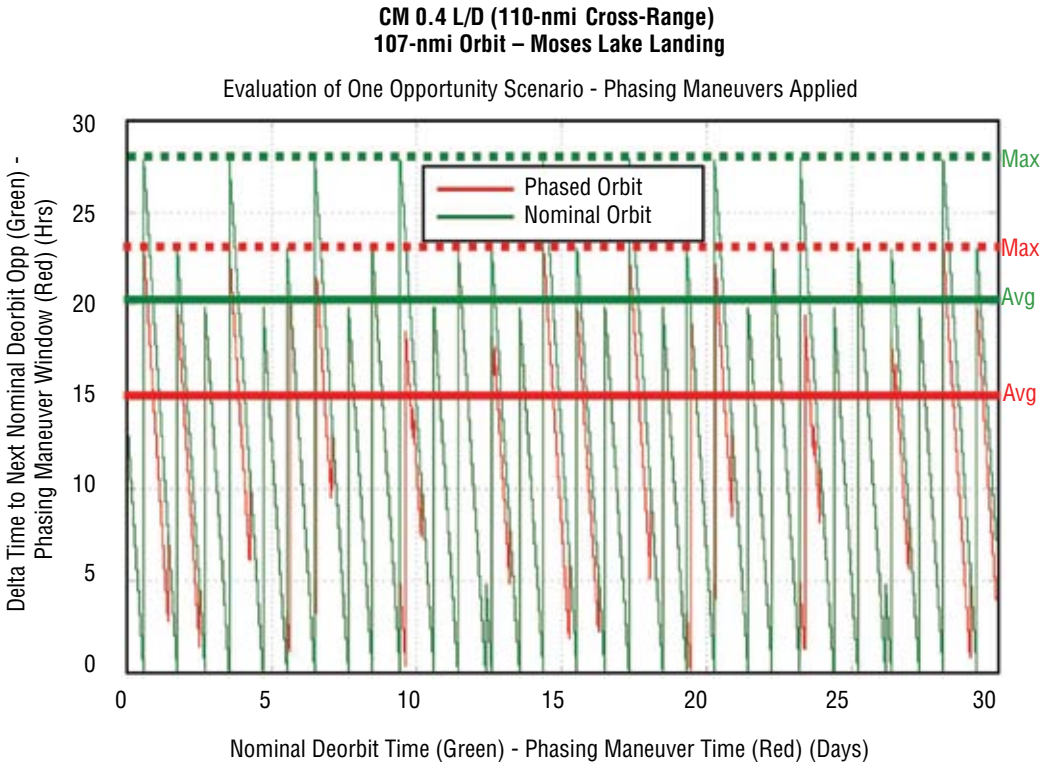

Figure 5-52. Moses Lake Deorbit Opportunities

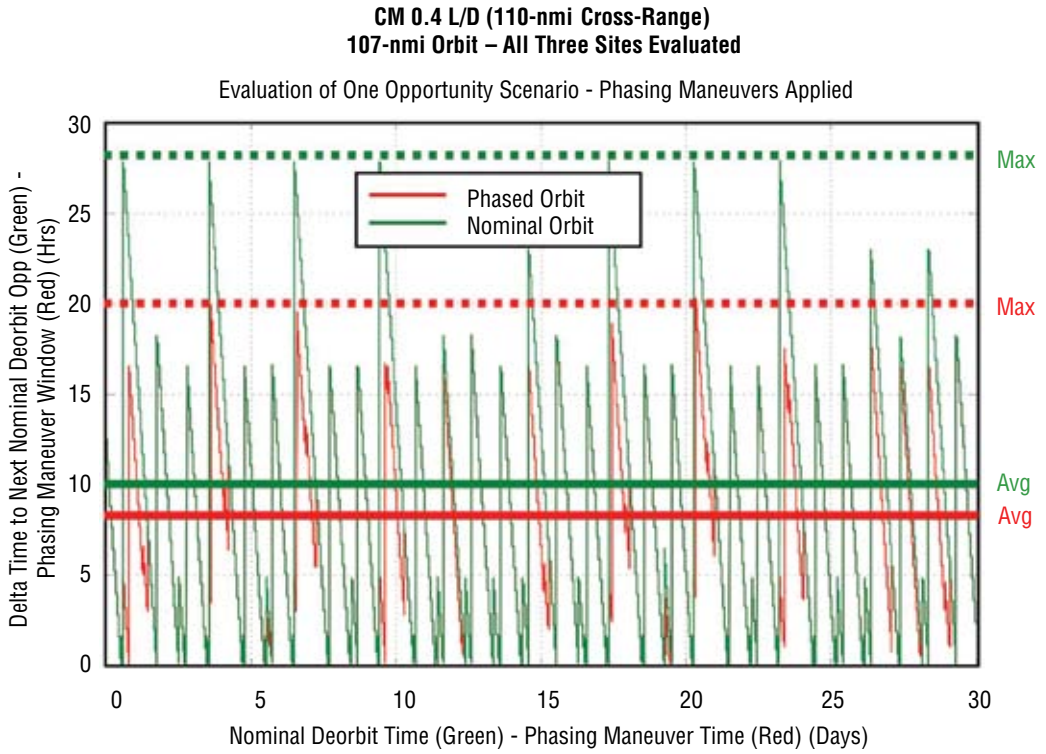

Figure 5-53. Deorbit Opportunities for All Three Sites Combined

It should be noted that the vehicle's operational altitude, vehicle cross-range capability, and site latitude location will change the landing opportunity wait times. Also, consideration of densely populated areas along the ground track to the landing site will have to be a part of a detailed safety analysis in the site selection process. At the present time, an acceptable orbital wait time requirement for the CEV has not officially been determined. Previous program studies such as X–38 and OSP only addressed the maximum wait time allowed for medical emergencies (18 hours).

Results show that the average orbital wait time for the nominal case for Moses Lake was 21 hours. This is considerably less than either Edwards AFB (39 hours) or Carson Flats (35 hours). The gap is even wider for the maximum wait time cases. However, if all three sites are considered together, the average time lowers to 10 hours and the maximum to 28 hours. If phasing is used, almost all times are reduced considerably, with the exception of combining the three sites together. In that case, the average wait time is reduced by only 2 hours and the maximum by 7 hours.

As a general rule, the higher the north or south latitude of the site, the more opportunities are available. This makes Moses Lake a good candidate as a potential landing site. However, there are other important factors that must be considered. The possibility of a water landing should be seriously considered as an option since it would alleviate many of the problems presented in this analysis.

The plots in **Figures 5-50** through **5-53** show both the nominal (green) and the phased (red) deorbit opportunities. All nominal landing opportunities are plotted for the entire mission segment, as are the predicted phasing opportunities, which are based on a current time using a

maximum allowable dwell time of 36 hours. The Y-axis shows delta time to the next opportunity in hours, and the X-axis is the mission elapsed time in days, which shows the approximate time that the deorbit opportunity needs to be performed. It should be noted that a single landing site opportunity scenario was used, as opposed to one that includes a backup site, since this information does not need to be addressed at the present time.

5.3.5.2.3 Entry Trajectory for CEV CM Returning from ISS

Process

An evaluation of the CEV returning from the ISS was conducted as part of the ESAS. A simplified CEV vehicle model was used in the 4-DOF Simulation and Optimization of Rocket Trajectories (SORT). The vehicle model consisted of an L/D of 0.4 which included constant lift-and-drag coefficients as well as a constant ballistic number throughout the entry. A complete list of the simplified CEV model can be seen in **Table 5-20**.

Table 5-20. Simplified CEV Model

Lift Coefficient	0.443
Drag Coefficient	1.11
L/D	0.4
Aeroshell Diameter (m)	5.5
Mass (kg)	10,900
Ballistic Number (kg/m^2)	413.32

All entry scenarios were flown assuming two entry techniques, guided and ballistic (spinning). The guided trajectories were all flown using the Apollo Final Phase Guidance (AFPG) logic to converge on a range target. This guidance was used for all Apollo reentries, and a derivative is currently being slated as the Mars Science Laboratory (MSL) entry guidance. The ballistic entry cases were flown at the same angle-of-attack as the guided cases, which produced the same amount of lift; however, the vehicle was given a constant spin-rate (bank-rate) to null out the lift force.

Each of the two entry modes had its own set of constraints for the entry design to accommodate. An ISS return mission had the following constraints for a nominal guided entry:

- The g-load profile experienced during entry had to be less than the maximum limits for a deconditioned crew member. (Limits are provided in **Appendix 5E**, **Crew G-Limit Curves**.)
- The vehicle had to fly at least approximately 450 nmi more range than the SM disposal to ensure proper disposal of the SM in the Pacific Ocean.
- The vehicle had to converge on the target within 1.5 nmi using the current chute-deploy velocity trigger.

Ballistic entry constraints were:

- The g-load profile experienced during the ballistic entry had to be less than the maximum crew limits for an abort scenario. (Limits are provided in **Appendix 5E**, **Crew G-Limit Curves**.)
- The ballistic vehicle must land in the Pacific Ocean.

For an ISS return mission, the primary design parameters are the EI flight-path angle and the entry guidance design. Even though each entry technique had its own constraints, the flight-path angle chosen for the guided mission also had to accommodate the ballistic entry mission. Therefore, different constraints were applied to each entry technique, but both sets of

constraints had to be satisfied with a single flight-path angle and entry guidance design. The flight-path angle and guidance design were adjusted until all nominal constraints were met. The associated ballistic case was then examined with the same flight-path angle to confirm that all ballistic constraints were met.

Results

The CEV trajectory for the ISS return mission met all nominal mission constraints. Assuming the nominal guided entry may become a ballistic entry in an abort scenario, the ballistic entry was also confirmed to meet all ballistic constraints. The entry flight-path angle that met all constraints was found to be –2.0 deg. This correlates to an inertial velocity at EI of 8 km/s, and the guidance design reference trajectory at 52 deg bank. **Figures 5-54** through **5-56** depict the nominal guided entry trajectory.

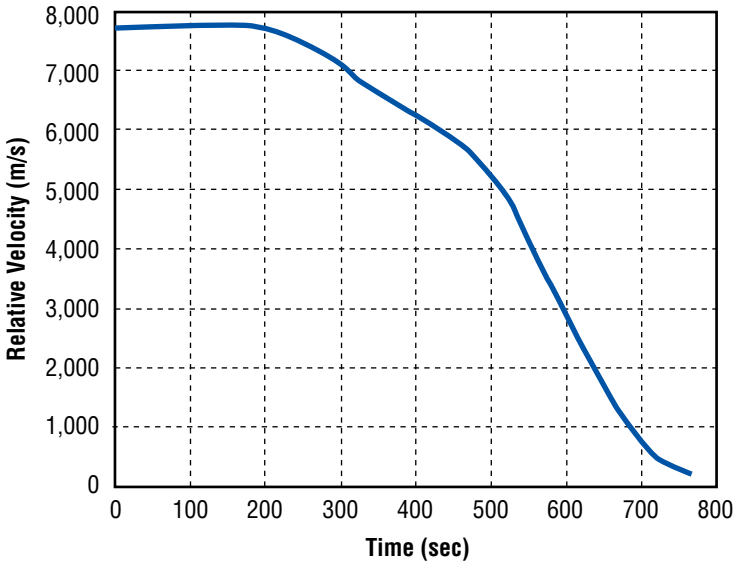

Figure 5-54. Nominal Guided – Relative Velocity Profile

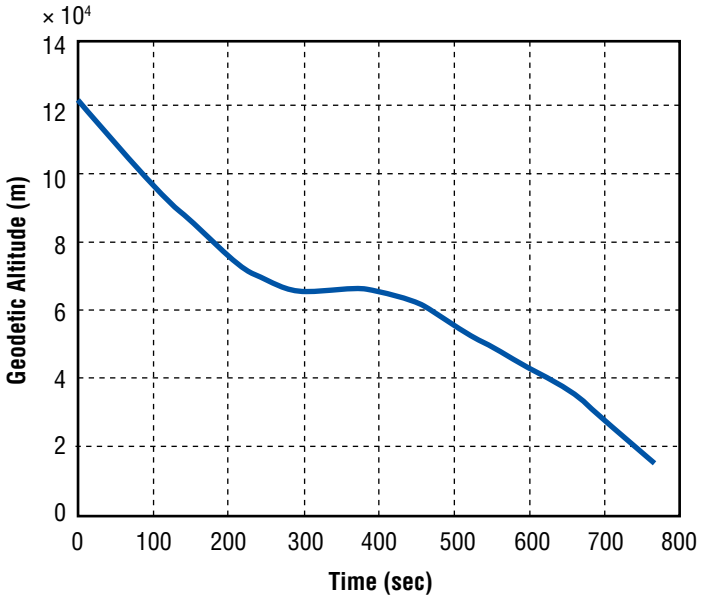

Figure 5-55. Nominal Guided – Altitude Profile

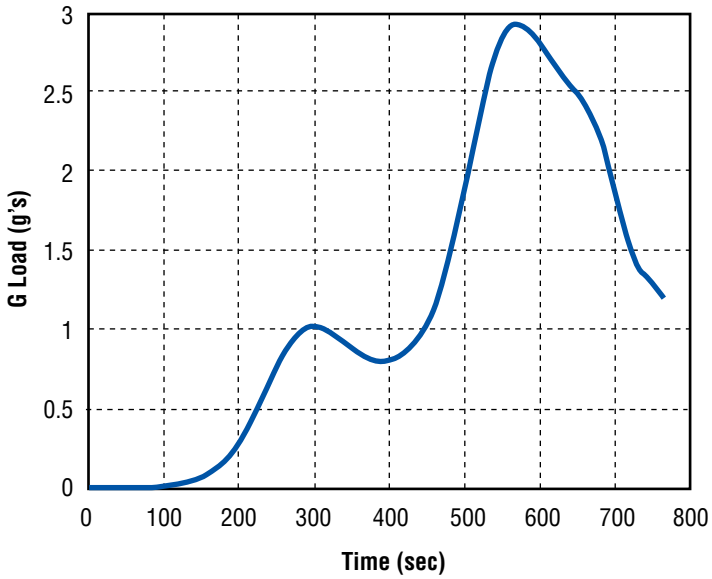

Figure 5-56. Nominal Guided – g-Load Profile

The ballistic entry (spinning) trajectory is shown in **Figures 5-57** through **5-59**).

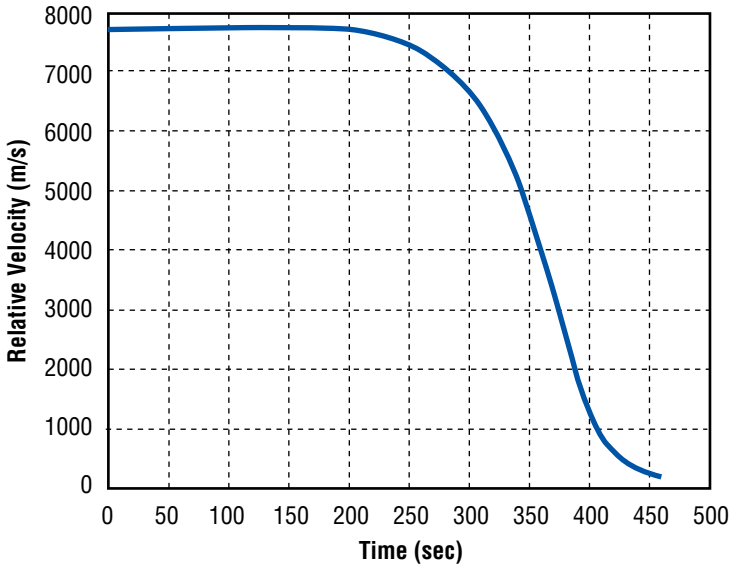

Figure 5-57. Ballistic Entry – Relative Velocity Profile

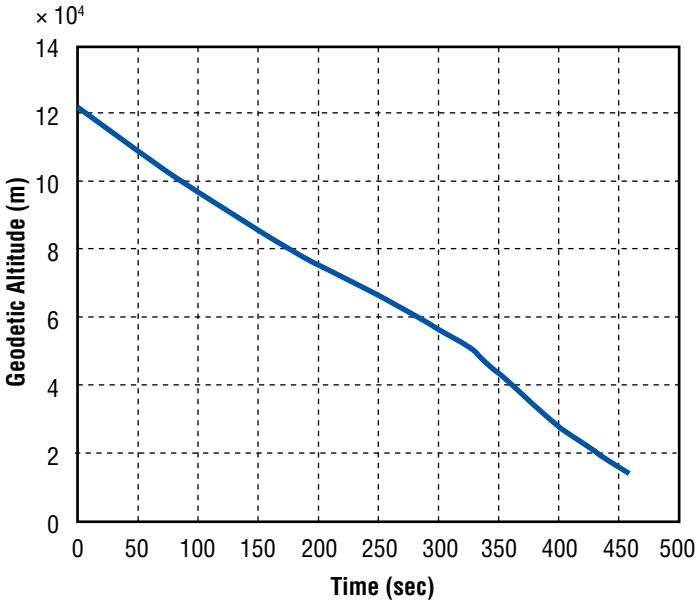

Figure 5-58. Ballistic Entry – Altitude Profile

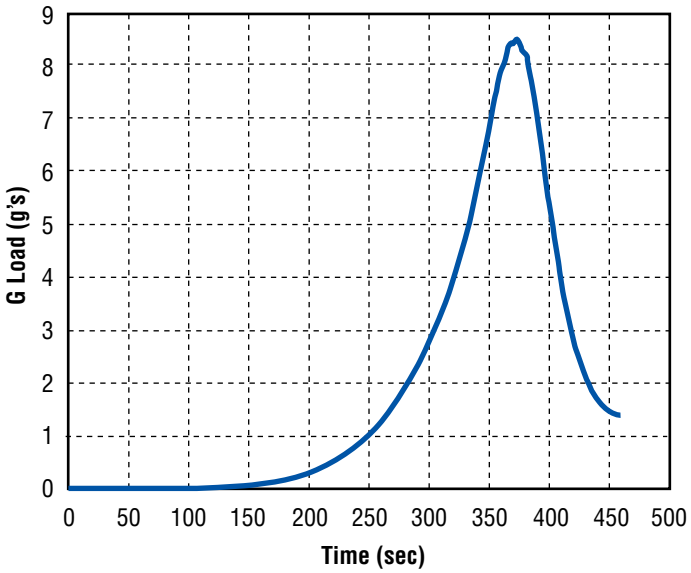

Figure 5-59. Ballistic Entry – g-Load Profile

Once the initial design analysis was completed, a corridor analysis was conducted using the nominal flight path angle and guidance design. The goal of a corridor analysis is to understand the overall capability of the vehicle to converge on the target and stay within constraints. The process starts by setting up the nominal guidance design and entry flight-path angle. The trajectory is then dispersed by steepening or shallowing the entry flight-path angle along with +30 percent of the atmospheric density for the steep case and –30 percent for the shallow case. The guided entry simulation is run using the nominal guidance design with the trajectory dispersions to confirm the vehicle's ability to still achieve the target and stay within constraints. The bounds of the corridor are determined when the vehicle no longer achieves the target or a trajectory constraint is not met. The corridor analysis revealed a corridor size of approximately 1 deg, which is sufficient, with margin, for the ISS return mission.

The ISS return mission was designed using an undispersed trajectory; thus, the design had to have margin so that the constraints would still be met when dispersions were applied. In order to confirm that all constraints would be met when dispersions were applied, a Monte Carlo analysis was conducted for both the nominal guided and ballistic entries. The Monte Carlo analysis is a statistical analysis meant to encompass all possible dispersions that may be encountered during a real-world entry. The Monte Carlo analysis included dispersions in the initial state at EI (including flight-path angle), aerodynamic uncertainties, atmosphere disturbances, and ballistic number uncertainties. For the analysis, 2,000 entry cases were simulated that applied different dispersion levels in each of the areas previously listed. The Monte Carlo analysis was used to confirm that all constraints could be met for the nominal guided and ballistic missions within the dispersed (real-world) environment. **Figure 5-60** shows a histogram plot of the maximum g-loads experienced during each of the 2,000 cases.

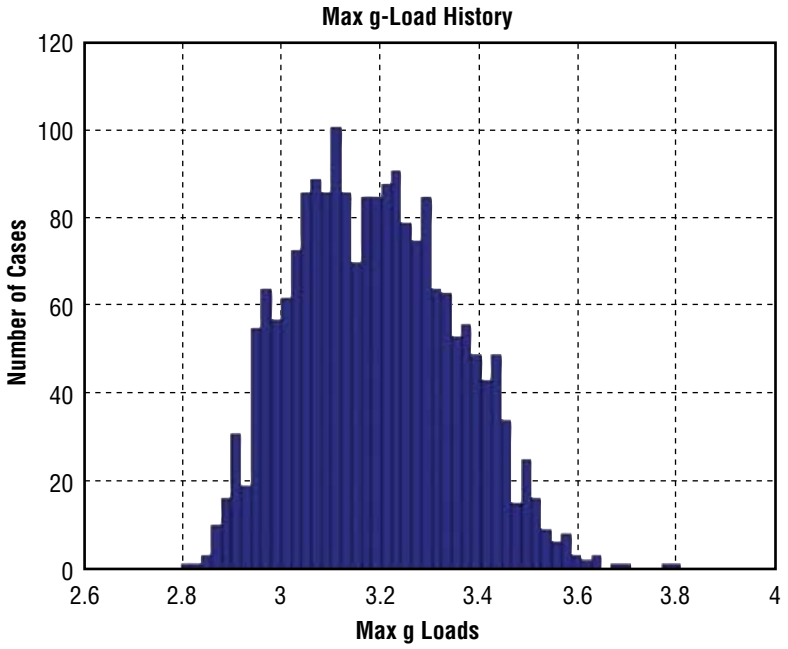

Figure 5-60. Nominal Guided Monte Carlo g-Load Histogram

As can be seen from the g-limit curves in **Appendix 5E**, **Crew G-Limit Curves**, a deconditioned crew member can withstand a 4-g load sustained (greater than 100 sec) in the X-axis ("eyeballs in") direction. Since the maximum g-load achieved for all 2,000 cases was 3.8 g's, it can be confirmed that all nominal guided cases are within the g-load limits for a deconditioned crew member.

Figure 5-61 shows the chute deploy accuracy for the same 2,000 cases.

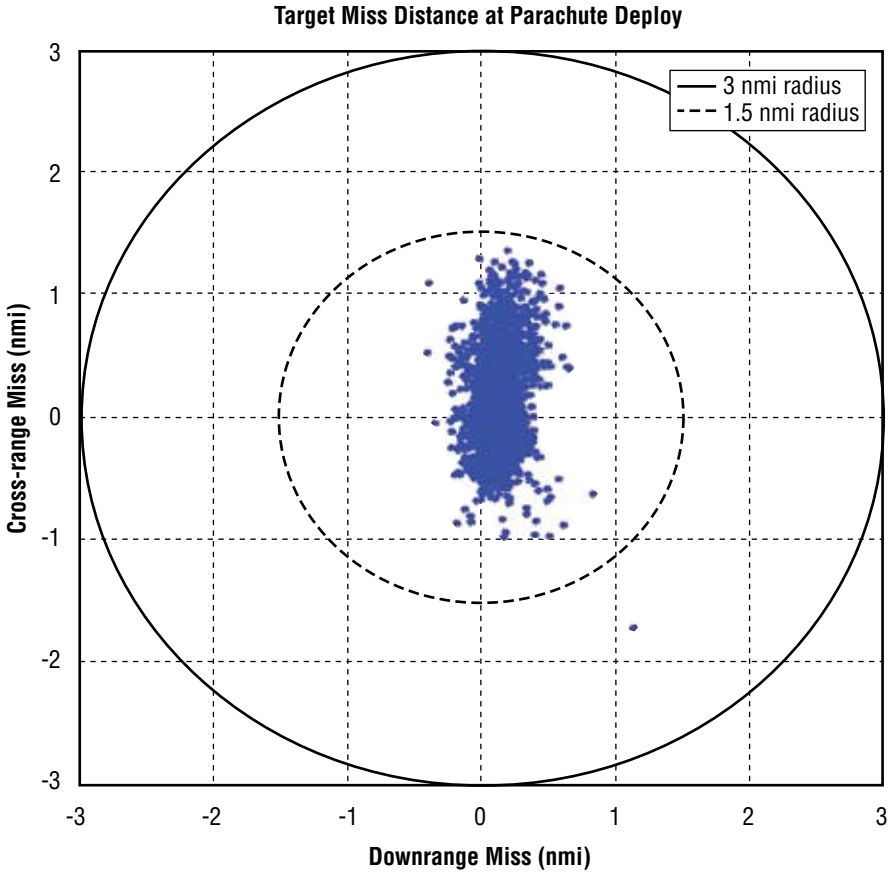

Figure 5-61. Nominal Guided Monte Carlo Target Miss Distance

All cases, except for one, are within the 1.5-nmi constraint. However, this is with a single iteration through the guidance design process. With further detailed design, this case could be brought to within 1.5 nmi. Also, the chute deploy trigger is based solely on velocity. With a more advanced chute deploy trigger and near-target guidance technique, it is believed that the target miss distance could be improved to be within 0.5 nmi or better. Based on those two assumptions, the range convergence constraint of 1.5 nmi was considered to be achieved.

The analysis for disposing of the SM in the Pacific Ocean was conducted with only a single trajectory meant to determine where the toe of the debris footprint would land relative to the target landing site. The trajectory associated with the debris toe was designed to include sufficient margin in order to represent the worst case that would come from a Monte Carlo analysis. The debris toe trajectory was given an original ballistic number of approximately 463 kg/m^2 (95 psf) and transitions to approximately 600 kg/m^2 (123 psf) at a 300,000 ft altitude. Throughout the entire entry, the debris piece was assumed to produce 0.075 L/D, which would extend the range of the toe trajectory even farther. This was determined to be very conservative and could be used to represent a worst case from a Monte Carlo analysis. The debris toe trajectory was found to land approximately 500 nmi uprange of the nominal landing target, which meets the nominal mission constraint of 450 nmi with some margin. Based on this analysis, it can be confirmed that a CEV ballistic entry would also land at least 500 nmi uprange of the target landing site, placing it in the Pacific Ocean. This is because the CEV

ballistic number is less than the toe ballistic number, resulting in less range flown, and the ballistic CEV will be spinning, thus nulling the lift force and resulting in less range flown. Therefore, the ballistic constraint of landing in the ocean is met.

A Monte Carlo analysis was also conducted assuming a ballistic entry; however, in the interest of time, only 100 cases were run instead of 2,000. This will result in less confidence in the statistical analysis, but should still allow a general trend to be established and a good approximation of the maximum value if 2,000 cases had been simulated. The histogram plot of the maximum g-loads is shown in **Figure 5-62**.

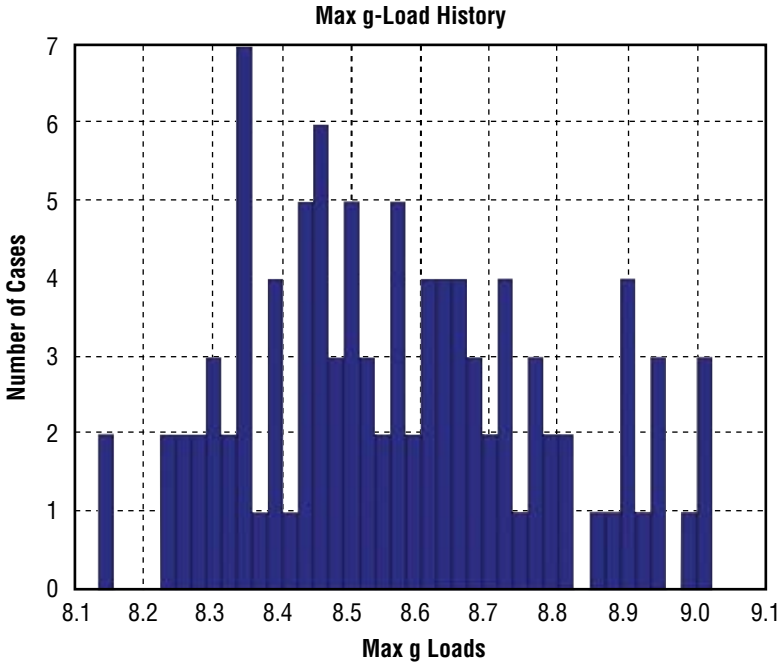

Figure 5-62. Ballistic Entry Monte Carlo G-Load Histogram

The histogram charts show a maximum g-load of roughly 9 g's. It is believed that a 2,000-case Monte Carlo would result in a maximum g-load of roughly 9.2 g's. An assessment of the g-load profile was conducted against the maximum g-load limits for an abort scenario and found to be within the limits in **Appendix 5E**, **Crew G-Limit Curves**.

All ISS return mission constraints were met with single-case trajectory designs and later confirmed with Monte Carlo analysis. Further analysis could be conducted to strengthen the confidence in the ballistic entry scenario. Analysis could also be conducted with updated models that would more accurately model the CEV capability for EI targeting, aerodynamic uncertainty, and navigation capability. Based on this first iteration approach at an entry design with the CEV, acceptable entry trajectories can be designed and flown to meet all entry constraints for a nominal guided and ballistic entry.

5.3.5.3 Return from Lunar Missions CEV Entry Trajectories

5.3.5.3.1 Landing Mode Skip-Entry Technique Description

The "skip-entry" lunar return technique provides an approach for returning crew to a single CONUS landing site anytime during a lunar month. This is opposed to the Apollo-style entry technique that would require water or land recovery over a wide range of latitudes, as explained in the following sections. This section will discuss the top-level details of this technique, as well as the major technological and vehicle system impacts.

The skip-entry trajectory approach is not a new concept. The original Apollo guidance was developed with skip trajectory capability, which was never used because of navigation and control concerns during the skip maneuver. The Soviet Union also used skip trajectories to return Zond robotic vehicles to a Russian landing site. Considerable analysis was completed in the 1990s to investigate the long-range capability of vehicles in the 0.5 L/D class, which, at that time, was considered the minimum L/D required to enable accurate skip trajectory entry capability. Skip-entry in its current formulation for the ESAS effort differs in two ways from previous approaches for capsule vehicles. First, the inclusion of an exoatmospheric correction maneuver at the apogee of the skip maneuver is used to remove dispersions accumulated during the skip maneuver. Secondly, the flight profile is standardized for all lunar return entry flights. Standardizing the entry flights permits targeting the same range-to-landing site trajectory flown for all return scenarios, stabilizing the heating and loads that the vehicle and crew experience during flight. This does not include SM disposal considerations that must be assessed on a case-by-case basis.

The Standardized Propulsive Skip-Entry (SPASE) trajectory begins at the Moon with the targeting for the TEI maneuver. The vehicle is placed on a trajectory that intercepts EI (121.9 km, 400,000 ft) at Earth at the correct flight-path angle, latitude, time (longitude), range, and azimuth to intercept the desired landing site. **Figure 5-63** shows the geometry and the resulting ground tracks at two points, 11,700 km (6,340 nmi) and 13,600 km (7,340 nmi) antipode range, along two Constant Radius Access Circles (CRACs). The antipode is targeted to slide along the desired CRAC during the lunar month, fixing the range to the desired landing site. The flight-path angle, longitude, and azimuth are controlled via the TEI maneuver back at the Moon, establishing the required geometry to accomplish the return entry flight. The Moon is shown at a maximum declination of ±28.6 deg. The entry vehicle enters the atmosphere at lunar return speed (approximately 11.1 km/sec) and then steers to a desired exit altitude and line-of-apsides. Currently, this altitude is approximately 128 km (420,000 ft). During the coast to apogee, the navigation system is updated via GPS communication. Just before apogee of the skip orbit, a correction burn is executed using small engines on the capsule to correct for dispersions (if required) accumulated during the skip phase of flight. This maneuver steers the vehicle to an optimal set of conditions (flight-path angle and range) at the second entry point. The second entry is initiated at LEO entry speeds. The vehicle enters the atmosphere a second time and steers to the desired landing site location. The change in targeting to the shallow side of the entry corridor for the first entry enables the skip trajectory to be safely designed within guidance capability and remains a distinct difference between targeting direct-entry versus skip-entry.

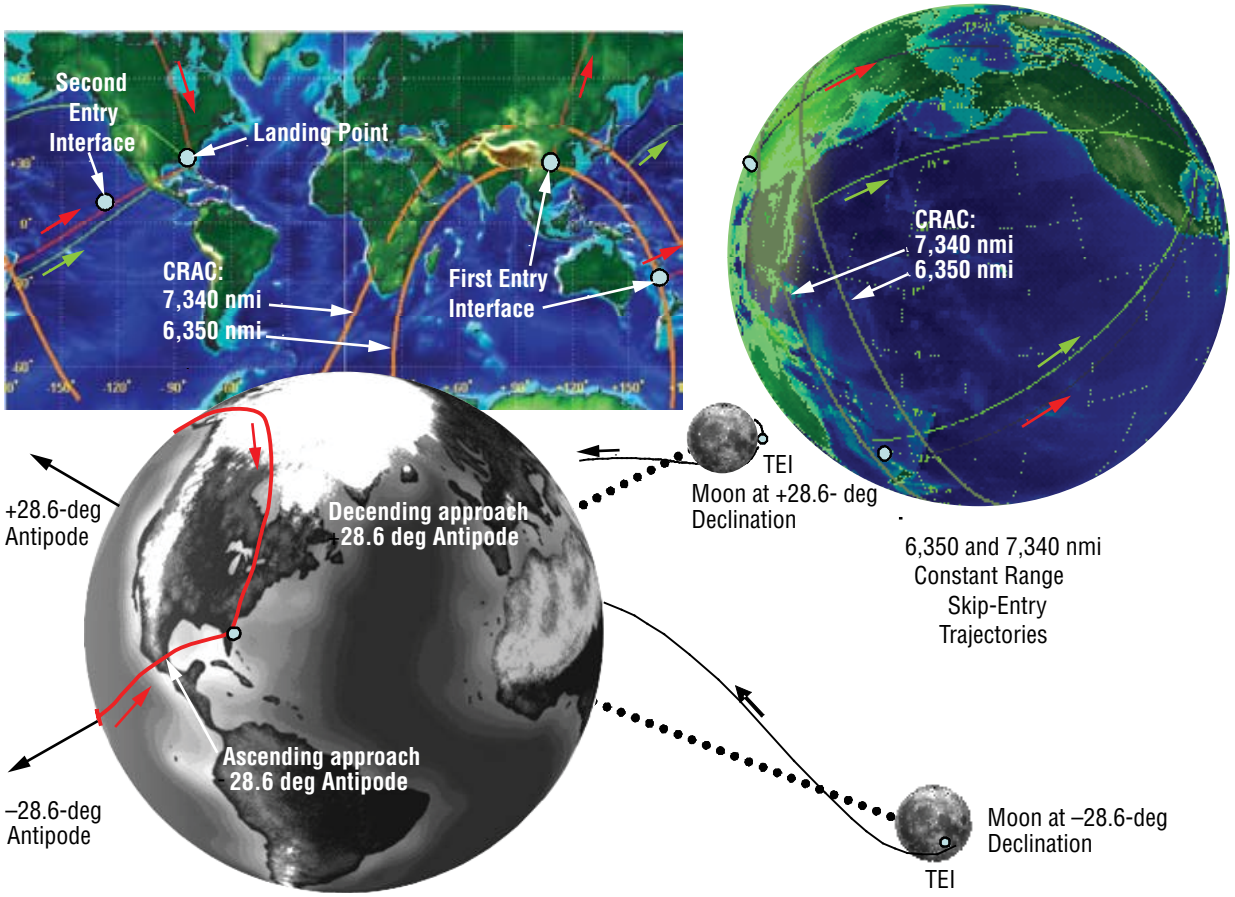

Figure 5-63. SPASE Entry Design Concept

Several state-of-the-art guidance algorithms are currently used for steering the vehicle. The generic vehicle design with 0.3 L/D used in this preliminary analysis is shown in **Figure 5-64**. The vehicle is controlled by steering the lift vector via a bank angle about the relative velocity vector. The angle-of-attack is fixed by appropriately designing the vehicle CG. The Hybrid Predictive Aerobraking Scheme (HYPAS) is used for steering the vehicle during hypersonic skip flight. The Powered Explicit Guidance (PEG) is used for the exoatmospheric correction maneuver. The Space Shuttle Entry Guidance (SEG) is used for steering the hypersonic and supersonic phases of the second entry. Finally, the Apollo Entry Guidance (AEG) is used for steering the supersonic and transonic flight phases down to parachute deployment. Ballistic chutes are released at a 6–km (20,000–ft) altitude.

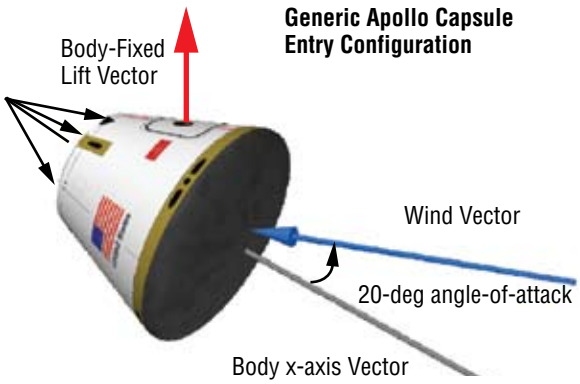

Figure 5-64. Generic SPASE Entry Capsule Concept

Figure 5-65 shows the time line of events for a 7,340-nmi CRAC SPASE flight to NASA's KSC for the Moon at +28.6-deg declination and the antipode at –28.6 deg. Note that the entire entry phase from first entry to landing is completed in less than 40 minutes. **Figures 5-66** through **5-70** provide trajectory plots for nominal flight, and **Figures 5-71** through **5-75** provide trajectory plots for a 100-case Monte Carlo. The Monte Carlo used Global Reference Atmospheric Model (GRAM) atmosphere and winds, initial state, weight, and aerodynamics uncertainties, with perfect navigation.

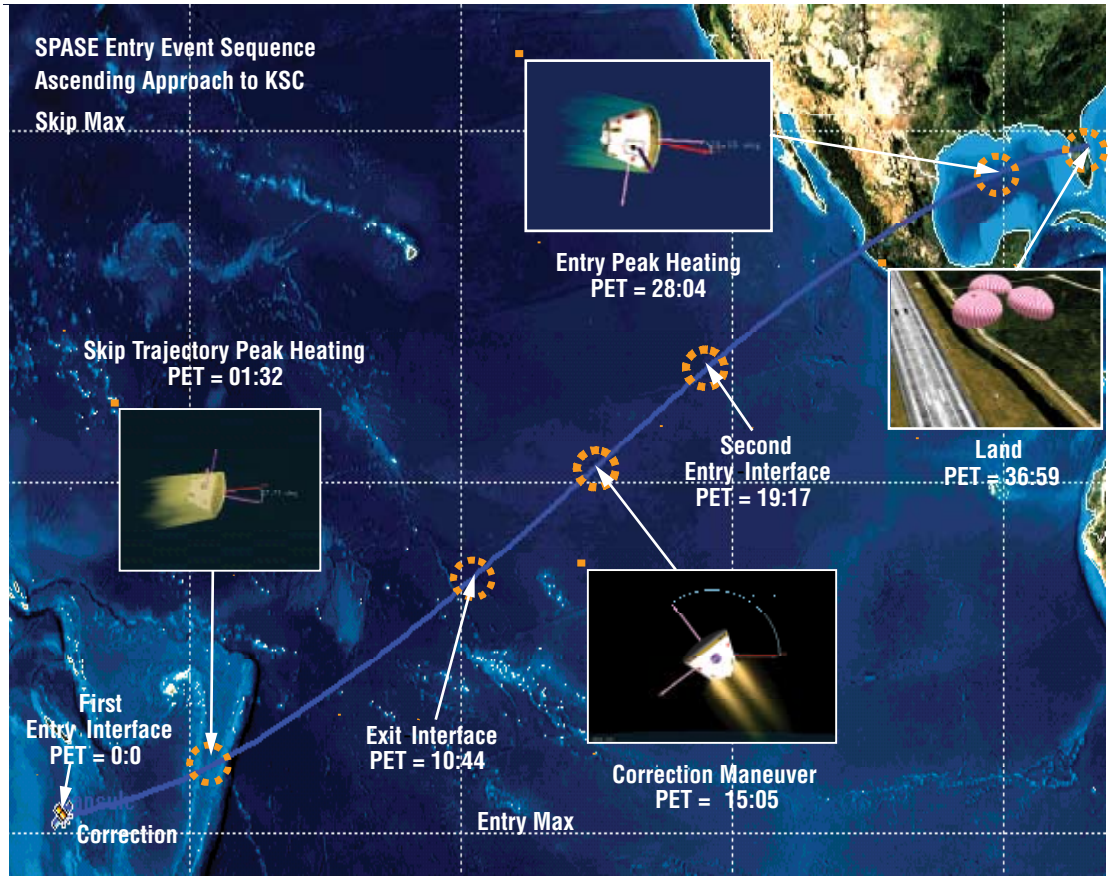

Figure 5-65. SPASE Nominal Flight Entry Event Sequence, (times shown in minutes: seconds)

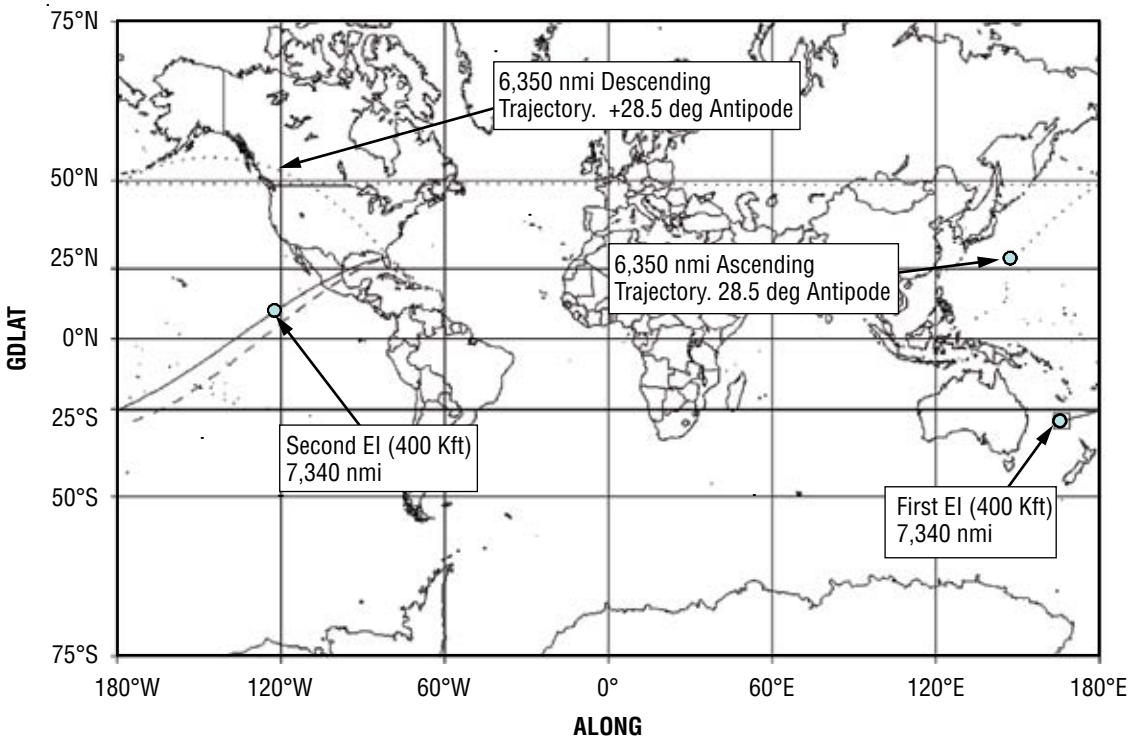

Figure 5-66. SPASE Nominal Flight Groundtrack to KSC

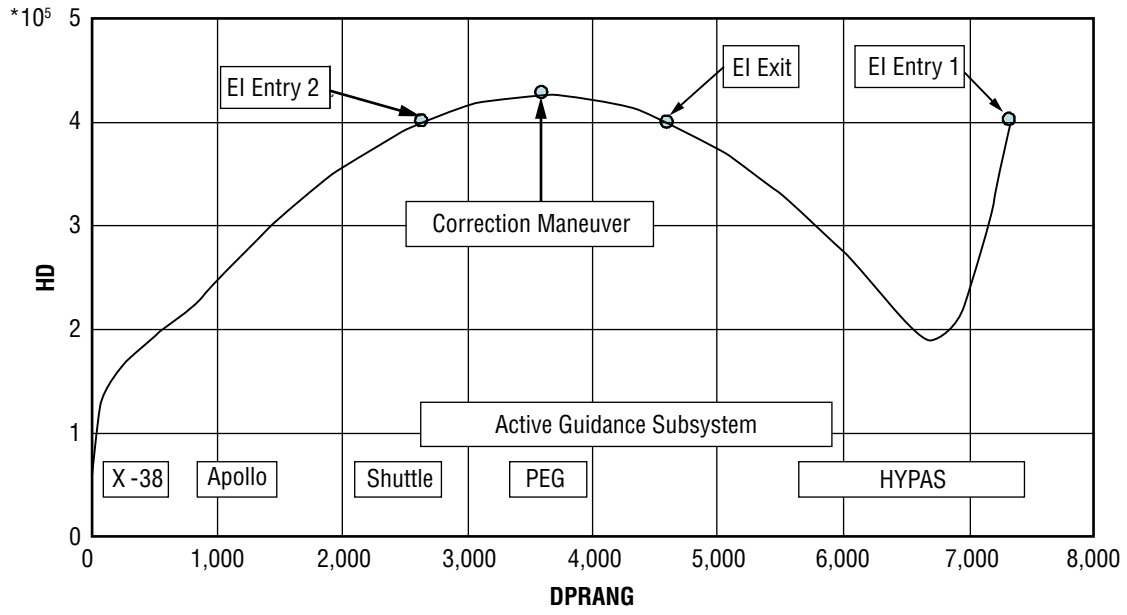

Figure 5-67. SPASE Nominal Flight Geodetic Altitude (ft) versus Range (nmi) to Landing Site

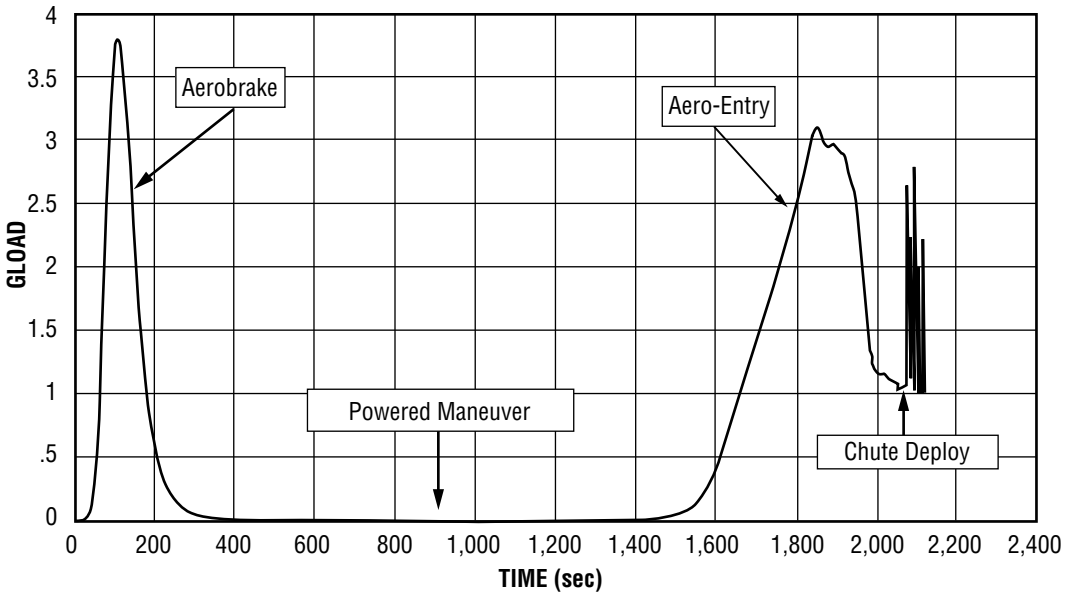

Figure 5-68. SPASE Nominal Flight Total Aerodynamic/Propulsive Acceleration (g's) versus Time (sec)

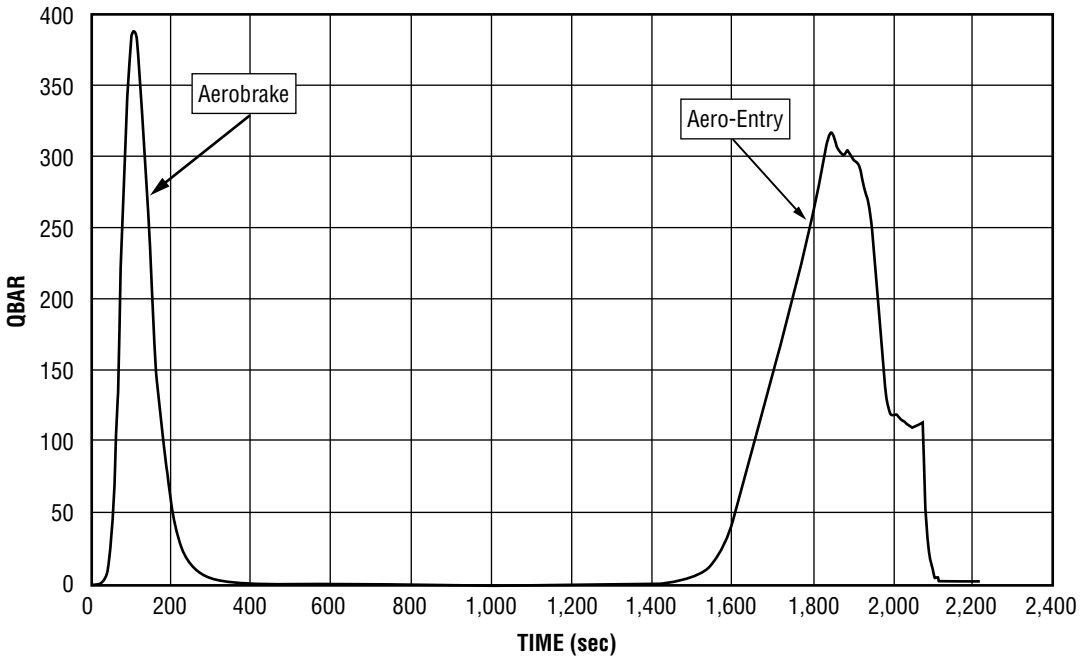

Figure 5-69. SPASE Nominal Flight Dynamic Pressure (psf) versus Time (sec)

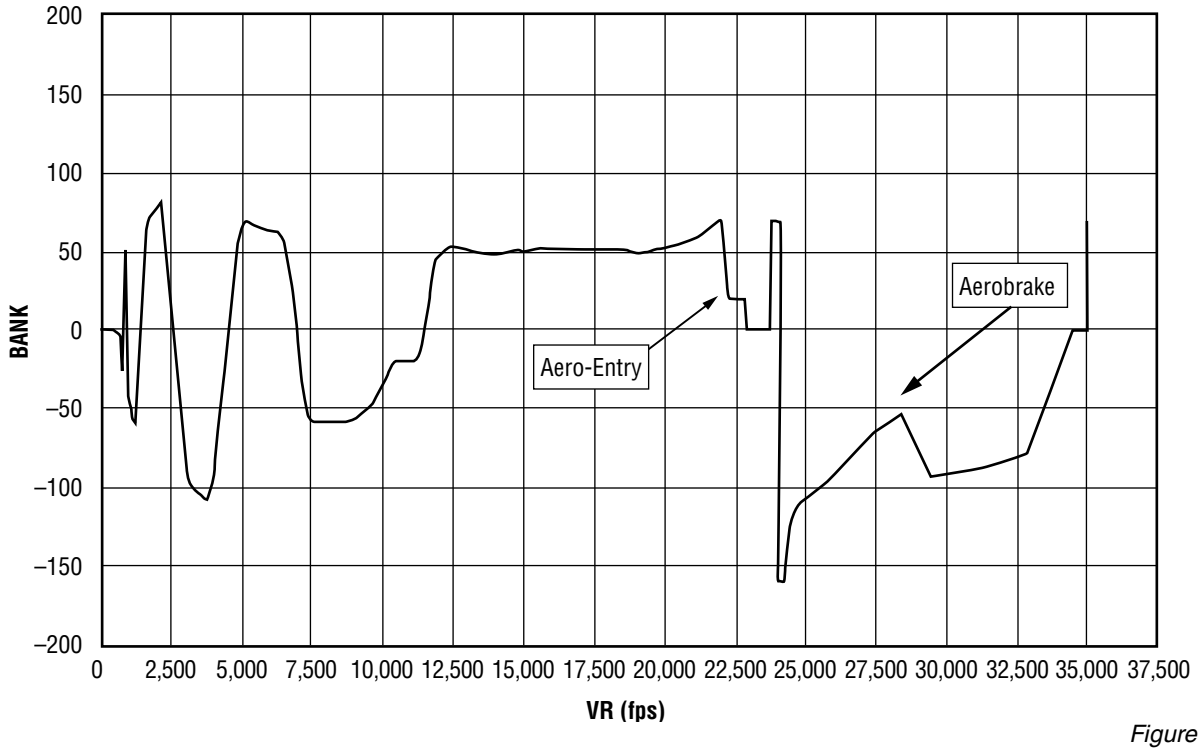

Figure 5-70. SPASE Nominal Bank Angle (deg) versus Relative Velocity (fps)

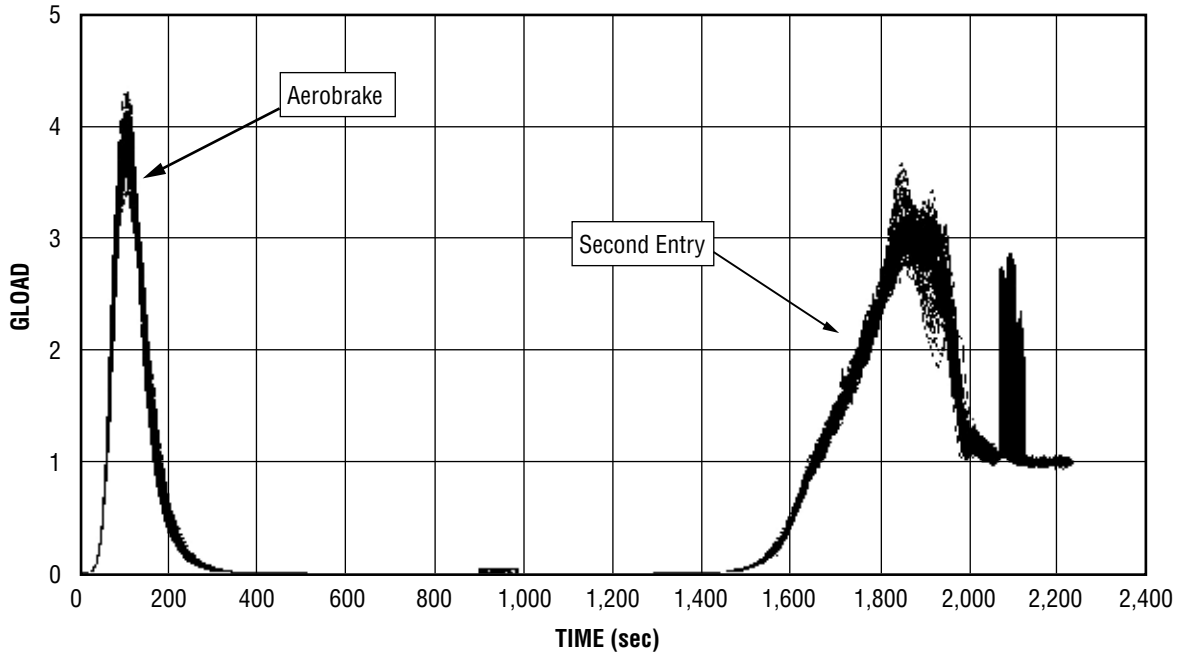

Figure 5-71. SPASE Dispersed Flight Acceleration (g's) versus Time (sec) (100 Cases)

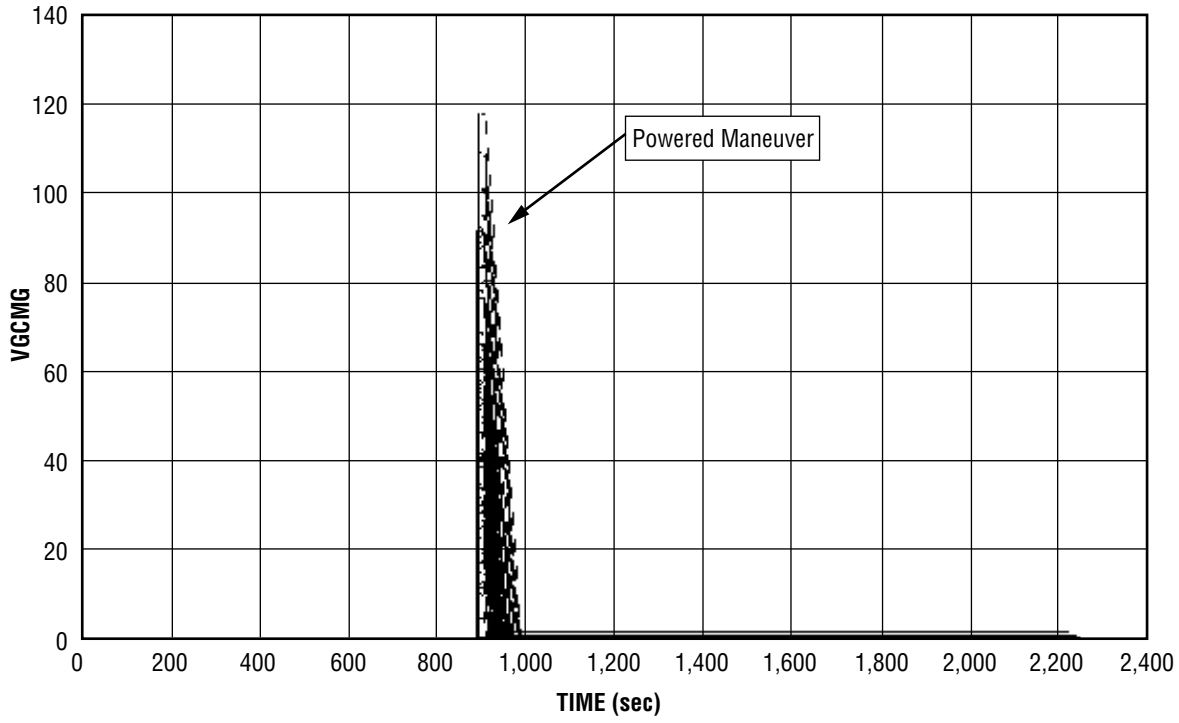

Figure 5-72. SPASE Powered Maneuver Delta Velocity Required (fps) versus Time (sec) (100 Cases)

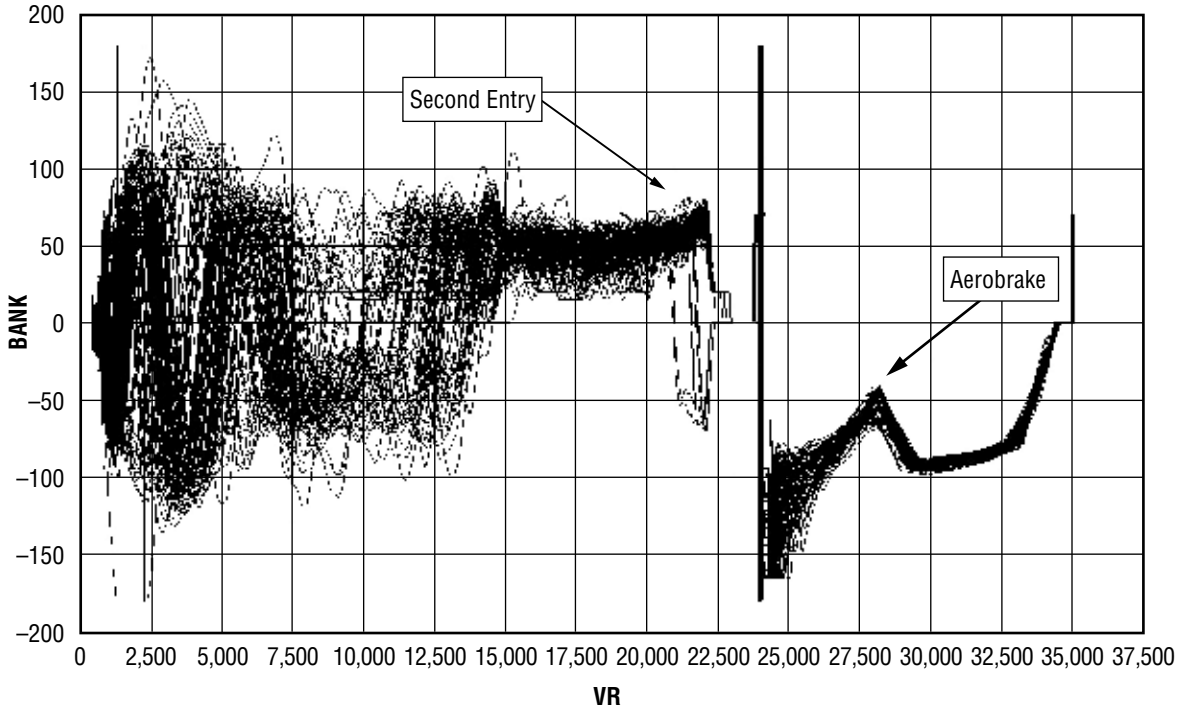

Figure 5-73. Bank Angle (deg) versus Relative Velocity (fps)– Dispersed Flight (100 Cases)

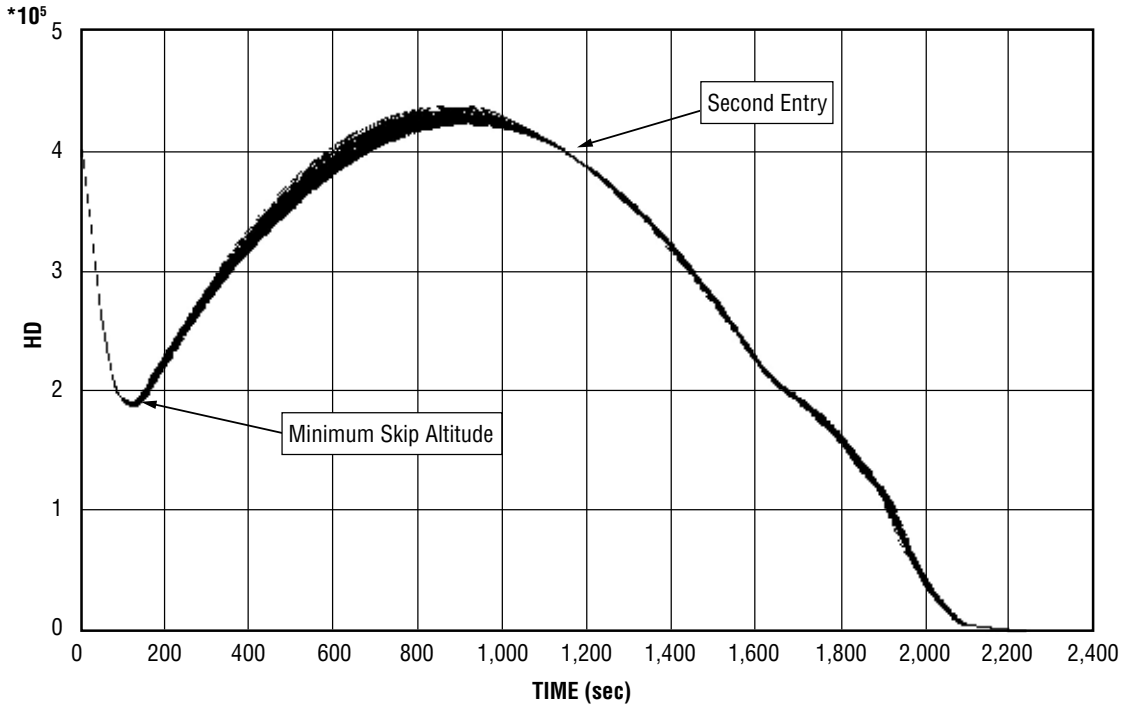

Figure 5-74. Geodetic Altitude (ft) versus Time (sec)–Dispersed Flight (100 Cases)

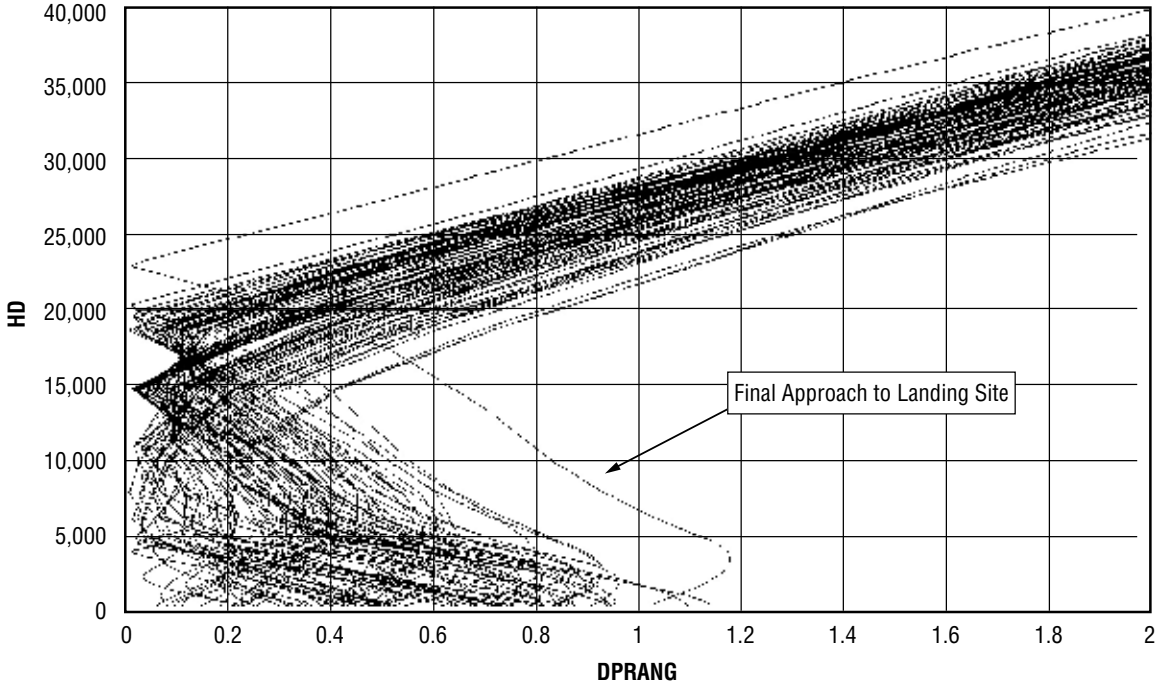

Figure 5-75. Geodetic Altitude (ft) versus Range at Final Approach (nmi)–Dispersed Flight (100 Cases)

5.3.5.3.2 Direct-Entry Versus Skip-Entry Comparison

This section will compare a lunar return direct-entry flight to a skip-entry flight. The vehicle used in this comparison will be an Apollo-style capsule with a ballistic number of 106 psf and a L/D ratio of 0.3. The drag coefficient is 1.29. The entry speed will be 36,309 fps at an EI altitude of 400,000 ft. The flight-path angle for the direct-entry flight is –6.65 deg and –6.0 deg for the skip-entry. The difference in nominal flight-path angle at EI is the most distinct difference in the targeting between skip-entry and direct-entry. The direct-entry flight is targeted to ensure capture of the vehicle and protect against skip-out of the entry vehicle. The skip-entry vehicle is designed to skip-out and, therefore, is biased into the skip side of the entry corridor. The vehicle must target lift-vector up during a majority of the skip phase to achieve the low-altitude skip target. Biasing the skip targeting to the steep side of the skip corridor is required to ensure that the vehicle will ballistically enter in case a failed control system and vehicle spin-up is required. This steep targeting is also required to ensure that the SM will ballistically enter and impact into a safe water location.

The Apollo-style direct-entry requires water- or land-landing over a wide range of latitudes. The antipode defines a vector connecting the Moon and Earth at time of lunar departure and closely approximates the landing site for a direct-entry mission. The lunar inclination, and, therefore, antipode varies from 28.6 deg to 18.3 deg over an 18.6-year lunar cycle. Therefore, depending on the lunar cycle, appropriate recovery forces or ground landing zone would have to be available within this antipode range approximately 3 days from lunar departure. For an L/D of approximately 0.3, this implies a landing site or recovery ship within 2,200 km of the EI location, or 200 km of the antipode location.

The guidance bank angle command is used to steer the entry vehicle to drogue chute deployment. The target range is 1,390 nmi for the direct-entry mission. The 1969 version of Apollo guidance is used for modeling the direct-entry flight. For the skip-entry trajectory, the HYPAS aero-braking guidance algorithm is used for the skip phase of the skip-entry flight. The Powered Explicit Guidance (PEG) algorithm is used for the exoatmospheric flight phase. For the second entry, the hypersonic phase of the SEG is used. Finally, the final phase of the AEG algorithm is used for sub-mach-5 flight to chute deployment. The target range for the skip-entry flight under analysis is 13,600 km (7,340 nmi) from EI.

The intent of this section is to quantify the trajectory differences between flying a 0.3 L/D vehicle using the standard Apollo-style direct-entry versus a skip-entry method. As can be noted from the plots in **Figures 5-76** and **5-77**, the skip-entry method provides a lower heat rate but higher heat loads than the direct-entry method. The skip-entry trajectory also has a “cooling off” period following the first aerobrake maneuver before the second entry. This will allow the heat pulse absorbed during the aeropass to soak into the structure and must be accounted for in the TPS design. The dramatic difference in range flown from EI is the most distinct difference between the trajectories. This not only extends the flight time but greatly extends the distance between the location of the SM disposal footprint. It also locates the ballistic abort CM location close to the perigee of the lunar approach orbit. The great distance between the SM disposal location could be advantageous for inland landing site locations or populated over-flight geometries; however, the great distance between the ballistic abort landing point and the nominal landing point would necessitate a mobile Search and Rescue Force to recover the crew and vehicle from the abort landing location.

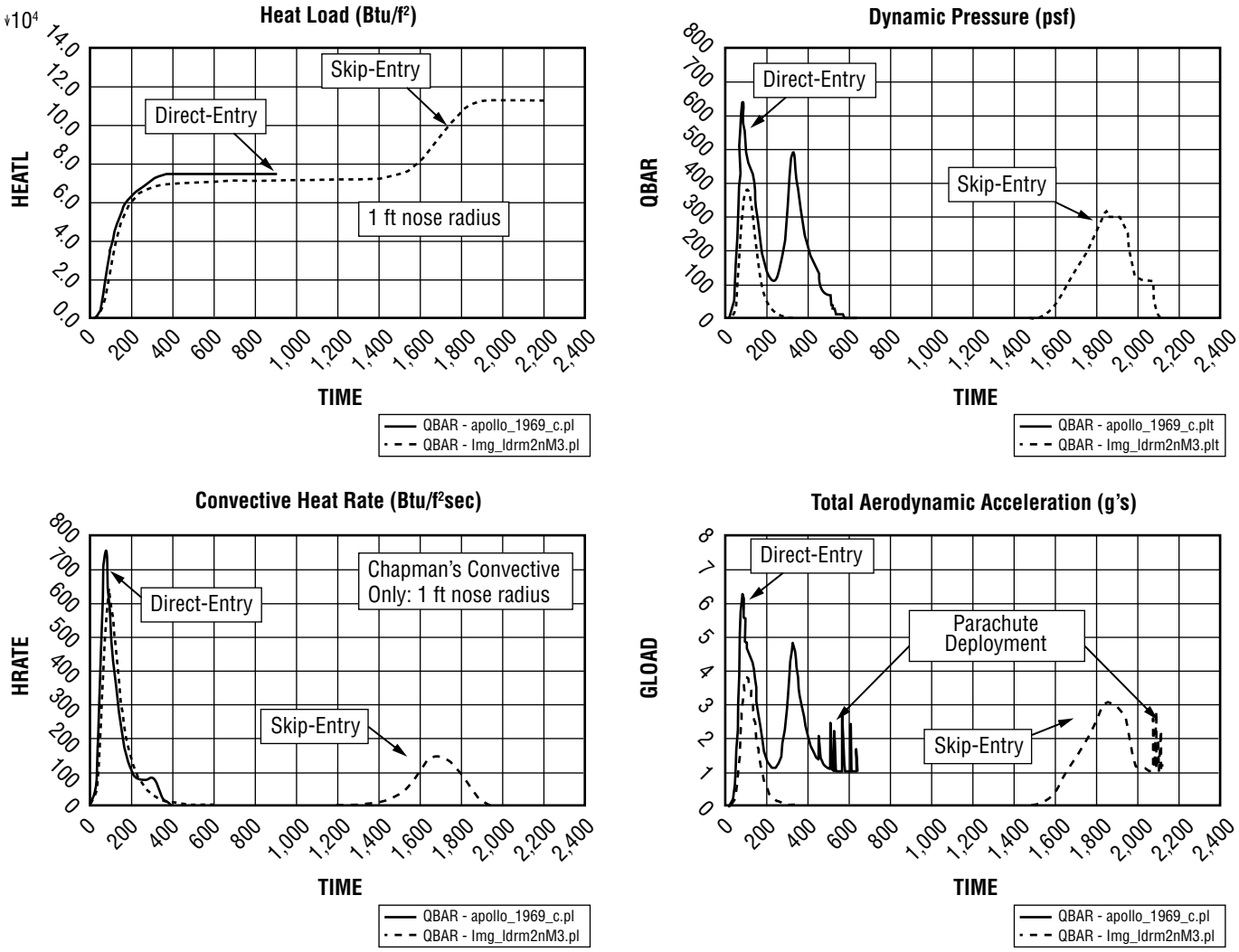

Figure 5-76. Trajectory Comparisons Direct versus Skip-Entry

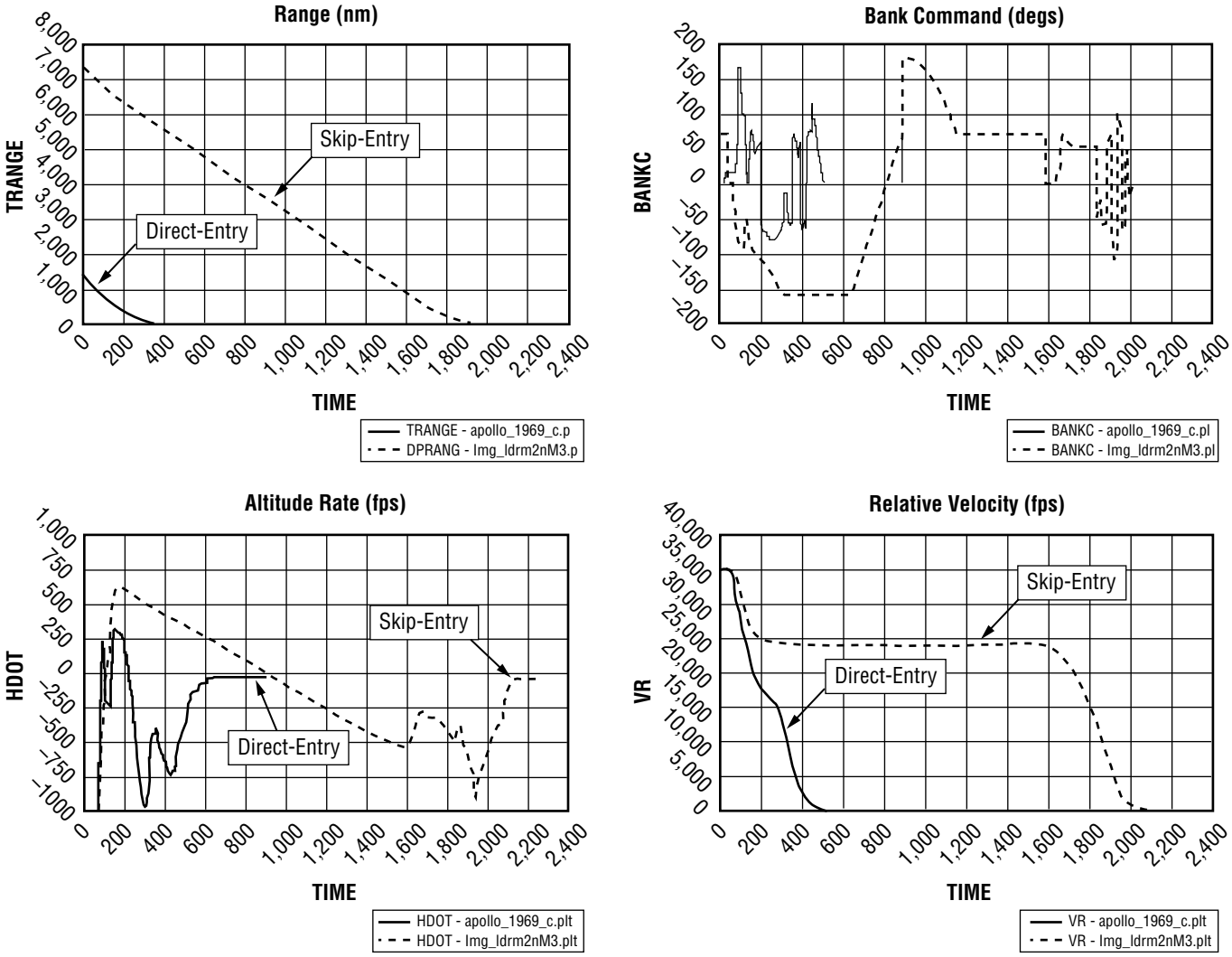

Figure 5-77. Trajectory Comparisons Direct versus Skip-Entry

5.3.5.3.3 Skip-Entry Vehicle Configuration Comparison

This section will provide a comparison of three different vehicle comparisons (**Figures 5-78** to **5-85)** for a skip-entry trajectory. The vehicles considered will be a capsule (L/D = 0.3, ballistic number = 64 psf), a biconic (L/D = 0.82, ballistic number = 199 psf), and an ellipsled (L/D = 0.66, ballistic number = 197 psf). Targeting was completed that ensured the proper amount of energy is depleted for an exoatmospheric apogee altitude of approximately 420,000 ft. This implied a capsule EI flight-path angle of –5.83 deg, a biconic EI flight-path angle of –6.94 deg, and an ellipsled EI flight-path angle of –6.5 deg. The steeper flight-path angles required for the ellipsled and biconic are a result of the higher ballistic number and the increased lift acceleration used for exit-phase targeting. The entry conditions for all vehicles simulate a lunar return with an inertial entry velocity of 11.1 km/sec (36,300 fps).

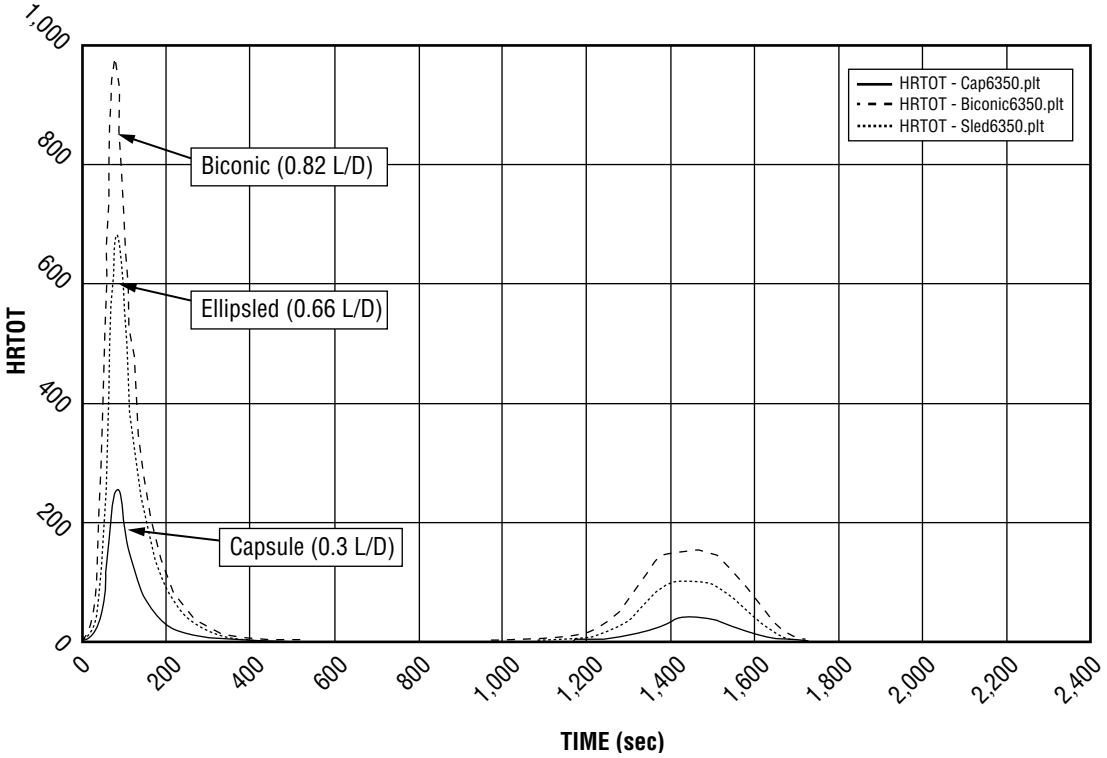

Figure 5-78. Total Heating - Radiative Plus Convective (1-ft Radius Sphere)

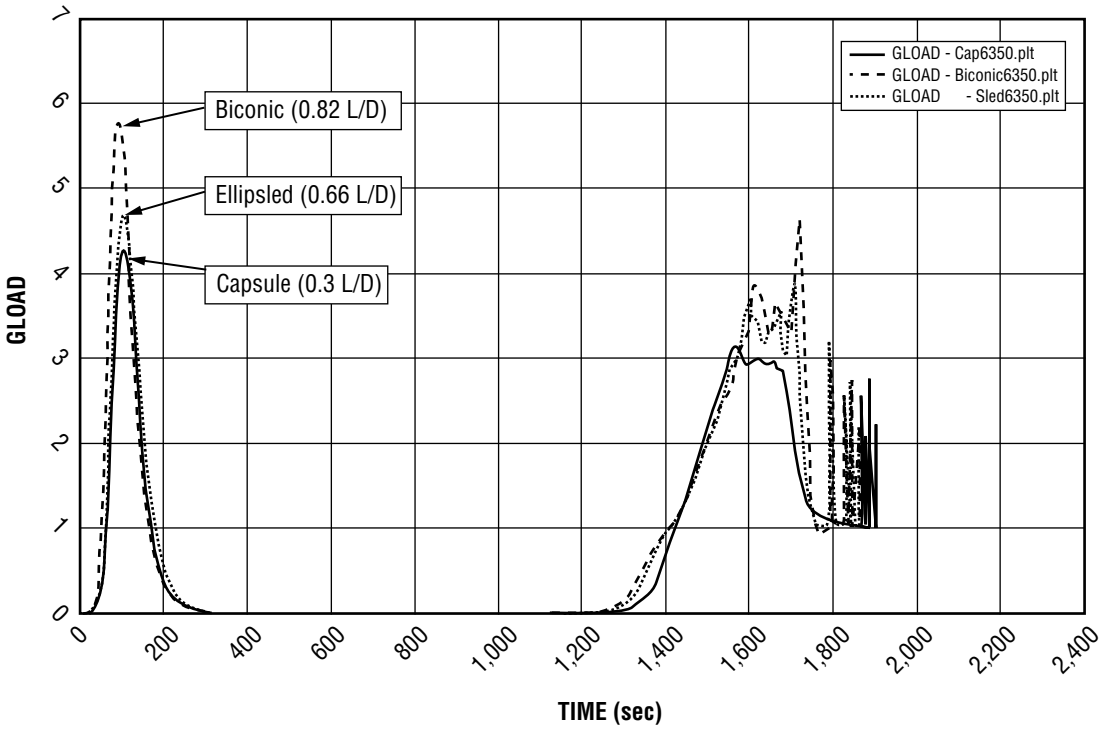

Figure 5-79. Total Aerodynamic Acceleration (g's) versus Time from EI (sec)

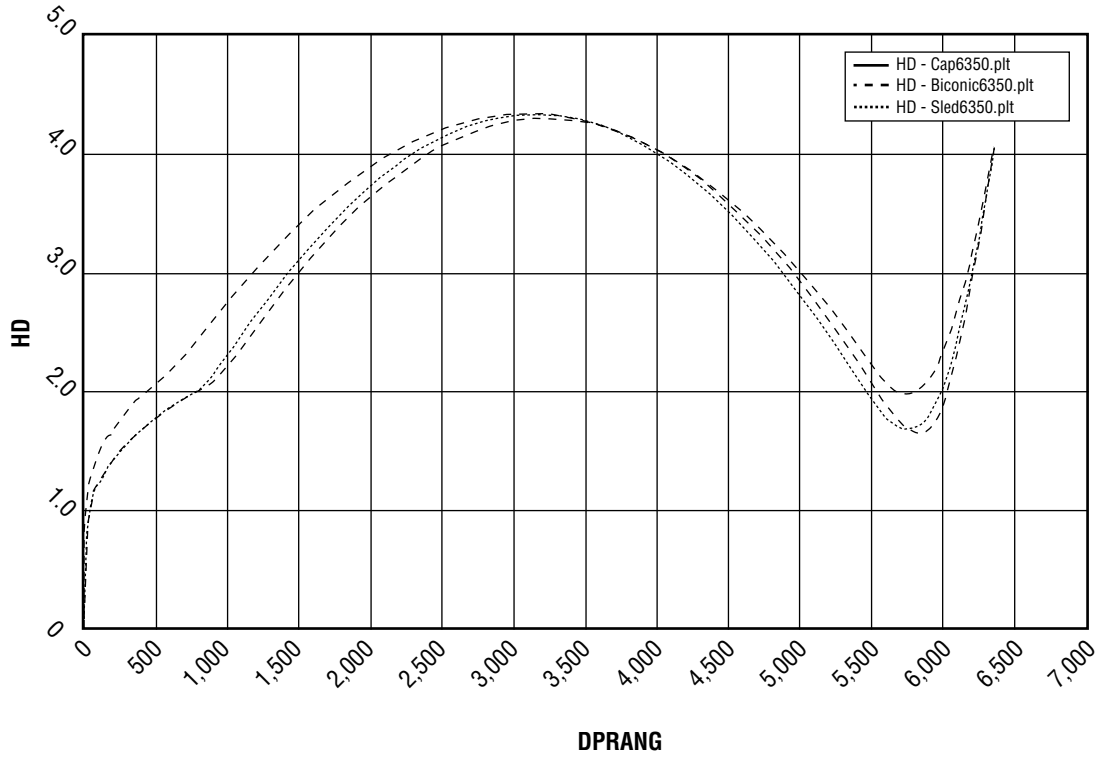

Figure 5-80. Geodetic Altitude (ft) versus Range-to-Target, DPRANG (nmi)

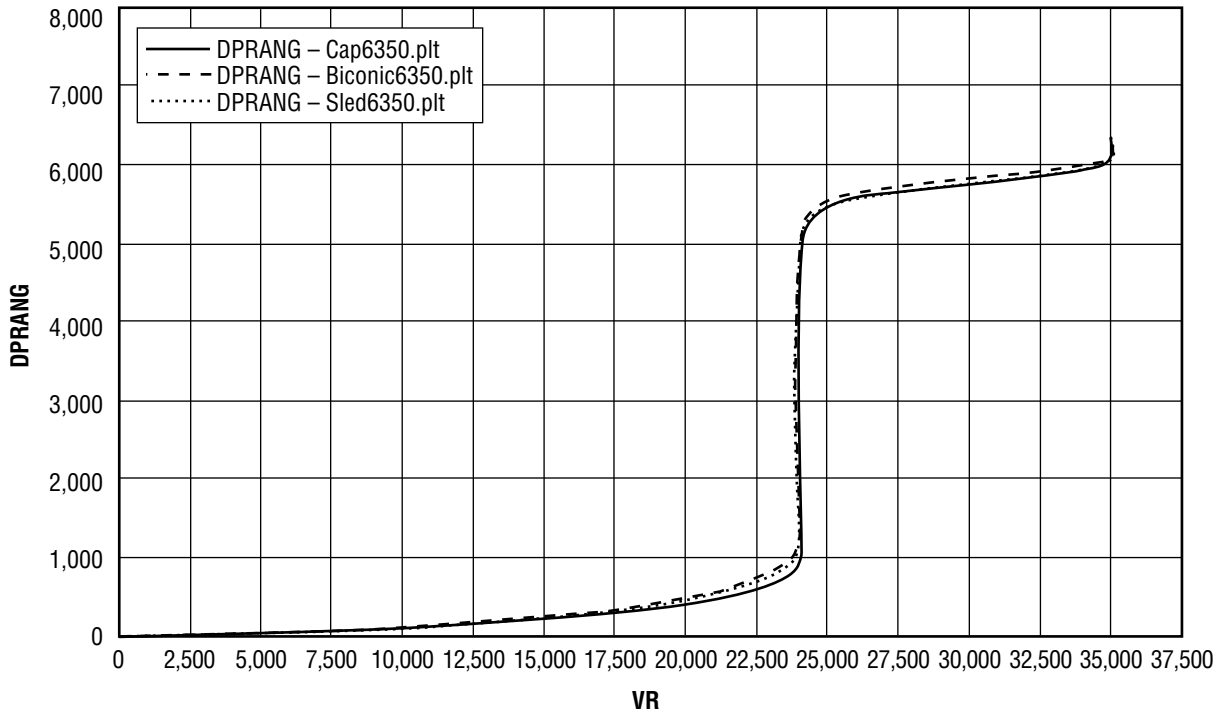

Figure 5-81. Range-to-Target (nmi) versus Relative Velocity (fps)

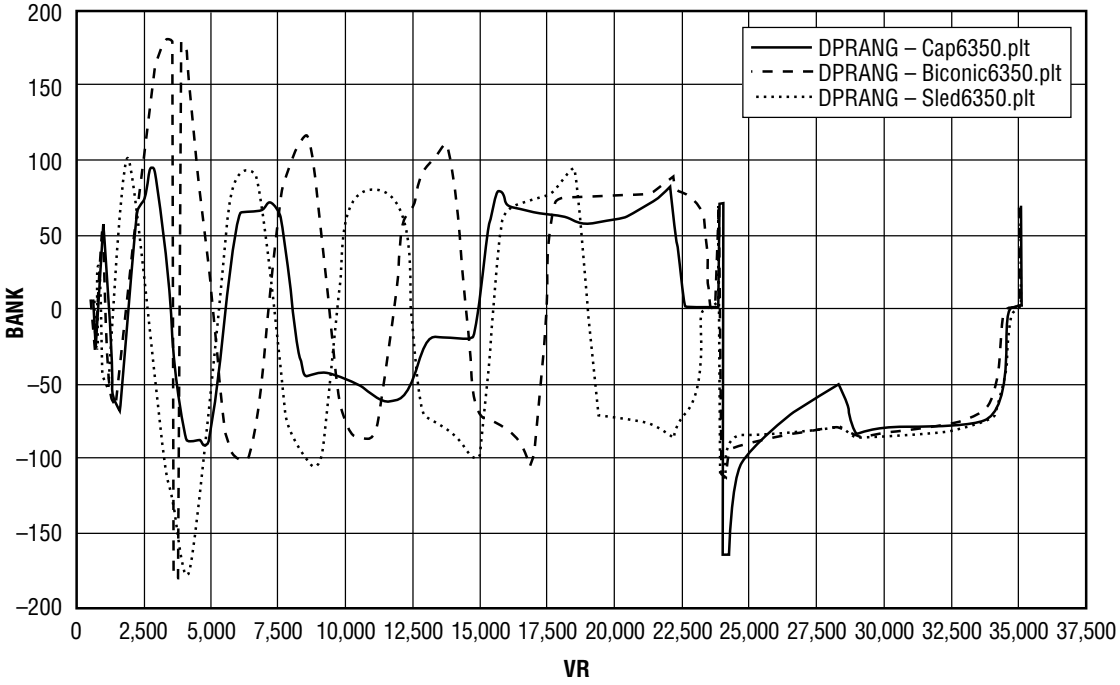

Figure 5-82. Bank Angle versus Relative Velocity (fps)

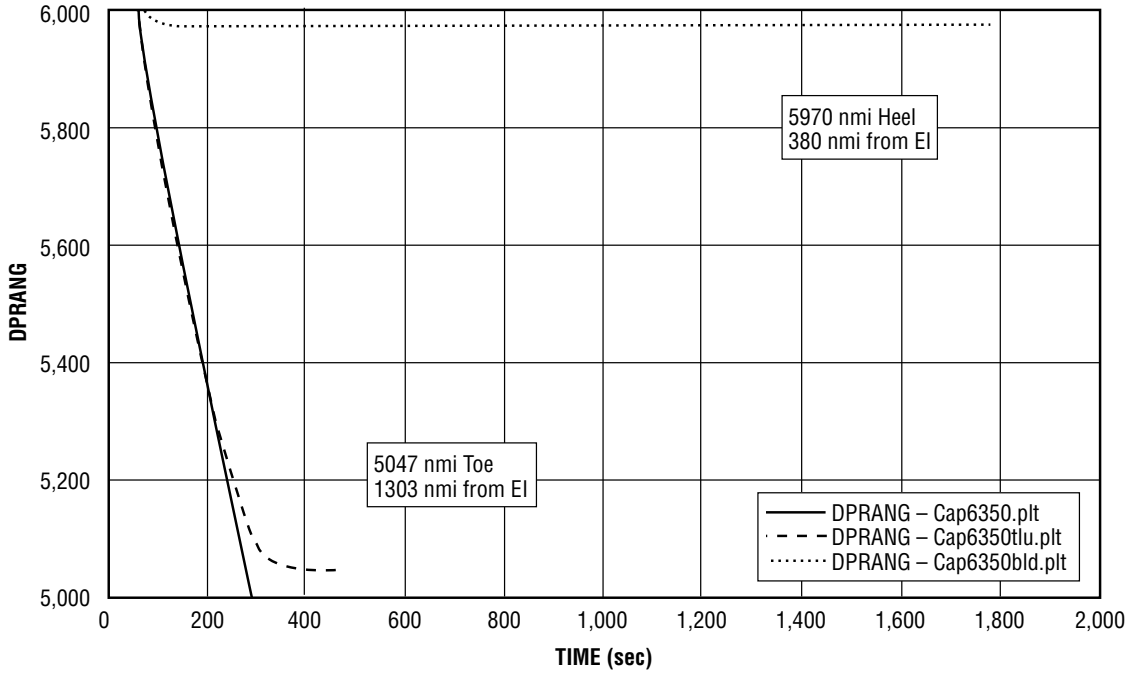

Figure 5-83. Capsule SM Footprint

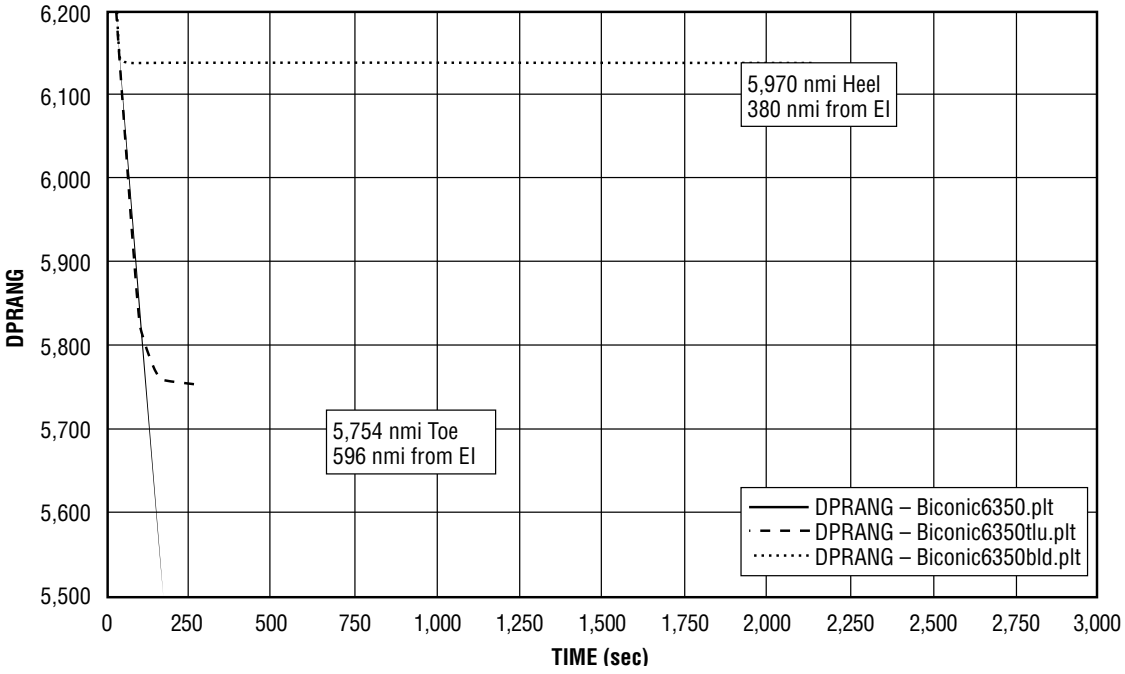

Figure 5-84. Biconic SM Footprint

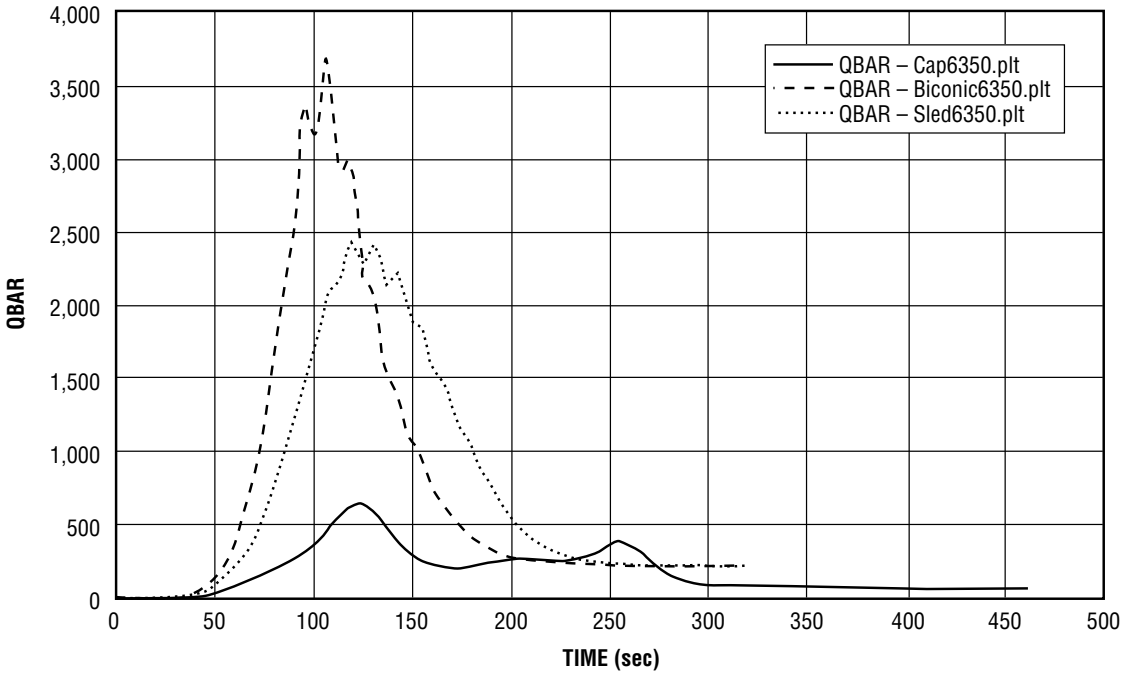

Figure 5-85. Ballistic Entry Comparison - Dynamic Pressure (psf) versus Time

5.3.5.3.4 Skip-Entry Vehicle (0.3 and 0.4 L/D) Site Accessibility

This section provides information on the site accessibility for the 0.3 and 0.4 L/D vehicles. **Figures 5-86** and **5-87** provide the footprint comparisons and the strategy for controlling the approach azimuth to the landing site using co-azimuth control during the TEI maneuver at the Moon. (Note that the footprint can be rotated about the antipode by controlling the entry azimuth.) This technique permits an alignment of the approach geometry with the desired landing site. For direct-entry scenarios, this permits alternatives for approaching the landing site for SM disposal considerations, or perhaps populated over-flight concerns. For SPASE trajectories, this enables the antipode and the landing site alignment to achieve the desired landing site. Note that the 0.4 L/D vehicle provides more than 500 km of additional direct-entry footprint than the 0.3 L/D vehicle. This has important implications for achieving direct-entry inland landing sites while maintaining the required coastal SM disposal clearance.

EI, Vacuum Perigee (VP), and the entry footprint are all interrelated via the entry design process (**Figures 5-86** and **5-87**). The antipode is fixed to the landing site at the time of lunar departure. However, VP moves relative to the antipode, and, therefore, to the landing site, by as much as 430 km over ±12 hours of flight time variation. This variation in flight time is controlled by the TEI maneuver and is required to allow the Earth to spin into proper entry orientation. The amount of flight time variation required to achieve the desired Earth-relative longitude is not known until lunar departure; therefore, as much as 430 km of footprint must be "reserved" to account for the flight time variation. If this is not done, an opportunity could arise where the footprint would lie outside of the desired landing site.

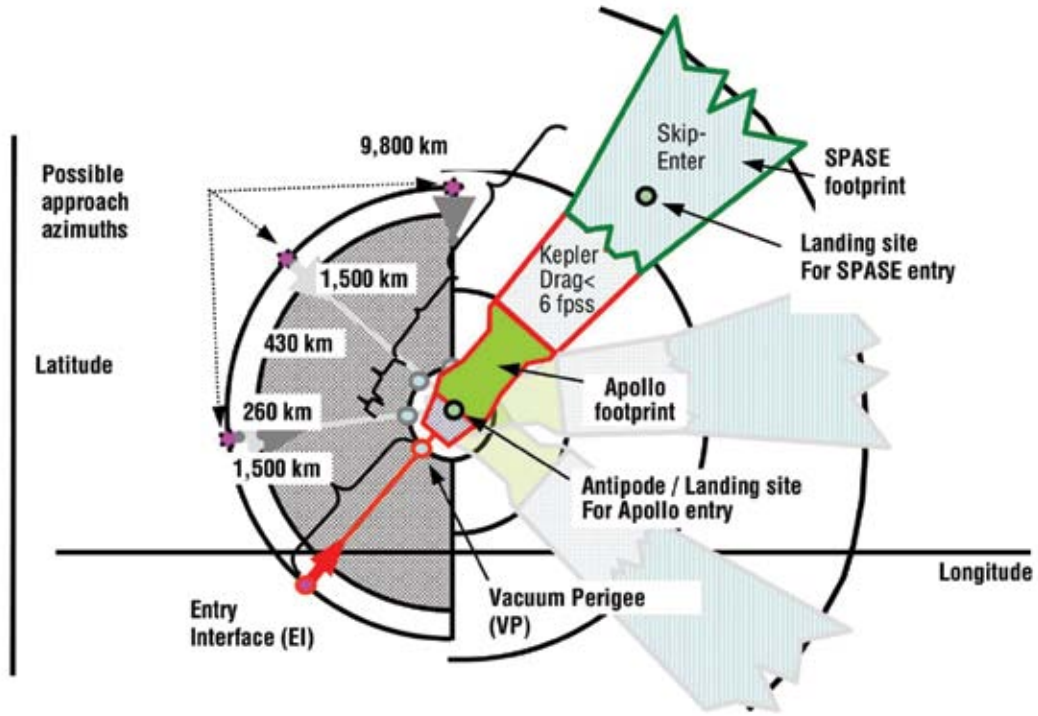

Figure 5-86. Entry Footprint with Co-azimuth Control (Direct-Entry and Skip-Entry), 0.3 L/D

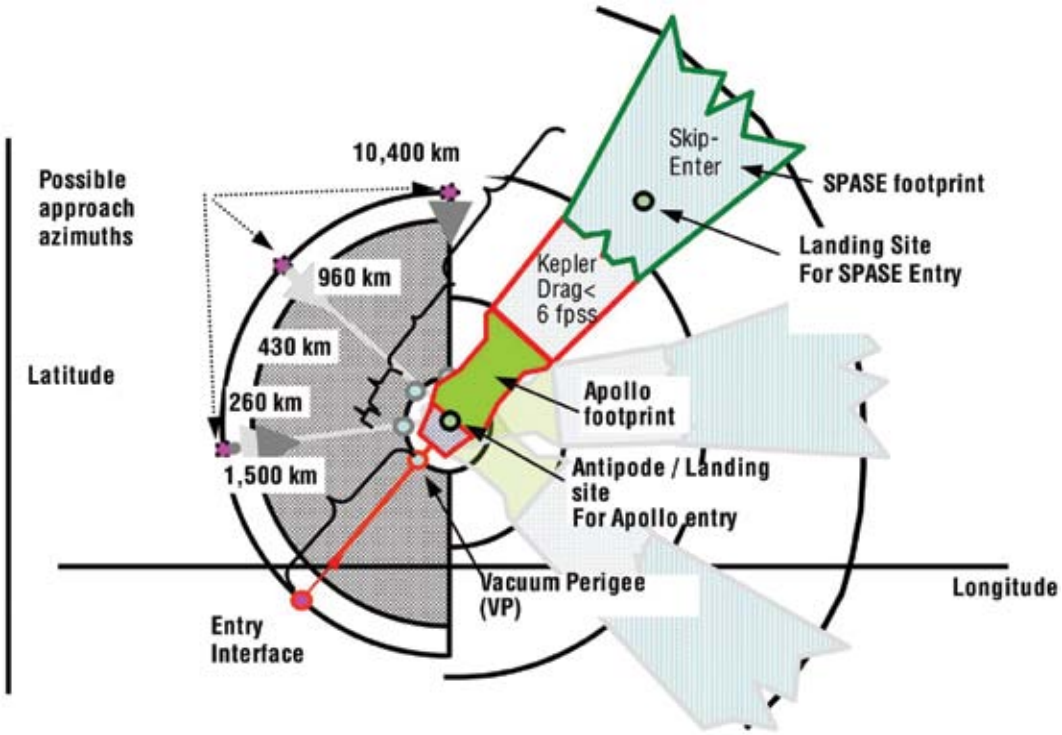

Figure 5-87. Entry Footprint with Co-azimuth Control (Direct-Entry and Skip-Entry), 0.4 L/D

The original Apollo guidance formulation provides for achieving long-range targets via a "Kepler" phase of guidance, which was exercised in only one test flight and never operationally flown due to concerns with controlling the up-control Kepler skip errors. **Figure 5-88** demonstrates that at least 9,200 km of range is required to achieve the Vandenberg landing site when the antipode is at maximum southerly location (–28.6 deg).

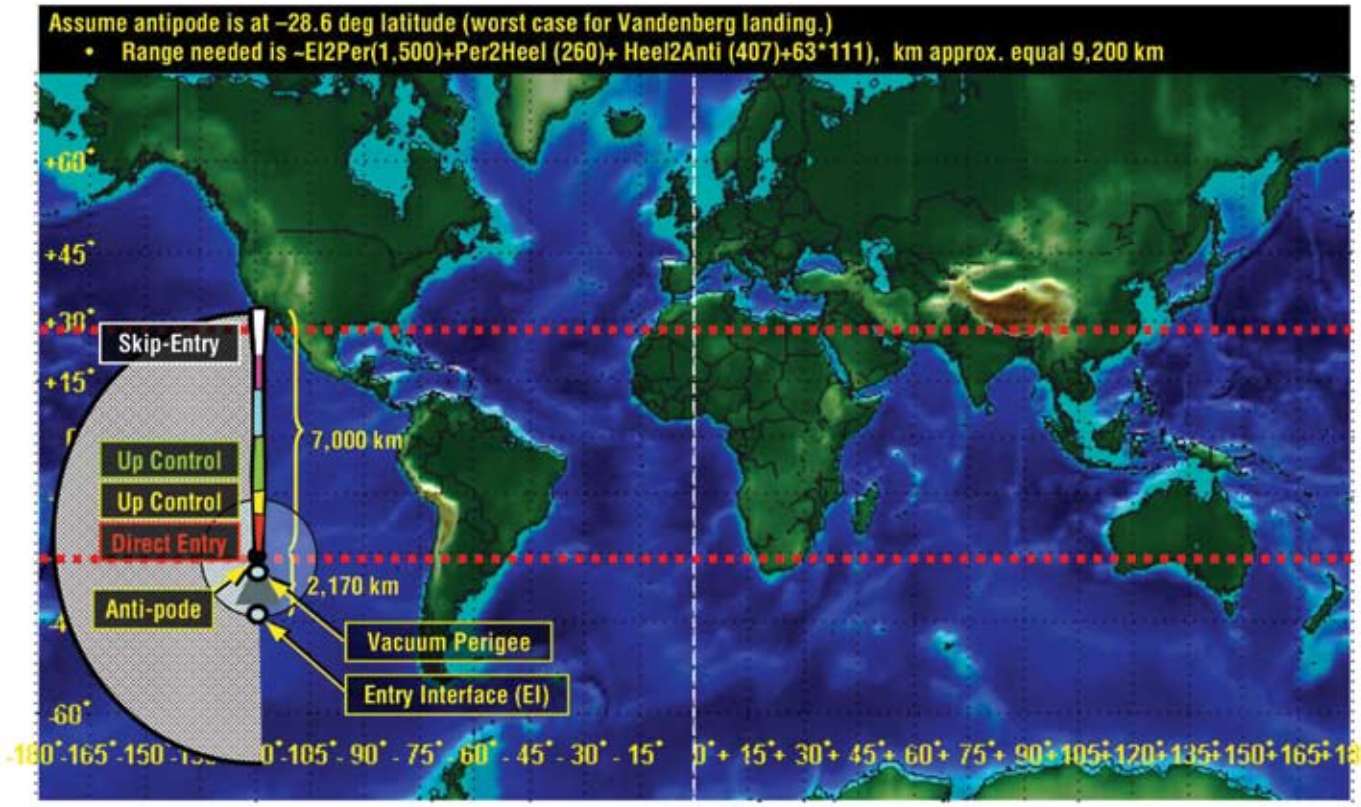

Figure 5-88. Flight Range Required to Reach Vandenberg AFB

Figures 5-89 and **5-90** provide the site accessibility of Vandenberg AFB for a 0.3 L/D capsule vehicle for different range flights. The current Apollo guidance provides an access circle of approximately 1,000 km, taking into account the loss of footprint due to the affect of ±12 hour flight time variation on the relative position of the landing site and the antipode. (Note that the original Apollo guidance capability would currently provide no access to Vandenberg AFB for maximum antipode in the ±18.3 deg cycle and less than 1 day for the ±28.6 deg cycle.) Each successive range circle increases the accessibility for the Vandenberg landing site until a range of 5,900 nmi for the ±18.3 deg cycle, or 9,300 nmi for the ±28.6 deg cycle, provides full-month coverage.

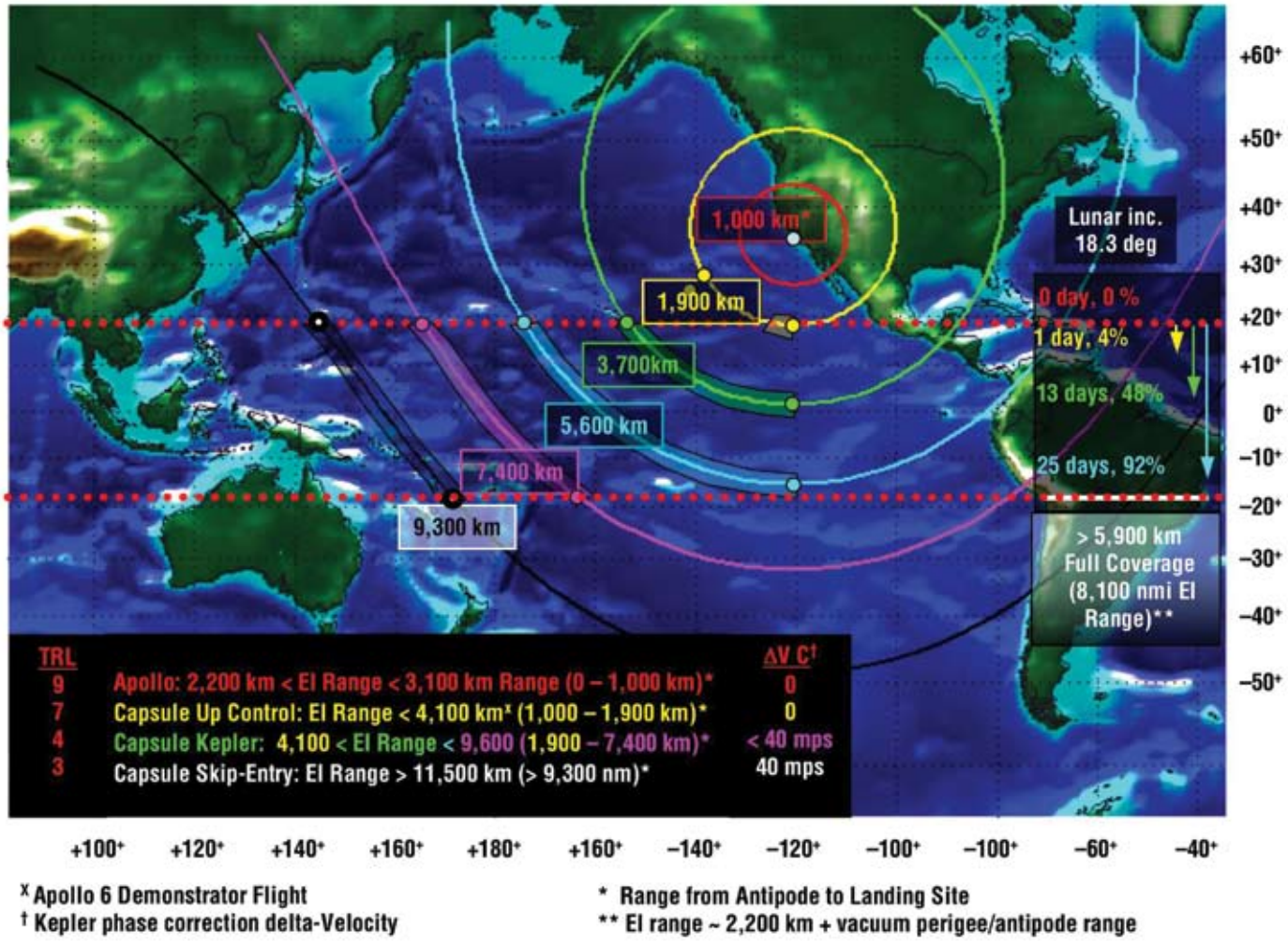

Figure 5-89.
Vandenberg AFB Site Accessibility (0.3 L/D Capsule, ±18.3 deg Lunar Inclination

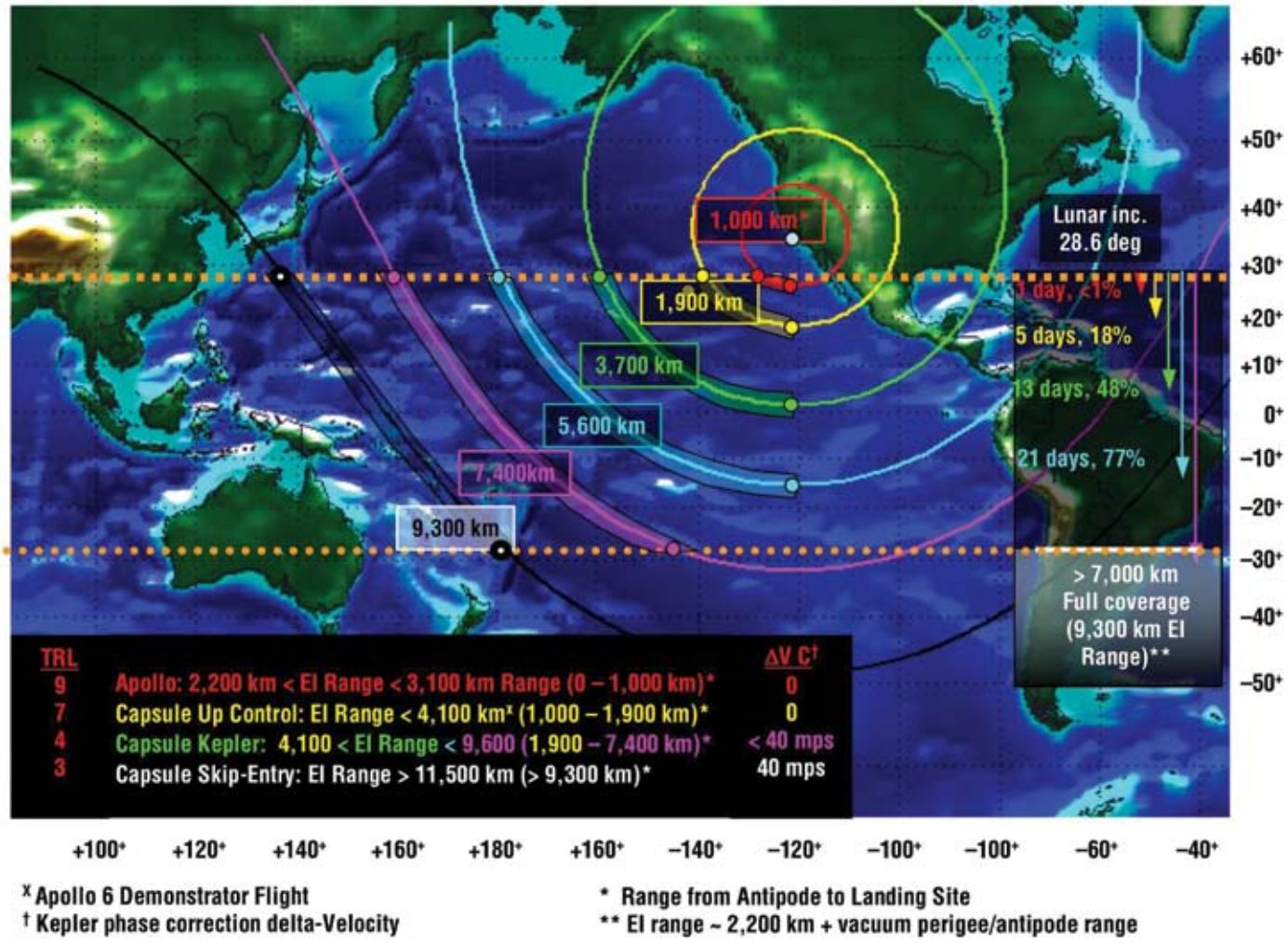

¤ Apollo 6 Demonstrator Flight
† Kepler phase correction delta-Velocity

* Range from Antipode to Landing Site
** EI range ~ 2,200 km + vacuum perigee/antipode range

Figure 5-90. Vandenberg AFB Site Accessibility (0.3 L/D Capsule, ±28.6 deg Lunar Inclination)

Figure 5-91 provides Edwards AFB site access for a 0.4 L/D capsule vehicle. Even with the extended range provided by the increased L/D, Edward's site accessibility is not possible for the most northerly +18.3 deg antipode location using standard direct-entry Apollo guidance (1,500 km range).

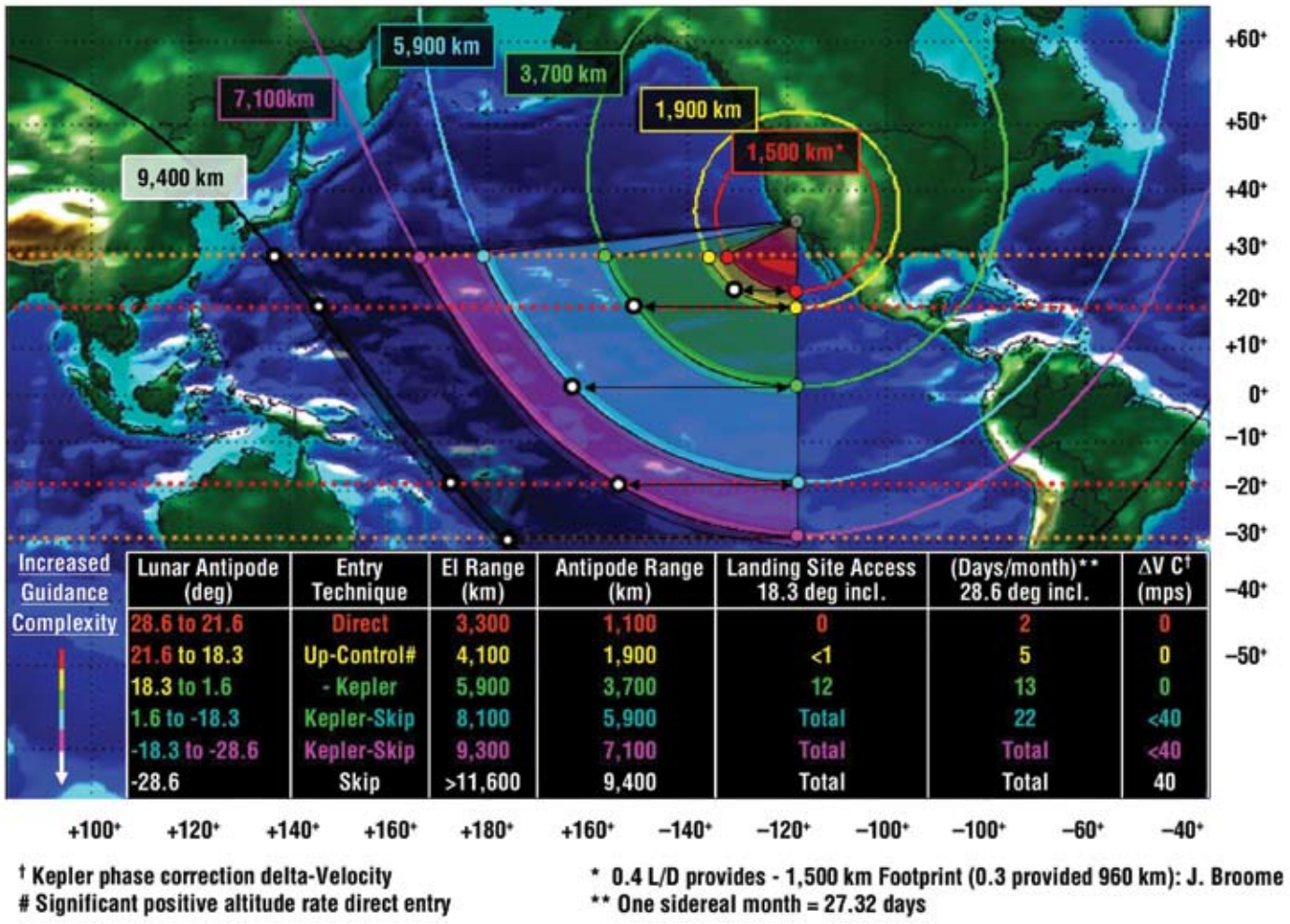

Increased Guidance Complexity	Lunar Antipode (deg)	Entry Technique	EI Range (km)	Antipode Range (km)	Landing Site Access 18.3 deg incl.	(Days/month)** 28.6 deg incl.	ΔV C† (mps)
	28.6 to 21.6	Direct	3,300	1,100	0	2	0
	21.6 to 18.3	Up-Control#	4,100	1,900	<1	5	0
	18.3 to 1.6	- Kepler	5,900	3,700	12	13	0
	1.6 to -18.3	Kepler-Skip	8,100	5,900	Total	22	<40
	-18.3 to -28.6	Kepler-Skip	9,300	7,100	Total	Total	<40
	-28.6	Skip	>11,600	9,400	Total	Total	40

† Kepler phase correction delta-Velocity
# Significant positive altitude rate direct entry
* 0.4 L/D provides - 1,500 km Footprint (0.3 provided 960 km): J. Broome
** One sidereal month = 27.32 days

Figure 5-91. Edwards AFB Site Accessibility, 0.4 L/D Capsule (±28.6 deg, ±18.3 deg, Lunar Inclination

5.3.6 SM Propulsion Trades

A wide variety of SM propulsion trades were performed prior to selecting a LOX/methane pressure-fed system that has a high degree of commonality with the LSAM ascent stage. These trade studies and their results are presented in **Section 4**, **Lunar Architecture**.

5.3.7 Radiation Protection Trades

Detailed radiation analyses were performed on various CEV configurations to assess the need for supplemental radiation protection for lunar missions. These analyses and conclusions are presented in **Section 4**, **Lunar Architecture**.

5.4 Ascent Abort Analyses for the CEV

5.4.1 Summary

This analysis examines ascent aborts for a number of different CEV and LV combinations and focuses on total loss-of-thrust scenarios after jettison of the LAS. The general goal is to determine the abort options that might reasonably exist for various points in the ascent and characterize the CEV entry environment (e.g., in terms of loads and temperatures).

For the major portion of the analysis, the CEV is an Apollo-like capsule with a corresponding SM. SM delta velocities (ΔV's) are assessed from 330 to 1,732 m/s (1,083 to 5,682 fps) and Thrust-to-Weight (T/W) ratios from 0.38 to 0.17. Ascents to both 51.6 deg and 28.5 deg inclinations are considered.

The focus of the later portion of the analysis is on a Shuttle-derived LV: a four-segment SRB with a single SSME upper stage, LV 13.1. The sensitivity of abort coverage and abort mode boundaries to variations in available ΔV and T/W are key factors that received appropriate emphasis. Other important factors include the minimum operating altitude of the thrusting CM and SM (i.e., can they safely perform in the 335-kft altitude region where the effects of aeroheating cannot be ignored?) and the ignition delay of the propulsion system (i.e., how quickly can the CM/SM separate and maneuver to burn attitude?). These factors are particularly important for LV 13.1, because the ascent trajectory is quite depressed. Abort coverage will not be good if, for example, the CM/SM cannot perform safely below approximately 340 kft, has a T/W of less than 0.2, cannot ignite the propulsion system fairly quickly, and is launched on a very depressed ascent trajectory. This analysis tries to quantify the effects of all of these factors.

The analysis sought to define near-optimal abort coverage by using numerically optimized pitch profiles during thrusting phases. The intent was to try to avoid limitations that available guidance algorithms might impose. New guidance algorithms may well be needed to automatically target and fly some of the abort trajectories from this analysis.

The results indicate a fairly robust abort capability for LV 13.1 and a 51.6 deg mission, given 1,200 m/s of ΔV, a T/W of at least 0.25, a CM/SM minimum operating altitude of 335 kft, and the ability to initiate propulsion system burns in about one-third the time budgeted for Apollo. (Apollo budgeted 90 sec to initiate posigrade burns and 125 sec for retrograde burns.) Abort landings in the mid-North Atlantic can be avoided by either an ATO or posigrade TAL south of Ireland. Landings in the Middle East, the Alps, or elsewhere in Europe can be avoided by either an ATO or a retrograde TAL south of Ireland. At 28.5 deg, landings in Africa can be avoided by either an ATO or a retrograde TAL to the area between the Cape Verde islands and Africa. However, it appears that even with 1,732 m/s of ΔV, some abort landings could occur fairly distant from land. However, once the ballistic impact point crosses roughly 50°W longitude, posigrade burns can move the abort landing area downrange near the Cape Verde islands.

The next section will briefly introduce some of the various abort modes, including a summary of the Apollo abort modes. Key assumptions will also be discussed. Subsequent sections will then review the detailed results, beginning with the Shuttle-derived boosters, followed by the Evolved Expendable Launch Vehicles (EELVs). Lastly, results for two different lifting bodies will be reviewed that address mostly abort loads and surface temperatures. Some results from earlier analyses are also presented to illustrate the effect of dispersions and other operational considerations.

5.4.2 Introduction

The Apollo literature on ascent aborts has quite proven useful to these studies. **Figure 5-92** presents a summary of the abort modes for Apollo 11. Four abort modes are identified. Mode I covers aborts using the LAS. Mode II aborts are simple, unguided lift-up entries, terminated when the landing area begins to impinge on Africa. Mode III uses lift reduction and retrograde thrust to land short of Africa. Mode IV is a contingency orbit insertion (or ATO in Shuttle jargon). A large ATO capability exists, especially with use of the S-IVB stage. Interestingly, the abort plan did not include use of posigrade thrust to target some aborts off Africa. For this CEV analysis, use of posigrade thrust is considered for suborbital abort modes like TAL.

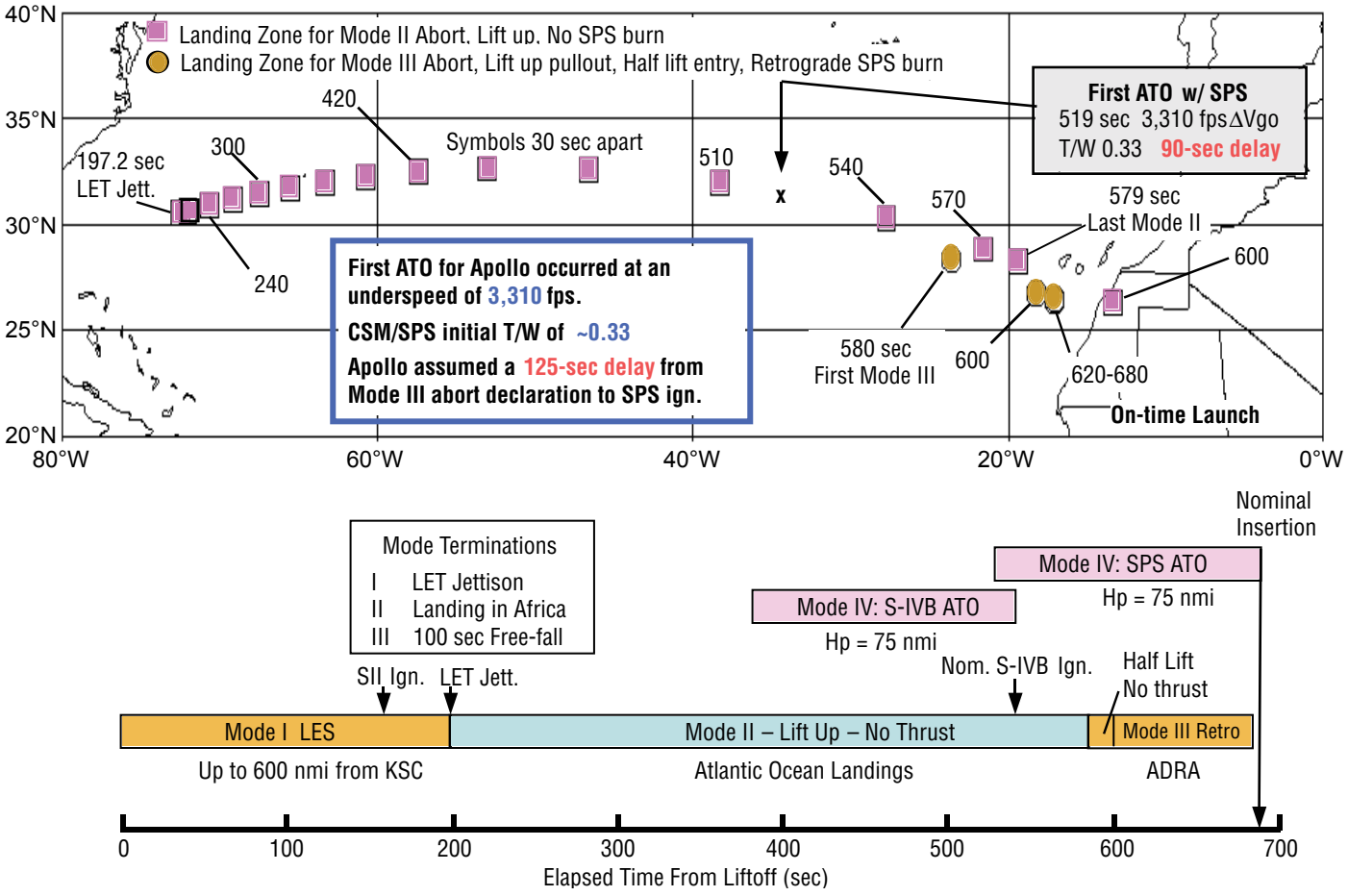

Figure 5-92. Apollo 11 Abort Modes

A key parameter in the Apollo ascent abort analyses is “free-fall time” to 300 kft altitude. For instance, Mode II aborts require 100 sec of free-fall time from abort declaration to 300 kft altitude on the abort-entry trajectory. This amount of time is budgeted to terminate thrust on the LV, separate the CM/SM from the stack, separate the CM from the SM, and then orient the CM for entry. Likewise, Mode III aborts require 100 sec of free-fall time from termination of the Service Propulsion System (SPS) burn to 300 kft on the abort-entry trajectory. While no specific free-fall time requirement has been established for the CEV, the parameter has been included in the analyses. It is a useful parameter for assessing the reasonableness of abort scenario timelines from ascent trajectories with varying amounts of loft.

Figure 5-92 identifies other guidelines for abort time lines. Ninety seconds are budgeted for startup of the SPS engine for Mode IV aborts (ATO). One-hundred-twenty seconds are budgeted for startup of the Mode III retrograde burns. This CEV study took the approach of initially using a much more aggressive time line (20 sec for SPS startup) and assessing the sensitivity to larger delays.

5.4.3 Assumptions and Methodology

Key assumptions are made relative to aerodynamics and the estimation of surface temperatures. Where possible, the Apollo aerodynamic database is used. For a capsule with 0.3 L/D, the Apollo angle of attack (α) versus Mach tables for the Command Module are used with an angle-of-attack of 160 deg. For ATO studies, the free-molecular coefficients for the Command and Service Module are used. For vehicles with an L/D other than 0.3, aerodynamics are typically modeled with a coefficient of L/D and the given reference area.

Figure 5-93 presents the methodology for estimating surface temperature. The approach has provided reasonable surface temperature estimates for preliminary assessment purposes. The results are evaluated relative to the single mission limit for TPS materials developed for the Shuttle and X–38 (i.e., 3,200–3,300°F for the C/SiC-coated Reinforced Carbon-Carbon (RCC) developed for the X–38.

The 1976 Standard Atmosphere is used, with no winds.

SORT is used to define the trajectories for the analyses. SORT is a versatile 3-DOF simulation tool that is controlled by the Aerosciences and Flight Mechanics Division at NASA’s JSC.

Heat rates use the modified Detra-Kemp-Riddell (DKR) formulation embedded within a Newton-Rhapson temperature convergence.

T_{surf} is the estimated surface temperature in degrees Rankine.

Modified DKR Heat Rate for an Equilibrium Wall Temperature

$$\dot{Q} = \frac{17600}{\sqrt{R_N}} \sqrt{\frac{\rho}{\rho_o}} \left(\frac{V_{fs}}{26000} \right)^{3.25} \left(\frac{H_{stag} - H_{wall}}{H_{stag} - 129.6} \right)$$

V_{fs} = freestream velocity (fps)

ρ = atmospheric density (slugs/ft^3)

$H_{wall} = 0.24 * T_{Surf}$

$H_{Stag} = \left(V_{fs}\right)^2 / 50073.12$

Radiation Equilibrium Temperature: T_{surf}

$$T_{Surf} = \left(\frac{\dot{Q}}{0.85 * S_{bc}} \right)^{\frac{1}{4}}$$

$S_{bc} = 4.75833 \times 10^{-13}$

Emissivity = 0.85

Effective nose radius (R_N) for capsule derived from "ACRV Landing Accuracy Study" NASA Memo EG3/9104-24, 4/4/91: R_N = 8 ft for a 14 ft diameter Apollo capsule

For this study, R_N (in ft) = 8 x capsule diameter (in ft) / 14

Figure 5-93. Methodology for Estimating Surface Temperature

ATOs are defined using two burns. The pitch profile to raise apogee consists of a constant segment followed by a linear segment. To raise perigee, a single linear segment is used. A SORT optimizer is used to define profiles for minimal ΔV. The optimizer defines the value for the constant segment, the transition time to the linear segment, the slope and length of the linear segments, and the coast period between burns. ATOs are targeted to a 100- x 100-nmi circular orbit to provide a 24-hour orbital life.

5.4.4 Shuttle-Derived Vehicles (SDVs)

Ascent aborts are analyzed for several different Shuttle-Derived Vehicles (SDVs): in-line crew vehicles with four- and five-segment SRBs (LV 13.1 and 15, respectively) and an in-line crew/cargo vehicle with five-segment SRBs and four SSMEs on the tank (LV 26). The LV numbers correspond to those defined in the LV data summary. These numbers are typically included on the figures to aid booster identification (usually contained in parentheses).

Ascent trajectories for the three boosters are presented in **Figure 5-94**. Subsequent sections will first address the loads, estimated surface temperature, free-fall time characteristics, and impact points for "Mode II" aborts from the various boosters. This will be followed by a discussion of preliminary abort mode boundaries and the sensitivities to T/W and other factors.

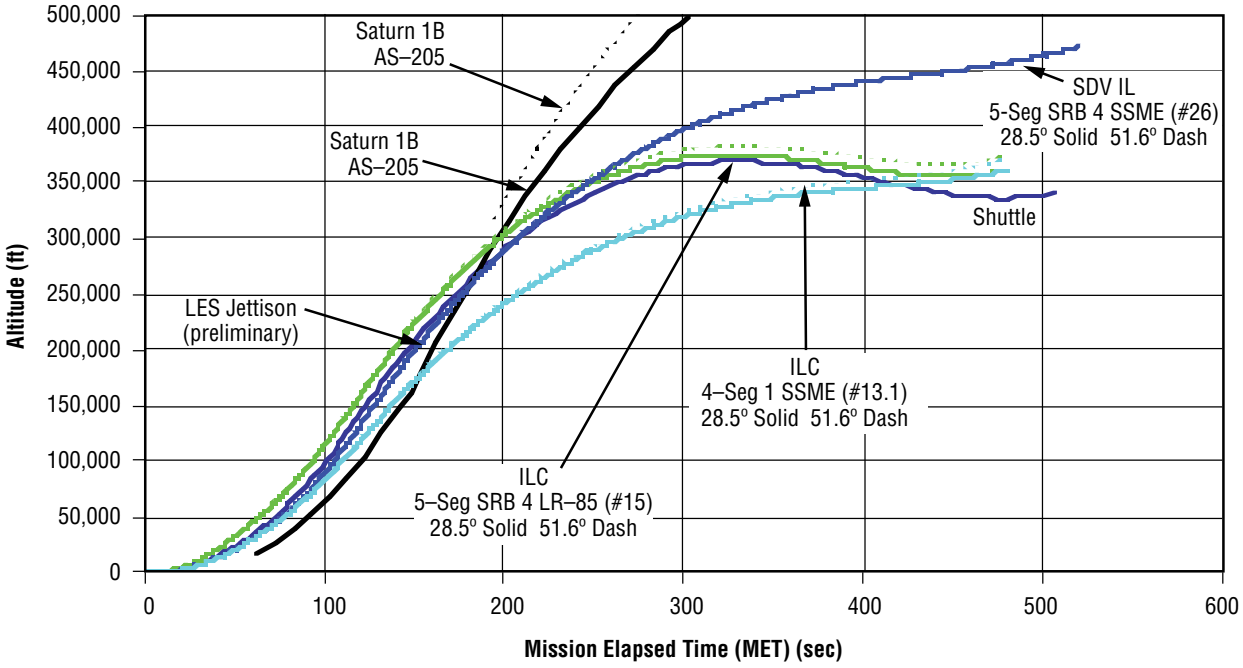

Figure 5-94. Ascent Trajectories for SDVs

5.4.4.1 Loads, Surface Temperature, Free-fall Time, and Impact Points

Peak loads, estimated maximum surface temperatures, and free-fall time are presented for ballistic (i.e., nullified lift) and lift-up aborts in **Figures 5-95** to **5-99**. Data from the Apollo Program are included for ballistic and lift-up abort loads and free-fall time for comparison. Data for CEV aborts from a representative Shuttle trajectory are also included.

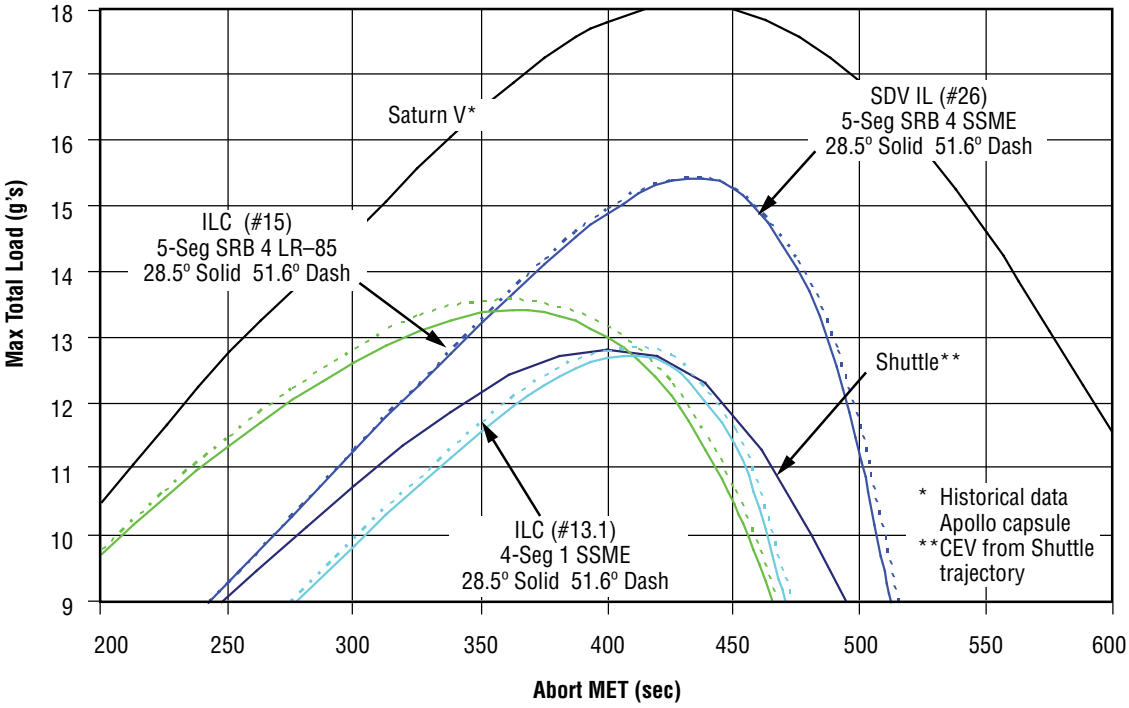

Figure 5-95. Ballistic Loads for Aborts from Shuttle-Derived Boosters

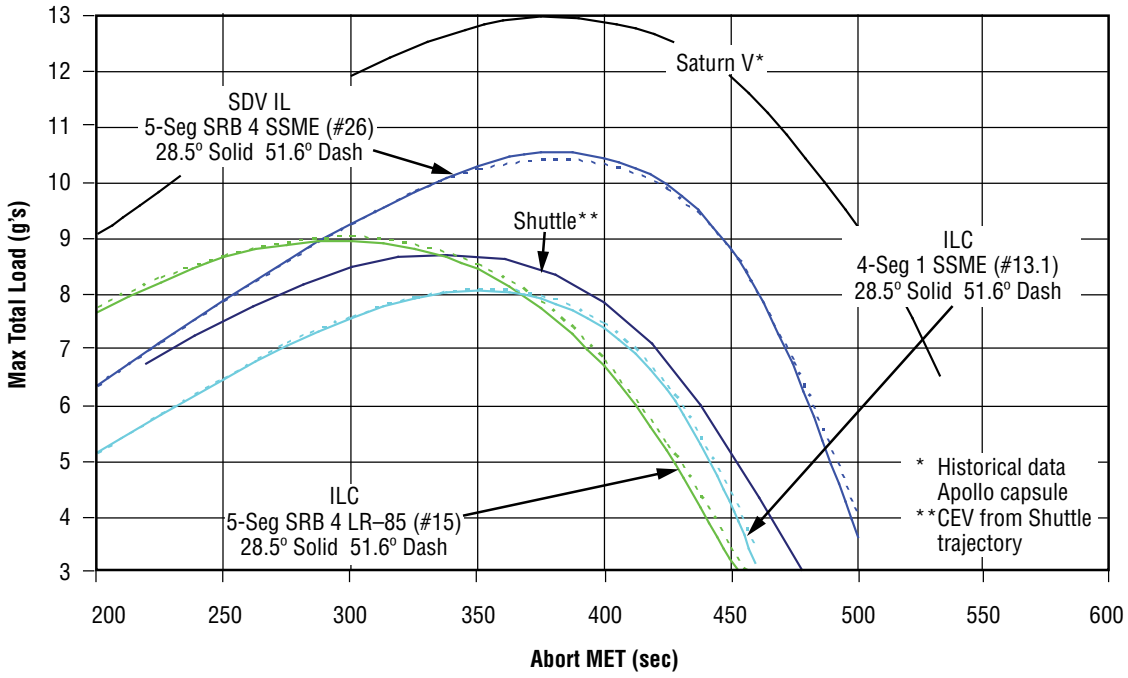

Figure 5-96. Lift-up Loads for Aborts from SDVs

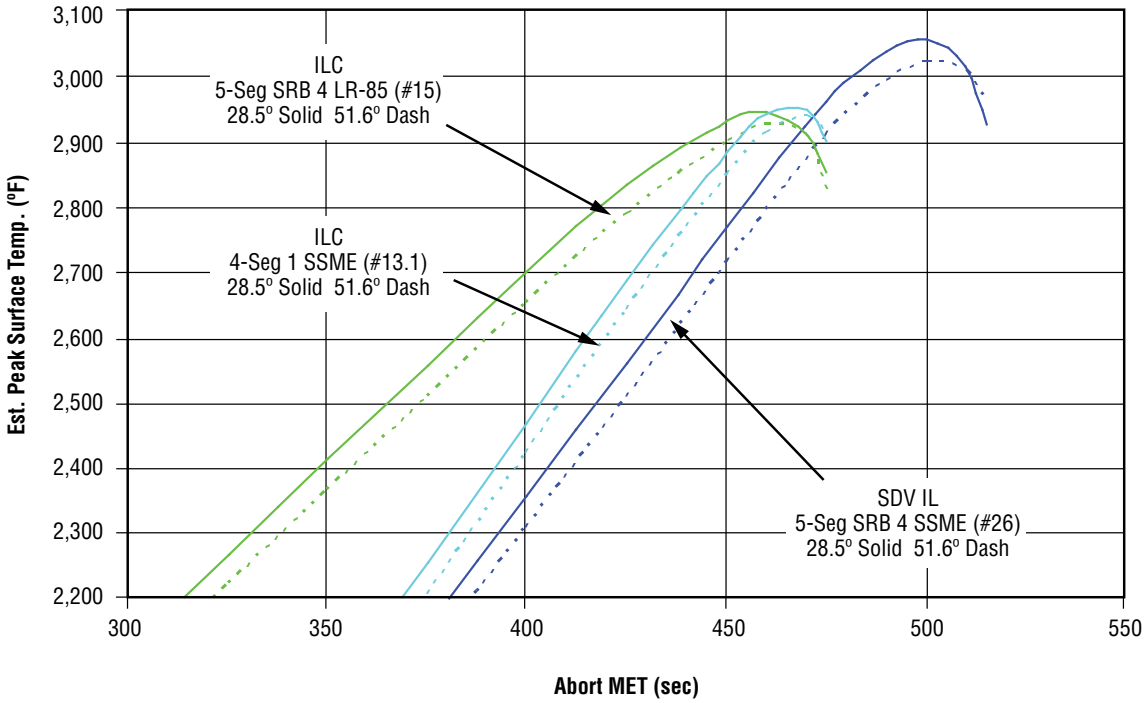

Figure 5-97. Maximum Surface Temperatures for Ballistic Aborts from Shuttle-Derived Boosters

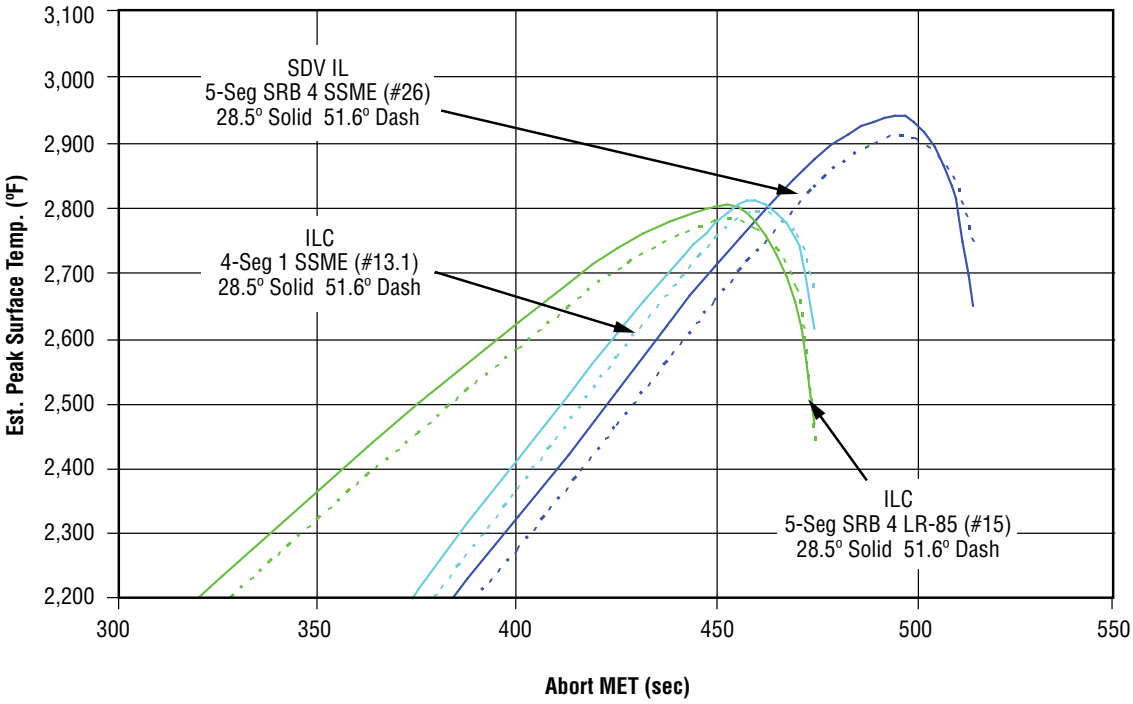

Figure 5-98. Maximum Surface Temperatures for Lift-up Aborts from Shuttle Derived Vehicles

Data at 28.5 deg are for the lunar CEV (Block 2) with an L/D of 0.3 and a ballistic number of 81 psf. Data at 51.6 deg are for the ISS CEV (Block 1) with an L/D of 0.3 and a ballistic number of 67 psf. (Note that, in general, the abort parameters for the depressed LV 13.1 trajectory are lower than for the other, more lofted ascent trajectories). The lower loads and temperatures are obviously a benefit. However, since the LAS most likely will not be available after approximately 240 sec (and possibly earlier), the limited amount of free-fall time before encountering the atmosphere could be an issue. Free-fall times near 50 sec indicate abort scenarios that probably deserve more attention.

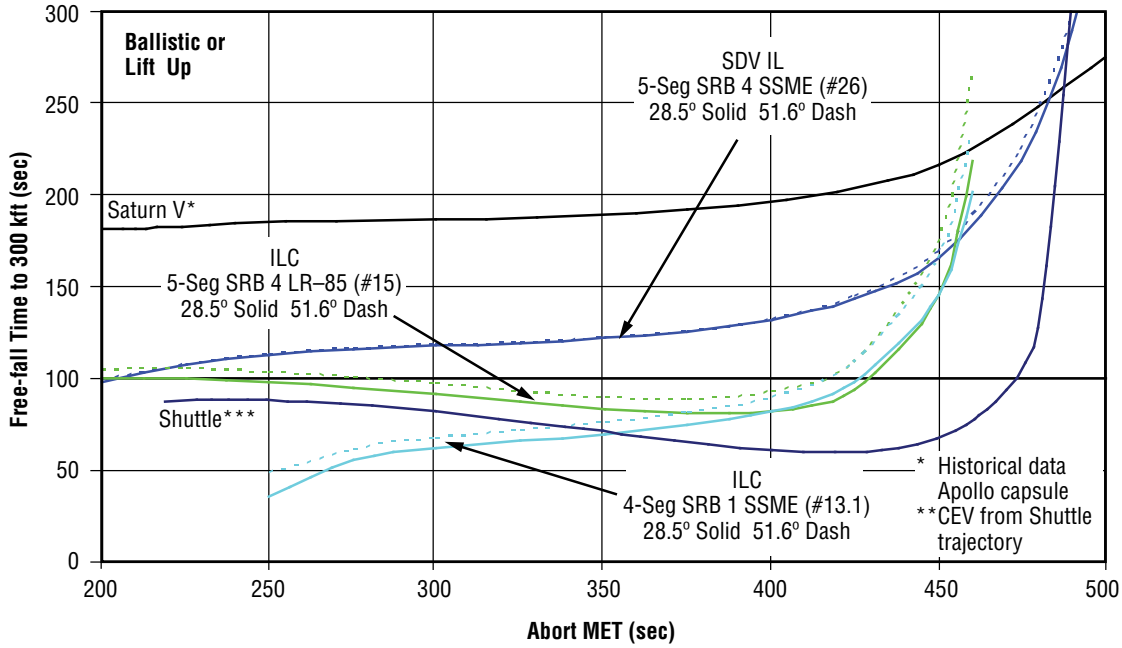

Figure 5-99. Free-fall Time for Aborts from SDVs

Load durations for the worst-case ballistic aborts are well within the crew limits for escape. (Note the duration histories relative to the red line on **Figure 5-100**.) Estimated maximum surface temperatures are within the single mission limits for TPS materials developed for the Shuttle and X–38. However, higher fidelity aeroheating analyses are needed to confirm this data.

Alternate capsule designs evolved during the analysis. **Figure 5-101** compares abort loads and estimated surface temperatures for the Cycle 1 and Cycle 2 CEV CMs and LV 13.1. The Cycle 2 capsule has a higher ballistic number (87 psf versus 67 psf for the ISS versions). This causes the ballistic loads and surface temperatures to increase slightly. (The ballistic loads are also driven up slightly by the increase in L/D from 0.3 to 0.4.) For the lift-up aborts, the increased L/D helps the loads and appears to almost cancel the effect of the increased ballistic number on the temperatures for the lift-up aborts. **Figure 5-102** indicates that the load durations for the worst-case ballistic aborts are well below the crew limits.

Ballistic impact points for the Cycle 1 capsules (ballistic numbers of 67 and 81 psf) are presented in **Figure 5-103.** The high T/W ratios (for second stage) limit North Atlantic abort landings to approximately 3–5 percent of the ascent trajectory. Powered abort options (discussed below) were also examined to totally avoid the North Atlantic and other undesirable landing areas along the 51.6 deg inclination ground track.

It is worth noting the ATO times on **Figure 5-103** for 28.5 deg. The first ATO of LV 15 has a significantly lower "under speed" (i.e., the velocity magnitude short of the nominal engine cutoff velocity). Although this LV was not carried forward in the later analyses, it is worth noting the impact on ATO of the negative altitude rate during the later portion of the trajectory. (Note that a minimum operating altitude of 345 kft was used for this comparison; it is difficult to meet this limit with a trajectory shaped like the one for LV 15.) A higher Second-Stage Engine Cutoff (SECO) altitude will bring ATO performance for LV 15 closer to that of LV 13.1.

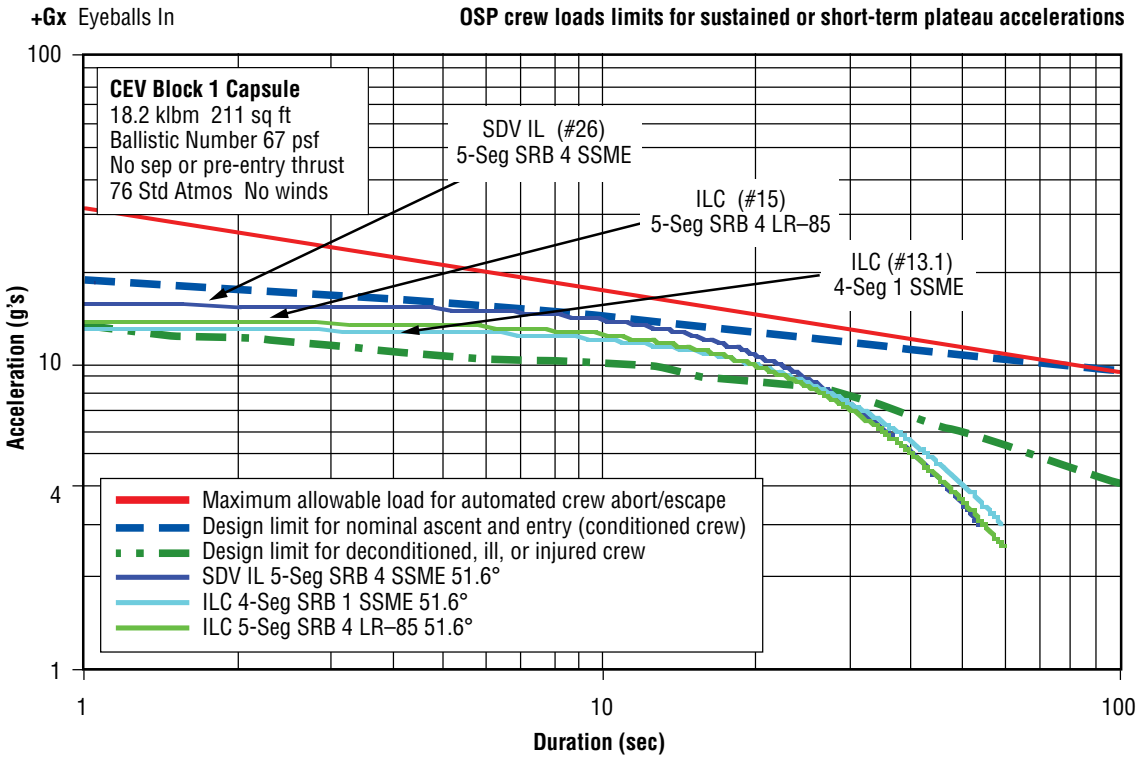

Figure 5-100. Worst Case Ballistic Load Durations versus Crew Limit Lines

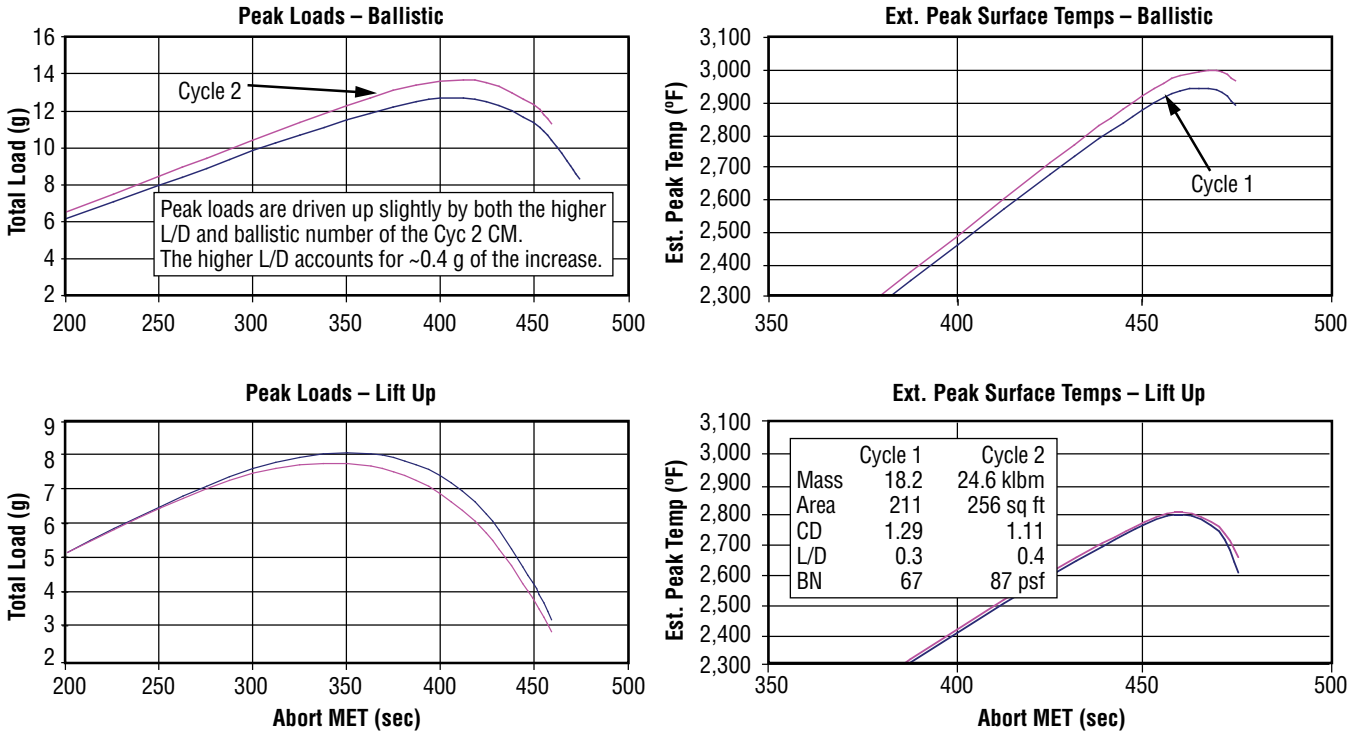

Figure 5-101. Comparison of Aborts for Cycle 1 and 2 ISS CEV and LV 13.1

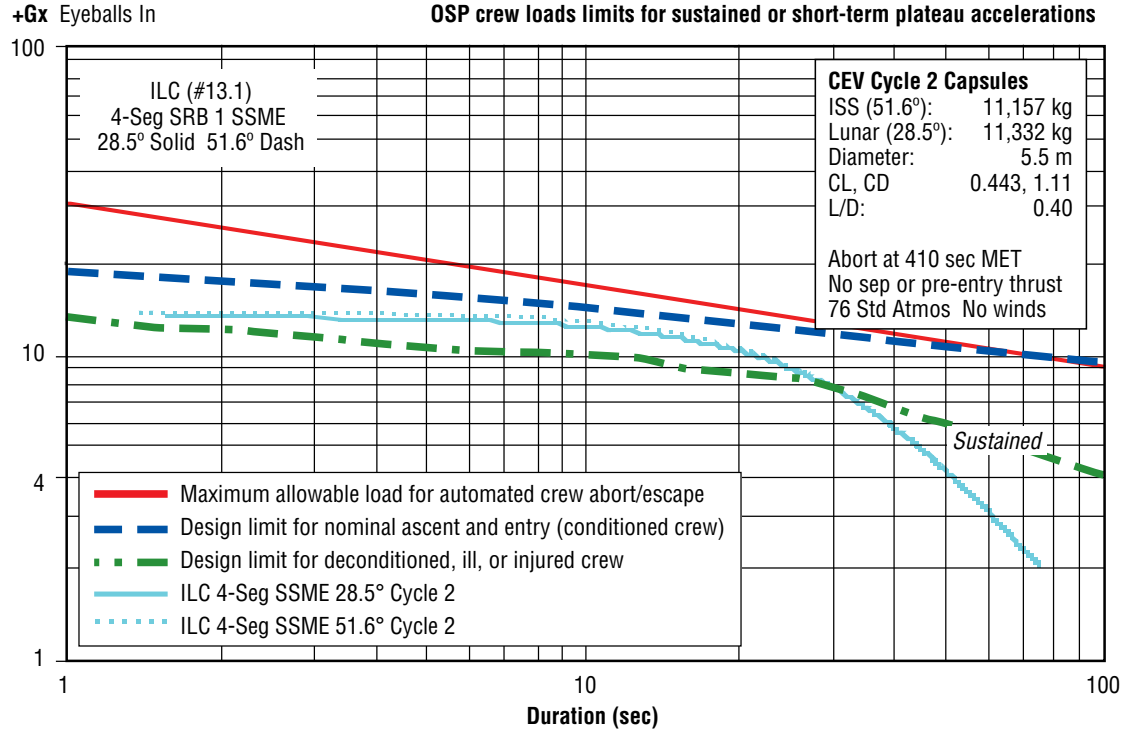

Figure 5-102. Worst Case Ballistic Load Durations for Cycle 2 CEV and LV 13.1

5.4.4.2 Abort Mode Assessments for 51.6-deg Inclination

5.4.4.2.1 Abort Modes for Two Different Propulsion System Configurations

Abort modes were initially assessed for an ISS CEV (Block 1) with the baseline and an alternate propulsion system delta-V and thrust: 330 m/s and 44.5 kN, and 1,200 m/s and 66.75 m/s (1,083 fps and 10 klbf, and 3,937 fps and 15 klbf). Abort modes for LV 13.1 were assessed for both propulsion system configurations, while LV 26 only used the baseline configuration. This latter study was undertaken to understand the effects of the depressed ascent trajectory for LV 13.1. The effect of various T/W levels and propulsion system ignition delays was briefly studied for LV 13.1.

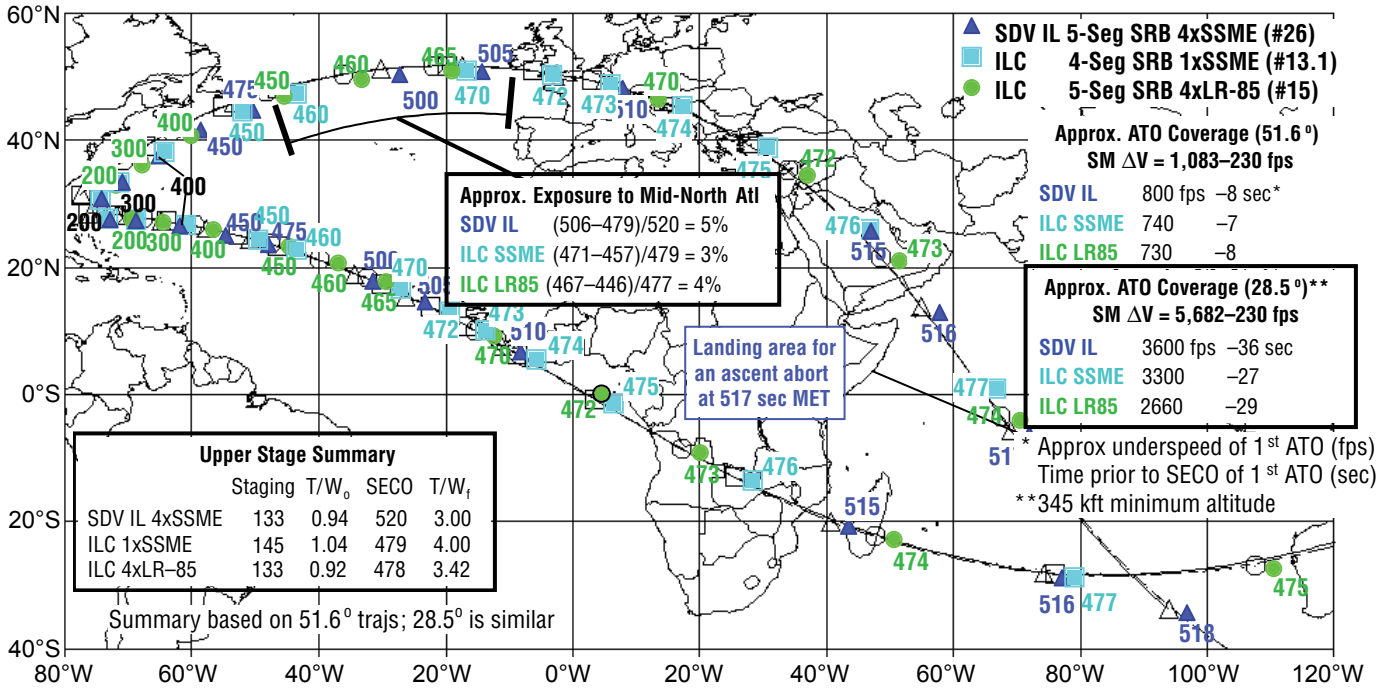

Figure 5-103. Ballistic Landing Areas for SDVs

Figure 5-104 presents the results for LV 13.1 and the baseline propulsion system configuration. The turquoise symbols and time tags indicate landing areas for no thrust-and-lift (i.e., a ballistic entry). The first ATO occurs at 472 sec—corresponding to the ballistic landing symbol near Ireland and England—indicating that the ATO abort mode avoids abort landings in the Alps and Middle East. The red symbols and time tags indicate landing areas for a retrograde burn that minimizes downrange, combined with a "half lift" entry at a 60-deg bank. The landing areas are shifted well to the left when all available ΔV is used. The implication is that for METs between 472 sec and SECO (479 sec), retrograde burns of a lesser magnitude can target a landing area south of Ireland (in a manner similar to the way Apollo targeted a landing area near the Canary Islands for Mode III aborts). This provides another potential abort mode for avoiding the Alps and the Middle East, but will require a more thorough examination since the free-fall time is only approximately 50 sec for the 472-sec abort and an aggressive-maneuver time line is used for the retrograde burn. The green symbols and time tags indicate landing areas for a posigrade burn that maximizes downrange, combined with a full-lift entry. The landing area for a 462-sec abort is in northern France. If the retrograde burn-abort mode were available at 462 sec (note the red square with a landing area near Newfoundland), landings in the middle of the North Atlantic could be avoided by landing on either side of the Atlantic. However, a very short free-fall time after the burn (17 sec) does not make this abort appear practical.

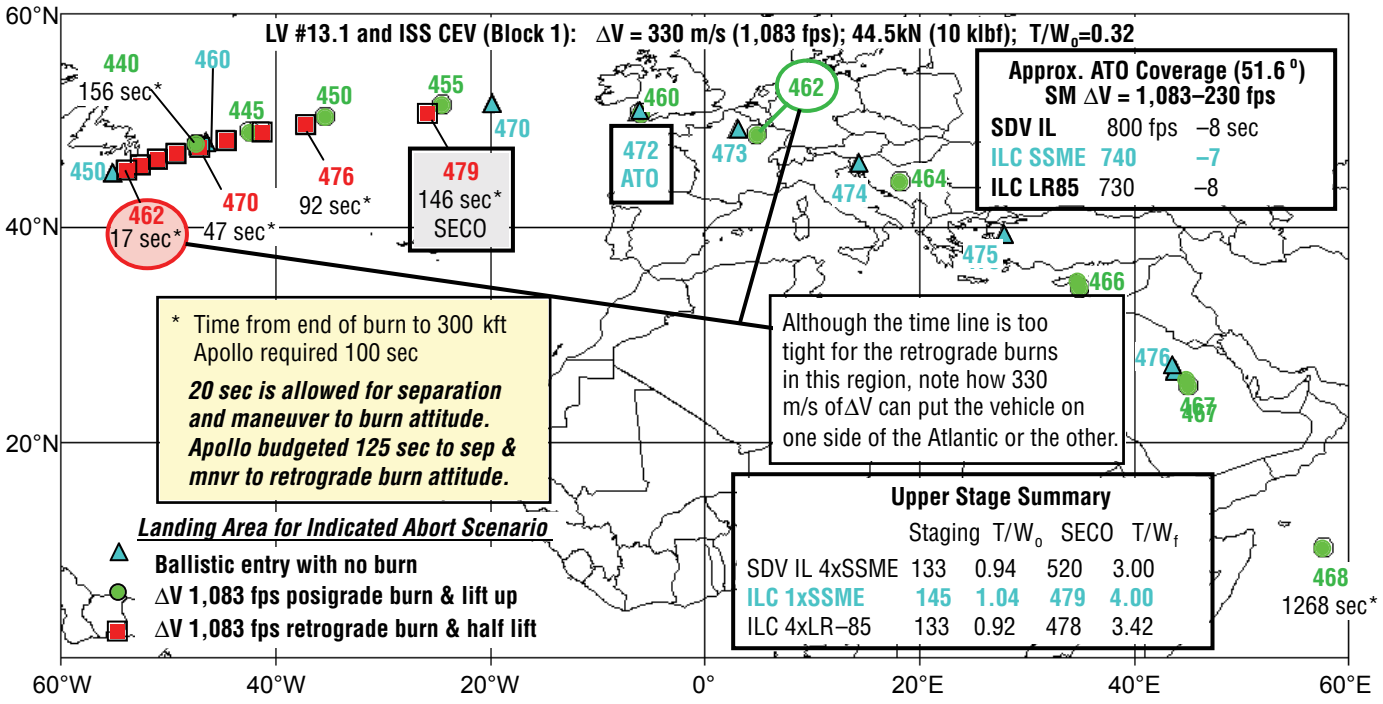

Figure 5-104. Effect of 330 m/s on Landing Areas for LV 13.1

A similar analysis was performed for LV 26 to assess the effect of a more lofted ascent trajectory (**Figure 5-105**). (Note how landings are possible on either side of the North Atlantic for aborts at 490–491 sec). For the more lofted ascent, the 490-sec retrograde abort has 69 sec of free-fall time from the end of the burn. Given a CEV with a robust RCS that allows a quick separation and maneuver to retrograde burn attitude, this abort mode may be feasible. Another important observation is that the first ATO does not provide protection from landing in the Alps; the first ATO is at 512 sec, which corresponds to the ballistic landing area in Bosnia. This is not due to the lofted ascent trajectory, but rather due to the 3-g maximum acceleration for LV 26 (versus 4-g limit for LV 13.1).

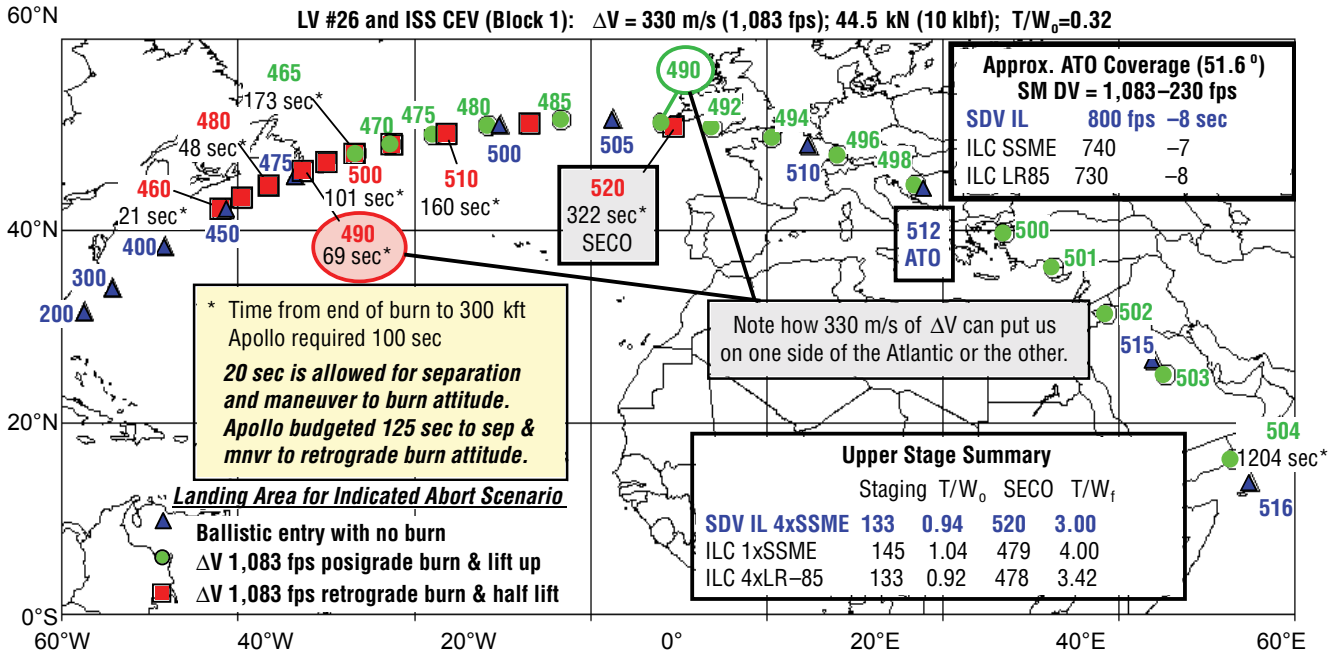

Figure 5-105. Effect of 330 m/s on Landing Areas for LV 26

The results of these two analyses are summarized in the top half of **Figure 5-106** and **5-107**. The conclusion is that, with a more lofted ascent trajectory, the North Atlantic and other undesirable landing areas can be avoided with a limited amount of ΔV, if the CEV RCS is robust enough to separate and maneuver to burn attitude quickly and if the CEV propulsion system can ignite quickly.

The bottom half of **Figure 5-106** summarizes the LV 13.1 abort modes for the alternate propulsion system configuration. To summarize briefly, this configuration provides two abort modes for avoiding a landing in the middle of the North Atlantic, in the Alps, or in the Middle East: ATO and a posigrade TAL, or ATO and a retrograde TAL, respectively.

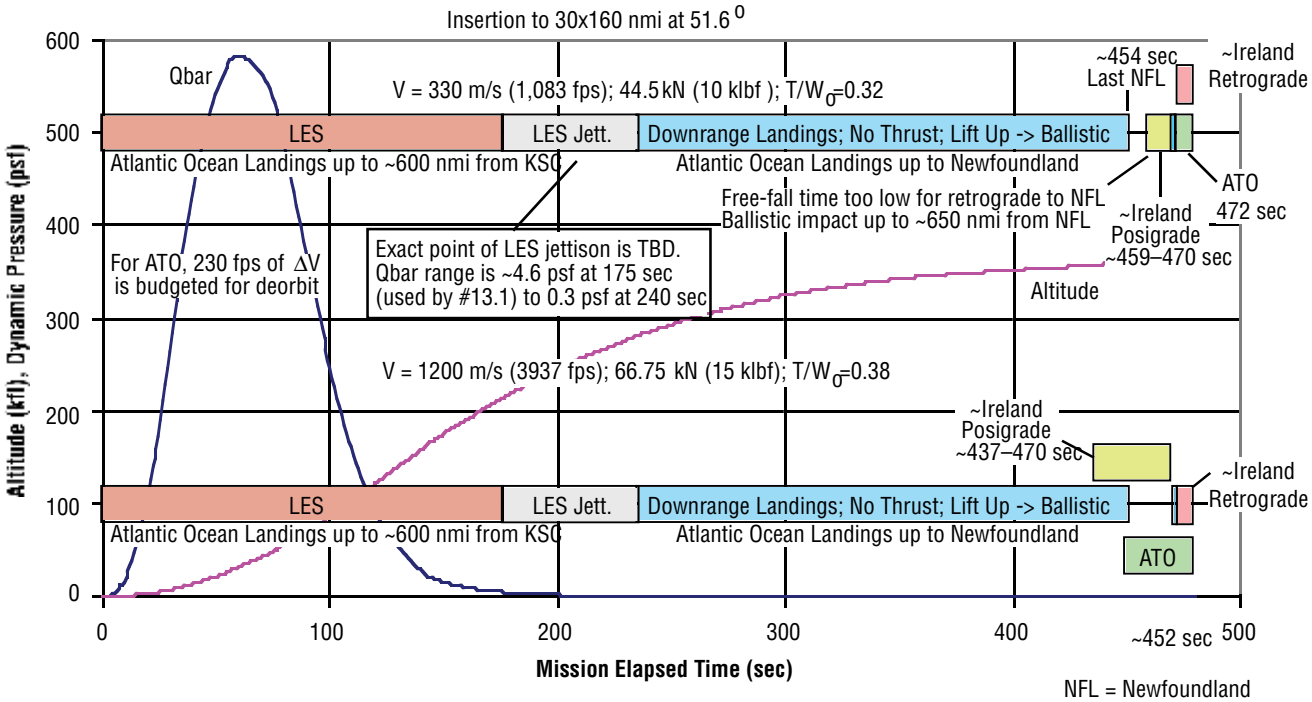

NFL = Newfoundland
Nom. insertion: 479.3 sec

Figure 5-106. Abort Modes for Launch Vehicle 13.1 with the ISS CEV and Two Propulsion System Configurations

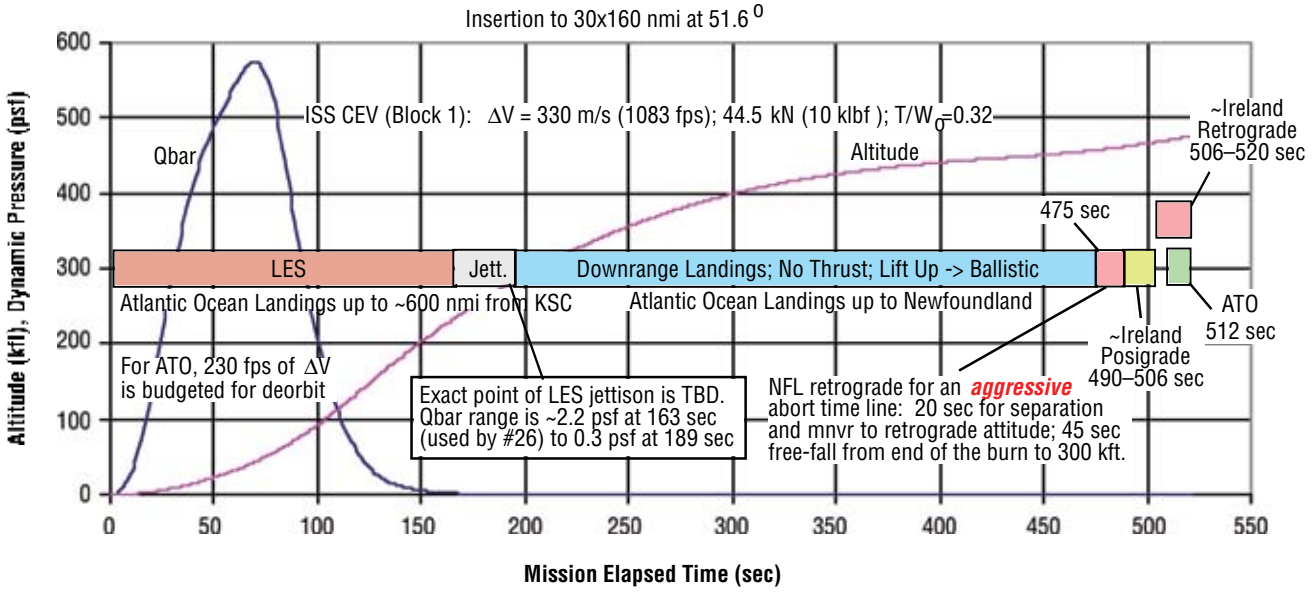

NFL = Newfoundland
Nominal insertion: 520 sec

Figure 5-107. Abort Modes for LV 26 and the ISS CEV with Limited OMS Propellant

5.4.4.2.2 Abort Mode Sensitivities to T/W and Propulsion System Ignition Delay

Figure 5-108 presents the sensitivity of TAL and ATO opportunities to variations in T/W for aborts from LV 13.1. The study assumes that 200 m/s (3937 fps) of propulsion system ΔV is available. (For ATO, 70 m/s is reserved for deorbit.) The horizontal limit line at approximately 453.5 sec indicates the point in the ascent when the distance from Newfoundland to the ballistic landing area begins to increase. The limit line is meant to provide a rough indication of the T/W required to avoid the middle of the North Atlantic with either an ATO (T/W ≈ 0.26) or a TAL (T/W ≈ 0.16). For T/Ws below approximately 0.21, selection of the first TAL time begins to be driven by having enough free-fall time from the end of the burn to the beginning of atmospheric entry. This study assumes the Apollo guideline of 100 sec of free-fall to 300 kft. Also, maintaining altitude above the assumed minimum operating altitude of the thrusting CM/SM (335 kft) is very important at these T/W levels. For ATO, the thrust pitch angle must be increased to maintain altitude, introducing a "steering loss" to the velocity gain. This effect is more apparent in **Figure 5-109**; as T/W drops below approximately 0.25, the rate of loss of ATO coverage begins to accelerate.

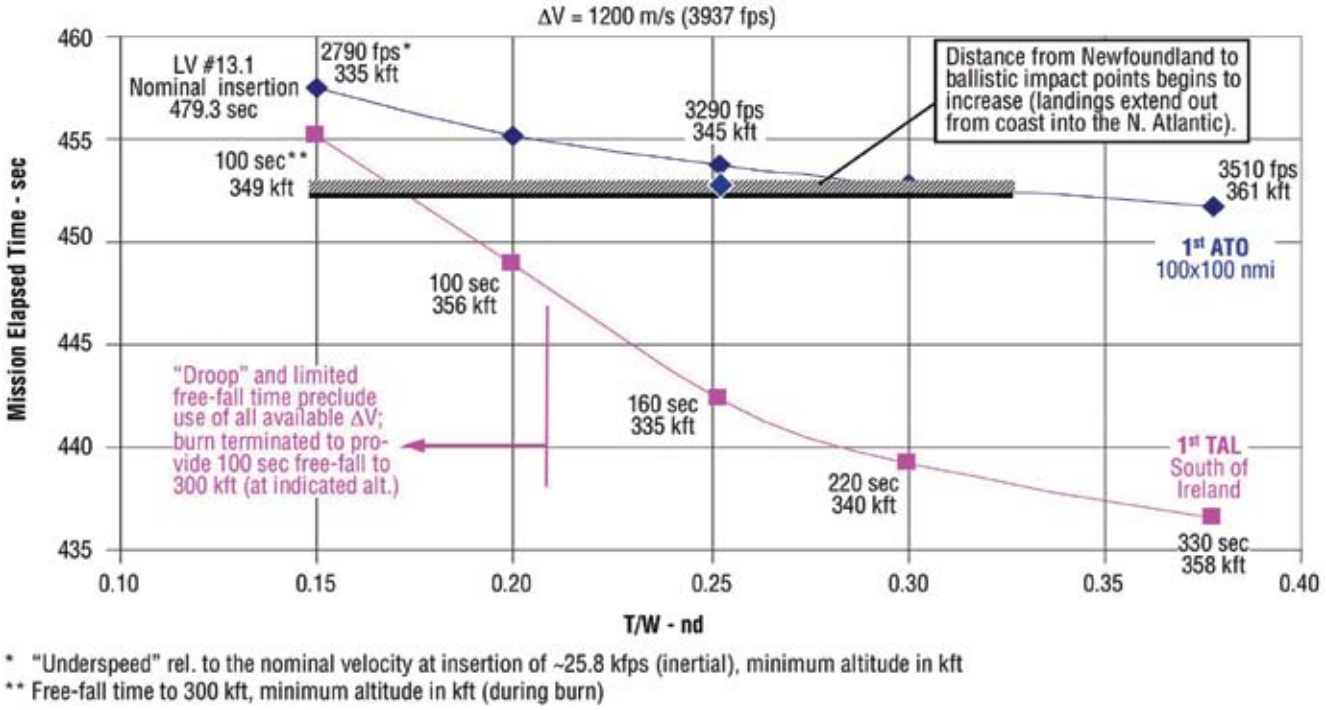

Figure 5-108. Sensitivity of First TAL and ATO to T/W for LV 13.1

The effect of propulsion system ignition delay on ATO coverage is presented in **Figure 5-110**. First ATOs are defined for delays from 20 to 80 sec for two T/W levels. The loss of ATO accelerates when the minimum operating altitude constraint gains prominence. The sensitivity to the propulsion system ignition delay is slightly less for the higher T/W.

It is interesting to note that, individually, the sensitivity to T/W or propulsion system ignition delay is not that significant (plus or minus a couple of seconds), but, taken together, they become more significant. The abort coverage for LV 13.1, with a given ΔV, can be significantly lessened given a low T/W, a propulsion system that takes as long as Apollo to ignite, and an SM that cannot operate below approximately 340 kft.

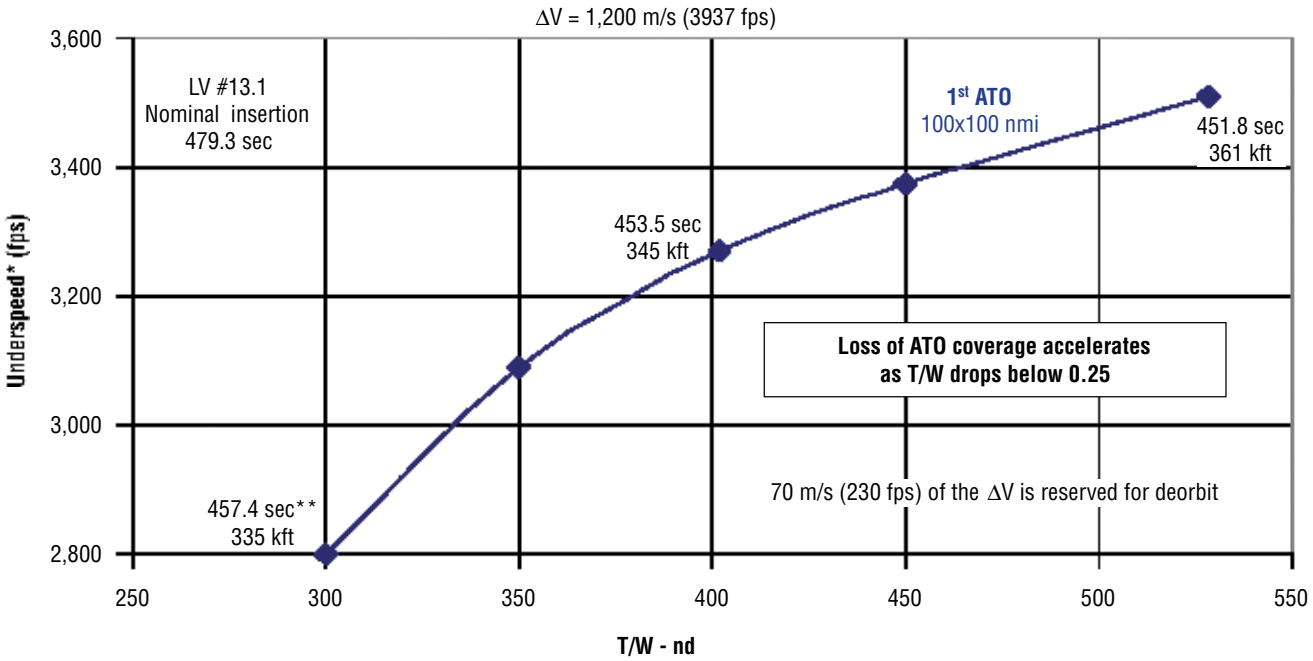

* Relative to the nominal velocity at insertion of approximately 25.8 kfps (inertial)

** MET of 1st ATO in sec, minimum altitude in kft

Figure 5-109. Sensitivity of First ATO to T/W for LV 13.1

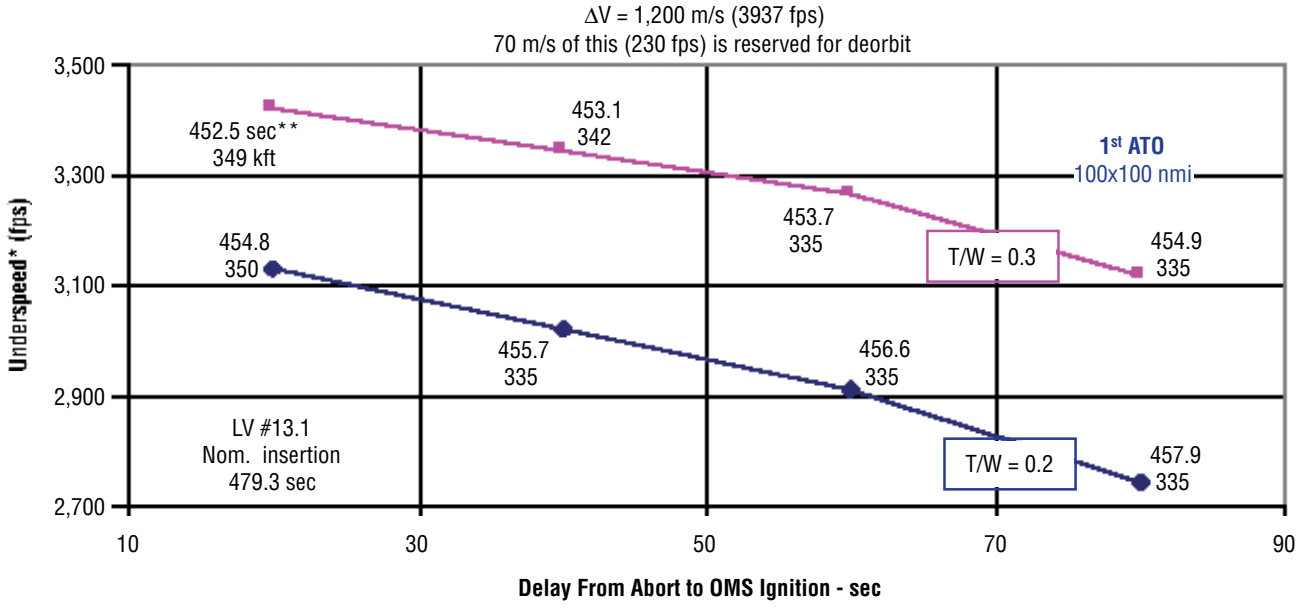

* Relative to the nominal velocity at insertion of approximately 25.8 kfps (inertial)

** MET of 1st ATO in sec, minimum altitude in kft (constrained to be greater than 335 kft)

Figure 5-110. Sensitivity of First ATO to Propulsion System Ignition Delay for LV 13.1

5.4.4.3 Abort Mode Assessments for 28.5-deg Inclination

Potential ascent abort modes for 28.5-deg inclination launches are shown for LV 13.1 and 26 in **Figures 5-111** and **5-112**, respectively. For posigrade and retrograde suborbital maneuvers, a recovery area is assumed between the Cape Verde Islands and Africa. Posigrade burns can access the recovery area once the ballistic impact point passes roughly 50°W longitude. The significance of this is that some abort landing areas will be far from land, even with the use of propulsion system thrust.

The effect of Earth oblateness should be noted: for the due east missions, the oblate Earth "rises up" during the ascent (the Earth radius increases); whereas, at 51.6 deg, the oblate Earth falls away. This phenomenon seems to explain the apparent reduction in the posigrade down-range abort capability at 28.5 deg. While not readily apparent from the abort mode diagrams, the down-range abort capability at 28.5 deg occurs significantly closer to the ATO abort boundary than at 51.6 deg. This oblateness effect should also impact the ATO boundary for LV 13.1, where minimum altitude is a concern. However, the effect probably is less than 300 fps of under-speed, which is the difference between LV 13.1 and 26. (Refer to **Figure 5-113**.) This effect could be negated by targeting the 28.5-deg engine cut-off at a higher altitude than 51.6°. The Space Shuttle Program used this strategy, targeting Main Engine Cutoff (MECO) 5 nmi higher when due-east missions were flown.

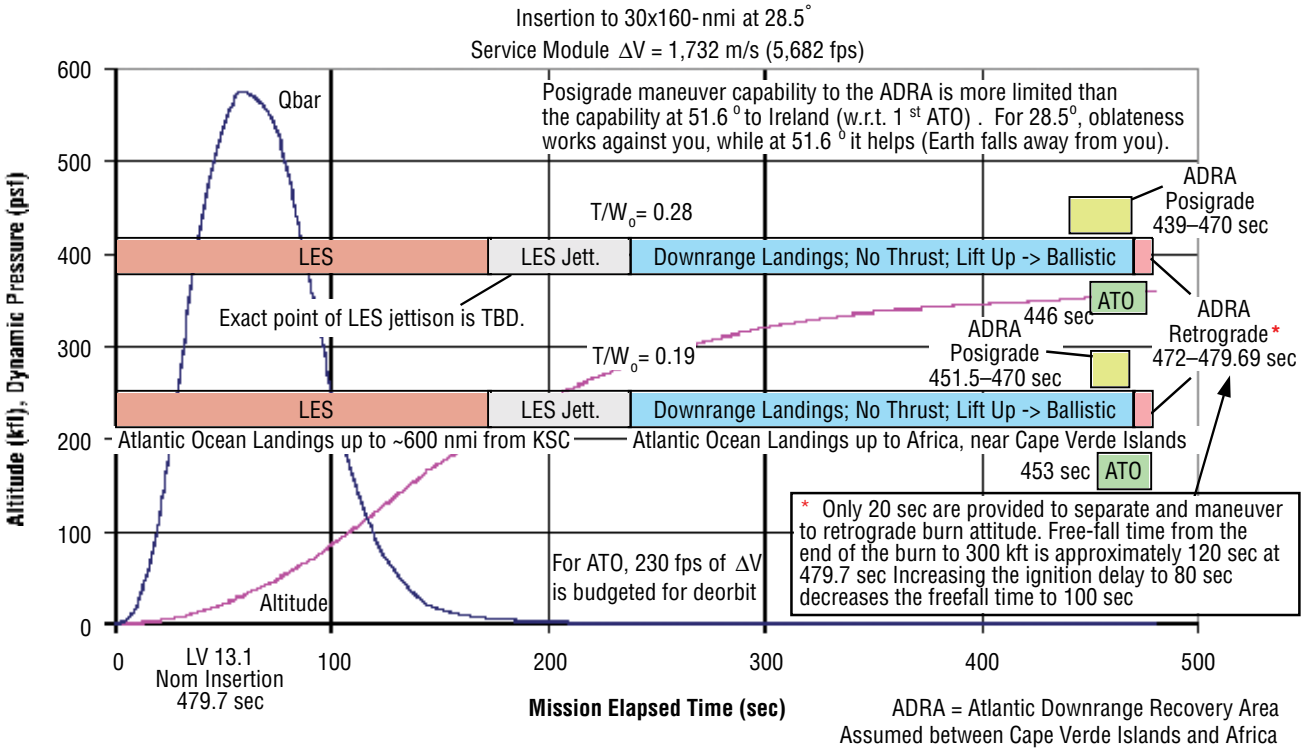

Figure 5-111. Abort Modes for LV 13.1 at 28.5 deg

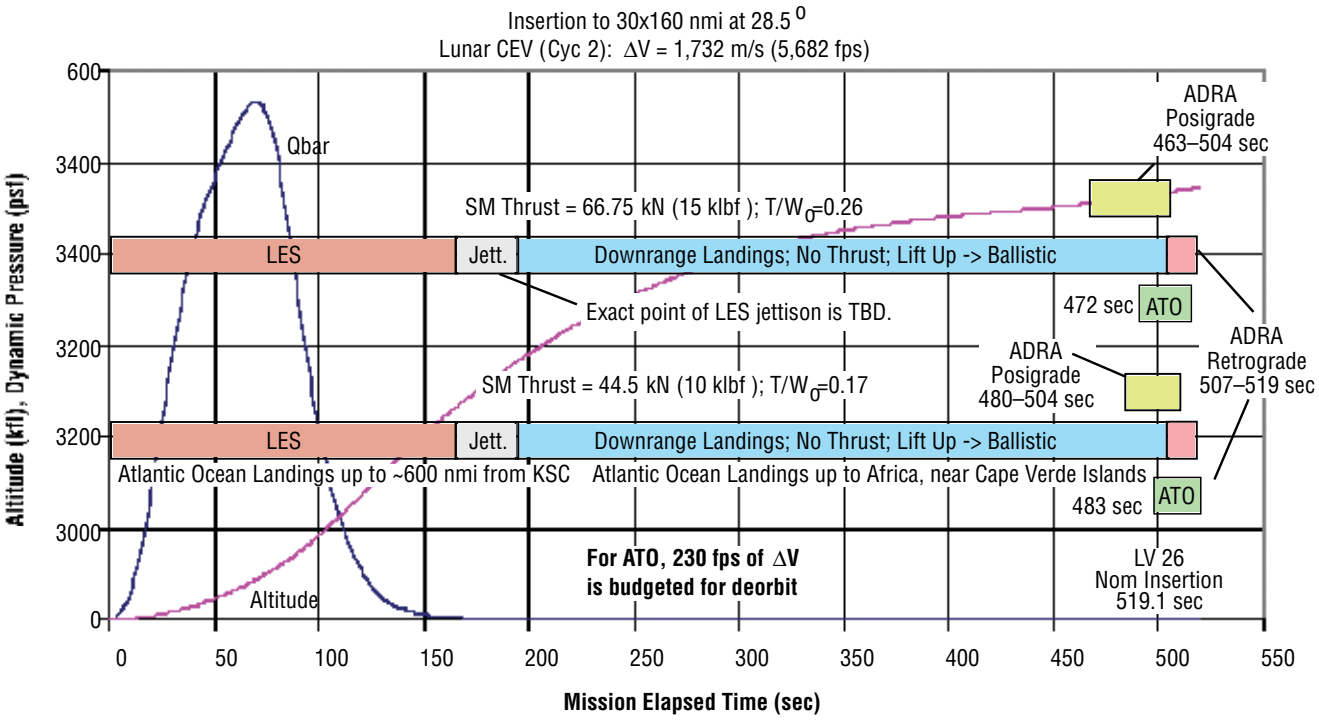

ADRA = Atlantic Downrange Recovery Area
Assumed between Cape Verde Islands and Africa

Figure 5-112. Abort Modes for LV 26 at 28.5 deg

Figure 5-113 presents a comparison of the ATO ΔV requirement for the LV 13.1 and LV 26 for two T/W levels. The data is presented as a function of abort "under-speed" (i.e., the velocity magnitude short of the nominal engine cutoff velocity). This is a useful parameter for comparing different LVs with different acceleration levels. Because LV 13.1 accelerates at 4g, and LV 26 at 3g, comparison of ATO times relative to nominal engine cut-off can be misleading. One can roughly convert from the under-speed domain to the time domain using the acceleration limits: approximately 100 and 130 fps2 for 3 g and 4 g, respectively (a 1,000 fps under-speed is roughly 10 sec prior to engine cutoff for a 3-g limit). Several interesting trends are presented on **Figure 5-113**. First, the benefit of higher T/W increases for earlier ATOs, which have larger under-speeds. (Note how the different slopes of the T/W curves cause them to diverge as the under-speed increases.) The earlier aborts provide more time for the larger gravity and steering losses of the lower T/W to accumulate. Conversely, the curves converge for smaller under-speeds, indicating that the effect of different T/W and ascent trajectory lofting diminishes as aborts occur closer to nominal engine cutoff. There is also a break point in the curves for LV 13.1. This particular study assumed a minimum operating altitude for the CSM of approximately 345 kft. The slope of the curve increases when the abort gets long enough that the altitude "droops" to the minimum. At that point, more thrust must be "diverted" upwards, making the burn less efficient. Since LV 26 has a more lofted ascent trajectory, this problem occurs at larger under-speeds than are shown on **Figure 5-113**.

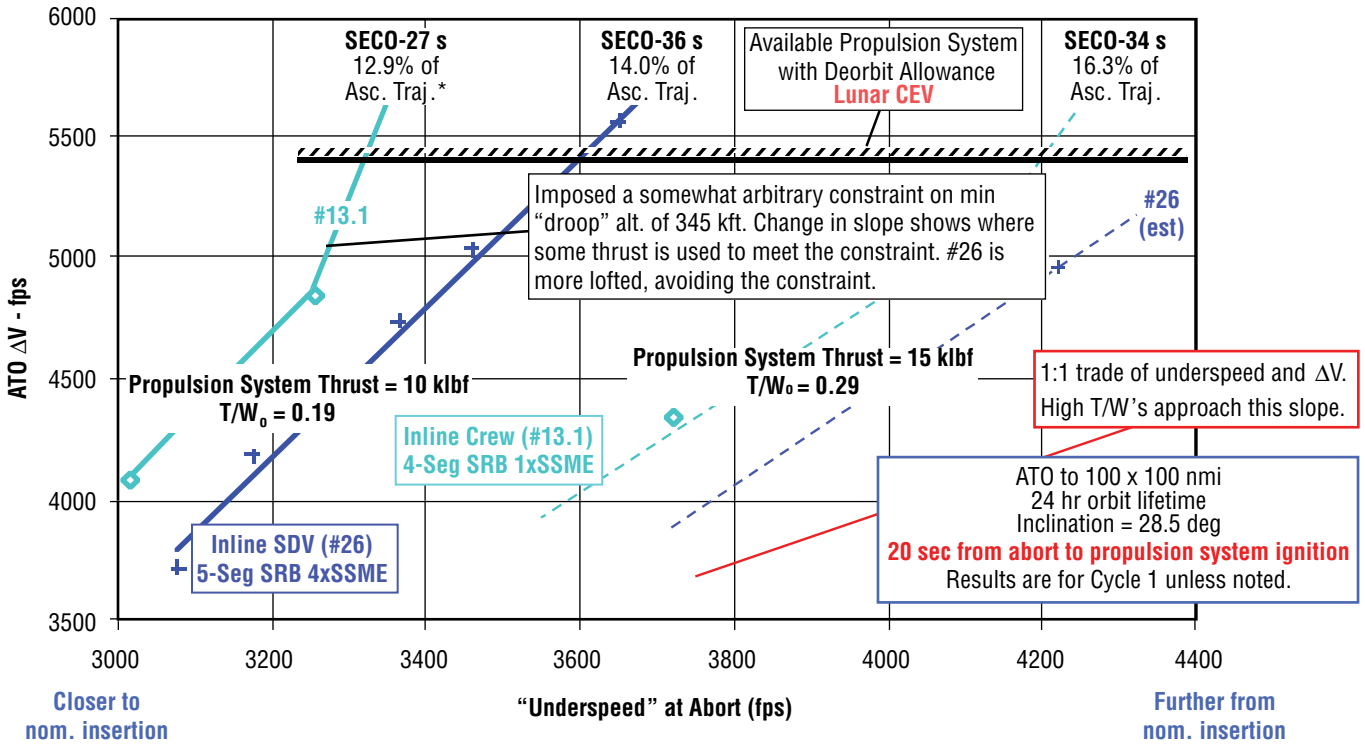

*Relative to the nominal velocity at insertion of ~25.8 kfps (inertial)

Figure 5-113. Comparison of ATO Delta-V Requirements at 28.5 deg